STUTZMAN

NATIONAL ACADEMIES OF SCIENCE AND ENGINEERING

NATIONAL RESEARCH COUNCIL

of the

UNITED STATES OF AMERICA

UNITED STATES NATIONAL COMMITTEE

International Union of Radio Science

National Radio Science Meeting

12-15 January 1987

Sponsored by USNC/URSI
in cooperation with
Institute of Electrical and Electronics Engineers

University of Colorado
Boulder, Colorado
U.S.A.

National Radio Science Meeting
12-15 January 1987
Condensed Technical Program

SUNDAY, 11 JANUARY

2000-2400	USNC-URSI Meeting	Broker Inn

MONDAY, 12 JANUARY
(Paper presentations will be held in the Engineering Center)

0855-1200		
A-1	Electromagnetic Measurements for RF Biological Effects Research	CR1-46
B-1	Electromagnetic Theory	CR2-28
F-1	Scattering, Attenuation, and Fading by Rain and Surface Obstacles	CR2-26
G-1	World-Wide Acoustic Gravity Wave Study	CR1-9
G-2	Wave Propagation	CR1-42
H-1	Plasma Chamber Simulation of Space Phenomena	CR1-40
0855-1035		
B-2	Antennas I	CR0-30
0855-0955		
J-1	New Techniques in Radio Astronomy	CR2-6
0955-1200		
J-2	Millisecond Pulsar Workshop I	CR2-6
1035-1200		
B-3	Transients	CR0-30
1355-1700		
B-4	Antennas II	CR2-28
C-1	Communication Theory	CR1-9
F-2	Surface Based Radar and Radiometric Remote Sensing of the Clear Atmosphere	CR2-26
G-3	Global Ionospheric Variations	CR1-42
G-4	Ionospheric Radio Techniques	CR1-46
H-2	RF Acceleration of Particles in Space	CR1-40
J-3	Millisecond Pulsar Workshop II	CR2-6
1355-1535		
B-5	Waves Near an Interface	CR0-30
1535-1700		
B-6	Random Media	CR0-30
1700-1800		
Commission A Business Meeting		CR1-46
Commission F Business Meeting		CR2-26
Commission G Business Meeting		CR1-42
Commission J Business Meeting		CR2-6

United States National Committee

INTERNATIONAL UNION OF RADIO SCIENCE

PROGRAM AND ABSTRACTS

National Radio Science Meeting
12-15 January 1987

Sponsored by USNC/URSI in cooperation
with IEEE groups and societies:

Antennas and Propagation
Circuits and Systems
Communications
Electromagnetic Compatibility
Geoscience Electronics
Information Theory
Instrumentation and Measurement
Microwave Theory and Techniques
Nuclear and Plasma Sciences
Quantum Electronics and Applications

Copy

14
18
26
63
68
133
134
136
137
215
216
219
220

NOTE:

Programs and Abstracts of the USNC/URSI Meetings are available from:

USNC/URSI
National Academy of Sciences
2101 Constitution Avenue, N.W.
Washington, DC 20418

at $2 for meetings prior to 1970, $3 for 1971-1975 meetings, and $5 for 1976-87 meetings.

The full papers are not published in any collected format; requests for them should be addressed to the authors who may have them published on their own initiative. Please note that these meetings are national. They are not organized by the International Union, nor are the programs available from the International Secretariat.

MEMBERSHIP

United States National Committee

INTERNATIONAL UNION OF RADIO SCIENCE

88-91 Bowhill Butler Dave Chang

Chairman:	Robert K. Crane*
Vice Chairman:	Sidney A. Bowhill*
Secretary:	Chalmers M. Butler*
Immediate Past Chairman:	Prof. Thomas B.A. Senior*

Members Representing Societies, Groups, and Institutes:

American Geophysical Union	to be appointed
American Astronomical Society	to be appointed
IEEE Antennas & Propagation Society	Dr. W. Ross Stone
IEEE Communications Society	Prof. Raymond Pickholtz
IEEE Geophysics and Remote Sensing Society	Dr. Robert E. McIntosh

Members-at-Large:

~~Dr. Alan T. Moffet~~ resigned

Dr. E.K. Smith

Mr. John A. Klobuchar 1987

~~Dr. Edmund K. Miller~~ Daniel Hill

Dr. Ray J. King 1987

~~Dr. Arthur D. Spaulding~~ Rino

Liaison Representatives from Government Agencies:

National Telecommunications & Information Administration	Dr. Hans Liebe
National Science Foundation	Dr. Tomas F. Gergely
Federal Communications Commission	Mr. William A. Daniel
	Mr. William J. Cook
Department of Defense	Dr. George L. Salton
Department of the Army	Lt. Col. Robert Clayton, Jr.
	Mr. Earl J. Holliman
Department of the Air Force	Dr. Allan C. Schell

Chairmen of the USNC/URSI Commissions:

Commission A	Dr. Harry Cronson
Commission B	Dr. Akira Ishimaru
Commission C	Dr. Jay W. Schwartz
Commission D	Drs. K.J. Button & A.A. Oliner
Commission E	Dr. Joel M. Morris
Commission F	Dr. Richard K. Moore
Commission G	Dr. Kung Chie Yeh
Commission H	Dr. Kenneth J. Harker
Commission J	Dr. William J. Welsh

Officers of URSI resident in the United States: (including Honorary Presidents)

Immediate Past President	Prof. William E. Gordon*
Honorary President	Prof. Henry G. Booker*

Chairmen and Vice Chairmen of Commissions of URSI resident in the United States:

Vice Chairman of Commission B	Prof. Thomas B.A. Senior
Vice Chairman of Commission F	Dr. Robert K. Crane
Vice Chairman of Commission G	Dr. Jules Aarons

Foreign Secretary of the U.S. National Academy of Sciences	Dr. William E. Gordon
Chairman, National Research Council, Commission on Physical Sciences, Mathematics, and Resources	Dr. Norman Hackerman
Chairman, National Research Council, Board on Physics and Astronomy	Prof. Norman Ramsey
Honorary Members	Dr. Harold H. Beverage Dr. Ernst Weber
NRC Program Officer	Dr. Robert L. Riemer
NRC Administrative Specialist	Ms. Helene E. Patterson

* Member of USNC/URSI Executive Committee

DESCRIPTION OF THE INTERNATIONAL UNION OF RADIO SCIENCE

The International Union of Radio Science is one of 18 world scientific unions organized under the International Council of Scientific Unions (ICSU). It is commonly designated as URSI (from its French name, Union Radio Scientifique Internationale). Its aims are (1) to promote the scientific study of radio communications, (2) to aid and organize radio research requiring cooperation on an international scale and to encourage the discussion and publication of the results, (3) to facilitate agreement upon common methods of measurement and the standardization of measuring instruments, and (4) to stimulate and to coordinate studies of the scientific aspects of telecommunications using electromagnetic waves, guided and unguided. The International Union itself is an organizational framework to aid in promoting these objectives. The actual technical work is largely done by the National Committee in the various countries.

The officers of the International Union are:

President:	Dr. A.P. Mitra (India)
Past President:	Prof. W.E. Gordon (U.S.A.)
Vice Presidents:	Dr. Ing. H.J. Albrecht (F.R.G.) A.L. Cullen (U.K.) S. Okamura (Japan) Prof. V. Zima (Czechoslavakia)
Secretary-General	J. Van Bladel (Belgium)
Honarary Presidents:	G. Beynon (U.K.) H.G. Booker (U.S.A.) W. Dieminger (West Germany) I. Koga (Japan) J.A. Ratcliffe (U.K.)

The Secretary-General's office and the headquarters of the organization are located at Avenue Albert Lancaster, 32, B-1180 Brussels, Belgium. The Union is supported by contributions (dues) from 38 member countries. Additional funds for symposia and other scientific activities of the Union are provided by ICSU from contributions received for this purpose from UNESCO.

The International Union, as of the XXth General Assembly held in Washington, DC in August 1981, has nine bodies called Commissions for centralizing studies in the principal technical fields.

Every three years the International Union holds a meeting called the General Assembly. The next is the XXIIst, to be held in 1987. The Secretariat prepares and distributes the Proceedings of the General Assemblies. The International Union arranges international symposia on specific subjects pertaining to the work of one or several Commissions and also cooperates with other Unions in international symposia on subjects of joint interest.

Radio is unique among the fields of scientific work in having a specific adaptability to large-scale international research programs, since many of the phenomena that must be studied are worldwide in extent and yet are in a measure subject to control by experimenters. Exploration of space and the extension of scientific observations to the space environment are dependent on radio for their research. One branch, radio astronomy, involves cosmic phenomena. URSI thus has a distinct field of usefulness in furnishing a meeting ground for the numerous workers in the manifold aspects of radio research; its meetings and committee activities furnish valuable means of promoting research through exchange of ideas.

Steering Committee:

S.W. Maley, Chairman
C.M. Butler
P.L. Jensen

Technical Program Committee:

C.M. Butler, Chairman
H. Cronson
K. Davies
E. Gossard
K.J. Harker
A. Ishimaru
M. Kanda
R.K. Moore
J.M. Morris
M. Nesenbergs
C. Rush
J.W. Schwartz
A.D. Spaulding
K.C. Yeh
W.J. Welch

Monday Morning, 12 Jan., 0855-1200

Session A-1 0855-Mon. CR1-46
ELECTROMAGNETIC MEASUREMENTS FOR RF BIOLOGICAL EFFECTS RESEARCH

Chairman: Howard I. Bassen, Dept. of Microwave Research, Walter Reed Army Institute of Research, Washington, DC 20307

A1-1 0900 **COMPARISON OF FIELD STRENGTH PREDICTED FROM A CALCULABLE TRANSMITTING ANTENNA, AND FIELD STRENGTH MEASURED WITH A CALCULABLE RECEIVING DIPOLE**

E.B. Larsen and W.J. Anson
Electromagnetic Fields Division, 723.03
National Bureau of Standards
Boulder,CO 80303

NBS offers calibration services for field strength meters, antennas, and rf hazard meters. Two independent approaches can be used to establish field strength standards. One is based on generating a known field in the main beam of a transmitting antenna in an anechoic chamber. The field is calculated from measured power delivered to the antenna, distance to the field point, and theoretical (or measured) gain of the transmitting antenna. The near-zone gain at a given frequency and separation distance can be derived in terms of the antenna dimensions. The antennas used at NBS for this approach consist of standard-gain pyramidal horns or open-end-waveguides (OEG's). The second approach used at NBS to produce a known field is to measure the strength at a field point in terms of the response and theoretical effective length of a calculable receiving dipole. The NBS "standard" dipoles cover a frequency range of 25 to 1000 MHz. The response can be measured either in terms of "open-circuit" rf voltage developed across the dipole center gap, or rf power delivered by the dipole to a 50 ohm power meter. In the latter case the dipole source impedance must be known from theory or measurement. The effective length of a thin cylindrical dipole is calculated from its length, length-to-diameter ratio and frequency.

Experiments were performed in the NBS anechoic chamber to determine the difference between field strength computed in terms of a <u>transmitting</u> antenna (power and gain) and <u>receiving</u> dipole (voltage and effective length). The frequency range tested was 200 MHz (lower limit for calculating fields in the anechoic chamber) to 1000 MHz (upper limit for the NBS standard dipoles). Data were taken in 50 MHz increments for 7 half-wave dipoles, each cut to a length for theoretical self resonance. Antenna separation distances (transmitting to receiving) of 1 to 5 meters were used. It was found that the "transmitted" field strengths were always greater than the "received" values. The <u>average</u> discrepancy was about 1 dB in the 0.2 to 0.5 GHz range (using OEG's) and about 0.6 dB in the 0.5 to 1 GHz range (using horns). Data were also taken with shorter (or longer) dipoles than a self-resonant length. The response versus length changed more rapidly (near resonance) than theoretically predicted. Reasons are postulated to explain these observed discrepancies, and suggestions are given to improve the accuracy of reference fields used for calibration services.

A1-2 0920 SHAPED FREQUENCY RESPONSE SURVEY INSTRUMENTS FOR RF & MICROWAVE FREQUENCIES: Edward Aslan, Narda Microwave Corp., 435 Moreland Rd., Hauppauge, NY 11788

The revision of the ANSI radio frequency protection guide in 1982 to the frequency dependent guide has produced the need for radiation monitors with a conforming frequency sensitivity. This paper describes monitors and the techniques to shape the frequency sensitivity curve to the ANSI RFPG.

Over the range of .3 MHz thru 1.5 GHz where the RFPG varies by 20 dB, the shaping is accomplished with discrete chip components for the lower frequency part of the curve and distributed resistive films for the upper frequency range. The detector is a beam lead diode operating in the square law region. Circuitry is included to provide the same sensitivity for CW and pulsed fields of the save average power density.

The second monitor described uses a combination of diode terminated dipoles and distributed resistive thin film dipoles. The latter function as both thermocouple detector and antenna. The thin film thermocouple detector element functions as a resistive dipole in the mid range and a travelling wave antenna in the highest frequency region. This combination of dipole designs extends the frequency range to 40 GHz. The elements are disposed in three orthogonal planes providing isotropic performance.

Combined Frequency Sensitivity, and ± 2 dB of ANSI C95.1-1982 RFPG

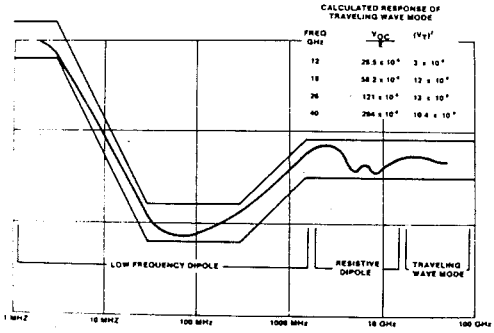

A1-3
0940

SOME PERFORMANCE CHARACTERISTICS OF
A SEMI-IMPLANTABLE E-H PROBE

Tadeusz M. Babij, Electrical Engr. Dept.
Florida International University
Miami, Florida 33199
Howard I. Bassen, Dept. of Microwave
Research, Walter Reed Army Institute
of Research
Washington, D.C. 20307

The purpose of this talk is to review various E-H probes recently developed for measuring intensities electric and/or magnetic fields near or in the phantom models constructed of thin fiberglass walls filled with synthetic tissue with dielectric properties similar to those of actual human tissue. The E-H probe uses dipole and loop antennas, and Schottky diode detectors that all fit in a cubic volume with dimensions of less than 10 mm per side (T.M. Babij, H.I. Bassen, U.S. Patent No 4,588,933, May 13, 1986),(See Fig. 1) An electrically small dipole and loop with nonlinear loads are analyzed theoretically using both analytical and numerical techniques. The nonlinear resistance of the diode is treated using the Newton-Raphson itaration technique. It was indicated that the resistive loading drastically reduces the sensitivity of magnetic response of a H probe, whereas its electric responses is not changed significantly. The analysis and experimental data are presented for models tested over the 0.5 MHz to 1000 MHz.

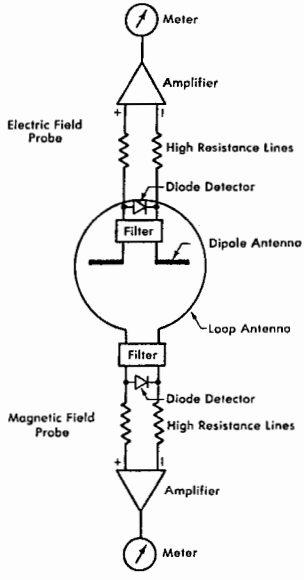

Fig. 1 - Fundamental Design of a single axis E-H probe

A1-4
1020

OUTDOOR MEASUREMENT OF SPECIFIC ABSORPTION RATE IN A MAN-MODEL

R. G. Olsen
Naval Aerospace Medical Research Laboratory
Bioenvironmental Sciences Department
Pensacola, FL 32508-5700

Continued reference to specific absorption rate (SAR) in recently promulgated electromagnetic radiation (EMR) exposure standards has prompted effort to measure SAR in the workplace. A portable man-model has been developed at the Naval Aerospace Medical Research Laboratory (NAMRL) to allow SAR data to be obtained in a wide variety of occupational exposure situations, both indoors and outdoors.

Localized SAR is rather easily determined from either measuring the temperature rate of rise in the model (using a nonperturbing temperature probe) or measuring the magnitude of the internal electric field (E-field) with a suitable miniature sensor. While localized SARs are valuable in determining potential hazards of EMR "hot spots" in the body, it is usually impractical to estimate average, whole-body SAR with many measurements of localized SAR.

At NAMRL, a portable system has been designed and constructed to measure average SAR in a full-size man-model outdoors. The system uses a matched pair of gradient-layer calorimeters each of which encloses a given volume with a surface array of many thermocouples to produce an output voltage proportional to the net heat flow rate (power) leaving the volume. Gradient-layer calorimeters are highly sensitive with a typical output signal of more than 0.75 mV per watt of power flow. Two identical man-models are initially brought to the same temperature, then one model is irradiated in the occupational location being studied while the second model is located nearby but not irradiated. Immediately after the timed irradiation, both models are placed inside the calorimeters, and the output voltages are monitored for the next 24-48 hours. Variations in ambient temperature do not affect the results so long as both calorimeters are placed in a homogeneous thermal environment.

The voltage difference between the two devices is proportional to the net rate of heat flowing from the irradiated model and can be integrated over time to obtain the total energy deposited in the man model. Average SAR then equals the energy deposited (in joules) divided by the irradiation time (in seconds) and further divided by the model mass (in kg).

A1-5
1040

ELECTROMAGNETIC FIELD MEASUREMENTS IN MODELS OF BIOLOGICAL BODIES

S.S. Stuchly[1]) and M.A. Stuchly[2])
[1])Dept. of Electrical Engineering,
University of Ottawa,
Ottawa, Ont. K1N 6N5
[2])Bureau of Radiation and Medical Devices,
Health & Welfare Canada, Ottawa, Ont. K1A 0L2

Biologocial effects of electromagnetic fields at radiofrequencies depend on the spatial distribution of the electric field induced in an exposed biological body. Two techniques have been developed to measure these fields in models of human and animal bodies. The thermographic technique was pioneered by Guy in the early seventies (A.W. Guy, IEEE Trans. MTT, 19, 205-221, 1971). More recently, in our laboratories another method has been developed.

A computer-controlled scanning system is used for positioning a small-size, isotropic electric field probe within a volume of 0.5m x 0.5m x 2m. The probe is interfaced by a custom designed electronic circuitry containing an optical fiber link with a minicomputer. The software developed controls the experiment and the data acquisition. It also provides data processing and graphical display and recording. The overall uncertainty in measurements of the electric field strenght is ± 1 dB and is mostly limited by the probe calibration accuracy (Stuchly et al, IEEE Trans. BME, 31, 526-531.

Extensive studies of the electric field distribution in two full-scale models of man have been performed. One model had average tissue electrical properties and the other was composed of a variety of tissue simulating materials such as the skeleton including the skull, spinal cord and all major bones, brains, lungs and muscle. Investigations were carried out for each model exposed both in the far-field and in the near-field for two field polarizations at three radiofrequencies. Results were compared for the two models, and comparisons were made with theoretical predictions.

A1-6
1100

BROADBAND MEASUREMENTS OF ELECTRICAL PROPERTIES OF BIOMATERIALS

M.A. Stuchly[1]) and S.S. Stuchly[2])
[1])Bureau of Radiation and Medical Devices,
Health & Welfare Canada, Ottawa, Ont. K1A 0L2
[2])Dept. of Electrical Engineering,
University of Ottawa,
Ottawa, Ont. K1N 6N5

The electrical properties of molecules, cells and tissues define their interactions with electromagnetic fields. These properties expressed in terms of the dielectric constant and loss factor or conductivity, change considerably, typically by six orders of magnitude, as the test frequency changes from a few hertz to tens of gigahertz, reflecting various relaxation phenomena. In many cases the properties in vivo are different from those in vitro. Temperature also affects the properties. For these reasons measurements of electrical properties of biomaterials pose several challenging problems.

Recently, several new sensors have been developed which are suitable for accurate in vivo measurements. Different types of sensors have to be used in the various frequency ranges, but one sensor, if properly designed, can ensure high accuracy in three decades of frequency (M.A. Stuchly and S.S. Stuchly, Int. J. Electronics, 56, 443-456, 1984). These sensors include: a short monopole (E.C. Burdette et al, IEEE Trans. MTT, 28, 414-427, 1980) and an open ended coaxial line (T.W. Athey et al, IEEE Trans. MTT,30, 82-86, 1982; G.B. Gajda and S.S. Stuchly, IEEE Trans. MTT,31, 380-384, 1983) at frequencies from 10 MHz to 10 GHz, and a multi-ring sensor (S.S. Stuchly et al IEEE Trans. IM, 35, 138-241, 1986) at frequencies from 10 kHz to 100 MHz. At present we are developing a sensor suitable for in vivo measurements below 10 kHz and at millimeter waves.

The permittivity of a test biomaterial is determined from measurements of the input reflection coefficient of the sensor, loaded with the test substance, by means of an automatic network analyzer. Commercial automatic network analyzers have been used for this purpose. With suitable calibration procedures accurate (within 2-3%) and fast measurements are performed.

Session B-1 0855-Mon. CR2-28
ELECTROMAGNETIC THEORY
Chairman: A.D. Yaghjian, Applied Electromagnetic Division, RADC/EEC, Hanscom AFB, MA 01731

B1-1
0900

SHEET SIMULATION OF DIELECTRIC LAYERS

T. B. A. Senior and J. L. Volakis
Radiation Laboratory
Dept. of Electrical Engineering and Computer Science
The University of Michigan
Ann Arbor, MI. 48109-2122

To facilitate the computation of the field scattered by thin non-magnetic layers, it is customary to model the layer as an infinitesimally thin resistive sheet. However, it has been found that this simulation becomes increasingly inaccurate at wide angles of incidence when the electric vector has a component normal to the layer.

By starting with the volume integral formulation, it will be shown that the accuracy of the sheet simulation is greatly improved by including a "modified" conductive sheet in addition to the resistive one. The boundary condition for this new sheet differs from that of a standard conductive sheet by the presence of a second normal derivative and the combination of the coincident sheets yields results for the thin layer/slab that are virtually identical to those provided by the volume integral equation. The advantages of this type of simulation will be discussed, and its extension to a layer of arbitrary shape and composition will be described.

B1-2 0920 **AN INTEGRAL EQUATION BASED LUNEBURG-KLINE DEVELOPMENT FOR THE CURRENT INDUCED ON A CONDUCTING SURFACE**

Gary S. Brown, Dept. of Electrical Engineering, VPI & SU, Blacksburg, VA 24061

Recently, Lee (S.W. Lee, IEEE Trans. Antennas & Propg., AP-23, 184-191, 1975) extended the work by Keller, et al.(J.B. Keller, R.M. Lewis, & B.D. Seckler, Commun. Pure Appl. Math.,IX,207-265,1956) who used ray techniques to generate a formal scattering solution in terms of inverse powers of the em wavenumber k, i.e. a so-called Luneburg-Kline series. Lee's contribution comprised developing a formal methodology for the vector problem and explicitly finding the coefficients of the first terms for the scattered field and the current induced on the surface. His approach was based on the electric field boundary conditions and Gauss's law.

In this paper, a formal Luneburg-Kline series for the current induced on the conducting surface is developed from the magnetic field integral equation (MFIE) under plane wave illumination conditions. After removing the spatially varying phase common to the incidence field from both sides of the MFIE, the residual part of the current is expanded in a Luneburg-Kline series. Because of the additional dependence of the kernel in the MFIE upon k, it also must be expanded in a L-K series. Equating like powers of k in the so expanded MFIE, leads to what appear to be integral equations for the coefficients in the current expansion, Fortunately, the integral term in these equations is evaluated as k becomes infinite and this has the effect of removing the expansion coefficients from under the integral. This, in turn , leads to an algebraic recurrance relation for the current coefficients. The complete Luneburg-Kline series thus hinges on the asymptotic behavior of a surface integral involving the gradient of the free space Green's function evaluated on the surface. The practical determination of the expansion coefficients for the current rests on our ability to develop a full asymptotic representation for this surface integral.

B1-3 0940 SURFACE INTEGRAL EQUATIONS FOR MULTI-WAVELENGTH, ARBITRARILY SHAPED, PERFECTLY CONDUCTING BODIES

A. R. Tobin, A. D. Yaghjian, and M. M. Bell
Applied Electromagnetics Division
RADC/EECT, Hanscom AFB, MA 01731

Conventional matrix solutions for surface integral equations applied to large bodies are limited only by computer time when using high-precision, large-memory computers. However, conventional electric and magnetic-field integral equations for a perfectly conducting body introduce spurious solutions at the resonant frequencies of the interior cavity formed by the scattering surface, and thus yield unreliable solutions, in general, for 3-D bodies larger than about a wavelength across. Among the alternatives that have been devised for eliminating the spurious solutions from the original integral equations, the combined-field equation (Mautz and Harrington, AEU, 32, 157-164, 1978) and the augmented electric or magnetic-field equation (Yaghjian, Radio Sci., 16, 987-1001, 1981) appear the more generally applicable and easily programable. However, for arbitrarily shaped, multi-wavelength bodies, the combined-field and augmented integral equations also have their drawbacks. The combined-field equation adds the magnetic-field equation to the electric-field equation, which takes considerably more ingenuity and computer time than the magnetic-field equation to achieve the same accuracy of solution. The augmented magnetic-field equation involves only the magnetic-field operator, but does not, by itself, eliminate all the spurious solutions from bodies of revolution.

Recently, we have derived the following "dual-surface" magnetic-field integral equation that differs only slightly and eliminates all the spurious solutions from the original magnetic-field integral equation:

$$\hat{n} \times \bar{H}_o = \bar{K}/2 - \hat{n} \times \int \bar{K} \times \nabla' \psi \, dS'$$

where

$$\bar{H}_o = \bar{H}_{inc}(\bar{r}) + \alpha \bar{H}_{inc}(\bar{r}_o), \quad \psi = \phi(\bar{r}', \bar{r}) + \alpha \phi(\bar{r}', \bar{r}_o)$$
$$(\bar{r}_o = \bar{r} - \delta \hat{n})$$

and ϕ is the free-space Green's function. We have applied this dual-surface integral equation to find the fields scattered by a cube of electrical sidelength as large as $s/\lambda=5$ (diagonal=8.7λ). To solve this problem our Cyber 750 takes about 7 hours of computer time proportional to $(s/\lambda)^6$. With computers 100 times faster than the Cyber 750, computer time for the same problem would reduce to a few minutes. In addition, scattering from bodies of revolution hundreds of wavelengths across could be found with such computers in a comparable amount of time. Still, when the integral equation is applied to arbitrarily shaped bodies more than a few wavelengths across, the sixth power dependence of the computer time on electrical size required by the conventional matrix solution taxes severely even the fastest available computers.

B1-4
1000 A NEW APPROACH TO THE SYNTHESIS OF WAVE SIGNALS: I.M. Besieris, A.M. Shaarawi, and M.E. Sockella, Dept. of Electrical Engineering, Virginia Polytechnic Institute and State Univ., Blacksburg, VA 24061

A rich class of novel, exact, finite- energy pulse solutions to a wide set of equations associated with wave motion can be constructed using a linear superposition of fundamental (irreducible) invariants of factorized embedded operators. Illustrative examples are given in connection with the scalar wave equation and the Klein-Gordon equation in space-time-independent unbounded domains. The essential differences between the ordinary Fourier method and the new spectral synthesis is discussed in detail.

B1-5
1040 WAVE PROPAGATION IN MEDIA WITH THREE-DIMENSIONAL QUADRATIC REFRACTIVE INDEX PROFILE

S. K. Jeng*, C. H. Liu and S. J. Franke
Department of Electrical and Computer Engineering
University of Illinois at Urbana-Champaign
Urbana, IL 61801-2991

A new method for computing the Green's function in an unbounded medium with three dimensional inhomogeneities will be presented in this paper. The method is based on results derived from the path-integral technique. When applied to a general 3-D quadratically inhomogeneous medium, the method yields an exact, one-fold integral expression that is numerically manageable. To check this technique, numerical results for the special case of a linearly stratified medium are computed using this technique and compared with those computed by the well established Fast Field Program (FFP) method for stratified media. Excellent agreements between the two results will be shown. The technique is then used to study the effects of range dependence of the medium on the various aspects of waves propagating in such a medium.

*On leave from National Taiwan University.

B1-6
1100

ON THE USE OF THE GENERALIZED BOUNDARY CONDITIONS IN THE SOLUTION OF SOURCE-EXCITED BOUNDARY-VALUE PROBLEMS OF ELECTROMAGNETICS

K.A. Michalski
Department of Electrical Engineering
University of Mississippi
University, MS 38677

The well-known boundary conditions on the behavior of the tangential field components across surface distributions of electric and magnetic currents have been generalized to cover the case where these currents have vector components normal to the surface (K.A. Michalski, Electron. Lett., 22, 921-922, 1986). The purpose of this paper is to demonstrate, in a tutorial manner, that these generalized boundary conditions make it possible to solve many source-excited boundary-value problems of electromagnetics in a systematic and direct way. The problems considered are that of an arbitrarily-oriented, time-harmonic dipole in a stratified medium consisting of planar or cylindrical layers, and in a cylindrical cavity.

B1-7
1120

ELECTROMAGNETIC ENERGY-HOW IS IT RADIATED AND ABSORBED?

John B. Smyth and John A. Durment
Smyth Research Associates
San Diego, California 92123

Einstein's (Ann. d. Phys., 18, 639-641, 1905) investigation, "Does the inertia of a body depend upon its energy content?", based on Maxwell's equations led to the famous conclusion: "If a body gives off energy L, in the form of radiation, its mass diminishes by L/c^2." Can Maxwell's equations describe how electromagnetic energy and inertial mass transform, one into the other?

There is an exact solution of Maxwell's equations (Smyth, Radio Sci., II, 977-984, 1976) which describes how a conceptual something associated with matter called "electrical conduction current" is related to its defining electromagnetic field when it is created and annihilated. Although Maxwell's equations represent a single relationship, the electromagnetic field points to a duality: One component of the electromagnetic field generates electric displacement providing energy in a form identified with matter exhibiting central force field interaction; the other two components of the electromagnetic field provide energy in a form which propagates with the speed of light through the energy of other electromagnetic fields in the vacuum universe without the slightest interaction.

This solution clearly depicts how the dipole antenna radiates and absorbs electromagnetic energy.

Session B-2 0855-Mon. CRO-30
ANTENNAS I
Chairman: L. Shafai, Dept. of Electrical Engineering, Univ. of Manitoba, Winnipeg, Manitoba, Canada

B2-1
0900

PHASE - ONLY ANTENNA SYNTHESIS FOR LINEAR AND PLANAR ARRAYS

John F. DeFord and Om P. Gandhi
Electrical Engineering Department
University of Utah
Salt Lake City, Utah 84112

Minimization of the maximum sidelobe level for a given array geometry by phase-only adjustment of the element excitations is considered. Optimum phases are obtained by using a numerical search procedure to minimize the expression for the pattern sidelobe level with respect to the element phases, and results for both linear and planar arrays of equispaced elements are presented. Data suggests that optimum sidelobe level is a logarithmic function of array size. Optimum patterns have relatively low efficiencies, with efficiency approaching an asymptotic nonzero limit as the array size is increased. Array efficiencies can be significantly improved by introducing a sidelobe taper, at the expense of raising the peak sidelobes somewhat. An analytic synthesis algorithm is presented for use on very large arrays for which the numerical search technique for the minimization of the sidelobe level is computationally impractical. This method produces patterns with characteristics similar to arrays synthesized using the numerical search method, and it may be used to synthesize either uniform or tapered sidelobes, allowing flexibility in determining the efficiency and peak sidelobe level for a given array.

B2-2
0920

NUMERICAL ANALYSIS OF WRAPAROUND ANTENNAS FOR MISSILES APPLICATIONS

Ahmed A. Kishk
The University of Mississippi
Dept. of Elect. Engr.
University, MS 38677

L. Shafai
University of Manitoba
Dept. of Elect. Engr.
Winnipeg, Manitoba, CANADA

Microstrip antennas have found widespread applications because of their numerous advantages as far as their weight, ease of fabrication and low profile. One of the microstrip elements that is commonly used in the surfaces of missiles and boosters is the wraparound microstrip, first described by Munson (R.E. Munson, IEEE Trans. AP-22, 74-78, 1974). The radiation characteristics of such an antenna have been previously examined using dyadic Green's functions (S.B. Fonseca and A. J. Giarola, IEEE Trans., AP-31, 248-253, 1983). Ashkenazy et al (J. Ashkenazy et al, IEEE Trans. AP-33, 295-300, 1985) replaced the printed radiator by an assumed current distribution. The previous analysis considered the cylinder as infinite to simplify the computations involved. However, the geometry with the infinite structure does not provide the practical problem of the finite structure.

In the present work, a numerical method applicable to the wraparound microstrip antenna over a finite cylinder, as shown below, is proposed. Integral equations are used, which are valid for the multiple region problem consisting of dielectrics and conductors. These integral equations are then applied for objects that are rotationally symmetric, and are reduced to a matrix equation using procedures common in solving the problem of bodies of revolution. The method also provides a convenient approach to solve for different number and location of the excitation probes under the microstrip patch. The radiation patterns are calculated for different dielectric materials, thicknesses, radii, and cylinder's height.

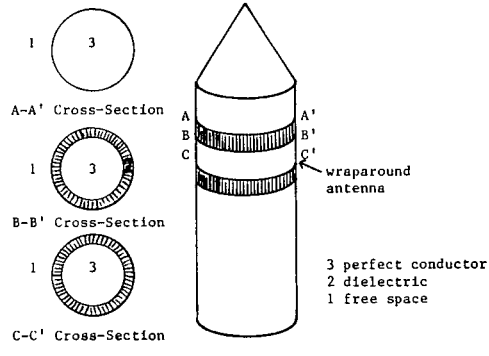

B2-3
0940

DIFFERENCE PATTERN OF A CIRCULAR APERTURE WITH FICTITIOUS BLOCKAGE

Anders G. Derneryd*
Department of Electrical and Computer Engineering
University of Colorado
Boulder, CO 80309

A number of techniques have been published for optimizing the performance of sum and difference circular aperture distributions in the absence of blockage. In a monopulse antenna where sum and difference radiation patterns are simultaneously required, it is not always possible to independently optimize the patterns. Thus a monopulse array antenna usually suffers from high sidelobes in the difference patterns. This is due to the amplitude discontinuity when phase reversing the antenna halves of the sum amplitude distribution to form the difference patterns.

The collapsed sum and difference optimum amplitude distributions of a circular aperture have the same general shape except close to the center of the aperture. The sum distribution has a maximum at the center while the difference distribution has a null. Thus it is possible to simulate approximately a difference distribution with a dip at the center by introducing a fictitious blockage in the sum distribution when forming the difference pattern. The size of the central blockage is set to achieve a smooth transition from one antenna half to the other half. The sum and the difference amplitude distributions are not completely independent of each other. However, a difference radiation pattern with lower sidelobes is realizable with this method compared to just a phase reversal of the sum distribtuion.

Results will be presented for the difference sidelobe level of a circular aperture with a fictitious circular blockage. The results have practical applications to monopulse slot array antennas where the same amplitude distributions have been used for the sum and difference patterns. An improvement of 7 dB is expected in the difference sidelobe level by introducing the central blockage.

---

* On leave from
ERICSSON RADIO SYSTEMS AB
S-43126 Molndal, Sweden

B2-4
1000

MONOPOLE IMPEDANCE AND GAIN MEASUREMENTS ON FINITE GROUND PLANES

R.G. FitzGerrell
National Bureau of Standards, 723.04
325 Broadway
Boulder, CO 80302

The purpose of the work described here is to determine, by a comparison of calculated and measured data, if it is possible to make acceptably accurate input impedance and gain measurements of monopoles on a reduced size ground plane. Ideally, monopoles are located on an infinite, perfectly conducting, plane ground. Practically, measurements are made on a test site with dimensions largely determined by the cost and availability of the space occupied by the site. Measured and calculated data show that the radius of a highly conducting ground plane should be at least 2 λ, where λ = wavelength, for measuring the input impedance of 0.25 λ monopoles. At 25 MHz, the lowest frequency considered here, such a ground plane will require a space at least 48 m in diameter. Model impedance measurements and calculations, a sample shown below, imply that a space only 8 m by 10 m is required by using 16 resistively loaded wire radials (E.E. Altshuler, IEEE Trans. Ant. and Prop, AP-9, 324-329, 1961) to extend a 4 m by 6 m solid metal ground plane. Measured insertion loss data acquired using a 1:5 scale modeled, resistively loaded, ground plane indicate that it is sufficiently large for gain measurements as well as input impedance measurements.

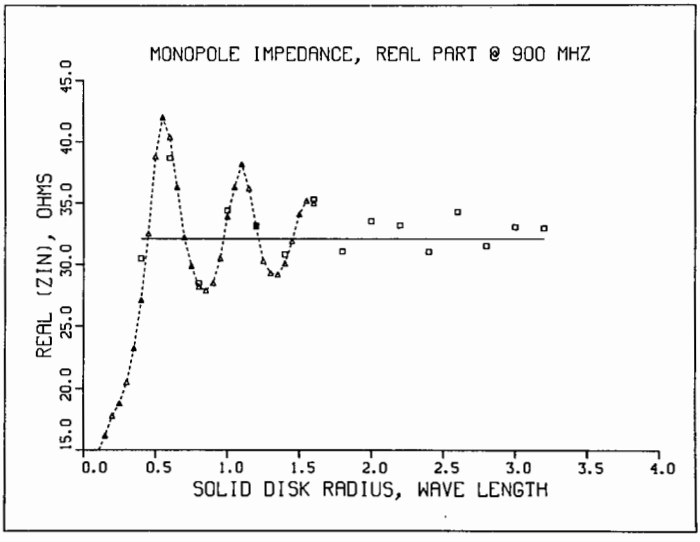

Measured □ □ □, calculated Δ Δ Δ, and ideal ——— real part of input impedance for a monopole on a solid disk.

B2-5
1020 LOW-COST MICROSTRIP PHASED ARRAY ANTENNA FOR USE IN MOBILE SATELLITE TELEPHONE COMMUNICATION SERVICE

F. W. Schmidt, Member, IEEE
Ball Aerospace Corporation
P. O. Box 1062
Boulder, CO 80306

A design for a low-cost phased array antenna used in a car-top application for a satellite communications link is presented. Microstrip stacked patch elements provide good pattern coverage over the 7% bandwidth. Three-bit distributed element microstrip phase shifters provide beam steering over a range of 0 to 70 degrees from boresight. Microstrip technology is also used in the corporate power divider and polarization hybrids.

A hybrid tracking system consisting of an inertial sensor for open loop tracking and a sequential lobing scheme for closed loop tracking provides accurate tracking of the signal through brief signal outages. A novel scheme is used to minimize the effects of varying multipath on closed-loop tracking accuracy. A single board PC-compatible computer is used in conjunction with an interface board to steer the antenna and interface with the transceiver.

Session B-3 1035-Mon. CRO-30
TRANSIENTS
Chairman: A.T. Adams, 111 Link Hall, Syracuse Univ., Syracuse, NY 13210

B3-1
1040 A MODIFIED MARCHING-ON-IN-TIME METHOD FOR TRANSIENT ELECTROMAGNETIC DIRECT-SCATTERING PROBLEMS: Anton G. Tijhuis, Dept. of Electrical Engineering, Delft Univ. of Technology, P.O. Box 5031, 2600 GA Delft, The Netherlands

We consider the solution of time-domain electromagnetic direct-scattering problems with the aid of the marching-on-in-time method. This method utilizes the common property in the relevant integral equations that the scattered field at each space-time point is expressed in terms of one or more integrals of field values at previous instants. The most important difficulty in its application is the occurrence of exponentially increasing instabilities in the solutions obtained. Up to now, this instability problem has been solved by either improving the discretization [1], or applying a gradient-type method to minimize a squared error in the equality sign of the discretized integral equations [2,3]. Both these methods have the disadvantage that they become computationally expensive for multi-dimensional scattering problems.

In the present work, the marching-on-in-time method is interpreted as the recursive solution of a lower-triangular matrix equation of a large dimension. The instabilities can then be envisaged as the inaccurate components of the solution vector along a few problematic eigenvectors of the system matrix associated with a small eigenvalue. Since these components are located in a small subspace of the total solution space they may be designated as "local" errors. Such "local" errors may appear regardless of the accuracy of the discretization. On the other hand, the marching-on-in-time method will determine the components of the solution vector along the majority of the eigenvectors of the system matrix up to some small "global" accuracy.

An iterative method will be described that uses this property as well as the lower-triangular structure of the matrix equation in determining a regularized solution that does not have components along the problematic eigenvectors. This method leaves us with a gradually varying solution whose "global" error may still increase gradually with increasing time. To that error, we apply the analysis of [1], which argues that it can be controlled by taking care that the discretization error is at most proportional to the square of the space-time mesh size and by choosing that mesh size sufficiently small.

The validity of the analysis will be demonstrated with the help of some representative results for one- and two-dimensional scattering problems.

[1] A.G. Tijhuis, Radio Sci. 19, 1984, pp. 1311-1317.
[2] G.C. Herman and P.M. van den Berg. J. Acoust. Sco. Am. 72, 1982, pp. 1947-1953.
[3] T.K. Sarkar, Radio Sci. 19, 1984, pp. 1156-1172.

B3-2
1100 ANHARMONIC FREQUENCY ANALYSIS: AN EXAMINATION OF ITS USE IN IDENTIFYING "NATURAL" RESONANCES: W. Ross Stone, IRT Corp., 1446 Vista Claridad, La Jolla, CA 92037

A.K. Paul (Math. Comp., 26, 1972, pp. 437-447) has presented a numerical method for frequency analysis which he terms "anharmonic analysis." The name is appropriate because the method accurately determines the presence, magnitude, and phase of the constituent frequencies of a signal, regardless of the presence or absence of any harmonic relationships. Although apparently not well known, this method has potential application in a variety of electromagnetic problems. An example occurs in system identification. There has been considerable interest in the use of "natural" resonances in the scattering response of a target for identifying and/or characterizing the target. These resonances are often analyzed in terms of their associated poles in the complex plane. A major practical problem in doing this is the fact that noise in the response produces spurious poles. These often cannot be readily separated from those due to the target's noise-free response without a priori knowledge. A number of techniques have been investigated for this problem, with varying degrees of success. Prony's method is perhaps the best-known example of one "resonance-extraction" technique which suffers from this problem. Also central to this problem for many approaches is the need to know the "order" of the system (corresponding to the order of the polynomial used to represent the system response).

Two distinctive properties of anharmonic frequency analysis are that the method remains robust in the presence of noise, and does not require foreknowledge of the "order" of the system. Although Paul commented on the relevance of these properties of his technique vis a vis Prony's method, it does not appear that the usefulness of the technique for practical system identification problems has been fully explored. This paper reviews Paul's technique, identifying how it differs from other approaches. Examples are then given to illustrate the characteristics of the technique in comparison to both Prony's method and other published approaches, including the effects of noise.

B3-3
1120

COMPUTATIONAL FEATURES OF THE WAVEFRONT/ RESONANCE HYBRID REPRESENTATION OF THE TRANSIENT FIELD EXCITED BY A MAGNETIC LINE SOURCE ON A PERFECTLY CONDUCTING CYLINDER

Radhakrishna Naishadham
Dept. of Elec. Engr.
University of Kentucky
Lexington, KY 40506

L. W. Pearson
McDonnell Douglas Research Laboratories
P. O. Box 516
Saint Louis, MO 63166

In this presentation we explore some computational ramifications of the wavefront/resonance hybrid expansion for the time-domain Green's function of a magnetic line source residing on a perfectly conducting cylinder. This hybrid representation was developed recently by Heyman and Felsen (I.E.E.E. Trans. Ant. and Propag., AP-31, 426, 1983).

The development of the wavefront/resonance hybrid representation can be viewed in terms of the following steps, beginning from azimuthal propagation representation of the frequency-domain Green's function: (1)The sum over circumnavigations is split into early, recent, and late arrivals of creeping waves and the late-arrival terms are observed to be zero due to causality. (2)The early arrivals are summed as a finite geometric series, yielding the singularity expansion of the original Green's function and a correction term due to the finite-length of the geometric series. (3)The inversion into the time domain is accomplished by way of asymptotic evaluation of the recent wavefront arrivals and the correction term and by exact inversion of the residue series--i.e., singularity expansion, corresponding to the early arrivals. The asymptotic evaluation introduces a partial residue series that anihilates the high-frequency portion of the early arrival residue series, which is effectively a systematic truncation procedure for the singularity expansion.

Computed results from the wavefront/hybrid representation are presented. It is observed from these computations that the wavefront and correction terms add destructively so that their net contribution is small compared with the singularity expansion contribution. It is shown that the finite number of poles resulting from the systematic truncation of the singularity expansion expresses the peaked behavior of the transient response near a wavefront arrival. However, a numerically based truncation criterion consistent with computer precision retains fewer poles than indicated by the hybrid representation. It is shown that the asymptotic evaluation deteriorates after a given wavefront arrival and contributes to the error in the representation between wavefront arrivals.

B3-4
1140

PULSE DATA PREPROCESSING TECHNIQUES
TO RECOVER SEM PARAMETERS

C. D. Taylor*, S. Giles**, and E. Harper***
* Stocker Visiting Professor
Ohio University
Athens, OH 45701-2979
** Lawrence Livermore National Laboratory
Livermore, CA 94550
*** Air Force Weapons Laboratory
Kirtland AFB, NM 87117

Generally, the response of a system to a high power electromagnetic transient can be expressed in terms of a singularity expansion. This technique is called the singularity expansion method (SEM). Knowning the SEM parameters it is possible to characterize the system response and to search for conditions required to maximize a particular attribute of the response signal. Thus it is the goal of this study to present techniques whereby the SEM parameters can be extracted from measured data, and in particular, data with a low signal-to-noise ratio. Both linear and nonlinear filter techniques are considered.

A nonlinear digital filter technique that uses a serial correlation test is shown to provide a preprocessing technique which allows the classic Prony method to be applied to the data. The technique also estimates the noise level and detects the presence of nonstationary noise. Results are presented for typical noisy data, as well as for analytical data with added White-Gaussian noise.

Session F-1 0855-Mon. CR2-26

SCATTERING, ATTENUATION AND FADING BY RAIN AND SURFACE OBSTACLES

Chairman: R.K. Crane, Dept. of Electrical Engineering, Dartmouth College, Dartmouth, NH 03755

F1-1 0900 THREE BODY SCATTERING PRODUCES PRECIPITATION SIGNATURE OF SPECIAL DIAGNOSTIC VALUE

D. S. Zrnic'
National Severe Storms Laboratory
1313 Halley Circle
Norman, OK 73069

Examples are given of three body scatter signatures produced by high reflectivity cores in thunderstorms. The process consists of: 1) scattering by the hydrometeors, 2) backscattering by the ground to the hydrometeors and 3) scattering by the hydrometeors to the radar. When viewed on radar displays, the signatures have an elongated shape, radially aligned behind strong (60 dBZ) reflectivity cores. A radar equation for echo power is developed and predicted r^3 dependence of the echo power on the range between the center of scattering volume, and a reflecting ground ring is confirmed by a least squares fit to actual data. It is shown theoretically that mean Doppler shifts associated with three body scatter signatures are caused by the vertical components of hydrometeor velocities; this is also verified from least square fits of range profiles of measured Doppler velocities to theoretical curves based on geometrical considerations.

F1-2
0920

MILLIMETER-WAVE RAIN ATTENUATION PARAMETERS AND DISTRIBUTIONS

E.J. Dutton
National Telecommunications and Information Administration
Institute for Telecommunications Sciences
325 Broadway
Boulder, CO 80303-3328

In the past couple of years, methods that involve matrix solution of equations relating the specific attenuation measured at three millimeter-wave frequencies and the theoretical relationship of individual raindrop cross-sections integrated over the distribution of raindrop sizes in a given volume of air have been introduced. A recent method will be discussed here.

If we use a parabolic representation of the form

$$n(D) \approx b_1 D^2 + b_2 D + b_3$$

we will have three coefficients, b_i ($i = 1$ to 3) for the three measurement frequencies to describe the dropsize density function, $n(D)$. The function is defined as the number of spherical raindrops per cubic meter of air per centimeter of drop diameter between diameters D and D + dD. We have used units of centimeters for the diameter, D.

One of the major purposes of the millimeter-wave propagation experimentation at the Institute for Telecommunications Sciences has been to develop millimeter-wave propagation characteristics through rainfall across the conterminous United States of America (CONUS). This requires a rainfall attenuation climatology in CONUS. However, this climatology must be achieved as economically as possible, yet be of sufficient breadth to represent CONUS. It is believed that this can be minimally achieved by measurement of three rain-climate types. In this presentation two of these three climatic types, represented by Gasquet, California and Boulder, Colorado, will be discussed.

F1-3
0940

TWO DIMENSIONAL SIMULATION OF RAIN RATE FOR TELECOMMUNICATION APPLICATIONS

K.C. Allen
National Telecommunications and Information Administration
Institute for Telecommunication Sciences
Boulder, Colorado 80303

Simulation techniques surpass present modeling capabilities to predict the limitations placed on microwave and millimeter-wave telecommunication systems by rain. Current models predict little more than the cumulative distribution of attenuation on a line-of-sight path for the average year. Some models predict year to year variability or path diversity improvement to a limited extent. The prediction of other statistics, such as the distributions of fade duration and of time between fades, is extremely limited. Reliable predictions are also not available for complex systems such as the NASA ACTS satellite or networks of paths in which connections can be rerouted. Simulation modeling can predict any measurable performance statistic for simple or complex systems.

Since most models predict the propagation effects of rain as dependent upon the rain rate, it is necessary to simulate the spatial and temporal occurrence of rain rate. In this presentation we explore one approach to simulating the two dimensional occurrence of rain rate.

The first hypothesis is that the rain rate is "frozen in" so that the spatial statistics and the wind velocity determine the temporal statistics. An array represents the rain rate field with the wind moving the columns across the array. A multiple output digital filter generates the random data. After exponentiation, the outputs of the filter replace the first column on the windward side of the array. With normally distributed random inputs to the filter, the distribution of the simulated rain rate is lognormal. The autocorrelations for each output and across the outputs of the digital filter determine the spatial autocorrelation of the rain rate.

F1-4
1100

THE AFGL WEATHER ATTENUATION PROGRAM

Arnold A. Barnes, Jr.
Atmospheric Sciences Division/LYC
Air Force Geophysics Laboratory
Hanscom AFB, MA 01731-5000

AFGL conducted experiments between 15 March and 22 May 1986 in the greater Boston area to measure attenuation in the K_a-band due to precipitation. Emphasis was placed on attenuation in the melting layer (where mixed phase snow and rain coexist) since some previous work indicated that attenuation at these frequencies in the melting layer could be as much as ten times the attenuation in rain for the same precipitation rates. Attenuation was measured in three ways: (1) total attenuation of 38.04 GHz signals from Lincoln Laboratory experimental satellite LES-8, (2) horizontal attenuation from an airborne K_a-band (35.4 GHz) radar, and (3) attenuation in the vertical from co-located, vertically pointing S-band (2710 MHz) and K_a-band (34.512 GHz) radars. Meteorological conditions were monitored by weather radars at AFGL/LYR (Sudbury) and at MIT (Boston), by cloud physics equipment on an aircraft, by sounding balloons, and by ground based equipment at Sudbury and at Hanscom AFB. Eleven cases were obtained with data suitable for in-depth analyses. Preliminary results of the analyses will be presented. This work has applications to the effects of clouds and precipitation on satellite communication systems operating in the EHF range.

F1-5
1120

THE DURATION OF FADES IN SATELLITE TO LAND MOBILE PROPAGATION

R. G. Schmier, W. L. Stutzman, M. Barts, and C. W. Bostian
Virginia Polytechnic Institute and State University
Department of Electrical Engineering
Satellite Communication Group
Blacksburg, VA 24061

While several models exist which predict the cumulative distribution of fades on satellite to land mobile radio paths, relatively little progress has been made in developing techniques for predicting the statistical distribution of fade durations. This distribution is important to link designers who, for example, want to employ error correcting codes to compensate for signal dropouts. Classical methods yield only the average fade duration for certain idealized conditions, and even this has not been predictable for paths with significant shadowing by vegetation. This paper describes two approaches to solving the problem. One uses a software simulator which predicts the complete distribution of fade durations on any path for which it has as input the cumulative fade distribution. The other is an analytical approach which derives fade duration statistics from a recently developed model for propagation on a vegetatively-shadowed path.

Session G-1 0855-Mon. CR1-9
WORLD-WIDE ACOUSTIC GRAVITY WAVE STUDY
Chairman: Paul E. Argo, Los Alamos National Lab
Mail Stop D466, Los Alamos, NM 07545

G1-1
0900 GRAVITY WAVE SOURCES IN THE HIGH LATITUDE IONOSPHERE

G. Crowley
High Altitude Observatory
National Center for Atmospheric Research*
Boulder, CO 80307

K. Schlegel
Max Planck Institut für Aeronomie
Lindau, West Germany

A. D. Richmond
High Altitude Observatory
National Center for Atmospheric Research
Boulder, CO 80307

During the Worldwide Atmospheric Gravity-wave Study (WAGS) an array of instruments monitored the European ionosphere from high- to mid-latitudes. Analysis of the mid-latitude data reveals an increase of wave activity with magnetic activity for both large and medium scale waves. Equatorward propagation is observed predominantly in association with active auroral conditions.

Using a simple source model, auroral measurements made by EISCAT will be related to mid-latitude data from an HF Doppler network.

*The National Center for Atmospheric Research is sponsored by the National Science Foundation.

G1-2 0920 ATMOSPHERIC GRAVITY WAVE OBSERVATIONS: AURORAL SOURCE REGIONS THROUGH MID-LATITUDES

D. D. Rice
Geophysical Institute
University of Alaska-Fairbanks
Fairbanks, AK 99775-0800
R. D. Hunsucker, Professor of Physics
and Electrical Engineering
Geophysical Institute
University of Alaska-Fairbanks
Fairbanks, AK 99775-0800
L. J. Lanzerotti
AT&T Bell Laboratories
Murray Hill, NJ 07974

During the first campaign of the Worldwide Atmospheric Gravity Wave Study (WAGS) on October 18, 1985, large Joule heating events were observed throughout the northern auroral oval, particularly between 1200-1600 UT. Large-scale traveling ionospheric disturbances (TIDs) were subsequently detected by stations in Sondrestrom Greenland and along the east coast of the United States. Correlation between the quasi-periodic Joule heating event and the gravity wave periods suggests that the waves may represent forced oscillations. Evidence suggests several gravity waves may have been launched from different regions of the auroral oval between 1500-1600 UT, possibly exhibiting the quasi-period of the Joule heating source event.

G1-3 0940 GRAVITY WAVE SPECTRA DURING THE WORLD ACOUSTIC GRAVITY WAVE STUDY (WAGS)

D. R. Sheen and C. H. Liu
Department of Electrical and Computer Engineering
University of Illinois, Urbana-Champaign, IL 61801

The incoherent scatter (ICS) radars were used during the WAGS campaign of October 14-18, 1985 to measure line-of-sight ion velocity and electron density. The background spectra of these two parameters will be examined and compared to a gravity wave model. The analysis is based on Hooke's 1968 results of how a monochromatic neutral atmospheric gravity wave affects ionospheric parameters in the F-region. Hooke's analysis was extended to include a spectrum of waves with a horizontal background wind. A flexible computer model was written. The inputs to this model include the observation geometry and an assumed neutral atmospheric velocity spectrum (e.g., a Garrett-Munk spectrum). The outputs from this model are a theoretical line-of-sight ion velocity spectrum and a theoretical electron density spectrum. It will be shown that the experimentally observed ionospheric data are consistent with the acoustic-gravity wave model. Particular attention will be given to data collected from the Sondrestrom facility in Greenland.

G1-4
1000

GRAVITY-WAVE STUDIES WITH A CLOSE-SPACED NETWORK OF RAPID-RUN IONOSONDES AT CHIBOUGAMAU, QUEBEC ($L \simeq 4.5$)

M. G. Morgan, Radiophysics Laboratory
Thayer School of Engineering
Dartmouth College
Hanover, NH 03755

Using a three-station network of rapid-run ionosondes, mutually about 35 miles apart, daytime TID's and their causative gravity waves have been studied. The station-spacing is but one-third that used in our previous studies in northern New England ($L \simeq 3.3$) and results in proportionately smaller lag times between the stations. Although these lag times must therefore be measured with greater precision, the correlations are much higher which, in turn, means that much shorter correlation time windows may be used. At the suggestion of C. O. Hines, this feature has been used to study local-time dependence of the TID parameters. It is found that the waves regularly travel toward the southeast in the morning and toward the southwest in the afternoon, moving through south in midday. Although it is plausible to account for this behavior in terms of energetic particle precipitation patterns fixed in sun-earth space, it seems more likely that it is a manifestation of thermospheric wind behavior. If so, the prospect of finding the sources becomes elusive. In contradiction of previously reported results, using the wider-spaced network in New England and single stations lying northward, no north-going TID's are seen. No obvious error has been found in the previous analysis and it seems that the contradiction must be ascribed to aliasing due to excessive separation of the single stations from the network.

G1-5
1040 MONITORING F-REGION VARIATIONS WITH A RADIO TELESCOPE

Adolf K. Paul
Naval Ocean Systems Center (Code 544)
Ocean and Atmospheric Sciences Division
San Diego, CA 92152-5000

The Clark-lake radio astronomical antenna array can measure the apparent position of a radio star with very high accuracy (fraction of a degree) and its beam can be switched from one source to another in a very short time (msec). The frequency range of the system extends from the VHF-band down into the HF-band where the apparent position of a source is significantly influenced by even small changes in magnitude and spatial distribution of the electron density in the F-region. It is expected that the combination of those properties will provide the possibility to study the structure and motion of medium scale (in the order of 100-500 km) irregularities in the F-region. Results of model studies in preparation of data recording will be presented.

G1-6 1100 TRAVELLING IONOSPHERIC DISTURBANCES (TIDs) AT MIDLATITUDES: SOLAR CYCLE PHASE DEPENDENCE

Haim Soicher
Center for Communications/Automatic Data Processing
US Army Communications-Electronics Command
Fort Monmouth, NJ 07703

Faraday observations of total electron content (TEC) at Haifa, Israel (32.87° N, 35.09° E), during periods near the maximum and minimum phases of the current solar cycle have yielded information on TIDs in terms of their frequency of occurrence, amplitude, period and time of occurrence.

While at both epochs, the TID structure is seasonally dependent, important differences are evident. For example, during summer, the TIDs at the near minimum phase occur more frequently, are of longer period, and are of lesser magnitude than those during the near maximum phase. During winter, the TIDs at the near minimum phase occur less frequently, are of longer period, and are of lesser magnitude than those during the near maximum phase.

A post sunset secondary peak in the diurnal TEC variation is a common occurrence during the near maximum phase, but it is absent during the near minimum phase. While the post sunset peak is not considered an effect attributed to TIDs but to the "equatorial fountain" phenomenon, it is nevertheless a characteristic which is solar phase dependent.

G1-7 1120 **ON THE OBSERVATIONS OF INFRASONIC WAVES AND ACOUSTIC-GRAVITY WAVES AT GROUND LEVEL**

XIE Jin-Lai, YANG Xun-Ren, TIAN Shi-Xiu
(Institute of Acoustics, Academia Sinica)
and
LI Qi-Tai
(Meterological Science Institute of Guizhou)

Abstract

The investigation on atmospheric infrasonic waves from various sources is significant in many fundamental aspects concerning atmosphere. In this paper, a systematic description of observations at ground level is given, including the detailed discussions about the equipment system, the multi-element detector array, the data analysis and some typical results.

The infrasonic signals we have detected during the period more than twenty years involve both natural and man-made natures, such as those from typhoon, thunderstorm, hailstorm and other severe weathers and also from the eruption of Volcano St. Helens(1980) referred to the former, and those from atmospheric tests of nuclear bombs and also from the tragic explosion of space shuttle "Challenger"(1986) referred to the latter.

Especially, we have joined the WAGS campaign of October 1985, and lots of data have been recorded at our infrasonic observation stations situated in Yongan, Guiyang and Lasa respectively. The analysis to these data shows there are strong AGWs with periods within 5-42 minutes attached to the variations in solar cycle, and the coupling effects between ionosphere and ground layer is obvious.

The advantages of our observation means lie in the simplicity and economy in equipments, the continuity and reliability in records and the easiness in operation and maintenance. Futhermore, the advantages express also in the intuition of results and in the fact that the analogue data can be reserved on paper or magnetic tapes and thus can be real-time processed.

Session G-2 0855-Mon. CR1-42
WAVE PROPAGATION
Chairman: K.C. Yeh, Dept. of Electrical and Computer Engineering, Univ. of Illinois, Urbana, IL 61801

G2-1 0900 IONOSPHERIC IMAGING USING COMPUTERIZED TOMOGRAPHY

J. R. Austen, S. J. Franke and C. H. Liu
Department of Electrical and Computer Engineering
University of Illinois at Urbana-Champaign
Urbana, IL 61801-2991

A two-dimensional image of the electron density in the ionosphere can be produced from TEC data by using Computerized Tomography (CT) techniques. The imaging of large-scale structures such as the ionospheric trough and equatorial bubble should be possible. Different reconstruction algorithms will be compared and the effects of noise on the reconstruction will be discussed. Images produced from simulated TEC data as well as from actual data will be presented.

G2-2
0920

THE CALCULATION OF FOCUSING IN RAY THEORY

L. J. Nickisch
Mission Research Corporation
2300 Garden Rd., Suite 2
Monterey, CA 93940

When a wave front is decomposed into component plane waves in an angular spectral representation, the dominant contributions are seen to come from directions where the phases of nearby components add together constructively, i.e. from angles for which the phase changes only slightly with direction (stationary phase). Hamilton's equations, which are obtained via the principle of stationary phase, provide a means of tracing through space the dominant plane wave components of an incident wave through rather arbitrary three-dimensional ionospheric structure. Focusing effects however, require information about the curvature of the wave front, or alternatively information about neighboring plane wave components. Thus from the point of view of fields, second order phase information must be retained, and this information is lost in the first order stationary phase approximation. From the point of view of rays, more than one ray must be propagated to get focusing information.

A method is presented whereby focusing is computed along a single ray path by retaining second order information. The essence of the method is to calculate the infinitesimal deviation in ray landing point per infinitesimal deviation in ray launch angle, calculated along the undeviated ray. Equations appropriate for this calculation are derived by considering secondary variations of Hamilton's equations. An isotropic, collisionless ionosphere is assumed, and the calculations are performed in spherical coordinates. The generalization to anisotropic ionospheres or other coordinate systems is obvious.

Tests of the method are performed. Analytical tests are possible for the spherically stratified quasi-parabolic layer, and the method is shown to be capable of essentially arbitrary accuracy. Tests for three-dimensional structure are made by comparison to the more conventional finite flux tube approach. The disadvantage of the finite flux tube approach (limits in accuracy and computational precision) and the corresponding advantage of the single ray differential flux tube method is demonstrated.

G2-3 ANALYTIC RAY TRACING USING ERMAKOV INVARIANTS
0940

Stanford P. Yukon
Rome Air Development Center
Electromagnetic Sciences Directorate
Hanscom AFB MA 01731

Analytic raytracing in a physically realistic model ionosphere is developed using the theory of Ermakov invariants. The method starts from the scalar wave equation in the paraxial approximation. By redefining the distance along a great circle path as a time coordinate, the paraxial equation can be cast into the form of the time dependent Schroedinger equation. A class of time dependent potentials for the Schroedinger equation has recently been shown to be exactly soluble by using the techniques of Ermakov invariant theory (J.R. Ray, Phys Rev A, 729, 1982). This result may be used in the ray approximation for the range varying potentials of the ionospheric case. By approximating the variations in the ionospheric potentials such that they belong to this class, analytic ray paths may thus be obtained.

Ionograms and ray traces for various great circle paths obtained using these methods will be shown and compared with results obtained by numerical integration of the Haselgrove Hamiltonian equations.

G2-4
1000 SIMULATION OF THE PROPAGATION OF HF WAVES BELOW AND NEAR THE REFLECTION HEIGHTS IN A TURBULENT IONOSPHERE

J.-F. Wagen and K. C. Yeh
Department of Electrical and Computer Engineering
University of Illinois
Urbana, IL 61801-2991

The propagation of HF wave in a turbulent and stratified ionosphere is simulated by the phase screen diffraction layer method. This scheme is used to compute the received complex amplitude which provides information on the signal scintillation.

The simulation method computes sequentially the effects of phase fluctuations due to the irregularities and of diffraction due to phase mixing. Below the reflection height, this method is equivalent to the split-step method used in ocean acoustics. The mathematical justification can be made naturally under the forward scatter approximation since the complex amplitude satisfies a parabolic equation. The solutions are written in terms of WKB solutions. Near the reflection height the method must be generalized by replacing the WKB solutions by the Airy functions. This generalization is desirable since earlier investigations have demonstrated that the irregularities in this reflecting region are most important in producing effects on the reflected wave. However, in the region of reflection, previous computations accounted for phase changes only, but not diffraction effects. The improved scheme is derived based on the Green's function technique. This generalizes the split-step method at the reflection level and justifies the use of the sequential computations even near the turning point. It also provides a proper expression which takes into account both diffraction and phase change.

The improved simulation scheme will be described and numerical results, including statistics of the received wave will be presented.

G2-5
1040 COMPACT DIRECTIONAL ANTENNAS FOR USE BY SHORTWAVE LISTENERS AGAINST EITHER GROUNDWAVE OR SKYWAVE INTERFERENCE: O.G. Villard, Jr., K.J. Harker, and G.H. Hagn, SRI International, Menlo Park, CA 94025; and M.J. Tia, Office of Engineering and Technical Operations, Voice of America, Washington, DC 20547

In urban environment groundwave radio noise due to gap and corona discharge from power lines, fluorescent lights, automobile ignition systems, etc. is severe. In addition, crowding of the shortwave broadcasting and amateur bands is leading to increased co-channel skywave interference. This paper describes the evolution of several compact portable antenna designs useful against interference propagated by both mechanisms and capable of being operated immediately beside a receiver either indoors or outdoors. Proximity allows listener adjustment of tuning and spatial orientation for best reception. Low-impedance magnetic-field antennas (e.g., loops) proved superior to high-impedance electric-field antennas (e.g., whips) for this application. One design is capable of attenuating groundwave interference more or less irrespective of its direction of arrival, while at the same time accepting skywaves arriving from essentially any direction. Another design gives a deep, steady unidirectional null which is insensitive to the vertical-plane angle of arrival. This design is especially useful at mitigating intereference caused by a multipath skywave signal emanating from a specific location. The philosophy for each design is discussed and examples of measured data are presented to show the amount of interference rejection achieved with prototypes.

G2-6
1100

HF RADAR STUDIES OF THE HIGH LATITUDE IONOSPHERE

R. A. Greenwald, K. B. Baker, J. M. Ruohoniemi, and J.-P. Villain
The Johns Hopkins University
Applied Physics Laboratory
Johns Hopkins Road
Laurel, Maryland 20707

Since October 1983, an electronically-phased HF radar has been operated from the Air Force Geophysics Laboratory High Latitude Ionospheric Observatory in Goose Bay, Labrador. The radar operates in the frequency band from 8-20 MHz and is capable of sensing coherent backscatter from electron density irregularities located in the E- and F-regions of the auroral zone and polar cap ionospheres. The radar scans over a 52° azimuth sector centered approximately on geographic north and typically monitors backscatter from 300 km to more than 2000 km in range. The duration of each scan is normally 80 s. A unique multipulse transmission pattern is used so that full autocorrelation functions of the backscattered signals are obtained without any Doppler or range ambiguities.

To date, the radar has been used for a variety of studies. Observations made in conjuncton with the Sondre Stromfjord incoherent scatter radar have clearly demonstrated that at least some types of F-region irregularities move at the plasma drift velocity. Two-dimensional convection patterns have been obtained by combining data from the Goose Bay and Sondre Stromfjord radars. Similar studies are possible with the SHERPA HF radar that has recently begun operation from Schefferville, Quebec. The Goose Bay radar has been used to detect oscillatory ionospheric motions in the vicinity of the polar cusp that may be related with magnetospheric boundary layer phenomena and it has provided evidence of a new type of E-region instability process. In the future, the Goose Bay radar will be used with the French SHERPA radar for a variety of two-dimensional convection studies. It will also be used for coordinated measurements with an identical HF radar at the near-conjugate location of Halley Bay, Antarctica. This program, known as PACE, will commence in January 1988.

G2-7 1120 ON THE USE OF MAXIMUM ENTROPY SPECTRUM ESTIMATION IN IONOSPHERIC PROBLEMS: Paul F. FOUGERE, AFGL/LIS, HANSCOM AFB, MA 01731

The Burg Maximum Entropy Method (MEM) will be presented and briefly described. A series of computer simulations which compare Burg-MEM to periodogram will be reviewed. The simulations show that careful windowing and/or end matching are required for periodograms. Even then, periodograms are much noisier than MEM spectra and if periodograms are stacked and averaged to reduce the spectral variance, time resolution is lost. In contrast the MEM spectrum is always smooth and requires only a short segment of time series data. Thus MEM is an ideal method for analyzing data sets whose properties change slowly with time in such a way that short segments are approximately stationary (in the weak sense).

MEM will be applied to a number of real ionospheric data sets, including scintillation measured at ground stations on signals launched from satellites (e.g., MARISAT and HILAT), in-situ ion density and velocity data from the atmospheric explorer (AE) satellite, PIIE rocket campaign data, and neutral air density data measured on a polar orbiting satellite.

We hope to prove convincingly that Burg-MEM is a reliable tool that belongs in every ionospheric experimentalist's tool-kit--and we will even provide a complete Fortran package to assist all those who want to try it.

G2-8
1140

SCINTILLATION PROBLEMS OF HF/VHF DIRECT SATELLITE BROADCASTING

Jules Aarons
Dept. of Astronomy
Boston University
Boston, MA 02215

Charles Rush
NTIA
Dept. of Commerce
Boulder, CO 80303

Direct Satellite Broadcasting at the upper end of the HF Band is a means of communicating information with modest equipment at the reception end. It is possible for certain areas and times of reception to have relatively low power satellite transmissions reach large numbers of listeners with audio modulation. However the requirements for a system are limited by the ionospheric propagation problems. One of these is the fading produced by scintillation. Irregularities in the ionosphere both at high latitudes and in the equatorial region put restrictions on comprehension of voice because of the effect of fading on the HF/VHF signals. The strongest effects are from irregularities at night in the equatorial region (plus or minus 20 degrees of the magnetic equator) or at any time from irregularities at auroral oval latitudes during magnetic storms. During many hours fading is noted at polar latitudes particularly during periods of high sunspot number.

The assessment of the scintillation problem involved statistics and observations first made with transmissions from Sputnik 3 then with the BEB and BEC satellites of the S66 set, and finally with 40 MHz observations from ATS-6. The available data will be shown. The results indicate sectors where fading will be severe at certain times of day and under certain geomagnetic conditions. Auroral and polar latitudes will show effects as a function of sunspot number and geomagnetic conditions. The equatorial region will show fading levels which are a function of longitude, geomagnetic conditions and solar flux.

As in any system development the limitations must be taken into consideration but the possibility of broadcasting at HF/VHF frequencies from the viewpoint of scintillations exists. An area to be explored is the deterioration of speech as function of fading rate and fading depth.

Session H-1 0855-Mon. CR1-40
PLASMA CHAMBER SIMULATION OF SPACE PHENOMENA
Chairman: R. Stenzel, Dept. of Physics, Univ. of California, Los Angeles, CA 90024

H1-1 0900 LABORATORY STUDIES OF BASIC PLASMA PHYSICS RELATED TO SPACE EXPERIMENTS

A. Y. Wong, P. Y. Cheung, T. Tanikawa, A. Kuthi, L. Schmitz, D. Chelf, K. Lam
University of California, Los Angeles
Department of Physics
405 Hilgard Avenue
Los Angeles, CA 90024

A series of experiments in large chambers are described which study the electron beam and RF interactions with plasmas. In the electron beam case we have studied the generation of strong turbulence and its relation to the perturbation on zeroth order conditions and EM radiation. Relation to the auroral ionosphere will be made.

In RF experiments we have studied the profile modification, the emission of multiples of half harmonics, the production of double layer and the overshoot phenomena when plasmas with nonuniform density profiles are subject to strong EM radiation. The laboratory results have predicted a number of findings in active ionospheric modification experiments such as the generation of cavities at the critical layer, the excitation of low frequency waves and wave trapping inside such cavities. Our magnetized plasmas with very high mirror ratios have been used to interpret results of auroral plasmas in both MHD and kinetic regimes. The scaling of endloss processes with mirror ratios have been completed in both collisional and collisionless regimes and relate to plasma confinements in the ionosphere.
Research supported by NSF PHY85-02490 and ONR N00014-78-C-0754.

H1-2 0920 THE PLASMA DYNAMICS OF HYPERSONIC BODIES IN SPACE: APPLICATIONS OF LABORATORY SIMULATIONS EXPERIMENTS

N. H. Stone
Space Science Laboratory
NASA Marshall Space Flight Center
Huntsville, AL 35812

Attempts to gain an understanding of spacecraft plasma dynamics via experimental investigation of the interaction between artificailly synthesized, collisionless, flowing plasmas and laboratory test bodies date back to the early 1960's. In the past 25 years, a number of researchers have succeeded in simulating certain limited aspects of the complex spacecraft-space plasma interaction reasonably well. Theoretical treatments have also provided limited models of the phenomena. However, the available insitu data was framentary, incomplete, and unable to provide a good test of the results from the ground-based experiments and theory. Several active experiments were recently conducted from the space shuttle that specifically attempted to observe the Orbiter-ionospheric interaction. These experiments have contributed greatly to an appreciation for the complexity of spacecraft-space plasma interactions but, so far, have answered few questions. Therefore, even though the plasma dynamics of hypersonic spacecraft is fundamental to space technology, it remains largely an open issue. A brief overview will be given of the primary results from previous ground-based experimental investigations and the preliminary results of investigations conducted on the STS-3 and Spacelab 2 Space Shuttle missions. The laboratory results discussed will include recent "process simulation" experiments that look promising in their potential application to the space shuttle-ionospheric interaction and certain solar system plasma phenomena.

H1-3
1000

TEMPORAL DYNAMICS OF PLASMA WAKES

Chung Chan
Dept. of Electrical and Computer Engineering
and Center for Electromagnetics Research
Northeastern University
Boston, MA 02115

The formation of plasma wakes has been an important issue in many aspects of space research. The most common examples are the interactions of planetary bodies with the solar wind, aerodynamics of spacecrafts in the ionosphere, and the structuring of the comet tails. We have performed a series of laboratory experiments to investigate the temporal dynamics of the near wake of a conducting body. By immersing the body in a pulsed plasma stream, we were able to observe the wake evolution process in time and study a number of interesting phenomena which are associated with the wake formation. These phenomena include the charging of the body, the focusing of plasma particles in the near wake, wave activities in the plasma-wake boundary, and the filling-in of the wake.

We will review these laboratory results and attempt to provide a possible explanation for a controversial issue in plasma wake research, namely, the existence of an electron temperature enhancement region in the near wake of an electrically floating body.

H1-4
1020

SELF-SIMILAR POTENTIAL IN THE NEAR WAKE

D. Diebold, N. Hershkowitz, T. Intrator, and A. Bailey
Nuclear Engineering Department
University of Wisconsin
Madison, WI 53706

We present plasma potential measurements of the near wake of a planar obstacle in a plasma flow in DOLI, a triple plasma device. Both fluid theory and data show that under certain conditions the near wake is non-neutral and its potential is self-similar. Strong electric fields are found near the obstacle and equipotential contours are found to conform to all boundaries. The theory shows that plasma density is not self-similar. Argon gas was used at a pressure of 5×10^{-5} torr to produce a plasma flow of density $\sim 10^{5} - 10^{7}$ cm^{-3} in a chamber 0.5 m in length and 0.25 m in radius. Ion beam energy was 30 eV to 150 eV. The inflection point of an emissive probe in the limit of zero emission was used to measure potential.

*This work was supported by NASA Grant NAGW-275.

H1-5
1040

EXPANSION OF A COLLISIONLESS, MAGNETIZED, NON-MAXWELLIAN PLASMA INTO VACUUM*

G. Hairapetian and R. L. Stenzel
University of California, Los Angeles
Department of Physics
Los Angeles, CA 90024

The expansion of plasma into free space leads to an acceleration of ions which can be an important process in space plasma physics (wakes, artificial comets, ion acceleration in the magnetosphere and ionosphere). We have investigated the physics of the expansion process in a controlled laboratory experiment and shown the importance of an energetic tail in the expansion process. Using a pulsed ($t_{on} \simeq 2$ ms, $t_{rep} \simeq 3$s) neutral gas/plasma source, we allow a discharge plasma ($n \simeq 10^9$ cm^{-3}, $kT_e \simeq 3$ eV, $E_{tail} = 80$ eV) to expand into an evacuated chamber (working pressure 7×10^{-6} Torr). Atomic collisions are negligible in the expansion process. The ion front expands supersonically ($v_{flow} > 10^6$ cm/s) along an axial B-field (10-40G). Plasma potential measurements indicate a propagating potential gradient of up to the discharge voltage (≤ 80 V). Since the thermal electrons ($kT_e \simeq 3$ eV) cannot penetrate the potential gradient, the primary electrons ($E \simeq 80$ eV) drive the expansion. At the expansion front, the ions have a beam-like distribution function. While the beam temperature decreases from 3 eV near the source ($z \leq 5$ cm) to 0.7 eV further away ($z \geq 70$ cm), the streaming velocity increases up to 130 eV. During early expansion ($t \leq 70$ μs), the ions at the front have a pencil-shaped angular current profile of half-width $\sigma \simeq 4^\circ - 10^\circ$, which broadens ($\sigma_{max} \simeq 40^\circ$) at later times ($t \geq 1000$ μs). In contrast, the initial electron current profile is broad ($\sigma \simeq 70^\circ - 80^\circ$) and remains relatively unchanged over time. In summary, the plasma expansion which leads to production of energetic ions, is controlled by the energy of the fastest electrons and the inertia of the massive ions.

*Work supported by NSF grants ATM 84-01322 and PHY 84-10495.

H1-6 1100 **ELECTROSTATIC DETECTORS IN SPACE CHARGE DOMINATED PLASMAS***

T. Intrator, M.H.Cho, E.Y. Wang, N. Hershkowitz, D. Diebold, and J. De Kock
Department of Nuclear Engineering
University of Wisconsin
Madison, WI 53706

In space, electrostatic satellite detectors are used to measure wave electric fields. For altitudes greater than one earth radius, solar wind photons can generate considerable photo electron emission from the spacecraft surface. These antennae operate as (photo)emitting probes in a non neutral sheath plasma that can be space charge dominated.

We present two dimensional laboratory measurements of the local plasma potential near a hot cathode subject to space charge limited emission. This is intended to resemble a satellite in the solar wind emitting copious photoelectrons. The current bias technique (R. Grard, K. Knott, R. Pedersen, Space Sci. Rev. 34, 289, 1983) is compared with the inflection point method (J.R. Smith, N. Hershkowitz, P. Coakley, Rev. Sci. Instrum. 50, 210, 1979) for different conditions of surplus local electron density. Time response as well as absolute potential measurements will be evaluated.

At the boundary between a plasma and a charged particle source, or even far away in the bulk plasma itself space charge effects can determine or dominate the balance of potential, particle density and current flow. Data will be shown that demonstrates these effects for distances greater than 75 Debye lengths from the hot cathode as well as double layer formation.

*This work supported by NASA Grant # NAGW275.

H1-7
1120

ON NONLINEAR CURRENTS IN MAGNETOPLASMAS; WILL THE TETHERED SATELLITE SYSTEM WORK?*

J. M. Urrutia and R. L. Stenzel
University of California, Los Angeles
Department of Physics
Los Angeles, CA 90024

In collisionless magnetoplasmas, electron currents produced by electron beams or positively biased electrodes are generally thought to flow along the magnetic field, $\underline{B}_o$, and their magnitude to be limited by the electron saturation current, $I_{e,sat}$. These assumptions from linear theories are made when predicting the behavior of currents produced by the proposed Tethered Satellite System (NASA A.O. No. OSSA-1-84). Recent laboratory studies [J. M. Urrutia and R. L. Stenzel, Phys. Rev. Lett., 57, 715 (1986); R. L. Stenzel and J. M. Urrutia, Geophys. Res. Lett., 13, 797 (1986)] have shown the dominant role of nonlinear effects in determining a current system which is driven by a voltage $\phi >> kT_e$. In these experiments, a field-aligned electron beam and a return electrode, located on separate flux tubes, are immersed in a large, afterglow plasma. It is found that large currents ($> 10 \times I_{e,sat}$) can be obtained for short periods of time ($\Delta t \sim 2$ μsec) independent of the electrode orientation with respect to $\underline{B}$. Detailed diagnostics reveal that such currents are made possible by anomalous cross-field transport due to self-consistently produced ion-acoustic instabilities. In the vicinity of the return electrode, current-driven turbulence ($v_d \gtrsim v_e >> c_s$) increases the plasma resistivity, builds up anomalous electric fields ($E = \eta^* j > 4$ V/cm), which expel ions, lead to a density depletion ($n_e \simeq n_i \to 0$) and disrupt the current. Thereafter, ions return and the process repeats like a relaxation oscillation but at low average currents ($I < I_{e,sat}$). Thus, nonlinear effects prevent the formation of a large amplitude current system on MHD scales as extrapolated from linear theories.

*Work supported by NSF grants ATM 84-01322 and PHY 84-10495.

H1-8
1140

LABORATORY OBSERVATION OF ION CONICS

R. McWilliams and R. Koslover
Department of Physics
University of California
Irvine, CA 92717

Ion conics are observed in the Earth's lower magnetosphere through the use of ion energy analyzers on satellites (R.D. Sharp, R.G. Johnson, and E.G. Shelley, J. Geophys. Res., 82, 3324, 1977). These conical distributions in velocity space are seen in conjunction with double layers, electrostatic ion cyclotron waves, and lower hybrid waves. One suggested mechanism (T. Chang, and B. Coppi, Geophys. Rev. Lett., 8, 1253, 1981) of ion conic formation is perpendicular (to the geomagnetic field) ion heating due to waves, followed by $\mu\nabla B$ forces folding the distribution into a conic. Laboratory experiments at U.C. Irvine are simulating the magnetosphere to examine the processes which may be responsible for satellite data. We report observations of drifting undisturbed maxwellian velocity distributions and ion conic production in the presence of radio frequency waves. Specifically, we measured ion distributions in the presence of electrostatic ion cylcotron waves, and also lower hybrid waves. These measurements were made using a new technique of optical tomography in velocity space, which relies on laser induced fluorescence (R.A. Stern and J.A. Johnson, Phys. Rev. Lett., 34, 1584, 1978; D.N. Hill, S. Fornaca, and M.G. Wickham, Rev. Sci. Instrum., 54, 309, 1983). Optical tomography differs from physical-space tomography due to subtleties associated with velocity space projections, along with Zeeman splitting of the electronic transitions involved.

The magnetospheric simulation experiments reported here were performed in a single-ended Q-machine which provided a low density ($n \sim 10^{10}$ cm^{-3}) low temperature ($T_i \cong T_e \cong 0.2$ eV), nearly completely ionized barium plasma 1.0 m long and 5 cm in diameter. The confining magnetic field was 6 kG.

In summary, a direct, non-perturbing optical tomography diagnostic has been developed which measures multidimensional ion velocity space distribution functions. In laboratory simulations of the Earth's magnetosphere, large amplitude waves can modify a drifting maxwellian plasma to form ion conic distributions similar to those observed by satellite measurements.

This work supported by National Science Foundation Grant No. ATM-8411189.

H1-9 1200 THREE-DIMENSIONAL TEARING INSTABILITIES OF ELECTRON CURRENT SHEETS*

H. Pfister, W. Gekelman and R. L. Stenzel
University of California, Los Angeles
Department of Physics
Los Angeles, CA 90024

Reconnection of magnetic fields have been studied at UCLA in a laboratory experiment [R. L. Stenzel, W. Gekelman and J. M. Urrutia, UCLA PPG 995 (1986) (see Adv. Space Res., 1987)] which models the basic two-dimensional neutral sheet geometry. In contrast to magnetotail models, the current sheet is thin compared with an ion Larmor radius; there is a magnetic field component $|B_y| \simeq |\vec{B}_x + \vec{B}_z|$; the reconnection electric field E_y is localized self-consistently at a boundary layer; the current is carried by electrons whose distribution consists of a Maxwellian and high-energy tail. In the present experiment the width of the current sheet is further narrowed by limiting the electron flow with a plane slotted grid ($\Delta x \simeq 70$ cm, $\Delta z \simeq 1$ cm $\simeq c/\omega_{pe}$, y = const.) rapidly pulsed to a large negative potential ($-V_g \simeq 200$ V $>> kT_e/e$, $t_{rise} \simeq 3$ μsec $<< f_{ci}^{-1}$). Given these initial and boundary conditions the temporal and 3D spatial evolution of the magnetic field configuration $\vec{B}_{(x,y,z,t)}$ is measured with magnetic probes from repeated events. The digitized data sets of 1024 time increments at each of 5000 spatial positions are processed by a state-of-the-art computer system [W. Gekelman and L. Xu, Rev. Sci. Instrum. 57, 1851 (1986)]. The observations show that the constriction of the current sheet propagates in the y-direction at the speed of whistlers rather than Alfvén waves. Subsequently, the magnetic field develops multiple X and O points in the x-z plane with growth times approximately given by the collisionless electron tearing mode. The magnetic islands also exhibit periodic structures in the y-direction. Coalescense of islands in three dimensions and time will be shown.

*Work supported by NSF grants ATM 84-01322 and PHY 84-10495.

Session J-1 0855-Mon. CR2-6
NEW TECHNIQUES IN RADIO ASTRONOMY
Chairman: Wm. J. Welch, Radio Astronomy Lab,
Univ. of California, Berkeley, CA 94720

J1-1 0900 PLANS FOR THE LARGE DEPLOYABLE REFLECTOR (LDR)

Paul N. Swanson, 168-327
Jet Propulsion Laboratory
California Institute of Technology
Pasadena, CA 91109

The Large Deployable Reflector (LDR) is to be a dedicated astronomical observatory placed in orbit by NASA in the 1990's. It will operate in the 30-1000 micron region of the spectrum that is obscured by the Earth's atmosphere. LDR will complement other orbiting observatories such as the Hubble Space Telescope and SIRTF by providing sub-arc second resolution and extreme sensitivity in the far infrared and submillimeter region.

The LDR Science Coordinating Group has defined the science requirements for LDR in a report to be published in 1986. These requirements have led to a conceptual design of a 20-m circular aperture telescope made up of a mosaic of 2-m ultralightweight hexagonal panels. Active figure control is accomplished by a two-stage optical system with an active quaternary mirror of the exit pupil of the primary reflector.

The 30-1000 micron spectral range can be covered by eight instruments with an initial complement of four instruments and the capability for orbital replacement of instruments.

Technical challenges for LDR include thermally stable composite reflector panels, submillimeter coherent receivers, long lifetime space cryogenics systems, precision control systems and space assembly and testing.

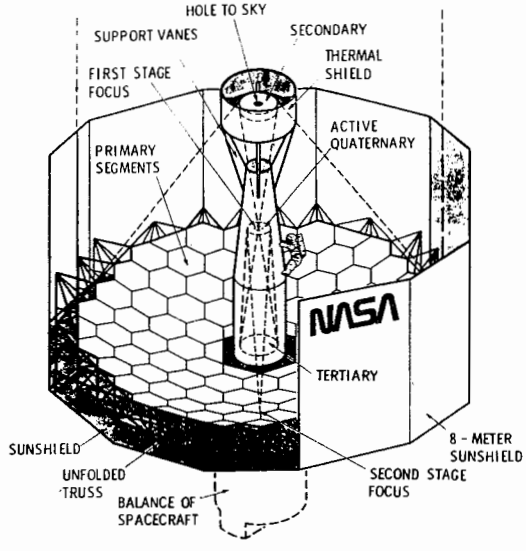

J1-2 LUNAR RADAR POLARIMETRY
0920 T.W. Thompson, H.A. Zebker, J.J. Van Zyl (NASA/JPL)

Two of us (HAZ and JJV) have developed polarimetry techniques for the NASA/JPL Airborne Imaging Radar whereby the amplitude and phase of all elements of a radar scattering matrix can be synthesized from simultaneous recording of vertically and horizontally polarized reflections from terrestrial targets. An adaptation of these techniques have been applied to the simultaneous recording left and right circularly polarized radar reflections from the moon obtained with the 430 MHz (70-cm wavelength) radar at the Arecibo Observatory, Puerto Rico. Although the original data recording of the lunar echoes at Arecibo in 1981 through 1984 were not intended for these techniques, the phase difference between the two circular polarizations remains constant for at least fifteen minutes and all elements of the scattering matrix for the lunar surface can be generated.

We obtained the polarization signatures of mare, terra and the young, radar bright crater Tycho. The lunar terra are unpolarized consistent with a large amount of volume scattering in the lunar subsurface. The radar scatter from the large young crater Tycho is consistent with a Bragg scattering model like rough terrestrial lavas in the Snake River Plain, Idaho. Mare and terra have different polarization signatures suggesting that the maria have less subsurface volume scattering and more surface scattering from wavelength sized rocks. Thus, the first adaptation of these radar polarization techniques to a solar system object have been successful.

Session J-2 0955-Mon. CR2-6
MILLISECOND PULSAR WORKSHOP I
Chairman: David W. Allan, Time and Frequency Division, National Bureau of Standards, Boulder, CO 80303

J2-1 1000 MILLISECOND PULSAR TIMING RESULTS

Lloyd A. Rawley and Joseph H. Taylor
Princeton University
Michael M. Davis
Arecibo Observatory

A study of the pulse arrival times of PSR 1937+21 between 1982 and 1984 showed that this "millisecond pulsar" is an extremely stable rotator (M.M. Davis *et al.*, Nature 315, 547-550, 1985). Two more years of data taken with an improved measurement system show no evidence of timing noise intrinsic to the pulsar. Apparently the main cause of arrival time fluctuations prior to October 1984 was the variable propagation delay of LORAN signals used to calibrate the Arecibo Observatory's clocks. A GPS satellite link has removed this source of error.

Arrival times obtained at each of two radio frequencies (1408 and 2380 MHz) fit a simple model with root-mean-square errors of 300 nanoseconds. The values of the model parameters differ for the data sets at different frequencies. This discrepancy can be explained if the integrated electron density along the line of sight to the pulsar fluctuates by 10 parts per million on time scales of about 1 year. The noise spectrum of the timing residuals has a $1/f$ character.

If other stable pulsars could be timed with submicrosecond precision, one could form a time standard which would rival UTC in stability. Among known pulsars, only the recently discovered PSR 1855+09 (D.J. Segelstein *et al.*, Nature 322, 714-717, 1986) could potentially serve as a clock comparable to PSR 1937+21. The latest timing results on these pulsars will be presented.

J2-2 1020 TIMING AND SCINTILLATIONS OF THE MILLISECOND PULSAR 1937+214: J.M. Cordes, A. Wolszczan, R.J. Dewey, and M. Blaskiewicz, Astronomy Dept. and National Astronomy and Ionosphere Center, Cornell Univ., Ithaca, NY 14853; and D.R. Stinebring, Dept. of Physics, Princeton Univ., Princeton, NJ 08544

We present results from a multifrequency timing and scintillation program at the Arecibo Observatory whose aim was to monitor the time dependence of interstellar scattering and measure the frequency dependence of pulse phase. The timing program extended from April 1982 through December 1985. Data at 0.43,0.61, and 1.4 Ghz were digitally filtered to remove distortion from cold plasma dispersion, then folded to yield pulse wave forms averaged over 32 sec. The data were also Fourier analyzed to yield dynamic spectra with the same averaging time. At each epoch, the pulse arrival times were determined at each available frequency and scintillation parameters were determined at 0.43 GHz. We show how arrival time estimates are degraded by scattering induced frequency structure in the receiver bandpass. We also estimate the characteristic amplitudes and time scales of angle of arrival, time of arrival, and dispersion measure variations. The implied constraints on the electron density wavenumber spectrum along the line of sight to PSR 1937+214 are also given.

J2-3 1040 SOME TIME DOMAIN ANALYSIS OF THE RESIDUALS OF PSR 1937+214: David Allan

The measurement time residuals have been significantly reduced between the millisecond pulsar PSR 1937+214 and the reference atomic time scale UTC(NBS). The most recent 658 day period analyzed indicated a fractional frequency stabilities of parts in 10^{-15} . Three significant things have occurred since the first two years of analysis to give this significantly improved stability. First, an upgraded data acquisition system was installed at Arecibo Observatory, substantially reducing several kinds of systematic measurement errors. Second, the Loran C link to the AO clock was replaced by a GPS common-view link, which effectively removed the link noise from consideration. And third, the measurements were made in two widely separated frequency bands in order to determine whether the total electron content along the 15,000 light year path from the pulsar to the earth varies. The interstellar total electron content was found to random-walk by up to 12 ppm over the 658 days. The primary analysis of the above has been reported by Dr. Rawley. This paper reports in a support role on some statistical implications regarding time series analysis of the pulsar's residuals. Some remarkable improvements are noted.

J2-4
1100 THE ALLAN VARIANCE AND SPECTRAL DENSITY FUNCTION ESTIMATION: D.B. Percival, HN-10, Applied Physics Lab, Dept. of Statistics, Univ. of Washington, Seattle, WA 98105

In the 20 years since Allan's 1966 landmark paper, the Allan variance has become the primary time domain tool for evaluating the statistical properties of the time and frequency generated by atomic clocks. This talk focuses on some statistical questions concerning the use of the Allan variance as a spectral density function (sdf) technique. We discuss some techniques for computing the correlation between estimators of the Allan variance for different sampling times and describe how this correlation affects the estimation of the sdf. We compare the sampling properties of sdf estimators based upon the Allan variance to those of the direct frequency domain techniques that are used in many branches of the engineering and physical sciences. Finally, we give some perspectives on the applicability of the Allan variance for general use in exploratory data analysis and in determining models of physical processes.

J2-5
1120 INTERSTELLAR PROPAGATION EFFECTS AND THE PRECISION OF PULSAR TIMING: J.M. Cordes, Astronomy Dept., Cornell Univ., Ithaca, NY 14853; and D.C. Backer, Astronomy Dept., Univ. of California, Berkeley, CA 94720

Dispersion and scattering of pulsar signals in the interstellar medium cause a number of effects that limit the precision of pulse time of arrival (TOA) measurements. We discuss

1) dispersion measure variations;
2) angle of arrival (AOA) variations;
3) errors in estimating (solar system) barycentric arrival times caused by AOA variations;
4) refraction-induced variability of the diffraction smearing time.

We also consider

5) the effects of pulse to pulse phase jitter; and
6) time variable polarization and the use of imperfect feed antennas.

The first four kinds of error are estimated assuming that a Kolmogorov wavenumber spectrum describes electron density variations in the interstellar medium. We emphasize, however, that TOA variations are associated with low wavenumber components of the spectrum that are, to date, poorly probed and may depart from a Kolmogorov spectrum. Consequently, TOA studies of millisecond pulsars are likely to reveal considerable information about fine scale turbulence in the interstellar medium as well as about the proper motion, parallax, and pulse phase stability of the pulsars. Results from numberical simulations will be presented to show the conditions under which the highest precision measurements may be obtained.

J2-6
1140 SOLAR-SYSTEM-PARAMETER-ADJUSTMENT FILTER FOR PULSAR TIMING ANALYSIS: Ronald W. Hellings, Jet Propulsion Lab, Pasadena, CA

Results are presented from a Monte Carlo determination of the transfer function of the solar-system-parameter-adjustment filter applied to the millisecond pulsar data. Random data were simulated at a frequency of one point per week for the period 1980-2000. These data were then passed through the parameter adjustment software. and the spectra of the pre-fit and post-fit residuals were compared to find the fraction of power which was subtracted out as a result of the parameter adjustment. The final transfer functions represent a stable mean of several such runs of sinmulated data. Because the solar system parameters are constrained by the existence of other non-pulsar astrometric and radiometric data, the transfer functions are not independent of the assumed size of the pre-fit data.

Monday Afternoon, 12 Jan., 1355-1700

Session B-4 1355-Mon. CR2-28
ANTENNAS II
Chairman: H. Steyskal, Electromagnetic Science Directorate, Rome Air Development Center, Hanscom AFB, MA 01731

B4-1
1400 **CLOSED-FORM EXPRESSIONS FOR STATIC COUPLING BETWEEN TWO COPLANAR POLYGONS**

David C. Chang and Bradley L. Brim
Department of Electrical and Computer Engineering
University of Colorado
Boulder, CO 80309

Numerical solutions to many electromagnetic boundary-value problems using integral-equation formulation often involve four-dimension coupling integrals such as those found in moment methods. Even with the use of the simplest basis and weighting functions, these integrals often are not expressible in closed-form and they have to be computed numerically. Efficient computational schemes can be developed only if the dominant contribution to these integrals can be subtracted out and evaluated analytically in closed-form.

In this paper we present a method by which exact closed-form expressions for static (R^{-1}) coupling between two arbitrary coplanar polygons may be derived. We assume constant distributions within each polygon and zero elsewhere (i.e., subsectional pulse expansions and weights). The method involves performing the four- dimensional spatial integration analytically by going to the Fourier transform domain, thereby reducing them to two-dimensional spectral integrations. The spectral integrals are then converted to an integral of a group of sums, which, after some algebraic manipulations, give rise to a closed-form expression consisting of a group of terms involving logarithmic and other known functions of distances corresponding to the separations between any given pair of vertices in the two polygons.

Examples will be presented of rectangle-rectangle and triangle-triangle static coupling. It will be shown that these results hold equally well for both mutual and self coupling. The application of this method to both static and dynamic problems will briefly be discussed.

B4-2
1420 ANTENNA DIAGNOSIS USING SPHERICAL NEAR-FIELD MEASUREMENT AND MICROWAVE HOLOGRAPHIC RECONSTRUCTION: Y. Rahmat-Samii, Jet Propulsion Lab, California Institute of Technology, Pasadena, CA 91109; and J. Hau Lemanczyk, Electromagnetics Institute, Technical Univ. of Denmark, DK-2800, Lyngby, Denmark

The application of surface diagnostic techniques for reflector and array antenna evaluations is receiving considerable attention. The main objective is to determine the surface profile distortion of reflectors or to locate defective array elemens. Among the many different techniques, microwave holography has been successfully applied in recent years (e.g., Y. Rahmat-Samii, Radio Science, 19, 1205-1217, 1984). In this technique, the far-field amplitude and phase are measured and then the Fourier transform relationship which exists between the far-field pattern and a function related to the induced current is exploited to localize the distortion with the aid of an FFT algorithm. Up to now the technique has been applied to far-field data either directly measured in the far field or constructed from planar near-field measurement techniques.

In this presentation, for the first time, the results of an investigation demonstrating how the holographic technique can be applied to the data generated by the spherical near-field measurement technique are reported. This application would also allow an in-depth evaluation of the accuracy of the holographic technique because the spherical near-field measurement provides a very accurate result for the entire angular range.

Under controlled conditions, two spherical near-field measurements have been performed at the Technical University of Denmark on a 175 cm parabolic reflector at 11.3 GHz. In the first measurement, the antenna was measured in its existing condition while in the second measurement, several bumps of different sizes and heights were attached to the reflector surface. In addition, the amplitude and phase patterns of the feed was measured on the spherical near-field range. This measurement is needed in order to compensate for the surface error reconstruction which is due to the non-spherical phase pattern of the feed. These measured data have been used to carry out detailed investigation into the number of needed sample points, angular range selection, accuracy of the reconstruction process, etc. The availability of the far field patterns in both amplitude and phase allowed for the subtraction of the two measurements to purify the reconstruction of the attached surface bumps. Results clearly demonstrate that the simulated bumps can be re-

covered with a good degree of accuracy, however, care must be exercised in the proper interpretation of the reconstructed distortions that could be due to the diffraction effects from the struts, blockages, etc.

B4-3
1440

RADOME ANALYSIS USING BACKPROPAGATED NEAR-FIELD DATA

R. F. Schindel and A. J. Blanchard
Wave Scattering Research Center
Department of Electrical Engineering
University of Texas at Arlington
P.O. Box 19016
Arlington, Texas 76019

The electrical design of an airborne radome is a difficult process. The design is usually constrained by the mechanical and aerodynamic criteria. In most cases only a first pass electrical design, utilizing ray-tracing and flat plate approximations (D. G. Burks, Final Technical Report, Contract DAAk40-77-C-0022, U.S. Army Missile Command Redstone Arsenal, Alabama) is considered prior to building the prototype. The radome is compensated for aberrations in the transmitted field after the prototype has been constructed. The compensation generally takes the form of modifications to the electrical thickness of the radome wall. Compensation of this type is used to change the phase characteristics of the transmission coefficients. Most of the boresight error can be attributed to insertion phase delay differences over the radome surface for the different polarizations. If the transmission phase delay can be equalized for both principle polarizations over the entire radome surface, then the boresight error can be reduced significantly. (Fred German, private communication). The problem is knowing where on the radome surface compensation is needed. The technique presented in this paper utilizes plane-wave spectrum analysis and aperture integration to map the insertion phase delay over the radome surface. With this knowledge, the designer can determine the regions of the radome surface which must be modified in order to equalize the transmitted phase and reduce boresight error.

The technique of mapping the phase delay characteristics of the radome along the radome surface (R.F. Schindel, Masters Thesis, University of Texas at Arlington) is analogous to tomographic techniques used in medical diagnostics imaging (A. J. Devaney IEEE 1980 Ultrasonics Symposium, 979-983). Measurements of the field transmitted by the radome are taken in a plane in the near-field of the radome. These measured fields are decomposed into their angular spectrum of plane waves (Goodman, Introduction to Fourier Optics, 49-54, 1968). The spectrum is backpropagated to the antenna aperture inside the radome, and transformed into equivalent tangential sources (C. A. Balanis, Antenna Theory Analysis and Design, 447-454, 1982). Aperture integration is then used to project the resulting aperture distribution onto the outer radome surface. The transmission characteristics are obtained by subtracting a background measurement without the presence of the radome from the measurements which include the radome effects. This type of analysis allows two methods of compensation. The first is described above and consists of modifying the radome surface to equalize the transmission characteristics (G. Tricoles and E. L. Rope, General Dynamics Report No. R-7-038-7, April 1969). The second method of compensation is yet untried, and utilyzes the knowledge of the equivalent sources representing the radome effects on the antenna aperture. Since these equivalent sources are known, compensation for the radome effects on the aperture can be accomplished by subtracting these equivalent currents from the original aperture currents.

B4-4
1500

ON THE THEORY OF THE SYNTHESIS OF SINGLE AND DUAL OFFSET SHAPED REFLECTOR ANTENNAS

Victor Galindo-Israel, Fellow IEEE; William Imbriale, Member IEEE; Raj Mittra, Fellow IEEE
V. Galindo-Israel and W. Imbriale are with the Jet Propulsion Laboratory, California Institute of Technology, Pasadena, CA 91103.
R. Mittra is with the Department of Electrical Engineering, University of Illinois, Urbana, IL 61801, and Consultant to JPL.

Since Kinber (Radio Technika and Engineering - 1963) and Galindo (Antennas and Propagation - 1963/64) developed the solution to the circular symmetric dual-shaped synthesis problem, the question of existence (and of uniqueness) for offset dual (or single) shaped synthesis has been a point of controversy. Many researchers thought that the exact offset solutions may not exist. Later, Galindo-Israel and Mittra (AP-1979) formulated the problem exactly and obtained excellent and numerically efficient but approximate solutions.

Based on a technique first developed by Schruben (Journal of the Optic Society - 1973), Brickell and Westcott (IEE Proc - 1981) developed a Monge-Ampere (MA) second order non-linear partial differential equation for the problem. They solved this elliptic equation by a technique introduced by Rall (1979) which iterates, by a Newton method, a finite difference linearized MA equation. The elliptic character requires a set of simultaneous finite difference equations to be developed and solved iteratively. Existence still remained in question.

Although the second order MA equation is elliptic, the first order equations from which the MA equation is derived can be integrated progressively as for an initial condition problem - a more rapid and non-iterative type solution. In addition to demonstrating in a general format that the MA equation can be derived for both the single and dual reflector synthesis, we have further solved, numerically, the first order equations. Exact solutions are thus obtained by progressive integration. Furthermore, we have demonstrated that an infinite set of such solutions exist. These conclusions are inferred, in part, from numerical results.

The practical consequences are significant for current contour beam synthesis problems with regard to the single reflector synthesis. Spacecraft low cross-pol and high gain requirements which frequently prefer an offset geometry will substantially benefit from this new exact synthesis method. Other ground system applications include shaped beam waveguides. The speed of the earlier approximate method (Galindo-Israel and Mittra - 1979) coupled with this new exact method will make powerful complementary design tools.

B4-5
1520

ACCURATE ANALYSIS OF METAL-STRIP-LOADED IMAGE GUIDE LEAKY WAVE ANTENNAS

M. Guglielmi and A. A. Oliner
Polytechnic University
333 Jay Street
Brooklyn, NY 11201

In the past decade, many types of leaky wave antennas for the millimeter wave range have been investigated. One class of such antennas for which a sound theoretical analysis was not available in the past is the metal-strip-loaded dielectric image guide which consists of a dielectric rod of rectangular cross section on a ground plane. We present here a complete and detailed analysis of the dispersion behavior of this class of antennas. We also show how the dispersion behavior and the antenna performance can be effectively controlled, thereby providing for the first time a solid theoretical basis for the design of these antennas.

We first characterize a key constituent of the antenna structure, namely, a multimode metal strip grating at a dielectric interface. The relevant boundary-value problem leads to a rigorous singular integral equation with a static kernel, which is solved in the small obstacle limit. This solution yields a very simple equivalent network description for the discontinuity, which is also both novel and accurate. The network developed is used in the formulation of the transverse resonance equation for the propagation behavior of the infinitely wide antennas. The transition from the infinitely wide antenna to the one of finite width is performed using the effective dielectric constant (EDC) method.

From a parametric analysis we exhibit the effects of changes in the dimension of the metal strips, and we show that the leakage rate can be varied over a wide range of values. Our analysis also permits the design of tapered antenna apertures in order to control the sidelobe behavior.

B4-6
1540 A METHOD FOR SENSITIVITY ANALYSIS OF SERIES-FED ARRAYS OF RECTANGULAR MICROSTRIP PATCHES

Abdelaziz Benalla and K.C. Gupta
Department of Electrical and Computer Engineering
University of Colorado
Boulder, Colorado 80309

Analysis of single-port and two-port rectangular microstrip patches using two-dimensional analysis and segmentation method (Gupta, IEEE AP-S Symp. 1985, pp. 71-73; and Gupta and Benalla, IEEE AP-S Symp. 1986, pp. 821-824) has been extended for calculation of the sensitivities of the array performance to various designable parameters such as substrate height and dielectric constant, fabrication tolerances, etc.

The method consists of the evaluation of the modified Z-matrix for the multiport-network model of each cell of the array. A single cell typically consists of a single patch with two sections of interconnecting lines on each side. The segmentation method is then used to calculate the currents at the ports of each cell. These currents are used to compute the voltage distributions at the radiating edges of array elements. This yields the radiation performance of the array. Also, the input impedance of the array is computed by the segmentation method.

This procedure has been implemented for a 19 element linear series-fed array with Taylor amplitude distribution. Detailed results will be presented.

The method is also applicable to other types of series-fed arrays, such as series-fed arrays of circular patches, and planar arrays consisting of a number of series-fed linear arrays.

B4-7
1600

MUTUAL COUPLING COMPUTATIONS FOR RECTANGULAR MICROSTRIP PATCH ANTENNAS WITH A DIELECTRIC COVER LAYER

Yinggang Tu, K.C. Gupta, and D.C. Chang
Department of Electrical and Computer Engineering
University of Colorado
Boulder, CO 80309

Dielectric cover layers are often used as protective coverings for microstrip antennas and arrays. However, a dielectric overlay alters the antenna characteristics, and the design procedure needs to be modified. Effect of a dielectric layer on edge admittance of microstrip antenna has been discussed earlier (Tu et al., 1986 National Radio Science Meeting, Boulder, CO). The present paper describes a method for evaluating the external mutual coupling between the two radiating edges of a rectangular microstrip antenna with a cover layer.

Rectangular microstrip patch with a cover layer is modelled by two magnetic current line sources (one for each radiating edge) placed on a conducting ground plane and covered with the dielectric layer. Obviously, this model is accurate when the substrate is electrically thin (which is true for most commonly used microstrip antennas and arrays). For computation of the mutual coupling, the two magnetic line sources are divided into a number of small sections and the mutual admittance between each pair of two sections on different edges is evaluated by considering the 'reaction' between them. The key step in this computation is to find the near field of a magnetic dipole on the ground plane with a cover layer. The mutual admittance matrix (corresponding to various sections) thus obtained can be reduced to a 2×2 matrix for design of the antenna using the transmission line model, or to a multiport matrix for the design of the antenna using segmentation method.

Preliminary numerical results obtained so far indicate the mutual coupling between the radiating edges is increased considerably when a cover layer is present. The effect of resonance frequency on the resonance frequency and the input impednce of single rectangular patches will be discussed.

The method developed for calculation of the mutual coupling is also applicable to computation of mutual coupling among the radiating edges of different patches in an array environment.

B4-8
1620

THE MODIFIED DIAKOPTIC THEORY AND THE MOMENT METHOD FOR ANALYZING WIRE-STRUCTURE ANTENNAS

Chalmers M. Butler
Department of Electrical and Computer Engineering
Clemson University
Clemson, SC 29634

Felix Schwering
U.S. Army CECOM
Fort Monmouth, NJ 07703

The modified diakoptic theory (F. Schwering, N. N. Puri, and C. M. Butler, IEEE Transactions on Antennas and Propagation, AP-34(11), 1986) is, as the name implies, a modification of the general diakoptic theory introduced recently by Goubau. The modified theory retains almost all of Goubau's original notions but, in contrast to Goubau's original theory, it does not depend upon intermediate steps which violate Maxwell's continuity equation. In addition, the modified theory is founded upon well-established impedance matrix concepts common in microwave and distributed-parameter network theory. Consequently, the modified theory should be understandable to a larger group of antenna engineers than is the original theory. The purposes of this paper are to review the basic ideas embodied in the modified diakoptic theory, to draw attention to the close similarities of this theory and the method of moments, and lastly to point out the differences in these two methods. The general wire-structure antenna is used as a vehicle by the authors to illustrate the relationship between the modified diakoptic theory and the moment method. And a significant advantage in the numerical implementation of the modified diakoptic theory is discussed.

Subject to special, but very common, interpretation of sources (voltage generators) at ports, the Galerkin form of the moment method analysis of a wire-structure antenna is identical to the zero-order version of the modified diakoptic theory, provided the zero-order or dominant currents of the latter analysis are employed in the former. But, in the improvement of accuracy (process of achieving a converged solution), the two methods depart in principle. Convergence of the moment method is achieved by partitioning the structure more finely with an attendant introduction of more unknowns. On the other hand, convergence in the modified diakoptic theory depends upon an iterative solution of an integral equation to determine higher-order currents but the number of unknowns is not increased. This feature of the modified diakoptic theory enables one to analyze larger structures than could be handled otherwise.

B4-9 1640 **ARRAY ANTENNA POWER PATTERN SYNTHESIS WITH QUANTIZED PHASE SHIFTERS**

Hans Steyskal
Electromagnetic Sciences Directorate
Rome Air Development Center
Hanscom AFB, MA 01731

An antenna problem of theoretical and practical interest is to what extent the phase shifters in a phased array can be used not only to scan but also to shape the beam.

This paper reports a study on pattern synthesis for linear arrays with control of the array element phases only. The desired power pattern is synthesized directly since, in the absence of any far field phase constraints, this leads to a better approximation than conventional field pattern synthesis. A mean square error is adopted as a measure for the quality of the approximation and this error e is minimized by an exhaustive computer search over all possible combinations of the quantized phase shift values. Thus brute force approach has several merits: 1) it is suitable for relatively small arrays where classical phase-only synthesis methods (e.g. A. Dunbar, J. Appl. Physics 23, Aug. 1952) are not applicable, 2) it emulates the quantized real life phase shifters and 3) it avoids the risk of finding only a local rather than the global minimum, which the commonly used gradient descent method (e.g. A.R. Cherrette, D.C.D. Chang, IEEE AP-S Symp. Digest, 475-478, 1985) is subject to. In fact, an interesting by-product of the present approach is the map of the multidimensional surface e, which shows all the existing minima and thus indicates the severity of this risk.

Several illustrative cases of synthesized rectangular pulse patterns will be discussed.

Session B-5 1355-Mon. CRO-30
WAVES NEAR AN INTERFACE
Chairman: E.F. Kuester, Dept. of Electrical and Computer Engineering, Univ. of Colorado, Boulder, CO 80309

B5-1
1400

A SIMPLE METHOD FOR DETERMINING THE FAR-ZONE FIELD DUE TO LINE SOURCES NEAR MEDIA INTERFACES

Chalmers M. Butler and Xiao-Bang Xu
Department of Electrical and Computer Engineering
Clemson University
Clemson, SC 29634

A simple method for deriving expressions for the far-zone field due to line sources near media interfaces is presented in this paper. The method, based upon reciprocity and notions of diffraction of a plane wave at a planar interface between two media, allows one to compute by elementary means the far-zone field due to line currents and line dipoles of both the electric and magnetic type. Resulting from this simple procedure are far-zone field expressions which vary as $\rho^{-1/2}$ and which are identical to the saddle-point contribution obtained from asymptotic evaluation of the appropriate Sommerfeld integrals. The lateral wave term is not included in the far-zone field expression but, of course, since this term varies as $\rho^{-3/2}$, it is insignificant compared to the dominant term in the radiation pattern, except in the very near vicinity of the interface. The far-zone fields due to electric and magnetic line currents are obtained from a direct application of reciprocity. But, in order to take advantage of reciprocity to calculate the fields due to line dipoles, it is necessary to introduce line-source doublets equivalent to the original line dipoles.

The analyses for determining the far-zone patterns due to line currents and line dipoles near interfaces are outlined. Expressions for far fields due to sources located in both half spaces are presented. Corresponding far-zone patterns are presented too for various combinations of source locations and electromagnetic properties of the two half spaces. It is demonstrated that these field patterns differ significantly from those which one would obtain from the same sources located in homogeneous space.

B5-2 SCATTERING FROM TE-EXCITED, PARTIALLY BURIED CYLINDERS
1420

Xiao-Bang Xu and Chalmers M. Butler
Department of Electrical and Computer Engineering
Clemson University
Clemson, SC 29634-0915

In this paper is presented an analysis of scattering from partially buried conducting cylinders at the planar interface between two semi-infinite, homogeneous half-spaces of different electromagnetic properties. The perfectly conducting cylinders of general cross section are of infinite extent and the excitation is transverse electric to the cylinder axes. Two types of coupled integral equations for the unknown currents induced on the cylinders are formulated: the magnetic field integral equations (MFIE) and the electric field integral equations (EFIE). Green's functions for the integral equations derived elsewhere are summarized, and numerical solution techniques for solving the integral equations are presented. A simple technique (Butler, C. M., and X.-B. Xu, "A Simple Method for Determining the Far-Zone Field Due to Line Sources Near Media Interfaces," 1987 National Radio Science Meeting, Boulder, CO, January 12-15, 1987) is employed to determine the far-zone radiated field from knowledge of the cylinder currents. The induced currents and the far-zone scattered field patterns are presented graphically as functions of various parameters of the problem.

B5-3
1440

NEAR-FIELD SCATTERING BY A BURIED DIELECTRIC SPHERE

Richard L. Lewis
Electromagnetic Fields Division
U.S. National Bureau of Standards
Boulder, Colorado 80303

The classical Mie (Annalen der Physik, 25, 377, 1908) formulation for scattering by a dielectric sphere is extended to the case of arbitrary incidence angles with respect to a preferred coordinate system, while the scattered field is expressed in terms of a plane-wave integral representation. This formulation is then combined with Fresnel's equations for reflection and refraction at a planar interface to obtain a plane-wave scattering formulation for buried dielectric sphere. This formulation is particularly convenient for calculating the scattered field just above the planar interface. Numerical results are presented for the special case of excitation by a normally incident plane wave.

B5-4
1500

FAST NUMERICAL COMPUTATION OF TWO-DIMENSIONAL SOMMERFELD INTEGRALS USING INCOMPLETE LIPSCHITZ-HANKEL INTEGRALS

Steven L. Dvorak and Edward F. Kuester
Electromagnetics Laboratory
Department of Electrical and Computer Engineering
University of Colorado - Campus Box 425
Boulder, CO 80309

Two-dimensional Sommerfeld integrals are often encountered in the analysis of electromagnetic field problems involving planar/layered geometries. Numerical computation of these integrals can be very time consuming due to their slow convergence properties. To address this problem, an efficient numerical method for evaluating two-dimensional Sommerfeld integrals will be discussed.

It is advantageous to use a polar transformation

$$\int_{-\infty}^{\infty}\int_{-\infty}^{\infty} f(\alpha_1,\alpha_2)d\alpha_1 d\alpha_2 \rightleftharpoons \int_{0}^{\infty} g(\lambda)\int_{0}^{2\pi} h(\lambda,\phi)d\phi d\lambda,$$

when doing the numerical integration. Now, the inner integral can be rewritten in terms of one, or more incomplete Lipschitz-Hankel integrals, each of which has the form

$$Je_0(a,z) := \int_0^z e^{-at} J_0(t)dt,$$

where a and z are functions of λ. The resulting incomplete Lipschitz-Hankel integrals can be efficiently computed to within a desired accuracy using factorial-Neumann, Neumann, and asymptotic series expansions. The two-dimensional Sommerfeld integrals are computed using the incomplete Lipschitz-Hankel expansions for the inner integral and a numerical integration routine for the outer integral.

The efficiency of this algorithm, as compared with a two-dimensional adaptive quadrature routine, was determined by computing the input impedance of a flat strip antenna positioned over a layered dielectric medium. In this example, a simple variational method was utilized, but the techniques developed in this paper can also be used to compute the integrals in a moment method formulation.

B5-5
1520

ACCURATE EVALUATION OF SOMMERFELD INTEGRALS USING THE FAST FOURIER TRANSFORM

B.C. Drachman
Department of Mathematics
D.P. Nyquist and M.J. Cloud
Department of Electrical Engineering and Systems Science
Michigan State University
East Lansing, MI 48824

Application of the conventional Hertzian-potential-based formulation of layered media electromagnetics necessitates evaluation of Sommerfeld-type integrals. An efficient and accurate method of computing these integrals is presented.

The Fast Fourier Transform (FFT) may be used in a straight-forward fashion to obtain accurate integrations of periodic functions. It is explained how, in these cases, the numerical integration method corresponds to the Corrected Trapezoidal rule (with error proportional to the fourth power of the step size). Attempts to use the FFT in such a fashion on aperiodic functions result in significant errors because, in these cases, the integration method corresponds to the Rectangular rule (error proportional to the first power of the step size). Thus it is often believed that the FFT is a quick but inaccurate way to compute an integral. When used in conjunction with Simpson's rule, however, the FFT gives extremely accurate results for aperiodic functions. An error analysis suggests a technique for integral truncation and choice of partition density. Examples are given in which this method is applied to the numerical evaluation of Sommerfeld integrals.

The method exploits the efficiency of the FFT algorithm, while deriving additional benefit from the fact that a single call of the FFT algorithm returns sample values of the Sommerfeld integral at many spatial locations. Moreover, this technique should be well adapted for use with the point-matching Galerkin's method of moments which requires values of the Sommerfeld integrals at a set of locations on a structure.

Session B-6 1535-Mon. CRO-30
RANDOM MEDIA
Chairman: A. Ishimaru, Dept. of Electrical Engineering, Univ. of Washington, Seattle, WA 98195

B6-1 1540 EFFECTIVE PERMITTIVITY OF A DIELECTRIC MEDIUM EMBEDDED WITH CONDUCTING NEEDLES

Leonard Lewin
Department of Electrical and Computer Engineering
University of Colorado, Boulder, CO 80309
Mohamed D. Abouzahra
Lincoln Laboratory
Massachusetts Institute of Technology
Lexington, MA 02173

A theoretical approach for predicting the complex effective permittivity of an inhomogeneous dielectric medium is described. This medium is comprised of a homogeneous dielectric region (host medium) weakly loaded with a three dimensional array of uniformly distributed, randomly oriented, thin ($ka<<1$) conductive needles. Each individual needle is assumed to be finite in length, electrically long ($kl>>1$), and possesses finite conductivity. A closed form formula describing the complex effective permittivity of this medium as a direct function of frequency and the scatterers concentration, size, and conductivity is developed.

Experimental samples of Teflon loaded with different concentrations of conductive needles have been fabricated and tested. The dielectric properties of these specimens were measured over a broad frequency range utilizing an HP8510 Automatic Network Analyzer. Comparison with the theoretical predictions is performed and the order of agreement is discussed.

B6-2
1600

MEASUREMENT OF A POINT SPREAD FUNCTION THROUGH A SLAB OF RANDOMLY DISTRIBUTED SPHERICAL PARTICLES AND APPLICATION OF SPECKLE INTERFEROMETRY

Yasuo Kuga and Akira Ishimaru
Department of Electrical Engineering
University of Washington
Seattle, Washington 98195

In astronomy it is known that a short-exposure image contains speckles whose size is close to the diffraction-limited optical system. It is also recognized that a long-exposure image causes an image blur due to the random motion of the atmospheric turbulence. Stellar speckle interferometry was invented in 1970, and the diffraction-limited image was obtained by using many short-exposure images. Image transmission through discrete particles such as rain is different from that of the turbulence case. However, it may be possible to use speckle interferometry for a random discrete medium and to obtain a diffraction-limited image.

In this paper, we present an experimental study of image transmission through random discrete media. The technique of speckle interferometry was applied to experimental data, and the result was compared with short- and long-exposure images. We measured the point spread function through a slab of randomly distributed spherical particles for different particle sizes, optical distances, and shutter speeds. The experimental system consists of a HeNe laser, a variable speed mechanical shutter, a 5 μm pin hole, a cell which contains latex spherical particles, and an imaging system. Experimental results are obtained for 2.02, 5.7, 11.9, and 45.4 μm particles; optical distances between 1 and 15, and shutter speeds between 10 msec and 30 sec. When the particle size is less than 11.9 μm, the speckles created by the particles are weak and the intensity distribution at the image plane is concentrated around the beam center. Because of this, the best quality image is obtained when a long shutter exposure time is used. On the other hand, speckles created by 45.4 μm particles are very strong and the intensity distribution at the image plane contains many peaks whose size is comparable to the image of the pin hole. In this case, it is shown that the average of the square of the MTF has a wider bandwidth than the average of the MTF. This shows that the image quality can be improved by using speckle interferometry.

B6-3
1620

ON THE APPLICATION OF THE MARKOV APPROXIMATION TO SCATTERING PROBLEMS FORMULATED IN THE SPECTRAL DOMAIN

by
Charles L. Rino
Mission Research Corporation
2300 Garden Rd., Suite 2
Monterey, Calif. 93940

The use of the Markov approximation to derive first-order differential equations for the complex moments of wavefields propagating in continuous randomly irregular media from the parabolic wave equation is well known, but the precise conditions under which the approximation is valid have been obscured because the derivation of the moment equations uses the parabolic approximation and neglects backscatter, for example in the formal computation of the functional derivative in the Navikov-Furutsu formula. What is needed is a more general transport-like formulation of the scattering problem.

We show that in the spectral domain the scalar Helmholtz equation admits an exact transport-like formulation. Applying the usual Neumann series approximation to the integral form of this equation shows that the Markov approximation is eqivalent to neglecting terms that are second order in the integral of the transverse wavenumber spectrum of the index of refraction fluctuations over the correlation along the propagation direction. Thus the validity of the Markov approximation depends only on the magnitude of the integral term.

We shall present these results and show that the more familiar spatial-domain forms are easily derived when the parabolic approximation is applied to the general result and discuss the ramifications for extending the limits of the scatter theory under the parabolic approximation.

B6-4
1640

SCATTERING AND DEPOLARIZATION BY LAYERS OF PARTICLES WITH ROUGH SURFACES EXCITED AT OBLIQUE INCIDENCE

Ezekiel Bahar and Mary Ann Fitzwater
Electrical Engineering Department
University of Nebraska-Lincoln 68588-0511

Optical and infrared electromagnetic scattering and depolarization by random distributions of particles of irregular shape and finite conductivity are determined by solving the equation of transfer (S. Chandrasekar, Radiative Transfer, Dover, N.Y., 1950; A. Ishimaru, Wave Propagation and Scattering in Random Media, Academic, N.Y., 1978). In this work excitations of both vertically and horizontally polarized waves obliquely incident upon parallel layers of particles are considered. The irregular shaped particles are characterized by their random rough surface height spectral density function or its Fourier transform the rough surface height autocorrelation function.

The full wave approach (Bahar and Fitzwater, Applied Optics, 23, 3813-3819, 1983; Bahar and Chakrabarti, Applied Optics, 24, 1820-1825, 1985) which accounts for specular point scattering as well as diffuse scattering in a self-consistent manner is used to evaluate the elements of the scattering matrix and the extinction cross section that appear in the equation of transfer. The equation of transfer is solved for the incoherent specific intensities using Gaussian quadrature and the matrix characteristic value techniques (Ishimaru et al. Radio Sci., 17, 1425-1433, 1982). Both single scatter as well as multiple scatter results for the co-polarized and cross-polarized incoherent specific intensities are presented for particles with smooth as well as rough surfaces. Thus the effects of particle surface roughness upon the co-polarized and cross-polarized intensities are investigated in detail. Special consideration is given to the degree of polarization of the incoherent specific intensities (modified Stokes parameters).

Session C-1 1355-Mon. CR1-9
COMMUNICATION THEORY
Chairman: A. Wyner, AT&T Bell Labs.,
600 Mountain Avenue, Murray Hill, NJ 07974

C1-1
1400 BASEBAND TRELLIS CODES WITH A SPECTRAL NULL AT ZERO

A.R. Calderbank, J.E. Mazo
AT&T Bell Laboratories
Murray Hill, NJ 07974
T.A. Lee
AT&T Information Systems
Middletown, NJ 07748

We describe a method of modifying classical N-dimensional trellis codes to provide baseband codes that combine a spectral null at d.c. with significant coding gain. The information rate of the classical code is decreased by one bit and this extra redundancy is used to keep the running digital sum bounded.

We present baseband trellis codes for several information rates together with complete spectral plots and performance comparisons. We also describe a method of constructing baseband codes with multiple spectral nulls.

C1-2
1440 ON DATA TRANSMISSION OVER CROSS COUPLED LINEAR CHANNELS

J. Salz, A.D. Wyner
AT&T Bell Laboratories
Murray Hill, NJ 07974

We discuss theoretical results related to digital communications over multi-input, multi-output linear channels. For this model we derive the structure of the optimum data sequence estimator and Shannon's channel capacity when the added noise is white Gaussian. We also derive the structure of the least mean-square equalizer/canceler and the formula for the least-mean squared error.

C1-3 1540 PROPERTIES OF CONSTRAINED MODULATION CODES:

Chris Heegard, School of Electrical Engineering, Cornell Univ., Ithaca, NY 14853

Many modulation codes that are incorporated in communication and recording systems can be described in terms of constraints on the set on allowed signals. Common examples are run-length limiting and charge constraints. In the former, constraints are introduced on the minimum and maximum time between transitions in the modulated signal. In the case of a charge constraint, a bound is maintained on the absolute value of the accumulated charge (the running integral of the modulated signal).

In this paper we discuss properties of run-length limiting and charge constrained modulated codes. We begin with a discussion of the maximum rate at which it is possible to map unconstrained data onto codewords that satisfy the appropriate constraint. It is shown that for i.i.d. data, the codewords can be described by a Markov chain that is consistent with the constraint. The maximum rate is then related to the maximum entropy obtainable from such a Markov chain. A description of this maximum entropy chain for the run-length limiting and charge constraints is presented.

The auto-correlation and spectral properties of constrained modulated codes is discussed. In the maximum entropy case, a simple method for computing the auto-correlation function and spectrum is derived. These results generalize to all cases where the codewords are described as a Markov chain. They approximate the spectrum of an arbitrary constrained modulated codes; the approximation is reasonable whenever the rate of the code is near the maximum entropy rate.

In the case of run-length limited codes, the method of computing the auto-correlation is generalized to non-maxentropic codes. This method gives the exact auto-correlation function for codes of practical interest. The simplicity of the result gives a way to easily compute the spectrum of simple codes rate 1/2 codes such Bi-Phase and MFM (results that where previously shown by more difficult calculations) and more complex codes such as rate 1/2 (2, 7) code and rate 2/3, (1, 7). The latter two codes are found in many high end magnetic disk systems; the closed form formulas for the auto-correlation and spectrum are new.

C1-4
1620

EQUALIZATION OF FADING DISPERSIVE CHANNELS WITH TRELLIS CODED MODULATION

K. Zhou*, J. G. Proakis*, and F. Ling**

*Department of Electrical and Computer Engineering
Northeastern University
Boston, MA 02115
**Codex Corporation
Mansfield, MA 02048Northeastern University
Boston, MA, 02115

Adaptive equalization techniques have been developed over the past few years for combatting intersymbol interference on time-dispersive channels such as HF and tropospheric scatter. When coding is used to improve performance performance, the adaptive equalizer is usually adjusted on the basis of tentative decisions made at the output of the equalizer, which precedes the decoder. Unrealieliable tentative decisions usually result in significant degradation.

In this paper we investigate the performance of adaptively equalized fading dispersive channlels when trellis-coded modulation is used to improve the performance of the system. The more reliable decisions at the output of the decoder are used to adjust the equalizer paramters. Performance results are presented that illustrate the advantage derived from using the more reliable information from the decoder.

Session F-2 1355-Mon. CR2-26
SURFACE-BASED RADAR AND RADIOMETRIC REMOTE SENSING OF THE CLEAR ATMOSPHERE
Chairman: Edgeworth Westwater, Wave Propagation Lab, NOAA/ERL, 325 Broadway, Boulder, CO 80303

F2-1
1400 RELATIONSHIP OF STRUCTURE PARAMETERS OF REFRACTIVE INDEX AND VELOCITY TO ATMOSPHERIC STABILITY

E.E. Gossard
CIRES, University of Colorado
Boulder, CO 80309
Nandini Sengupta
Post Doctoral Fellow
National Research Council
Wave Propagation Laboratory
NOAA
Boulder, CO 80302

Data collected on the 300 m tower at the Boulder Atmospheric Observatory are used to demonstrate that the ratio of temperature variance to velocity variance is a very good indicator of the height gradiant of potential temperature. Furthermore, the variances can be related to their corresponding structure parameters with good accuracy. However, clear air radars sense the structure parameter of radio retractive index rather than temperature, so conversions must be made to account for the influence of humidity on the refractive index. Appropriate relations are derived and discussed. Radar can, in principle, measure the structure parameter of velocity by use of the width of the Doppler velocity spectrum. The appropriate relations are shown and their accuracy is discussed.

F2-2
1420 REMOTE SENSING OF METEOROLOGICAL PARAMETERS UTILISING A CLEAR-AIR DOPPLER RADAR: Nandini Sengupta and R.G. Strauch, Wave Propagation Laboratory, NOAA, Boulder, CO 80302 and E.E. Gossard, CIRES, Univ. of Colorado, Boulder, CO 80309

Clear-air Doppler radars are being used extensively by scientists to measure wind profiles of the atmosphere. Radio refractive index fluctuations are usually presumed to be the cause of radar backscatter. The structure constant parameter C_n^2 is a good indicator of the intensity of the radio refractive index fluctuations. The Doppler spectral width can, in principle, provide the intensity of the turbulent velocity fluctuations and kinetic energy dissipation rate ε. Therefore, the backscattered power and the Doppler spectral width can be used to provide a radar-measured value of the ratio of refractive index variance to velocity variance for comparison with raob-observed refractive layers.

Data from the UHF wind profiling radar (Wave Propagation Laboratory, NOAA) at Stapleton Airport, Denver have been used to analyze elevated stable layers. The radar retrieved profiles of the structure parameter C_n^2 are shown to be well correlated with refractive index layers found in raobs launched at Stapleton Airport, Denver.

Enhanced echoes have also been obtained from the UHF wind profiling radar during rain and cloud conditions. An attempt has been made to obtain the drop-size from the Doppler spectrum of the fall velocities.

F2-3
1440

COMPARISON BETWEEN HEIGHT PROFILES OF C_n^2 MEASURED BY THE STAPLETON UHF WIND PROFILER AND MODEL ESTIMATES

J. M. Warnock
Aeronomy Laboratory

N. Sengupta and R. G. Strauch
Wave Propagation Laboratory

National Oceanic and Atmospheric Administration
U. S. Department of Commerce
Boulder, Colorado 80303

In recent years a statistical model has been developed to estimate height profiles of the reflectivity turbulence structure constant C_n^2 in the free atmosphere from standard upper air meteorological data. This data may be obtained from standard National Weather Service (NWS) balloon launches made twice daily from Denver's Stapleton International Airport. The Wave Propagation Laboratory's 915 MHz wind profiler is also located at Stapleton Airport. Thus the close proximity of the radar and the balloon soundings provides an unique opportunity to make detailed comparisons between the radar measurements and model estimates.

To make these comparisons, experiments were conducted during the summer and fall of 1986 with the Stapleton radar operating in a special high resolution mode. The height resolution was 150 m and an echo power profile was taken and recorded every 25 s. This operation began on the hour after the balloon launch on many mornings during the observing period, and lasted for about an hour. The power profiles were converted to C_n^2 using the system parameters and the known receiver temperature.

These radar and model comparisons are the first made at UHF, and also the first made with such high resolution data. A detailed study of the comparisons may give insight into the meteorological conditions responsible for the C_n^2 variability including the relative importance of turbulent intensity and the vertical gradient of refractive index.

F2-4
1540

ASPECT SENSITIVITY OF ST RADAR ECHOES FROM ANISOTROPIC TURBULENCE

Alan T. Waterman, Jr.
STARLab., Stanford University
Stanford, CA 94305-4055

It has been observed that radar echoes from the clear air within the troposphere and stratosphere are at times sensitive to the pointing direction of the radar. Echoes from the zenith are stronger than those off zenith, and echo strength continues to decrease with increasing off-zenith angle. Some of this variation may be due to a different reflection mechanism for vertically pointing beams, and some may be due to the same mechanism but from a structure that presents a different aspect when viewed from a different angle.

In the present paper we compute the reflectivity of an atmosphere that has an anisotropic turbulent structure. The anisotropy is characterized by different correlation distances along each of three orthogonal axes. Reflectivity is computed as a function of angle with respect to these axes. Results are compared with values quoted in published journals. It is also shown that, when horizontal anisotropy is present, the variation of echo strength with off-zenith angle can be very sensitive to azimuth.

F2-5
1600 FREQUENCY CHOICES FOR A GROUND-BASED MICROWAVE RADIOMETRIC PROFILER

J.A. Schroeder and E.R. Westwater
Wave Propagation Laboratory, NOAA
325 Broadway, R/E/WP5
Boulder, CO 80303

M.T. Decker
Cooperative Institute for Research in Environmental Sciences
University of Colorado
Boulder, CO 80309

Atmospheric temperature and humidity profiles, cloud liquid, precipitable water vapor, and pressure heights have been routinely inferred from ground-based microwave radiometer measurements at Stapleton Airport in Denver, Colorado since 1981. The meteorological variables are obtained by linear statistical inversion of radiance measurements at six frequencies (20.6, 31.65, 52.85, 53.85, 55.45, 58.80 GHz) plus surface measurements of temperature, pressure, and relative humidity. This six-channel system has proven the concept of unattended, continuous, passive ground-based measurement of meteorological variables. Such a system could become a valuable component of the next generation weather observation network if it can provide the necessary meteorological information at a reasonable cost. Since each channel represents a sizable fraction of the total cost, we investigated the possibility of reducing the number of channels without compromising the end result. Using the absorption model of Liebe (H.J. Liebe, Radio Sci., 20, 1069-1089, 1985) and the radiative transfer equation, we simulated radiance measurements for both clear and cloudy atmospheres at frequencies in the 60 GHz oxygen absorption complex and near the 22.235 GHz water line. We evaluated the performance of hypothetical systems by linear statistical inversion of various combinations of measurements. The method used and the results obtained are presented.

F2-6
1620

MULTI-LAYER WINDOWS IN MILLIMETER-WAVE RADIOMETRY

M.D. Jacobson
Wave Propagation Laboratory,
Environmental Research Laboratories,
NOAA
325 Broadway, Boulder, CO 80303

Millimeter-wave radiometers require the use of radomes or transmission windows to provide protection from the weather and to help maintain a constant temperature for the electronic components. In this paper, the design and performance of two different multi-layer windows operating at 20.6, 31.6 and 90.0 GHz are discussed. Theoretical brightness temperatures due to emission and reflection by the windows are compared with experimental measurements of these quantities made with the atmosphere as a source. Implications of these results on the design of multi-frequency radiometers for remote sensing of temperature, water vapor and cloud liquid in the atmosphere are considered.

Session G-3 1355-Mon. CR1-42
GLOBAL IONOSPHERIC VARIATIONS
Chairman: Robert W. Schunk, Center for Atmospheric and Space Sciences, Utah State Univ., Logan, UT 84322

G3-1
1400 TIME-DEPENDENT SIMULATIONS OF GLOBAL THERMOSPHERIC DYNAMICS

R. G. Roble
High Altitude Observatory
National Center for Atmospheric Research*
Boulder, CO 80307

The Earth's thermosphere responds to variations in solar X-ray, EUV and UV radiational outputs, to a wide variety of magnetospheric forcings, and to upward propagating tides, gravity waves and other disturbances from the middle atmosphere. One of the main problems in thermospheric dynamics is to properly specify the three-dimensional time-dependent distributions of these energy and momentum sources for studies in thermospheric and ionospheric dynamics. A review of our current understanding of the thermospheric response to these various energy and momentum sources will be presented. Time-dependent simulations of global thermospheric dynamics by the NCAR-thermospheric general circulation model (TGCM) will be used to display a wide variety of dynamic phenomena that depends upon the nature and time history of the forcings. Impulsive events generate large- and medium-scale disturbances that propagate to equatorial altitudes where they can interact with similar waves launched from the magnetic conjugate auroral region. Prolonged auroral disturbances, on the other hand, produce larger changes in the mean circulation and results in considerable temperature and compositional enhancements. Time-dependent thermospheric simulation that have been made for specific days where the results could be compared with measurements made along the orbital path by the Dynamics Explorer-2 satellite will be also described.

G3-2
1440

AN ANTARCTIC INCOHERENT-SCATTER RADAR: A NECESSARY ADDITION FOR GLOBAL STUDIES

Vincent B. Wickwar
Geoscience and Engineering Center
SRI International
Menlo Park, California 94025

Global studies of the ionosphere, today, require a comprehensive set of observations and close collaboration between observations and theory because the ionosphere is part of a complex system that also includes the neutral atmosphere and the magnetosphere. For example: the ionosphere is coupled to the neutral atmosphere chemically and dynamically; significant energy and momentum are transferred to the high-latitude regions from the solar wind and magnetosphere; high-latitude regions are coupled to low-latitude regions; altitude regions are coupled to the ones above and below them. Observationally, the incoherent-scatter radars have made very significant contributions to a large number of global studies (MITHRAS, GISMOS, GTMS, WAGS) and are to be major participants in future studies under CEDAR and WITS. These radars provide a wide range of geophysical parameters pertaining to the ionosphere, thermosphere, and magnetosphere. They are determined simultaneously and continuously for periods ranging from seconds to many days and from altitudes between 80 and 600 km. There is a long-standing tradition in the community of using the radars, as well as other complementary instruments, to make coordinated observations. These observations usually occur on the Coordinated World Days, which last from one to five days. The data are made widely available to researchers through the incoherent-scatter data base at NCAR.

However, these global studies are very heavily skewed toward the northern hemisphere. Four incoherent-scatter radars form a meridional chain in the American sector (between the polar cap and the magnetic equator), and two radars form a meridional chain in the European sector (in the auroral region and at mid latitudes). Because no other alternative currently exists, it is assumed, for instance, that high-latitude inputs are the same in both hemispheres and that June conditions in the northern hemisphere can be used to represent January conditions in the southern hemisphere. There are major departures from this simplification. Therefore, a radar located in the southern hemisphere high-latitude region, Antarctica, would significantly contribute to our understanding of global processes in the ionospheric-thermospheric-magnetospheric system.

G3-3
1520

SUNDIAL: A CONTINUING PROGRAM OF GLOBAL-SCALE MODELING AND MEASUREMENT OF IONOSPHERIC RESPONSES TO SOLAR, MAGNETOSPHERIC, AND THERMOSPHERIC CONTROLS

E.P. Szuszczewicz
Science Applications International Corporation
Plasma Physics Division
1710 Goodridge Drive
McLean, Virginia 22102

With a focus on the advancement of the understanding of global-scale interactive ionospheric processes, the SUNDIAL program combines theoretical and empirical modelling with a measurements activity that includes an international network of ionospheric monitoring stations at high-, middle-, and low latitudes in the American, European/African and Asian/Antarctican sectors. In the first campaign, measurements were taken with common data formats and around-the-clock data collection for the full eight-day investigation (5-13 October 1984). Solar, solar wind, interplanetary, magnetospheric and geomagnetic data were also included through the NOAA/SESC data center. The result was a unique and intensive eight-day period of global-scale ionospheric monitoring, during a period which saw the rise and fall of a high-speed corotating solar wind stream, and witnessed an ultimate coupling to the equatorial ionosphere. This coupling resulted in the most disturbed condition of equatorial spread-F ever recorded by the Jicamarca Observatory. The content of this paper presents the findings, recommendations, and future perspectives of the SUNDIAL activity in the ascending phase of the upcoming solar cycle.

Supported by NSF Grant No. ATM-8605210.

G3-4
1540

IONOSPHERIC CONVECTION DRIVEN BY ASYMMETRIES IN NBZ CURRENTS

C. E. Rasmussen and R. W. Schunk
Center for Atmospheric and Space Sciences
Utah State University
Logan, Utah 84322-3400

Computer simulations of Birkeland currents and electric fields in the polar ionosphere during periods of northward interplanetary magnetic field (IMF) were conducted. When the IMF B_z component is northward, an additional Birkeland current system is present in the polar cap. This additional system of currents, called the NBZ current system, depends upon the IMF y component as well as the z component. During periods of positive B_y, the area occupied by the downward flowing currents in the evening side of the polar cap is much larger than the area occupied by upward flowing currents in the morning side. These simulations show the effects of asymmetries in NBZ currents on ionospheric convection, particularly in the polar cap.

G3-5
1600

GLOBAL IONOSPHERIC VARIATIONS DURING SEPTEMBER 1984

G. Crowley and R. G. Roble
High Altitude Observatory
National Center for Atmospheric Research*
Boulder, CO 80307

H. Carlson
Air Force Geophysics Laboratory
Hanscom Air Force Base
Bedford, MA 01731

J. E. Salah
MIT Haystack Observatory
Westford, MA 01886

V. B. Wickwar
SRI International
333 Ravenswood Avenue
Menlo Park, CA 94025

During the ETS/GTMS period of 17-24 September 1984, two magnetic storms occurred, separated by an interval of low activity lasting about two days. The first storm had about half the amplitude of the second storm, which was the largest of the year. Both events caused major ionospheric perturbations in the American and Pacific sectors. For example, at Pt. Arguello, foF2 was reduced by 30 and 40% respectively, whilst foF2 at Maui was reduced by over 50% in both cases. In other sectors a smaller positive response was noted.

The thermospheric response to the two storms is simulated by means of the NCAR-TGCM. Neutral winds from Millstone Hill and Sondrestrom incoherent scatter radars are employed to validate the simulation. The neutral winds measured at Millstone Hill were perturbed on the storm days and remained strongly equatorwards during the morning hours.

An attempt to simulate the ionospheric response to both storms in the American sector will be described. The ionospheric model incorporates winds, temperatures and neutral composition predicted by the TGCM.

G3-6
1620

SOME IONOSPHERIC EFFECTS ASSOCIATED WITH THE STORM OF FEBRUARY 1986

K. Davies[1] and R. Conkright[2]

Following solar flare activity in early February 1986 one of the largest geomagnetic storms in recent history commenced on February 6 and intensified late on the Universal Day February 8 when K_p reached 9 (18 to 20 UT).

During this period the following ionospheric phenomena were observed and will be discussed: (1) an order of magnitude increase in the peak electron density over the USA, maximizing near 1600 LT (~ 2100 UT) starting in the east. (2) an order of magnitude increase in total electron content, over North America, seen from Good Bay, Canada to Ramey AFB, Puerto Rico and as far west as California. (3) severe scintillation of radio signals from GOES-2 received along the east coast of the USA. (4) a large (x2) increase in total electron content near Melbourne, Australia around 1900 local time. (5) an increase in riometer absorption near 18 dB in northern Scandanavia (at approximately 2100 UT).

[1]NOAA/ERL/Space Environment Laboratory, 325 Broadway, Boulder, CO 80303
[2]NOAA/ERL/NESDIS, 325 Broadway, Boulder, CO 80303

G3-7
1640 PRELIMINARY RESULTS ON EFFECTS OF THE FEBRUARY 1986 MAGNETIC STORM ON MF SKYWAVE SIGNALS RECORDED AT FAIRBANKS, ALASKA

Robert D. Hunsucker
Geophysical Institute
University of Alaska-Fairbanks
Fairbanks, AK 99775-0800
Brett S. Delana
Geophysical Institute
University of Alaska-Fairbanks
Fairbanks, AK 99775-0800
John C. H. Wang
Spectrum Engineering Division
Office of Science & Technology
Federal Communications Commission
Washington, DC 20554

The magnetic storm of 8-9 February 1986 was one of the largest in 40 years and has been very well documented. The magnetometer H-component data recorded a maximum value of --6110 nT at the USGS College, Alaska observatory -- the largest variation ever observed at that location. Medium frequency (MF) skywave signals from standard broadcast band stations located in the continental U.S., Canada and Alaska recorded at College, Alaska showed profound variation during this period. A preliminary analysis of the behavior of signal amplitude from these stations on short and long propagation paths before, during and after the storm will be described.

Session G-4 1355-Mon. CR1-46
IONOSPHERIC RADIO TECHNIQUES
Chairman: Bodo W. Reinisch, Univ. of Lowell Center for Atmospheric Research, Lowell, MA 01854

G4-1 1400 IONOSPHERIC ROUGHNESS AND SPREAD-F: Gary S. Sales and Bodo W. Reinisch, Univ. of Lowell Center for Atmospheric Research, Lowell, MA 01854

A large increase in the roughness of the F-region ionosphere has been observed at night using the Digisonde 256 drift mode analysis. Roughness has been defined in terms of the angular spread in the scattering sources in the ionosphere when viewed by a vertically incident sounding. For comparison purposes the ionosphere after sunrise shows an order of magnitude decrease in this roughness index, indicating a relatively smooth daytime ionosphere which again becomes rough abruptly after sunset.

The observed angular distribution of nighttime sources has been analyzed in terms of a uniform spread convolved with the sounder antenna pattern. Finally a correlation is made with the spread F (range spreading) as seen on a vertical ionogram made every ten minutes following the "drift" measurement.

G4-2
1420 APPLICATION OF CHIRPED INCOHERENT SCATTER RADAR IN IONOSPHERIC PLASMA LINE OBSERVATIONS: B. Isham and T. Hagfors, National Astronomy and Ionospheric Center, Arecibo Observatory and Cornell Univ.; and W. Birkmayer, 2 MBB, 8000 Munchen 80, FRG

The method of chirped incoherent scatter plasma wave observations is briefly described. A discussion is given of the application of the method to the determination of electron density profiles, studies of ionospheric irregularities, electron temperature measurements, observations of electron gas vertical motion and field aligned currents and to the study of plasma line enhancements caused by photoelectrons and precipitating auroral electrons and to enhancements during ionospheric modification experiments. The method has been implemented at the Arecibo Observatory and at EISCAT. A few examples of the initial observations are presented.

G4-3
1440 FIRST DIRECT GROUND-BASED MEASUREMENTS OF ELECTRON DRIFT IN THE IONOSPHERIC F REGION:
S. Ganguly, Center for Remote Sensing, McLean, VA 22102; and Richard A. Behnke, National Science Foundation, Washington, DC

For the first time, vertical electron drift velocities in the F region of the ionosphere have been directly determined using the Doppler shift of the electron component of th incoherent-scatter spectra. Simultaneous measurements of ion drift velocities were also made. A large difference between the electron and ion velocities of the order of 100 ms^{-1} with corresponding currents of 10^{-5} Am^{-2} was observed at sunrise. The most likely source of these currents appears to be the action of the local thermospheric wind on the large conductivity gradients associated with the sunrise line.

G4-4
1500 OBSERVATIONS OF IONOSPHERIC CHARACTERISTICS DURING SLANT-E CONDITIONS BY A DIGISONDE 256 IN THE CENTRAL POLAR CAP

J. Buchau, Air Force Geophysics Laboratory,
Hanscom AFB MA 01731
P. Hoeg, Danish Meteorological Institute,
Copenhagen, Denmark
B.W. Reinisch, University of Lowell,
Center for Atmospheric Research, Lowell, MA 01854

Irregularities in the auroral zone and cusp region E-layer, observed as Slant-E Condition (SEC) in ionograms, and accompanying strong E-field intensities in the E-region, have been described in detail using the incoherent scatter radar, an HF backscatter radar, and standard ionosonde observations. To extend the observations of SEC deep into the polar cap, measurements were made with a Digisonde 256, recently deployed at the Danish Meteorological Institute's Qaanaaq Geophysical Observatory (86° CGL), during a SEC campaign conducted at Sondrestromfjord by DMI.

The Digisonde 256 multi-dimensional (amplitude-polarization-Doppler-direction) digital ionograms allow for an improved approach of synoptic investigations of SEC signatures in ionograms. The directional capability permits assessment of the poleward spread of the irregularity conditions, while high-resolution amplitude measurements allow quantification of the abnormal E-region absorption (Lacuna) generally accompanying SEC.

Between ionograms (1 every 5 min) the Digisonde 256 was operated as a multi-fixed-frequency (coherent) HF radar, and with the 7-antenna receive-array provided for multi-directional spectral measurements of the slant-E returns.

The technique will be described, and the first measurements of spectral characteristics of backscatter from E-region irregularities and of echo amplitude variations during SEC in the central polar cap will be discussed.

G4-5 1540 The PC Radar, A Digitally Controlled Ionosonde

PAUL E. ARGO, Los Alamos National Laboratory, Los Alamos, NM 87545, U.S.A.

A new digital ionosonde, based on the NOAA HF Radar, has been designed and built. This ionosonde uses an IBM-PC/AT for the control and data collection functions, and a pair of SKY320 coprocessors to do the signal processing. The "state" of the ionosonde can be controlled on a microsecond by microsecond timeframe, with a maximum scenario length (at that speed) of 64 milliseconds. Slower clock rates are available. Data is stored on a laser WORM disc, with 400 MBytes per disc.

The radar functions are controlled through programs written in the C programming language, and as such make the radar completely flexible in its' data collection modes. It can simulate the HF Radar's I, K, and G modes, the digisonde's standard data collection mode, and the oblique HF Radar (from Johns Hopkins) Doppler analysis.

Samples of data collected in a variety of manners will be presented.

G4-6
1600

CONCEPTS FOR A PORTABLE DIGITAL IONOSONDE:
D.M. Haines, T.W. Bullett, and B.W. Reinisch, Univ. of Lowell, Center for Atmospheric Research, Lowell, MA 01854; and F.J. Gorman, U.S. Army Communications-Electronics Command, Fort Monmouth, NJ 07703

Work has begun on a miniaturized version of the University of Lowell's Digisonde 256 vertical incidence ionospheric sounder. The major technical challenges inherent in such a development are the limits on transmitter size, weight and power and limits on transmit antenna size. Support data was collected during a variable power test conducted over a two week period at Wallops Island, VA. This data indicated that a few hundred watts of peak effective radiated power at mid-latitudes can reliably create ionograms of acceptable quality. A summary of this data is presented in the paper. Since it is feasible to carry only a few hundred watts of RF transmitter power in a portable system and even a 50% efficient portable broadband antenna would be a monumental achievement some exotic waveform design was necessary. A phase modulated complementary code set was selected and the required signal processing was implemented in real time on a personal computer. Interesting concepts in efficiency and compactness of circularly polarized magnetic transmitter antennas are presented as well as a discussion of signal processing for the elimination of narrow bandwidth interference.

Since the personal computer can provide the required signal processing, it is also available for data acquisition, system control, user interface, post processing, data storage and communications and indeed comprises the bulk of the new system. A lap-top version of a sufficiently powerful computer has just been announced which makes a truly man portable sounder intriguingly imminent.

G4-7
1620

APPLICATION OF MINIMUM-MEAN-SQUARE AND HOMOMORPHIC FILTERING TECHNIQUES TO AUTOMATIC SCALING OF OBLIQUE DIGITAL IONOGRAMS:
Water Kuklinski and John Huth, Univ. of Center for Atmospheric Research, Lowell, MA 01854

The utility of both minimum mean-square error (Wiener) and homomorphic filtering techniques for automatic identification of the individual traces in oblique digital ionograms is assessed. In developing both filters the received oblique ionograms were modeled as the sum of the desired oblique ionogram traces and an uncorrelated stationary noise/interference signal. The power spectral density of the noise/interference signal is obtained by averaging the magnitude squared of the two-dimensional discrete Fourier tranforms of ionograms containing only the noise/interference signals. An estimate of the oblique ionogram traces is synthesized from the vertical ionogram obtained at the receiver by using the secant law assuming a thin layer and taking the curvature of the earth into account.

Two filters, designed to recover only the one-hop oblique ionigram traces from the received oblique ionogram, was produced from the power spectral densities of the synthesized oblique ionogram traces and of the noise/interference signals. The performance of a Wiener filter, minimizing the mean-square error, and a homomorphic filter, producing an output with the same power spectral density as the synthesized oblique ionogram, are compared.

G4-8
1640 ROUND-THE-WORLD IONOSPHERIC DUCTING SIMULATION: Eli Tichovolsky, Rome Air Development Center, Electromagnetic Sciences Directorate, Hanscom AFB, MA 01731; and Chu-Hsien Lin, ARCON Corp., Waltham, MA 02154

Because of low absorption losses, ionospheric ducting has been associated with long range radio propagation. Under normal circumstances, these ducts are not accessible from ground-based transmitters. Natural or artificial mechanisms have to be utilized for injecting rays into the duct. Natural injection mechanisms have been demonstrated through model simulations in this study. High precision Jones-Stephenson ray tracing was used in conjunction with the ITS IONCAP median ionosphere and the RADC Polar models. Three injection mechanisms were identified: the Appleton's anomaly region, the auroral oval and the day-night terminator. An example of round-the-world (RTW) propagation is shown in the accompanying figure for a path originating in the southern hemisphere and traversing due north. The injection mechanism was the Appleton's anomaly.

These results were used to generate simulated ionograms which were calibrated against ground-based experiments. Oblique ionograms between ground and an orbiting receiver were also simulated. From these simulations, a test plan for optimum switching among several ground transmitters was formulated for a ducting experiment. The path with the most robust ducted propagation will be chosen in accordance with this test plan.

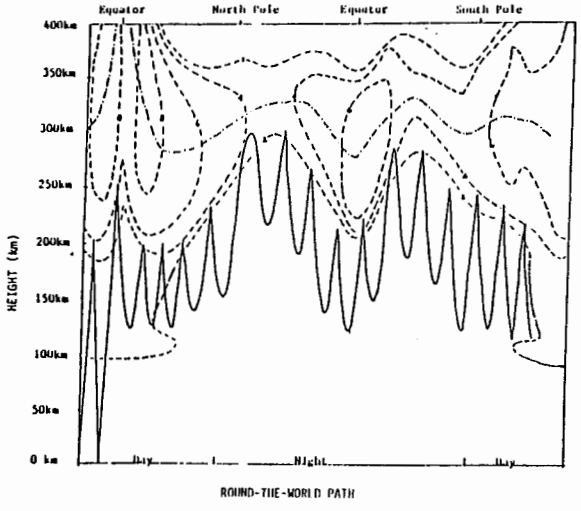

Session H-2 1355-Mon. CR1-40
RF ACCELERATION OF PARTICLES IN SPACE
Chairman: K. Papadopoulos, SAIC G-8, 1710 Goodridge Dr., McLean, VA 22103

H2-1
1400 RF ACCELERATION OF ELECTRONS IN THE IONOSPHERE

K. Papadopoulos
University of Maryland
Astronomy Program
College Park, Maryland 20742

The development of new high power sources of RF and microwaves as well as phased arrays is openning new research areas in ionospheric physics. A most exciting prospect is the possibility to generate electron fluxes with energy in the 50 KeV - 10 MeV range through the use of ground based or space born transmitters. In this talk we present a brief review of the possible acceleration concepts, the approximate power requirements and possible applications of the technique.

H2-2
1420 LASER ACCELERATION IN LABORATORY PLASMAS AND SCALING TO THE IONOSPHERE*, Tom Katsouleas, UCLA--Recently a growing experimental and theoretical effort has been directed toward the acceleration of particles in laser-driven plasma waves. Because of the unmatched peak power available from short pulse lasers and the ultra-high electric fields that can be supported by relativistic plasma waves, it may be possible to accelerate particles in plasma at rates three orders of magnitude higher than can be achieved in conventional accelerators. Such high gradients would enable the miniaturization of a high energy accelerator from kilometers to meters. One scheme for accomplishing this is the so-called beat wave accelerator in which two co-propagating lasers beat at the plasma frequency to resonantly excite a fast plasma wave ($V_{ph} = V_{group}(\text{lasers}) \approx c$). This process can be considered as seeded forward Raman Scattering. Injected electrons (or hot plasma electrons from the tail of the distribution) then surf on these plasma waves to gain energy.

General concepts and recent progress in laser acceleration of particles will be presented, and the potential for scaling these schemes to acceleration in RF-driven ionospheric plasmas will be discussed.

H2-3
1500

STOCHASTIC ELECTRON ACCELERATION IN OBLIQUELY PROPAGATING, ELECTROMAGNETIC WAVES

C.R. Menyuk
Science Applications International Corporation
1710 Goodridge Drive
McLean, VA 22102

Electron acceleration in space, both stimulated and natural, has long been a topic of interest in the study of space and astrophysical plasmas. Stimulated acceleration can be accomplished by rocket borne or ground-based transmitters. To date, coherent mechanisms have in most cases, been conjectured to cause the observed electron acceleration. This view is re-assessed here. It is shown that the stochastic mechanism can lead to ultra-relativistic electron energies under the appropriate circumstances. Moreover, in contrast to coherent mechanisms, this mechanism is robust. It is only weakly affected by changes in the plasma parameters, wave characteristics, and initial electron energies.

H2-4
1600

OBSERVATIONS OF RF ACCELERATED ELECTRONS IN SPACE

Herbert C. Carlson, Jr., Air Force Geophysics Laboratory, Hanscom AFB MA 01731

Strong RF fields can lead to the acceleration of electrons in space. Although a variety of processes have been hypothesized, there is not a concensus on which, if any, of these is primarily responsible for the electron acceleration found in ionospheric heating experiments. As a general rule, and particularly in this situation, experimental guidance can be very valuable in identifying promising candidate processes or theoretical approaches. To do this requires examining available data with a critical eye towards and concern for: the extent to which observables in the ionosphere relate back to the electron flux whose measurement is sought; and the extent to which such a flux if measured in a particular ionospheric altitude region relates back to electron acceleration in an electron flux source region. The very limited body of avaialble data is examined from this perspective.

H2-5 1640 ELECTRON ACCELERATION BY NONUNIFORM WAVE ELECTRIC FIELDS*

G. J. Morales, J. E. Maggs, Merit Shoucri, B. D. Fried, and A. Wang
Physics Department
University of California at Los Angeles
Los Angeles, CA 90024

An analytical and numerical study is made of the basic wave-particle interaction encountered when large amplitude wave fields are excited in nonuniform plasmas, as may be found in a variety of ionospheric and space applications. The central problem considered is the self-consistent determination of the waveform of excited electron plasma waves including the Landau acceleration of locally resonant electrons, i.e., electrons whose velocity matches the spatially varying wave phase velocity over a region of finite extent. Solutions to this problem have been obtained (without recourse to WKB approximations) for several cases of experimental interest, such as ionospheric HF heating, mode conversion of natural whistler noise, and beat-wave excitation in a density gradient. The nonlinear modification of the electron distribution function caused by the waves has been determined analytically by applying second order perturbation theory, and numerically for the large amplitude cases. The properties of particle trapping in the nonuniform wave troughs are examined.

* Work supported by ONR.

H2-6
1700

ELECTRON ACCELERATION BY CYCLOTRON HARMONICS IN THE IONOSPHERE

K. Hizanidis, P. Sprangle and K. Papadopoulos
University of Maryland
Astronomy Program
College Park, Maryland 20742

The acceleration of electrons in a bounded radiation field propagating obliquely with respect to the ambient magnetic field is studied. The numerical simulation is based upon the equations of the guiding center motion which are being obtained from the exact equations by fast time averaging. In the framework of this formulation, the interaction of particles with several high harmonics can be treated separately provided that overlapping of resonances does not considerably alter their motion. It also enables us to correlate the effectiveness of the acceleration with their spatial distribution as well as with the distribution of their gyro-phases. The regime of applicability, i.e. agreement with results from the exact equation of motion, is studied. Several wave amplitude profiles and fields with or without axial attenuation are studied.

Session J-3 1355-Mon. CR2-6
MILLISECOND PULSAR WORKSHOP II
Chairman: David W. Allan, Time and Frequency Division, National Bureau of Standards, Boulder, CO 80303

J3-1 1400 FREQUENCY STANDARD POSSIBILITIES WITH STORED IONS: J.J. Bollinger, National Bureau of Standards, Boulder, CO 80303

The method of ion storage provides a basis for excellent time and frequency standards. This is due to the ability to confine ions for long periods of time without the usual perturbations associated with confinement (e.g., wall shifts). In addition, Doppler effects can be greatly suppressed. The use of stored ions for microwave frequency standards and the future possibilities for an optical frequency standard based on stored ions will be discussed.

J3-2
1420

WORLD'S BEST CLOCK CONCEPT AND PRELIMINARY RESULTS

by

David W. Allan and Marc A. Weiss

Now that international timing centers can compare their time differences with precisions of the order of a nanosecond, this affords the opportunity to combine the readings from the world's set of high performance clocks and time scales. If these readings are statistically analyzed and optimum processing algorithms are employed, one can show, at least in terms how well the clocks are modeled, that algorithm's output is better than the best clock or time scale in the data base. The few nanosecond measurement noise via GPS in common view limits this approach to long-term stability improvement, but this is exactly what is needed as a reference for millisecond pulsar measurements with PSR 1937+214 approaching values for Mod.$\sigma_y(\tau)$ of 1^{-15} versus UTC(NBS).

Two approaches have been taken. First, we have performed a straight forward analysis estimating the stabilities of the major timing centers contributing to TAI via GPS in common view, and then combining their readings statistically weighted in the same algorithm used to generate UTC(NBS) we have generated a "best world" clock estimate. Secondly, we have combined the readings from the GPS common-view data base in a Kalman smoother with appropriate parameters set into the covariance matrix from the previous statistical analysis. A comparison along with the strengths and weaknesses of the two approaches will be discussed. In addition, for optimum long-term stability performance, the available periodic calibrations with respect to the world's primary frequency standards need to be optimumally included.

J3-3
1440

IMPROVED SENSITIVITY FOR FUTURE PULSAR OBSERVATIONS AT ARECIBO OBSERVATORY

Michael M. Davis
National Astronomy and Ionosphere Center
P.O. Box 995
Arecibo, Puerto Rico 00613

Major improvements being planned for the 1000 foot telescope at Arecibo will have a significant impact on future pulsar timing observations. The reflector surface has recently been readjusted to an accuracy of 2.3 mm rms, permitting observations up to 8 GHz. A 60 foot high ground screen around the perimeter of the main reflector will shield observations at high zenith angle from ground radiation which leads to increased system temperature. Plans are also well under way for a major improvement in the feed structure which illuminates the main reflector. A Gregorian subreflector system is being designed which will illuminate a 700 by 850 foot area, and provide a sensitivity of 12 K/Jy. The illuminated area is offset away from the edge of the reflector in the new design, so that the improved performance is maintained at high zenith angles. The system temperature, unaffected by losses in the currently used line feeds, is expected to drop to 20 K. These improvements will provide a factor of three increase in signal to noise at 21 or 12 cm at the zenith, and much greater improvement at high zenith angles. In addition, the correction to spherical aberration provided by the shaped subreflector system is wavelength independent. This opens up an opportunity to provide dedispersion of the pulsar signal over very much wider instantaneous bandwidth than at present. The combined effect of all of the improvements can provide a factor of ten increase in the sensitivity for pulsar measurements in the future. The Arecibo Observatory is part of the National Astronomy and Ionosphere Center, which is operated by Cornell University under contract with the National Science Foundation.

J3-4
1520

Millisecond Pulsar Surveys

D. C. Backer
Radio Astronomy Laboratory
University of California
Berkeley

In the past four years three pulsars with periods less than 10 milliseconds have been discovered. Two of these pulsars are in binary systems. These pulsars are interesting both for studies of the evolution of neutron stars and for use as astrophysical clocks. Many surveys have been initiated at radio observatories with the largest telescopes: Arecibo, Green Bank, Jodrell Bank and Molonglo. The status of these surveys will be summarized.

J3-5 1540 A SEARCH FOR SHORT PERIOD PULSARS IN OB ASSOCIATIONS AND GLOBULAR CLUSTERS: A. Wolszczan, J.M. Cordes, R.J. Dewey, and M. Blaskiewicz

According to standard evolutionary scenarios, short period pulsars appear in two distinct varieties: young Crab pulsar-like objects and extremely old pulsars which have been spun-up by accretion. We have begun a survey intended to cover these extreme ends of the age spectrum by searching for short period pulsars in OB associations and globular clusters. The survey is conducted at 1400 MHz with the Arecibo radio-telescope. At present a sensitivity of 0.5 mJy (8 sigma) is achieved in a wide range of periods and dispersion measures. The search data are processed with the Cornell Supercomputer Facility.

J3-6 1600

A NEW SYSTEM FOR HIGH ACCURACY TIMING OF MILLISECOND PULSARS

Daniel R. Stinebring and Joseph H. Taylor
Princeton University, Princeton NJ 08544
Timothy H. Hankins
Department of Electrical Engineering
Thayer School, Dartmouth College
Hanover, NH 03755

The timing accuracy of millisecond pulsar observations has improved by more than a factor of three in the last two years (see accompanying abstract by L. A. Rawley and J. H. Taylor). Most of this improvement is due to better time transfer between atomic time services and the Arecibo Observatory, where the pulsar observations are made. We are designing a system (Mark III) to improve the daily measurement accuracy of these observations by removing dispersion from the pulsar signal before detection of the signal. We anticipate a further factor of 2 – 5 improvement in timing accuracy within the next two years, which would yield daily measurement uncertainties of ~ 60 to 100 nanoseconds.

Propagation through the ionized interstellar medium degrades the accuracy of pulsar arrival time measurements in two ways. First, dispersion broadens the pulse over the observing bandwidth causing a degradation in our ability to precisely locate the pulse arrival time. For the current system, this broadening, which scales with observing frequency ν as ν^{-3}, amounts to 50 μs for observations of the millisecond pulsar PSR 1937+21 at 1400 MHz, compared to an intrinsic pulse width of 40 μs. The second effect is caused by time-varying spectral slopes across the filter bandpasses due to interstellar scintillation. These spectral slopes shift the effective center frequencies of the filters, resulting in time-varying systematic errors when the arrival times are corrected from the nominal center frequencies to infinite frequency. This is a significant source of systematic error for the current measurements, with an estimated rms level of ~ 1 μs at 1400 MHz.

The Mark III system will be immune to both of these effects. By removing dispersion before the signal is detected, the time resolution of the new system will be determined by the filter rise time ~ $\Delta\nu^{-1}$ rather than by the dispersion sweep time across the filters. Coherent dedispersion also removes the effect of frequency slopes across the filters since dispersion is removed exactly from each infinitesimal frequency element across the band. We will discuss recent tests of coherent dispersion removal on PSR 1937+21 and describe other features of the Mark III system.

J3-7 OPEN DISCUSSION ON THE POSSIBILITY OF DETECTION
1620 OF LOW FREQUENCY GRAVITATIONAL WAVES

Tuesday Morning, 13 Jan., 0835-1200

Session A-2 0855-Tues. CR1-42
ANTENNA AND EM FIELD MEASUREMENTS

Chairman: Motohisa Kanda, Electromagnetic Fields Division, National Bureau of Standards, Boulder, 80303

A2-1
0900

ANTENNA MEASUREMENTS AT NTT

Takehiko Kobayashi
NTT Electrical Communication Laboratories
P.O. Box 8, Yokosuka, 238 Japan
(guestworker until April, 1987
Electromagnetic Fields Division
National Bureau of Standards
Boulder, CO 80303)

Nippon Telegraph and Telephone (NTT), a telecommunication supplier in Japan, has been developing and operating a wide range of radio communication systems: terrestrial microwave relay systems, subscriber radio systems, mobile communication systems(automobile, maritime, aeronautical, paging, etc.), and satellite communication systems(6/4 and 30/20 GHz bands). NTT has been committed to research and development of antennas for these systems, and to their measurements.

These antenna measurements have been conducted using radio anechoic chambers, far-field antenna test ranges, space chambers, and mechanical and photogrammetric probes. With the more stringent requirements on antenna performances, the antenna measurement methodology itself has to be improved. NTT has introduced automatic antenna measurement systems, a vehicular motion simulator, and a satellite antenna test range.

System configurations, propagation characteristics, and antenna performances, as well as antenna measurement techniques are inseparably connected, and, consequently, must all be considered together in the design of radio communication systems. For example, the antennas for mobile communication in urban areas have to be designed with due consideration of the multi-path propagation. These antennas must be measured and validated in such propagation environments, and their performances directly influence the system configurations.

Highly sophisticated techniques are required for the measurements of frequency- and polarization-reuse multibeam antennas for future large-capacity communication satellites. Near field measurements could be advantageous to make antenna diagnosis, while analytical photogrammetry is essential for the tests in space chambers. Appropriate combination of several schemes are needed for reliable and economical measurements.

A2-2 0920 THE TIME-GATED ANTENNA RANGE. R. D. Coblin, O/6242; B/130, Lockheed Missiles and Space Co.,P.O. Box 3504, Sunnyvale, CA 94086-3504

Classical microwave metrology concentrates on measurement errors introduced by the measurement process. For standard transmission line components, the focus is typically on errors introduced by the equipment used. Therefore, self-calibrating instruments such as the automatic network analyzer have caused a revolution in readily achievable measurement accuracy. Such accuracy is not easily obtained in antenna measurements as the main source of error arises from extraneous radiation due to scattering from the antenna range itself.

A measurement method which addresses the multipath problem is the use of pulsed radiation and time-gating to isolate the desired direct radiation from the range reflected radiation. This paper reviews methods currently used to achieve time-gated antenna measurements. Considerations affecting the accuracy of such measurements are discussed such as pulse spreading due to antenna dispersion. Areas requiring better understanding are suggested.

A2-3
0940

DESIGN AND IMPLEMENTATION OF A CHECK STANDARD IN THE NBS RF ANECHOIC CHAMBER

W.J.Anson and E.B. Larsen
Electromagnetics Division 723.03
National Bureau of Standards
Boulder, CO 80303

The NBS check standard is a small stable receiving dipole antenna permanently mounted near the ceiling of the anechoic chamber. It's used to monitor the functioning of the field generation system. In use, the response of the check standard is recorded after an electric field has been set up in the chamber under pre-defined standard conditions. Since field strength is the "final product" of the field generation system, the established field is an indicator of the performance of each component and process in the system. The dipole check standard provides a dc voltage proportional to that field. This response is compared by the computer to pre-defined limits. If the response is not acceptable, the system components must be examined to find the cause before proceeding with a calibration.

The present check standard is a 1000-MHz half-wave dipole with sufficient response across the 200 MHz-to-2000 MHz band. It is permanently mounted near the ceiling of the anechoic chamber and midway between the front and back walls. Because it is small and positioned high in the chamber, reflections from the check standard are negligible. In this position it does not disturb the field at the antenna under test (AUT).

Since the state-of-the-system measurements take little time and are performed automatically under computer control, they are made just after the transmitting antenna has been positioned and just before it is removed to verify proper measurements during the use of that antenna. Several readings of the check standard response are recorded by the computer at three frequencies, i.e., at the top, bottom and middle of each transmitting antenna's frequency band. These will be compared with the system performance history and will be recorded on a computer file from which a control chart will be created. In the future the acceptable limits will be statistically determined from the control chart.

A2-4
1000

MAGNITUDE AND PHASE CALIBRATION OF MICROWAVE SENSORS*

R. R. McLeod and R. J. King
Lawrence Livermore National Laboratory, L-156
Livermore, CA 94550

Current network analyzer technology allows both magnitude and phase to be accurately recorded in antenna measurements, raising the possibility of fully characterizing antennas. This characterization can then be used in convolutions and inverse Fourier transforms. It requires, however, some standard calibration to measure against: a "standard phase horn" so to speak.

This paper first extends the definitions of several commonplace antenna parameters and equations to include phase. Given these necessary tools, a number of methods are used to derive a phase calibration and the results are presented. While every method used yields the proper results, only a few are easily applicable to phase measurements.

Using these results, the LLNL EMPEROR monocone is shown to be a nearly perfect, "flat" transmitter from 2 to 18 GHz. This allows it to be used as a magnitude and phase calibration range. In concert with the BEAMS measurement system, this allows engineers to quickly and accurately measure the complete response of antennas and other EM systems.

* Work performed under the auspices of the U.S. Department of Energy by the Lawrence Livermore National Laboratory under contract number W-7405-ENG-48.

A2-5
1040

ELECTROMAGNETIC FIELD MEASUREMENT ERRORS IN A SCREENROOM

J.E. CRUZ AND E.B. LARSEN
NATIONAL BUREAU OF STANDARDS
BOULDER, COLORADO 80303-3328

ABSTRACT

Most radiation measurements are done in a screenroom using antenna factors which have been determined in a known field at an open field site. These antenna factors are not necessarily applicable for making field measurements in a screenroom and the errors are difficult to determine. Measurement errors of electromagnetic fields in a screenroom are very large and non-repetitive because of multipath reflections, enclosure resonances, and near-field effects. These effects contribute to errors in determining antenna factor in the screenroom and hence to the accurate measurement of an EM field. An alternative technique for making EM field measurements in a screenroom is to measure an antenna factor in-situ and use this antenna factor to determine the EM field. However this technique has the problem that the antenna factor varies with antenna placement, screenroom dimensions, and screenroom loading. As a consequence the EM field measurement error is still difficult to determine.

In this paper we present the results for antenna factors determined in a screenroom using the two-antenna method. These antenna factors are compared with antenna fectors determined at an open field site. Experimental data are presented to show the variability of antenna factor as a function of frequency and location in a screen room. We also present data to show the dampening effect of absorber installed in the screenroom. Using a calibrated receiving probe to measure the fields in a screenroom while measuring antenna factor by the two-antenna method, a comparison was made of these two approaches for determining screenroom antenna factors.

A2-6
1100

THREE-DIMENSIONAL FIELD DETERMINATION OF CAVITY RESONANCE AND INTERNAL COUPLING

John D. Norgard and Ron M. Sega
Electrical Engineering Department
University of Colorado
Colorado Springs, CO 80933-7150

The effect of cavity geometry on the energy coupled through a slot aperture is investigated through the use of planar mappings of the internal field. A copper cylinder, closed at both ends, is constructed with copper mesh sections incorporated at the ends of the cylinder and in the cylinder wall opposite of a thin slot aperture placed in the wall. The frequencies used for testing are 2-4GHz.

Internal field mapping is accomplished by placing thin carbon-loaded sheets in the plane of interest and recording the digitized temperature distribution using an infrared scanning system. The sheets are calibrated such that the temperature data is transformed to current densities or electric field strengths.

Using several positions for the detection material, a three-dimensional field profile can be obtained. The onset of the internal cavity resonance is studied as it is related to the energy coupled through small apertures.

A2-7
1120 GRADIENT DISPLACEMENT ERRORS IN ANTENNA NEAR-FIELD MEASUREMENTS AND THEIR EFFECT ON THE FAR FIELD

L.A. Muth
National Bureau of Standards
Electromagnetic Fields Division, 723.05
Boulder, CO 80303

The effects of probe displacement errors in the near-field measurement procedure on the far-field spectrum are studied. Expressions are derived for the displacement error functions that maximize the fractional error in the spectrum both for the on-axis and off-axis directions. Planar x-y and z-displacement errors are studied first and, consequently, the results are generalized to errors in spherical scanning. Some simple near-field models are used to obtain order of magnitude estimates for the fractional error as a function of relevant scale lengths of the near field, defined as the lengths over which significant variations occur.

A2-8
1140

COMPACT RANGE AND SPHERICAL NEAR-FIELD SCANNING ANTENNA MEASUREMENTS

Doren W. Hess
Scientific-Atlanta, Inc.
P. O. Box 105027
Atlanta, Georgia 30348

Antenna pattern measurements yield the directional characteristic of an antenna, at a particular frequency. Compact range pattern measurements are made by recording the phasor response of an antenna under test as that antenna is illuminated by a plane wave. The plane wave is produced by collimating a point source of spherical wave radiation. Spherical near-field pattern measurements are made by recording the phasor response of an antenna under test as that antenna is illuminated by a spherical wave. The spherical near-field response can be transformed to yield the spherical far-field response via the Wacker algorithm. The result has been shown experimentally to the virtually identical to the compact range result.

In this presentation I review these two techniques and discuss the possibilities offered by application of pulse gating in the time domain.

Session B-7 0835-Tues. CR2-28
SCATTERING
Chairman: L.W. Pearson, McDonnell Douglas Research Lab, P.O. Box 516, St. Louis, MO 63166

B7-1 0840 HIGH FREQUENCY SCATTERING BY RESISTIVE, CONDUCTIVE AND IMPEDANCE STRIPS

M. I. Herman and J. L. Volakis
Radiation Laboratory
Dept. of Electrical Engineering and Computer Science
The University of Michigan
Ann Arbor, MI. 48109-2122

The resistive and conductive strips have been traditionally employed for the simulation of material slabs having relative permittivity and conductivity other than unity. In addition, a suitable combination of them forms an effective model for the impedance strip (T.B.A. Senior, *Radio Sci.,* 10, 645-650, 1975). It is therefore of interest to examine the scattering behavior of the resistive and conductive strips analytically.

In this paper explicit GTD expressions are presented for the scattered field (including multiply diffracted) by the aforementioned strips for either polarization of incidence. Our method of analysis employs the extended spectral theory of diffraction (R. Tiberio and R. Kouyoumjian, *Radio Sci.,* 14, 933-941, 1979) which involves the representation of the diffracted field from each edge as an integral of inhomogeneous plane waves. The diffraction of each of these plane waves at the next edge is subsequently treated in the known manner before the final asymptotic evaluation of the integral. The derived diffraction coefficients include up to third order interaction terms and are uniform in angle for all incidences. Particular attention is, of course, given to the rigorous evaluation of the surface wave field (and its interactions) which corresponds to the lowest order TM mode of the actual dielectric slab. Comparison of the GTD solution with numerical data indicates that the derived GTD coefficients are valid for strip widths as small as $\lambda/8$ in case of backscattering, and down to $\lambda/2$ near the forward scattering region for the bistatic case.

B7-2
0900

PHASE MATCHING OF HELICOIDAL SURFACE WAVES AND THE RESONANCE FREQUENCIES OF CONDUCTING SPHEROIDS

Anton Nagl[a], Barbara L. Merchant[b], and H. Überall[a]
[a]Department of Physics
Catholic University of America
Washington, DC 20064, and
[b]Naval Research Laboratory
Washington, DC 20375

The phase matching of surface waves on prolate conducting spheroids, generated e.g. by an incident electromagnetic wave, can be shown to explain the existence of the complex eigenfrequencies of the scatterer and the associated scattering resonances. This was demonstrated for the case of surface wave propagation along a meridian of the spheroid (B. L. Merchant, A. Nagl, and H. Überall, National Radio Science Meeting, Boulder, CO, Jan. 1986, and accepted for publication by IEEE Trans. A/P). We here treat the more complex case of an obliquely incident primary wave, whose scattering gives rise to helicoidally propagating surface waves. Only a discrete set of the required closed propagation paths exists, corresponding to a discrete set of allowed angles of incidence which can be associated with different "azimuthal quantum numbers" m of the surface wave propagation, m = 0 representing meridional paths.

The phase matching has been verified using sets of complex eigenfrequencies of the m>0 eigenvibrations of conducting spheroids as calculated by us previously using a T-matrix approach (B. L. Merchant, A. Nagl, H. Überall, and P. J. Moser, National Radio Science Meeting, Boulder, CO., Jan. 1986, and submitted to IEEE Trans. A/P). The phase matching integral is evaluated approximating the surface wave phase velocity locally by that on a sphere of equal radius of curvature. The ensuing fulfillment of the phase matching condition demonstrates the correctness of the phase matching principle, of the local-sphere approximation, and of the complex eigenfrequencies obtained by our T-matrix calculation.

B7-3
0920

T-MATRIX, EXTENDED BOUNDARY CONDITION METHOD APPLIED TO A DIELECTRIC ELLIPSOID: John B. Schneider and Irene C. Peden, Univ. of Washington, Seattle, WA 98195

The Extended Boundary Condition Method (ECBM) can be used to solve for the electromagnetic fields scattered from a single object when its size is of the order of a wave-length. The class of dielectric objects reported to date has been rotationally symmetric i.e., prolate and oblate spheroids.

The dielectric scatterer contains volume distributions of electric and magnetic currents. The resulting volume integral equations are applicable to arbitrary inhomogeneous dielectrics, but they require solution of six scalar three-dimensional integral equations. The EBCM provides an alternative to the surface integral formulation and its variants by focusing attention on the interior integral equation. Integral equation methods combined with finite difference techniques reduce the computational effort.

We apply the EBCM to dielectric ellipsoids which lack rotational symmetry as a step in a more general study of single-object scattering in the resonant range. Practical applications are thus extended to a wider class of targets, including irregular shapes that can be described in terms of "best fit" ellipsoids. Calculated results are presented for several elliopsoids having different dielectric constants, eccentricities and size parameters, and for a comparable spheroid. Differential cross-sections are presented, and some important details of the evaluation are discussed.

B7-4
0940

ON THE USE OF QUASI-STATIC TECHNIQUES IN ELECTRICALLY SMALL REGIONS OF ELECTROMAGNETIC PROBLEMS

R.G. Olsen, G.L. Hower
Electrical and Computer Engineering Department
Washington State University
Pullman, WA 99164

The analysis of three dimensional electromagnetic problems which contain conductors and dielectrics is a numerically difficult problem. In some cases, the analysis can be simplified considerably by using quasi-static analysis in an electrically small but geometrically complex region of the problem. A method for doing this is described here in cases for which the small region is weakly or strongly coupled to the rest of the problem.

The method is to first examine the conditions under which the integral equations of electromagnetic theory (A.J. Poggio and E.K. Miller, "Integral Equation Solutions of Three Dimensional Scattering Problems," in Computer Techniques for Electromagnetics, ed. R. Mittra, Pergamon, pp. 159-264) reduce to electrostatic integral equations. When valid, the electrostatic equations can be solved in the presence of a coupling field due to sources outside that region. Simultaneously, integral equations for the remainder of the problem can be solved in the presence of a coupling field due to sources inside the small region.

B7-5
1000

DETERMINATION OF SCATTERING CENTERS FOR A COMPLEX TARGET

Tinglan Ji
Nanjing Aeronautical Institute, P.R.C.
Visiting Scholar (with Professor James R. Wait)
Department of Electrical and Computer Engineering
University of Arizona
Tucson, AZ 85721

A complex target such as an aircraft is usually considered to consist of a number of scatterers having their movable scattering centers on the target. To set up a scattering model of the complex target, we should obtain the scattering center and strength for each scatterer of the target. This paper describes a method by which we can determine the locations of scattering centers of the target for arbitrary aspect angles.

The method is based on the fact that the scattering center (or the apparent center) of each scatterer must be in the direction of the phase gradient vector of its backscattering field, and then the exact position of the scattering center can be determined in terms of the relative phase of its backscattering field. The explicit formulas of the scattering center coordinates for each scatterer are presented in a target center coordinate system. The key to the problem is finding the analytical phase expressions of the backscattering fields and the relative phase for all the scatterers which compose the target. We have made calculations for a number of scatterers with typical shapes (e.g. ellipsoids, finite length cylinders and elliptical flat plates, etc.). The results show a good consistence with the actual situation.

In some particular cases, the analytical phase expressions of the backscattering fields are not known for some scatterers. Or even if we have their analytical phase expressions, there are a few singular points in their partial derivatives. We discuss these complications.

B7-6
1040

3D SCATTERING BY AN ANISOTROPIC CIRCULAR ROD.

J. Cesar Monzon
Damaskos, Inc., P.O. Box 469, Concordville, PA 19331

An arbitrarily polarized plane wave is obliquely incident on a homogeneous anisotropic cylinder which is embedded in free space as shown in the figure. The cylinder is characterized by tensors $\bar{\bar{\epsilon}}$ and $\bar{\bar{\mu}}$ of the form: $\bar{\bar{\alpha}} = \alpha_{xx}\hat{x}\hat{x} + \alpha_{xy}\hat{x}\hat{y} + \alpha_{yx}\hat{y}\hat{x} + \alpha_{yy}\hat{y}\hat{y} + \alpha_{zz}\hat{z}\hat{z}$, with the remaining components being identically zero.

This problem is a generalization of an earlier work (J.C. Monzon and N.J. Damaskos, IEEE Trans. Ant. and Propagat. AP-34, No. 10, 1986) where only normal incidence (i.e., 2D) was considered with the H and E polarizations treated separately and via duality. The 3D case is notoriously more complex than the 2D case since we have to deal with two coupled modes of propagation.

The axial fields in the anisotropic material are expanded in terms of extraordinary rays which define two unknown scalar spectral distributions. In addition, no inhomogeneous waves are handled which results in an attractive finite spectral range. By expressing the remaining field components in terms of the axial E and H and by appropriately matching boundary conditions, the problem is reduced to solving two coupled integral equations with nonsingular kernels.

Numerical results are presented, discussed and compared whenever possible with available published data or with a Gyrotropic type series solution implemented here for the sake of validation.

The extension of this work to an arbitrary number of different rods is clear.

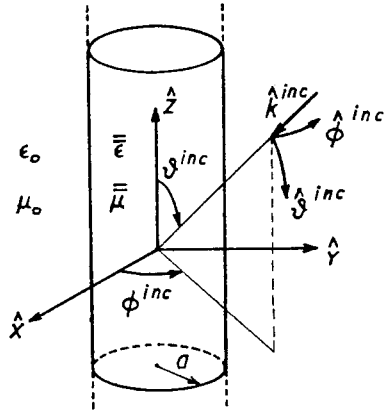

B7-7
1100

PHASED LINE SOURCE IN FRONT OF A UNIDIRECTIONALLY CONDUCTING SCREEN.

J. Cesar Monzon
Damaskos, Inc., P.O. Box 469, Concordville, PA 19331

A phased line source is located at a distance x_o from the screen and is parallel to it. The projection of the source on the screen forms an angle Ω with the direction of conduction as shown in the figure.

Karp and Karal (IEEE. Trans. Ant. and Propagat. AP-12, No. 4, 470-478, 1964) analyzed the case of $\Omega=\pi/2$ and arbitrary β; Seshadri (Cruft Lab. Harvard Univ. Tech Rep. No. 344, 1962) treated the case of arbitrary Ω but no phasing ($\beta=0$). Here we solve for arbitrary Ω and β. The problem is formulated in terms of a scalar u potential which satisfies Helmholtz equation. On the other hand (following Karp and Karal) the boundary conditions are composed of a second order differential jump condition on u (across the screen) plus an inhomogeneous second order ODE for u valid on the screen. The ODE on the screen is solved on the frame of the screen. This solution is then rotated into the frame of the filament where it is found that it can be easily generalized to all space. An exact integral representation for the scattered field is thus found by inspection of the solution on the screen. Surface wave information as well as the scattered far field are extracted from the integral representation. The waves excited to the right and left of the filament are in general different. They are both however circularly polarized and highly localized in the neighborhood of the screen. The scattered far field is symmetric on both sides of the screen and for $x>0$ admits an equivalent source located at the position of the image (as if the screen were p.c.) with a current amplitude independent of x_o but depending on the observation angle and with same phasing i.e., same cone. The transmitted field ($x<0$) is thus found to be independent of x_o.

Since the original integral representation is not suitable for numerical calculations an alternative expression for the field everywhere has been obtained which is attractive from the calculations viewpoint. Numerical results are presented.

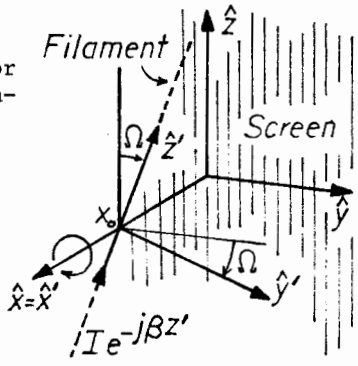

B7-8 1120 STEADY STATE AND TRANSIENT ELECTRIC FIELDS INDUCED BY A SPATIALLY UNIFORM MAGNETIC FIELD IN A CYLINDRICALLY INHOMOGENEOUS REGION

Charles Polk, Department of Electrical Engineering,
University of Rhode Island
Kingston, R.I. 02881

In experiments dealing with the effects of time varying magnetic fields on living tissue or cell cultures one frequently encounters the problem illustrated by the figure: A time varying magnetic flux density vector is perpendicular to the plane of the paper and its magnitude is uniform within a cylinder of radius R_o. Located off axis within this cylinder is another one, of radius a, which has different electric properties (conductivity σ_2 and dielectric permittivity ε_2) than the surrounding medium. The quantities of interest are the electric field and current in the smaller cylinder and the surface charge density ρ_s at the boundary between the dissimilar media.

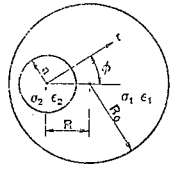

Although the frequency content of steady state and transient signals which are of interest may extend from ELF to the GHz region, the largest transverse dimensions L of the configuarations which are of interest (L~ cm for Petri dishes to L~ μm for cells), conductivities (σ), dielectric permittivities (ε) and magnetic permeabilities (μ) are such that the condition for validity of the quasi-static approximation

$$| j\omega\mu\ (\sigma + j\omega\varepsilon)\ L| \ll 1$$

is satisfied. It will be shown that under these circumstances Faraday's law, Gauss's law for the electric displacement and conservation of charge are satisfied in the region of interest, including the boundary at r = a, by solutions of the form

$$E_\phi = \frac{-j\omega Br}{2} + \frac{1}{r}\frac{\partial f}{\partial \phi}$$

$$E_r = \frac{\partial f}{\partial r}$$

where f is a solution of Laplace's equation in cylindrical coordinates. If it is assumed that $\rho_s = 0$ for $t \leq 0$, examples of the solutions for the electric field, which are obtained in this manner are for $r \leq a$

when $B = B_o \exp(j\omega t)$

$$E_{r2} = \frac{j\omega B_o R}{2}\sin\phi\left[K e^{j\omega t} + \left(\frac{\varepsilon_1}{\varepsilon_2} - K\right) e^{-t/\tau}\right] \qquad K = \frac{\sigma_1 + j\omega\varepsilon_1}{\sigma_2 + j\omega\varepsilon_2}$$

$$\tau = \frac{\varepsilon_2}{\sigma_2}$$

when B is a ramp function $B = Mt$ for $t \geq 0$

$$E_{r2} = \frac{MR}{2}\sin\phi\left[\frac{\sigma_1}{\sigma_2} + \left(\frac{\varepsilon_1}{\varepsilon_2} - \frac{\sigma_1}{\sigma_2}\right) e^{-t/\tau}\right]$$

B7-9
1140

BROAD SIDE COUPLED CYLINDRICAL STRIP LINES.

C.Jagadeswara Reddy & M.D.Deshpande
Radar & Comm. Center,IIT
KHARAGPUR-721 302,INDIA.

Using flexible dielectrics, it is possible to construct non planar strip lines,which can be warped around a cylindrical surface for the excitation of conformal arrays(K.K.Joshi et al,IEE Proc,pt.H, 127,287-291,1980). Various other applications of cylindrical strip lines are also reported(L.R.Zeng et al,IEEE-MTT,34,259-265,1986). In this paper a method for determination of even and odd mode impedances of a pair of broad side coupled cylindrical strip lines is presented.

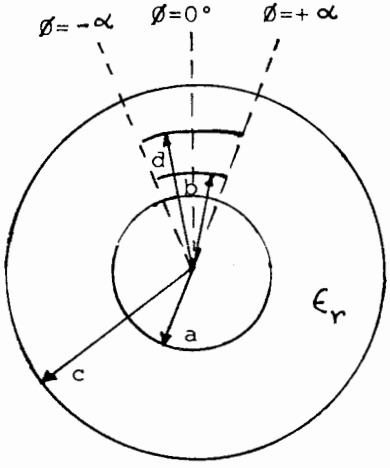

Fig.1

The cross section of the structure under consideration is shown in Fig.1 with the notation to be followed. It is assumed that only TEM modes exist. With transformation function $z=\pi-\phi+j\ln(\rho/a)$ the cylindrical structure transforms into a planar configuration. If the strip half width angle is small compared with 2π,the formulas available in literature for planar case(S.B.Cohn IEEE-MTT,8,633-637,1960) can be readily applied.

It is also shown that the analysis can be extended to find out the effect of environmental changes in an otherwise planar structure.

Session C-2 0835-Tues. CR1-9
MOBILE SATELLITE SYSTEMS
Chairman: F.M. Naderi, Jet Propulsion Lab, 4800 Oak Grove Drive, Pasadena, CA 91109

C2-1 0840 A NOVEL ELECTRONICALLY STEERABLE ANTENNA CONCEPT FOR LAND MOBILE SATELLITE COMMUNICATIONS: Donald G. Bodnar and B. Keith Rainer, Georgia Tech Research Institute, Georgia Institute of Technology, Atlanta, GA 30332; and Yahya Rahmat-Samii, Jet Propulsion Laboratory, California Institute of Technology, Pasadena, CA 91109

The Mobile Satellite Program (MSAT) is being developed to provide needed communication links to rural areas. A critical component in the system is the antenna for the vehicle. The antenna will be located on top of the vehicle (car, truck, etc.) and must acquire and track the desired satellite. Both electronically and mechanically scanning antenna configurations have previously been examined for this application. The purpose of this paper is to present a unique electronically steerable array approach for the MSAT program. This approach has the potential of reducing the cost of the antenna by eliminating most of the phase shifters in the array.

The proposed antenna design utilizes R-KR lenses to feed concentric rings of radiating elements in a planar array. Two diode switches and two power dividers are used to select the desired beam from the antenna. This arrangement replaces phase shifters at each element. The antenna provides azimuth only scan eliminating elevation search for the satellite.

The lens fed planar array described in this paper is a multilayer structure developed using stripline and microstrip design techniques. It has an aperture element packing arrangement consisting of two concentric rings of elements and a center element. The two rings of elements have twelve elements each and are fed by a switch and dielectric lens network which provides full duplex operation and 48 selectable azimuth beam positions which provide 360° of azimuth coverage. The beam is not scanned in elevation and provides coverage from 20° to 60°. Calculated patterns, losses, and inter-satellite isolation will be presented.

C2-2 0920 TRELLIS CODED MODULATION FOR MOBILE SATELLITE COMMUNICATIONS: Dariush Divsalar, Jet Propulsion Lab, California Institute of Technology, Pasadena, CA 91109

In Mobile Satellite (MSAT) communications, there is a need for conservation in both power and bandwidth. Several schemes using trellis coding with multilevel modulations are proposed. In particular, we are interested in transmitting 4800 bps over a 5 KHz MSAT channel which suffers from Rician fading and perhaps shadowing due to manmade or natural obstructions. Diversity and interleaving are considered as means for reducing the effect of fading bursts on trellis coded modulation. Two types of demodulation are considered, coherent demodulation with dual pilot tones and differentially detected demodulation. Dual pilot tone technique seems to be more appropriate for UHF operations where doppler spread is relatively modest whereas differential detection is preferable for L-band operation. For differential detection a novel doppler estimation system is proposed for doppler tracking in the presence of fading. Performance of the proposed systems has been computed for various system parameters, namely the speed of mobile, carrier frequency, fading parameters and interleaving. A simple model for fading channel is discussed.

C2-3 1020 THE OMNINET "OMNITRACS" MOBILE SATELLITE SYSTEM

Allen Salmasi
Omninet Corp.
2049 Century Park East
37th Floor
Los Angeles, CA 90067

Omninet applied to the Federal Communications Commission (FCC) in April of 1985 for authorization to establish a domestic Mobile Satellite System (MSS) offering affordable voice, data and position location services to non-metropolitan areas of the United States, Canada, Mexico, Puerto Rico and the Caribbean. The technologies that make this economically feasible include UHF and/or L-band satellite spot beams, omnidirectional mobile user antennas, spectrally efficient multiple access and modulation techniques, demand assignment of satellite capacity and flexible user interconnection to public and private switched networks. But such capabilities (herein called the "fully Capable" or "STARSAT^{SM}" system) cannot be realized in one fell-swoop. Rather, a gradual, revenue based rampup to this "fully capable" system, which determine the associated technical and business risks is being followed by Omninet. Accordingly, Omninet has announced a mobile alphanumeric data service employing receive only terminals at Ku-band. Omninet is also planning the early introduction of L-band MSS using host spacecraft currently under construction to carry an added L-band payload to geostationary orbit.

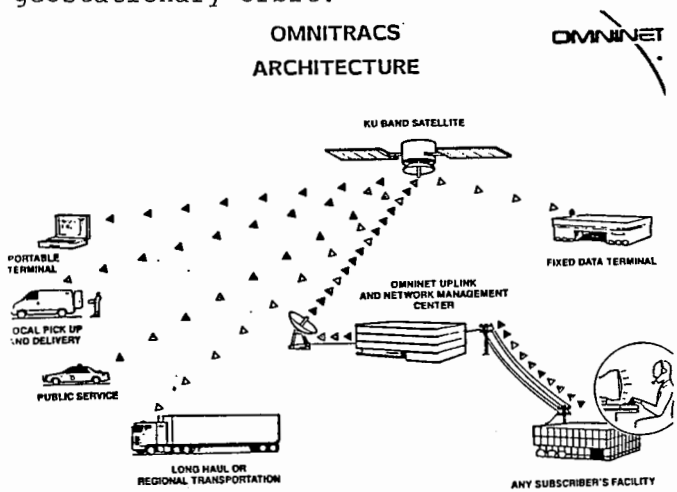

C2-4
1100

LOW-COST MICROSTRIP PHASED ARRAY ANTENNA FOR USE IN MOBILE SATELLITE TELEPHONE COMMUNICATION SERVICE

F. W. Schmidt, Member, IEEE
Ball Aerospace Corporation
P. O. Box 1062
Boulder, CO 80306

A design for a low-cost phased array antenna used in a car-top application for a satellite communications link is presented. Microstrip stacked patch elements provide good pattern coverage over the 7% bandwidth. Three-bit distributed element microstrip phase shifters provide beam steering over a range of 0 to 70 degrees from boresight. Microstrip technology is also used in the corporate power divider and polarization hybrids.

A hybrid tracking system consisting of an inertial sensor for open loop tracking and a sequential lobing scheme for closed loop tracking provides accurate tracking of the signal through brief signal outages. A novel scheme is used to minimize the effects of varying multipath on closed-loop tracking accuracy. A single board PC-compatible computer is used in conjunction with an interface board to steer the antenna and interface with the transceiver.

C2-5
1140 PROPAGATION CONSIDERATIONS FOR LAND MOBILE SATELLITE SYSTEMS: SIGNAL CHARACTERISTICS IN MOUNTAINOUS TERRAIN AT UHF AND L-BAND: W.J. Vogel and G.W. Torrence, Electrical Engineering Research Lab, The Univ. of Texas, 10100 Burnet Road, Austin, TX 78758; and J. Goldhirsh and J.R. Rowland, Applied Physics Lab, The Johns Hopkins Univ., Johns Hopkins Road, Laurel, MD 20707

A land mobile satellite system is currently being designed. It will provide communication services to vehicles traveling throughout the US, with an emphasis on low population density areas where land based systems are not available. In order to select system parameters which will result in satisfactory performance, the nature and severity of the various propagation related signal impairments has to be known. Of these, multi-path reflections are terrain dependent and for this reason a propagation experiment was carried out recently in the Rocky Mountains.

Tests were made in Poudre, Big Thompson and Boulder Canyon, all in the vicinity of Boulder, CO during a week of August 1986. They consisted of illuminating each canyon with cw signals at UHF and L-Band from a helicopter and measuring the received signal amplitudes and phases in a mobile receiving van. Repeated runs were made in which the helicopter followed the van as it made its way up or down the canyon, with the elevation angle help approximately constant to 30 and 45 degrees.

Of particular interest was whether rock faces would give rise to quasi-specular reflections which could lead to deep interference nulls and what the level of the signal was when the direct path was shadowed by a mountain ridge. Quantitative results will be presented, but preliminary ones indicate that multi-path reflections by canyon walls produced about +-3 dB fluctuations of the signal level, indicating the absence of strong specular components due to the natural surfaces. When the direct path was shadowed, the received signal level was reduced by about 15 to 20 dB. The dominant propagation problem in the mountains therefore appears to be the probability of having the satellite below the local horizon, whereas in flatter terrain it was found to be the probability of being shadowed by trees.

Session F-3 0855-Tues. CR2-26
THEORETICAL STUDIES OF PROPAGATION IN NON-IONIZED MEDIA
Chairman: Alan Waterman, Starlab, Stanford Univ.
Stanford, CA 94305

F3-1 0900 ON COMPUTATION OF THE GROUND WAVE OVER IRREGULAR AND/OR NONHOMOGENEOUS TERRAIN*

R. M. Bevensee
Engineering Research Division
Lawrence Livermore National Laboratory
Livermore, CA 94550

On flat earth the ground wave generated by a distributed antenna on or above ground is usually decomposed into a space wave and a surface wave component. The space wave contains a direct part plus an image part, the latter proportional to the Fresnel reflection coefficient. This paper discusses the propagation of both space and surface waves over nonuniform terrain, and their superposition to yield the ground wave.

Propagation of the surface wave component from flat earth over irregular and/or nonhomogeneous earth is treated by a Compensation Theorem version of WAGNER. This code has been validated by measurements in several test problems. However, the space wave component is not always negligible with respect to the surface wave component, particularly if the antenna is elevated. If so, the propagation of the space wave over the nonuniform terrain should be computed also.

It will be shown how the direct part of the space wave for a distributed source may be computed over irregular homogeneous terrain by a "direct-wave" version of WAGNER, and the image part computed over the same terrain by an "image-wave" version of WAGNER. The total relative space wave field (total field divided by a reference free-space Green function) is obtained by superposition. This is added to the relative surface wave field to obtain the relative ground wave field all along the irregular, homogeneous terrain.

This relative ground wave field is then inserted into a Volterra integral equation based on the Compensation Theorem to obtain the ground wave field over the irregular, nonhomogeneous terrain.

* Work performed under the auspices of the U.S. Department of Energy by the Lawrence Livermore National Laboratory under contract number W-7405-ENG-48.

F3-2 0920 GENERALIZED DOPPLER EFFECT COHERENT AND INCOHERENT SPECTRA: D. Censor, Dept. of Electrical and Computer Engineering, Drexel Univ. Philadelphia, PA 19104

The generalized Doppler effect produced by a particle moving along an arbitrary trajectory is analyzed. It is shown that to the first order in v/c, the observed spectrum is a convolution of the particle excitation spectrum produced due to the motion of the particle relative to the observer. For periodic motion in particular, the spectra can be expressed in terms of Fourier-Bessel series. The analysis is based on a Galilean transformation, however, time retardation and first order relativistic effects on the amplitude are incorporated into the formalism.

The statistical aspect is introduced by defining trajectory parameters as random variables with associated probability density functions specified. By defining an ensemble of non-interacting particles we create a scatterer whose shape, density and motion can be specified. The individual particles act as infinitesimal volume elements in a first order Born approximation. It is then possible to discuss, for example, rotating cylinders of circular or elliptical cross section, and derive the associated Doppler spectra.

It is shown that in special cases the coherent Doppler spectra degenerate to the incident field's frequency, i.e., the Doppler effect disappears. However, this cannot happen to the incoherently scattered field where intensities are summed.

F3-3
0940

INDUCED POLARIZATION AND RESISTIVITY RESPONSE FOR A BOREHOLE MODEL

James R.Wait and T.P.Gruszka
Electromagnetics Laboratory
ECE Department,
University of Arizona
Tucson, AZ 85721

Explicit results for the electrical resistivity and induced polarization responses are obtained for a four electrode array on the axis of a fluid filled hole.Quasi-static theory is employed(J.R.Wait,Introduction to Antennas and Propagation,Chap.2,PPL Dept. IEEE Service Center,1986).Electromagnetic coupling effects are neglected but the resistivities of the constitutive media may be complex and frequency dependent.We show that,in general,the frequency dependence of the apparent resistivity is a complicated function of the various parameters.In fact, even when the drill hole fluid is non polarizable, the masking effect involves both "dilution"and "distortion" of the intrinsic complex resistivity of the adjacent formation.

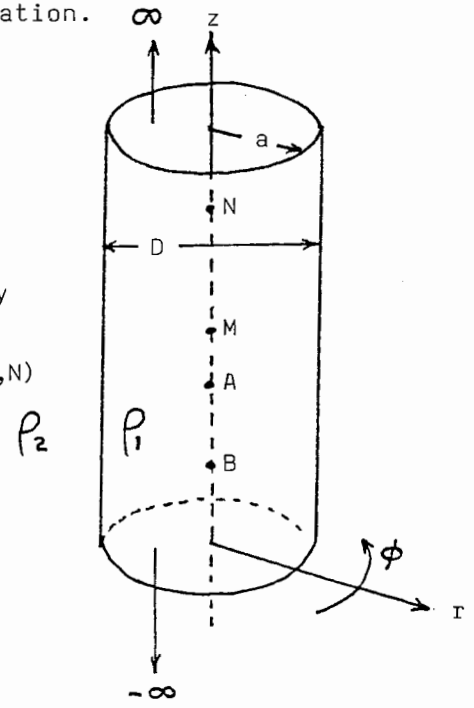

Figure

Borehole geometry showing location of current (A,B) and potential (M,N) electrodes.

F3-4
1100

ATMOSPHERIC RAY TRACING CORRECTIONS NEAR REGIONS EXCLUDING RAYS

Francis X. Canning
Naval Weapons Center
Code 3313
China Lake, CA 93555-6001

It has long been known that the basis of geometrical optics (and hence of ray tracing) "may be derived from the scalar wave equation in the limiting case $\lambda \rightarrow 0$" (Born and Wolf, Principles of Optics, Fourth Edition, pages 110-112). The derivation referred to above assumes that the products of λ with spatial derivatives of the fields go to zero as λ goes to zero.

In certain cases of atmospheric propagation, ray tracing predicts shadow boundaries. That is, it predicts that the spatial derivatives of the fields contain Dirac delta functions. Thus, whether the product of a small wavelength with these delta functions can be ignored requires careful consideration.

In this paper, we take a different approach. Simple refractive index profiles such that there is a minimum (of the refractivity) at a given altitude, are studied via the scalar wave equation. Ray tracing predicts that an incident ray will either cross the altitude of the minimum or be excluded from that region, depending on its original elevation angle. A calculation based on solving the wave equation directly shows that both always occur, though one is usually of negligible strength.

Reflection and transmission coefficients for this region are found in terms of analytical formulae. It is found that significant reflection and transmission simultaneously occur when several conditions are all satisfied. These conditions are that the wavelength is as long as the longer commonly used radar wavelengths, the refractivity has a sharp minima, and the rays either nearly reach or are near level at the altitude of the minimum of the effective refractive index. Quantitative examples are presented and discussed in terms of ray tracing parameters.

F3-5
1120

SMOOTH EM RESPONSE FUNCTIONS FROM NOISY DATA

J.C. Larsen
Pacific Marine Environmental Lab, NOAA
Seattle, WA 98115

Least squares methods are typically used to determine band average estimates of magnetotelluric response functions yielding estimates that are often not smooth functions of frequency due to noisy data. MT response functions should, however, be smooth function of frequency since the electromagnetic data can usually be treated as independent of the wavenumber of the source. Therefore a weighted least squares method has been developed to determine response functions and variances that will be smooth functions of frequency with the effects of noisy data removed.

To carry out the objective of obtaining smooth response functions that can also be approximated, as far as possible, by a response functions based on a one dimensional earth, the response is represented by a response based on a best fitting D+ Parker one dimension model earth (a stack of thin conducting sheets) times a smooth distortion factor given by a finite sum of simple frequency dependent functions. The response is then interatively estimated whereby a one dimensional model is computed at the end of each iteration and a new distortion factor for the next iteration is then computed by least squares from the electromagnetic data.

Since least square methods are sensitive to outliers, a time and a frequency weighting series are generated that are based, respectively, on the time and frequency residuals. The present iterative method then incorporates these weights and provides an unbiased method for removing the effects of outliers. The weighted residuals are plotted to determine whether a gaussian distribution is satisfied.

Session G-5 0855-Tues. CRO-30
WHAT IS THERE LEFT TO STUDY ABOUT THE IONOSPHERE AND WHY?
Chairman: S.A. Bowhill, Dept. of Electrical Engineering, Univ. of Lowell, Lowell, MA 01854
Organizer: J.A. Klobuchar, Air Force Geophysics Lab, Ionospheric Research Divsion, Hanscom AFB, MA 01731

G5-1 0900 IONOSPHERIC STUDIES: WHAT REMAINS TO BE DONE:
J.V. Evans, COMSAT Labs, Clarksburg, MD 20871

Over the last quarter of a century great strides have been made in understanding the earth's ionosphere from satellite, rocket and incoherent scatter radar soundings together with numerical simulation modelling. This paper reviews the current state of knowledge and addresses the question of what remains to be accomplished. Three key issues that are imperfectly understood are i) the behavior of the neutral atmosphere, its composition and wind fields as functions of day, season and sunspot cycle, ii) the establishment of electric fields through the action of neutral winds and/or the action of the solar wind dynamo, and iii) the erratic deposition of energy via particle precipitation at high latitudes. These three factors govern the dynamics of the ionosphere and control most of its variability. Their effects are difficult to separate since heating, winds and electric fields are all coupled. Time-dependent numerical models that include all of the known processes, have realistic boundary conditions and are compared with the best available data sets appear to be the means for greater understanding.

G5-2
0940 THE F REGION AND THE THERMOSPHERE: UNFINISHED PROBLEMS

John S. Nisbet
Communications and Space Sciences Laboratory
The Department of Eletrical Engineering
The Pennsylvania State University
University Park, Pa 16802

Factors affecting the ionization levels in the F region of the ionosphere are reviewed. The main sources of variability are the winds and electric fields that control the transport and the solar EUV and particle fluxes that control the ionization rates. The degree to which each of these parameters could be predicted is investigated in relation to predictive ionospheric models.

Validating ionospheric models requires the comparison of predictions with actual measured values over extended temporal and geographic ranges. Available sources of data are examined to determine their suitability for such comparison purposes. This leads to an examination of the information content of data bases, the requirements of models and the relations between them.

G5-3
1020 RESEARCH OPPORTUNITIES IN HF MODIFICATION OF THE IONOSPHERE: W.E. Gordon, Rice Univ.

Major facilities for modifying the ionosphere with high power HF radiowaves operate in Puerto Rico, Scandinavia and the Soviet Union. The research opportunities are available in plasma physics, geophysics/aeronomy and communications.

G5-4
1100 **ISSUES IN OUR CURRENT UNDERSTANDING OF THE IONOSPHERE, ITS GLOBAL-SCALE DISTRIBUTIONS, AND ITS ROLE IN THE SOLAR-TERRESTRIAL SYSTEM**

E.P. Szuszczewicz
Science Applications International Corporation
Plasma Physics Division
1710 Goodridge Drive
McLean, Virginia 22102

Ionospheric physics is perhaps one of the most mature sciences in the general area of space plasma research. Its current state of understanding has been the result of accumulating contributions from experimental and theoretical programs with substantial advances having been made in such apparently diverse elements as equatorial spread-F and magnetospheric-ionospheric coupling. These advances however are only now emerging in concerted efforts that recognize that our wealth of knowledge is balanced with an almost equal abundance of remaining issues... with the apparent dichotomy resulting from scientific thrusts that look to broad scale coupling processes and the development of ionospheric predictive capabilities within the framework of the entire solar-terrestrial network. This paper will attempt to develop a perspective on our current understanding of the multiplicity of ionospheric processes and establish a view on a number of outstanding issues to be faced in the next decade of investigation.

G5-5
1120

IONOSPHERIC PHYSICS--WHITHER WAY: N.C. Gerson, Lab for Physical Sciences, 4928 College Avenue, College Park, MD 20740

Although it began cursorily with studies of atmospheric electrification and magnetic variations, ionospheric physics received sustained attention only well after Marconi's transatlantic transmission in 1901. For four decades advances in the science were small but progressive, and in the practice (ionospheric communications), marked and dramatic. Concerted studies of the physics spurted in the 1950s and again in the 1960s when in situ experiments aboard rockets and satellites became possible.

Three decades of governmental largesse brought unprecedented advances in ionospheric and magnetospheric physics, not only of the earth but of other planets as well. However, resent budgetary restraints has evoked cries of concern about the future of the science--cries that should have arisen earlier.

This paper attempts to quickly survey the past, and then examine prospects for the future: fruitful areas for exploration, assistance to practical problems, overambitious future expectations, and critical present shortcomings.

G5-6
1140

ON BETTER DEFINITION OF THE D-REGION

W. Swider
Ionospheric Research Division
Air Force Geophysics Laboratory
Hanscom Air Force Base, MA 01731

Considerable effort has gone into observing and modelling the D-region. Nevertheless, our understanding of the D-region is unsatisfactory in a number of ways, as will be detailed. As one example, the International Reference Ionosphere overestimates absorption under most conditions (B. G. Ferguson and L. F. McNamara, J. Atmos. Terr. Phys., 48, 41-49, 1986).

The D-region is difficult to measure and/or to model. In-situ observations are hampered by low quantities of charged particles and relatively high neutral pressures. Radio-wave data appear to provide useful information on the electronic profile of the D-region only for a limited height interval. Physical-chemical models of the quiet D-region require a good knowledge of nitric oxide concentrations plus parameters like water vapor and temperature. Temperatures for the D-region are available in the climatological sense. Satellite data of nitric oxide are available for E-region altitudes. This gas apparently is more abundant in the winter (darker) hemisphere. Only rough models of water vapor are available. The positive ion chemistry of the D-region appears to be well understood, but serious deficiencies in our knowledge of the negative ion chemistry remain. There is not a single case where D-region electron and ion concentrations, both positive and negative, have been matched satisfactorily by a model.

Disturbances of the D-region from solar flares, electron, and proton precipitation events can be enormous. Order of magnitude enhancements of the charged particle concentrations commonly occur. For these cases, the ionization rate must be determined in real time.

The best approach to modelling the D-region under various ionization conditions may be through the parameter $\Psi = q/[e]^2$, where q is the ionization production rate, and where [e] is the electron concentration. This ratio apparantly increases monotonically with decreasing altitude. Furthermore, it is not strongly dependent on q or other parameters. Comparison of all D-region data and models in terms of Ψ might be the best way to make a more precise and utilitarian model of the D-region.

Session H-3 0835-Tues. CR1-40
WAVE, PARTICLE AND MASS INJECTIONS IN SPACE PLASMAS I
Chairman: W.W.L. Taylor, TRW Space and Technology Group, One Space Park, Redondo Beach, CA 90278

H3-1
0840 ALFVEN WAVES FROM AN ELECTRODYNAMIC TETHERED SATELLITE SYSTEM

R.D. Estes
Harvard-Smithsonian Center for Astrophysics
Cambridge, Massachusetts 02138

An orbiting system consisting of a long, vertically oriented, dielectric-coated, conducting tether and two terminating satellites capable of exchanging charge with the ionosphere transfers charge between the two vertical layers of the ionosphere with which it is in electrical contact. This current flow is induced by the Lorentz force acting on the charges in the system as they move through the geomagnetic field. The regions of net charge produced by the passage of the system travel away from the system in the form of Alfvén wave packets (the "Alfvén wings") along the magnetic field lines.

The present analysis considers a tethered system current distribution that takes into account the system's peculiar "dumbell" shape. The Alfvén wing currents and Alfvén wave impedance are calculated, and the results are compared with previous calculations. It is argued that the frequency band lying between the lower hybrid and electron cyclotron frequencies, recently found to have a very high wave impedance for the case of a thin orbiting cylinder, is of a greatly reduced significance for more realistic tethered system geometry and dimensions.

H3-2 0900 FEASIBILITY OF AN ORBITING ELECTRODYNAMIC TETHER AS A GENERATOR AND INJECTOR OF E.M. WAVES FROM A FEW HERTZ TO A FEW KILOHERTZ

M.D.Grossi
Harvard-Smithsonian Center for Astrophysics
Cambridge, Massachusetts 02138

The first use ever suggested for an orbiting tether (actually the reason put forward initially to develop such a tether at all) was to generate and inject into the ionosphere e.m. waves in several frequency bands, ranging from a few hertz to a few kilohertz. The scientific motivation was to simulate natural phenomena such as micropulsations and whistlers. It is therefore not surprising that experiments are being planned, both for the TSS demonstration flights and for post-TSS missions, aimed at providing the feasibility proof of the tether's ability to generate and radiate e.m. waves in a broad frequency band.

Among the related investigations, there is the study of a self-powered, drag-compensated, tethered satellite system, as an orbiting transmitter potentially of practical relevance, in a frequency band that extends from a few hertz (ULF) to a few kilohertz (VLF).

For this system,several issues of feasibility have already emerged, and numerous problem areas have been already identified. The most relevant are : (a) the tethered satellite lifetime must be at least six months - because the self-powered operation of the system uses kinetic energy to produce electric energy, drag-compensation is mandatory, in order to obviate with height losses as large as 500 Km/day; (b) the area illuminated by each satellite on the Earth surface must be of the order of 10^7 Km^2, in order to meet the requirement that a cluster of less than ten satellites be sufficient to cover the entire surface of the globe; (c) the required level of e.m. wave injected power must be sufficient to provide on the Earth surface a communication-rated Signal-to-Noise ratio, against a noise density that is as large as 10^{-7} At/m $Hz^{-1/2}$ at ULF and 10^{-8} At/m $Hz^{-1/2}$ at VLF- we are talking here of injected power levels of the order of 1 Kilowatt at ULF and of 100 Kilowatt (or larger) at VLF.

While for item (a) above, a practical and feasibile solution has been already identified, investigations are still underway to solve problems (b) and (c) . Solution of the former may reside in the tether's ability to excite from above long-range guided modes in the Earth-ionosphere waveguide, thus maximizing the area on the Earth surface that is illuminated by the orbiting tether.Solution of the latter must be sought both in the area of radiophysics and in the realm of space technology, and focus on the study and design of high-power, small-size e.m. generators, of the self-powered tethered variety.

H3-3
0920

A SELF-CONSISTENT INTEGRAL EQUATION FOR THE CURRENT IN AN INSULATED CONDUCTING ELECTRODYNAMIC TETHER

K. J. Harker and P. M. Banks
Space, Telecommunications, and
Radioscience Laboratory
Stanford University
Stanford, CA 94305

There is currently a great interest in using the electrodynamic tether for power generation, orbital control, and generation of low frequency waves. Important to these applications is a knowledge of the current flow in the tether induced by its motion across the geomagnetic field lines.

A theory based on the equivalence principle of electromagnetic theory is presented in this paper for the current induced in a conducting tether whose surface is insulated everywhere except at its extremities. The theory leads to a surface integral equation and is consistent, i. e. the fields generated by the currents induced in the tether by its motion satisfy the boundary conditions at the plasma-tether interface. Both conducting and perfectly conducting bodies are considered.

H3-4
0940

RADIATION FROM LARGE SPACE STRUCTURES IN LOW EARTH ORBIT WITH INDUCED AC CURRENT: D.E. Hastings, Dept of Aeronautics and Astronautics, MIT, Cambridge, MA 02139

Large conducting space structures in low earth orbit will have a significant motionally induced potential across their structures. The induced current flow through the body and the ionosphere causes the radiation of Alfven and lower hybrid waves. This current flow is taken to be AC, which it may be due either to inductive coupling from the power system on the structure or by active modulation, and the radiated power is studied as a function of the AC frequency. A typical Space Station and tether are studied and it is shown that for the Space Station the radiation impedance is particularly high for frequencies in the tens of kilohertz range.

H3-5
1040

AN ANALYSIS OF THE HARMONIC STRUCTURE OF VLF RADIATION GENERATED BY A SQUARE WAVE MODULATED ELECTRON BEAM IN SPACE.

G.D. Reeves, P.M. Banks, R.I. Bush, K.J. Harker
STAR Laboratory
Stanford Univ.
Stanford CA, 94305
D.A. Gurnett
Dept. of Physics and Astronomy
University of Iowa
Iowa City IA, 52242

During both the STS-3 and Spacelab-2 space shuttle missions a 1 keV, 100 mA, square wave modulated electron beam was injected in the ionospheric plasma and the resulting electric and magnetic fields measured with an array of plasma diagnostic instruments including a wide band spectrum analyzer. The results of both missions showed narrow-band emissions at the pulsing frequencies and harmonics of those frequencies. The harmonic structure showed considerable variation from one pulsing sequence to another.

The theory of Harker and Banks (1983, 1985 and 1986) predicts the amplitude of the fields generated by a coherent pulsed electron beam. Many pulsing sequences show good agreement with the results of the theory while others deviate significantly. Those deviations include not only variation from the predicted intensity but also the presence of emissions at frequencies not predicted by the theory and even occasional presence of half integral harmonics. Quantitative comparisons of the measured and predicted wave intensities will be presented and possible controlling plasma parameters will be discussed.

H3-6 1100 ECHO 7 - A NEW INVESTIGATION OF CONJUGATE ECHOES AND BEAM-PLASMA PHYSICS IN THE AURORAL IONOSPHERE

J. R. Winckler and K. N. Erickson
School of Physics and Astronomy, University of Minnesota
Minneapolis, MN 55455
P. R. Malcolm - Air Force Geophysics Laboratory
Hanscom Air Force Base, Bedford, Massachusetts 01731

ECHO-7 is a new electron beam sounding rocket experiment scheduled for a November 1987 launch from the Poker Flat Research Range in Alaska. The ECHO-7 experiment will consist of three free-flying diagnostic packages and a main payload containing a 40 KeV, 0.25 Ampere electron accelerator. All four payload sections will be equipped with a variety of electron detectors for making measurements of conjugate echoes. Following experience with ECHO 1, ECHO 3 and ECHO 4, ECHO-7 will be sent on a magnetic east trajectory to insure a high probability of echo detection. The echoes will be used as magnetospheric probes to study the acceleration, injection and diffusion of trapped particles. The importance of strong pitch angle diffusion for natural and artificial beams was shown by ECHO-5 and will be further investigated by the ECHO-7 experiment. In addition, magnetic field line inflation during moderately disturbed times will be analyzed through measurement of echo bounce times and energies. Finally, the extensive hot plasma region generated by electron beams as well as intense electric fields, flow patterns and ELF wave production shown particularly by the ECHO-6 experiment will be investigated by two of the free-flying payload sections equipped with orthogonal electric probes, wave analyzers and plasma particle detectors. The nose cone will comprise a third free-flying diagnostic package containing a plasma wave detection system. Other instrumentation on the free-flyers will include spectrometers for measuring transverse ion acceleration and a TV camera for imaging from a distance the luminous plasma around the electron beam and beam emitting main payload. In addition to the accelerator, the main payload will include a tethered probe for payload potential measurements, a Faraday rotation ammeter for emission current and return current measurements and other particle detectors and photometers. Ground based observations will be made with low light level TV cameras, radar, and electromagnetic wave receivers. The ECHO-7 effort involves a major collaboration between the Winckler group at Minnesota and the Air Force Geophysics Laboratory, as well as the Kellogg group at Minnesota, the Arnoldy group at the University of New Hampshire, the Hallinan group of the University of Alaska and the Torbert group of the University of Alabama. The program is sponsored by the Plasma Physics Division of NASA Headquarters.

H3-7
1120

CHARGE-2, A SOUNDING ROCKET PAYLOAD TO STUDY THE EFFECTS OF THE EMISSION OF A LOW POWER ELECTRON BEAM INTO THE LOW EARTH ORBIT ENVIRONMENT

W. J. Raitt, N. B. Myers
Center for Atmospheric and Space Sciences
Utah State University
Logan, UT 84322-3400
P. M. Banks, P. R. Williamson, R. I. Bush
STAR Laboratory
Stanford University
Stanford, CA 94305
S. Sasaki, K-I. Oyama, N. Kawashima
Institute of Space & Astronautical Science
6-1 Komaba 4-chome, Meguro-Ku
Tokyo 153 - Japan

In December, 1985, a NASA sounding rocket propelled an active space plasma experiment into the ionosphere above the White Sands Missile Range, N. M. The experiment designated Co-operative High Altitude Rocket Experiments (CHARGE-2) formed part of a continuing series of joint US/Japanese rocket payloads. The purpose of these payloads has been to study vehicle charging and related effects using a section of the rocket as a tethered, electrically connected reference electrode, relative to which the electrical potential of the platform containing an electron gun can be measured. The payload of this latest experiment was comprehensively instrumented to measure vehicle charging at very high time resolution, beam plasma interaction effects and tethered system characteristics in the low earth orbit space environment. In this paper a brief description of the payload and the flight program will be given. The charging results due to electron beam emission will be discussed in terms of the vehicle current/voltage relationship in the ionosphere. This behavior will be further related to strong evidence of a beam plasma interaction indicated by wave generation in the VLF and HF frequency ranges when the electron beam is being emitted.

H3-8
1140

ENHANCED PLASMA WAVE GENERATION OBSERVED DURING PULSED ELECTRON BEAM EMISSION

R. I. Bush, T. Neubert, P. M. Banks
STAR Laboratory, Stanford University
Stanford, CA 94305
D. A. Gurnett
Department of Physics and Astronomy, University of Iowa
Iowa City, IA 52242
W. J. Raitt
Center for Atmospheric and Space Sciences, Utah State University
Logan, UT 84322

The Vehicle Charging and Potential Experiment (VCAP) was flown on the STS 51-F Shuttle mission in July and August of 1985 as part of the Spacelab-2 payload. Part of the VCAP investigations was the observation of the interaction of electron beams emitted by the VCAP Fast Pulse Electron Gun (FPEG) with the ambient plasma. Electron beams were produced with an energy of 1 keV and currents of 50 or 100 milliamperes. In addition, the electron beam could be square wave modulated by switching the high voltage supply accelerating the electrons. Several different experiments were performed in which the electron beam pulsing frequency was varied between 10 Hz and 20 kHz.

One FPEG sequence was designed to test the dependence of plasma wave generation on the electron beam pulsing frequency. In this sequence, the electron beam was pulsed at nine different frequencies between 1.2 kHz and 8.7 kHz. Observations of plasma waves produced by the pulsed electron beams were made by instruments on the Plasma Diagnostic Package (PDP) which made wide band measurements of both the electric and magnetic field fluctuations up to 30 kHz. This pulsing experiment was operated both when the PDP was located in the Orbiter payload bay and on the Remote Manipulator System. The amplitude of the plasma waves generated by the pulsed electron beam in this experiment peaked between 5 kHz and 8 kHz. At the Orbiter altitudes flown during the Spacelab-2 mission, the oxygen lower hybrid frequency was also in the range of 5 kHz to 8 kHz. Comparisons of the plasma wave generation efficiency as a function of the relative positions of the electron beam and the PDP, and other environmental parameters will be discussed.

Session J-4 0955-Tues. CR2-6
MILLIMETER AND SUBMILLIMETER TECHNIQUES IN RADIO ASTRONOMY I
Chairman: P.F. Goldsmith, FCRAO, Univ. of Massachusetts, Amherst, MA 01003

J4-1
1000 PROGRESS REPORT ON THE JAMES CLERK MAXWELL TELESCOPE

Richard Hills *
Cavendish Laboratory
Madingley Road
Cambridge, England

The construction of this 15 metre diameter antenna, funded by the United Kingdom and the Netherlands, has recently been completed on Mauna Kea in Hawaii. The antenna is to be used for radio astronomy at millimetre and sub-millimetre wavelengths, the long-term goal being to provide useable performance at the 690 GHz transition of CO.

The presentation will review the design features of the telescope, which include a large rotatable housing to provide protection from storms, a membrane of PTFE in front of the dish to keep off wind and sun, a fully "homologous" backing structure, and the use of electrically driven adjustors to set the positions of the surface panels.

Special attention will be paid to the question of measuring the shape of the surface. Three independent methods are being employed, photogrammetry using a substantial number of camera positions, radio holography with a relatively nearby source, and an opto-mechanical measuring machine. Detailed descriptions of each method will be given together with the latest results achieved.

The drive system, pointing measurements, secondary mirror and instrumentation will also be described in outline.

*Present Address: United Kingdom Telescopes
665 Komohana Street
Hilo, HI 96720

J4-2 **THE CALTECH SUBMILLIMETER OBSERVATORY**
1020

T. G. Phillips
California Institute of Technology
Pasadena, California 91125

The Caltech Submillimeter Observatory has been under construction since 1984 on Mauna Kea, Hawaii. It consists of a 10.4 diameter radio style antenna, constructed by Dr. Robert Leighton, which has achieved a surface accuracy of 10 μm (rms) in the laboratory. The telescope is housed in a dome with moveable shutter doors which permit a clear aperture for observations. The dome also provides observing facilities such as data rooms, receiver preparation rooms and computer facilities.

All basic construction is now complete and instrumentation is being fitted to the telescope. Two foci will be used; side-cab which will support single mode heterodyne receivers; a Cassegrain mount which will be used for bolometer continuum detectors and arrays of various kinds. Because of the opacity of the atmosphere, even from the mountain top altitude of 4,200 m, observations can only be carried out to about 900 GHz, so that both heterodyne and bolometer detectors will be designed to reach this limit.

Telescope check out and optimization will commence this autumn. It is expected that some observations of limited types will be possible during 1987.

J4-3
1040

NOBEYAMA RADIO OBSERVATORY TODAY: THE 45 METER TELESCOPE AND THE MILLIMETER WAVE INTERFEROMETER

Tetsuo Hasegawa
Nobeyama Radio Observatory
Tokyo Astronomical Observatory
University of Tokyo
Nobeyama, Minamisaku, Nagano 384-13, Japan

The 45 meter telescope has been in regular operation including open use at frequencies ranging from 8.8 GHz up to 115 GHz. The topics to be covered are as follows:
1. Gain of the antenna. Improvement of the surface accuracy based on holographic measurements.
2. Pointing performance. Change of the subreflector from the Gregory type to the Cassegrain type, etc.
3. Multiband observation capability. Simultaneous observations using any two out of 22, 40, 80, and 100 GHz band receivers.
4. The 32,000 channel acousto-optical spectrometer system.
5. Receiver developments. SiS receivers being developed at Nobeyama.
6. Test at 230 GHz. The 45 meter telescope is being tested at 230 GHz this winter.

The 5 element millimeter wave interferometer starts its open use at 22 GHz this winter. Developments and test observations to bring it into regular operation at higher frequencies (40 - 115 GHz) are being made.

J4-4
1100

THE OWENS VALLEY MILLIMETER-WAVE ARRAY

L. G. Mundy
Owens Valley Radio Observatory
Caltech 105-24
Pasadena, Ca. 91125

The Caltech Owens Valley Radio Observatory (OVRO) Millimeter-Wave Interferometer currently consists of three 10.4-m telescopes operating at 95-115 GHz. The telescopes are movable on tracks arranged in an inverted T with baselines out to 100-m east and west and 140-m north. The instrument is equipped with low noise SIS receivers and continuum and analog filterbank correlators. The array is primarily used for spectral-line aperature systhesis mapping of molecular emission lines from star formation regions in our galaxy and external galaxies.

There are several improvements planned for the instrument over the next several years. The array is scheduled to begin limited operation at 230 GHz during the Winter of 1986-7 and go into normal operation at this frequency during the Winter of 1987-8. The design phase has begun for a high speed digital correlator which will replace the present filterbank correlator. The digital correlator will have a large number of channels of selectable frequency width which may be divided into sub-groups and independently placed within the overall 500 MHz bandpass of the system.

In addition, a NSF proposal for a major expansion of the array is pending. The proposed expansion will include 3 additional dishes, dual polarization capability, and sub-aperature illumination which will allow 5-m sub-areas of the primary dishes to be interferred. The total instrument will be capable of full imaging on spatial scales ranging from 0."5 to several arcminutes.

J4-5
1120

PRESENT STATUS AND FUTURE PLANS FOR
THE HAT CREEK MILLIMETER ARRAY

J. Welch and R. Crutcher
Radio Astronomy Laboratory
University of California
Berkeley, California 94720

The current status of the interferometer is summarized, including brief descriptions of the antennas and electronics. Plans for expansion from three to six antennas will be described. The expansion will be a joint project with the University of Illinois and will become the Berkeley-Illinois Array.

A key aspect of the larger array will be the development of an image processing capability at Urbana, based on the Cray super-computer, which will be the means for reducing the array data. Data will go directly from Hat Creek to Urbana, where it can be reduced by astronomers at Urbana, at Berkeley over a fast communication link, or at other Universities through the new high-speed links to super-computer centers. Because the array will be available to visitors for 50% of the time, this last connection is important. Although the number of baselines in the proposed array is modest, the multi-spectral-line capability (512 complex channels) of the instrument calls for the comprehensive image processing capability that is planned.

J4-6
1140

EXPERIENCES WITH THE IRAM 30-m MILLIMETER TELESCOPE

J.W.M. Baars
Max-Planck-Institut für Radioastronomie
5300 Bonn, Germany

The 30-m Millimeter Radio Telescope has been in operation for about 1.5 years. This telescope is the first instrument of the Institute for Radioastronomy in the Millimeterrange (IRAM), which is a French-German collaboration with headquarters in Grenoble, France. A complementary instrument, an array of three 15-m antennas is under construction.

The instrument is located at 2850 m altitude in the Sierra Nevada, near Granada in southern Spain. It is an exposed telescope, equipped with receivers for the 3, 2 and 1.2 mm wavelength atmospheric window.

The telescope employs a homologous design to minimize residual gravitational deformations. At the same time it is sufficiently stiff to carry the windloads. To decrease thermal deformations the entire structure is insulated. Moreover critical sections of the structure are actively controlled in temperature.

The experiences gained during the commissioning period will be described, as well as the presently achieved performance. The surface accuracy is about 80 μm, measured by radioholography at 22 GHz with the aid of the strong water vapor maser source in Orion. Tracking stability is better than 1" in winds up to 12 m/s, while the pointing accuracy is better than 2" rms over the entire sky. These characteristics can be maintained throughout the day with the aid of the active control of the temperature of the telescope's structure.

The performance will be illustrated with results of the commissioning program. Selected examples of astronomical results will be shown to illustrate the potential of this new instrument and plans for further development of the telescope and its instrumentation will be outlined.

Tuesday Afternoon, 13 Jan., 1355-1700

Session B-8 1355-Tues. CR2-28
NUMERICAL TECHNIQUES
Chairman: W. Ross Stone, IRT Corp., 1446 Vista Claridad, La Jolla, CA 92037

B8-1
1400

A SCHEME FOR AUTOMATIC COMPUTATION OF FOCK-TYPE INTEGRALS

L. W. Pearson
McDonnell Douglas Research Laboratories
P. O. Box 516
Saint Louis, MO 63166

This presentation concerns the evaluation of the transition functions that characterize the variation of the electromagnetic field in the vicinity of the geometrical-optics shadow-boundary on a curved surface, in both the distant-source/distant-observer and the distant-source/near-observer cases. These functions have come into extensive use in the Geometrical Theory of Diffraction (P. H. Pathak, Radio Science, 14, 419-435, 1979) and in hybrid numerical scattering computations (L. N. Medgyesi-Mitschang and D.-S. Y. Wang, I.E.E.E. Trans. Ant. Propagat., AP-31, 570-583, 1983). It is desirable to have an automatic scheme for evaluating these functions in computer routines in an as-needed fashion, rather than depending on tabulated values. It is also attractive to be able to compute the transition functions for arbitrary surface-impedance values.

The integrands of Fock-type integrals comprise a slowly varying factor involving Airy functions and an exponential factor exp(jxt). The integration contour can be chosen so as to optimize the asymptotic decay of the slowly varying factor, but at the expense of destroying the Fourier transform form associated with the exponential factor. When the parameter x is large, the integrands are highly oscillatory with respect to t and the direct quadrature of the integrals becomes ponderously inefficient.

This paper presents a method for computation of the integrals based on the Fourier-trapezoidal rule (Tuck, Math. Comp., 21, 239-241, 1967) extended to integration along a path comprising complex-valued points. The slowly varying factor in the integrand is approximated by a piecewise linear representation, which may be integrated analytically against the oscillatory factor. The principal cost in evaluating the integrand is associated with the Airy functions in the slowly varying factor. The present scheme significantly economizes the number of evaluations of this factor. Furthermore, the slowly varying factor is independent of the parameter x, so that the overall computation time is relatively insensitive to the number of observation points at which the field is computed. A representative computational time is 12 s. on a VAX 11/780 for the computation of the Pekeris integral for fifty values of the observation point.

B8-2
1420

ACCELERATED NUMERICAL COMPUTATION OF THE SPATIAL DOMAIN DYADIC GREEN'S FUNCTION OF A GROUNDED DIELECTRIC SLAB

Bradley L. Brim and David C. Chang
Department of Electrical and Computer Engineering
University of Colorado
Boulder, CO 80309

In solving microstrip junction discontinuity problems, one often needs to obtain a numerically-efficient technique for computing the dyadic Green's function for a grounded dielectric-slab whose spatial domain representation consists of a two-dimensional inverse Fourier transformation. By going to circular cylindrical coordinates, this inverse Fourier transformation may be reduced to a one-dimensional semi-infinite integration, which involves a branch cut and at least one pole very near the path of integration. It is well known that for large distances between source and observation points it is numerically efficient to deform this path of integration to yield at least one residue term and a branch cut integral (whose integrand decays exponentially very quickly). For small distances, however, the integration along the positive real axis is often more efficient.

We present a method that allows us to perform the same deformation of contour for moderate and even small distances and still maintain numerical efficiency. The method involves the subtraction of the asymptotic portion of the spectral domain Green's function from the Green's function itself. This asymptotic portion of the spectral domain Green's function physically represents the static field due to a point source and has an analytically known spatial domain counterpart.

Results will be presented that demonstrate this method's accuracy and its relative improvement of computation time for electrically small, moderate, and large separations of source and observation points.

In addition, we have also developed a cubic-spline approximation of the dyadic Green's function over a wide range of distances and proceeded to evaluate the four-dimensional surface integrals associated with the moment-method solution of a two-dimensional surface-current integral equation for a microstrip structure. The coupling integral associated with the static-field term, which we substrated out in the numerical computation, can in fact, be evaluated analytically. Numerical accuracy of the computed-moment integral also will be demonstrated.

B8-3
1440 A UNIFIED APPROACH TO THE SOLUTION OF ILL-CONDITIONED MATRIX PROBLEMS ARISING IN ENGINEERING AND PHYSICS

Byron Drachman, Department of Mathematics
Edward Rothwell and Michael A. Blischke,
Department of Electrical Engineering
Michigan State University
East Lansing, Michigan 48824

Ill-conditioned matrix problems arise often in engineering, typically through the discretization of a Fredholm integral equation of the first kind. Solutions are usually undertaken by using Tikhonov regularization or by employing the singular value decomposition and discarding certain singular values. However, each method has shortcomings. Employing Tikhonov regularization worsens the conditioning of the matrix problem (by squaring the condition number), whereas discarding singular values is a discrete process, and may overlook the solution of least error. Also, if the error in the problem is due to experimental inaccuracy (as opposed to truncation or roundoff error) then the proper number of singular values to discard is difficult to determine.

We show how the best features of each of the above approaches can be combined into a simple technique which is quite useful for solving engineering problems where experimental inaccuracy is the main source of error. The technique does not worsen the conditioning of the matrix problem, and allows a simple method for determining the solution of least error.

Important applications of this technique include deconvolution of measured scattering data and the extraction of radar target parameters from measured time domain signals.

B8-4
1500 APPLICATION OF THE CONTROL REGION APPROXIMATION TO ELECTROMAGNETIC SCATTERING

G. Meltz, B. J. McCartin and L. J. Bahrmasel
United Technologies Research Center
Silver Lane
East Hartford, CT 06108

The control region approximation is a finite difference discretization scheme applicable on arbitrary computational meshes. Among its desirable features are accomodation of general geometries, ease of enforcement of flux boundary conditions and automatic satisfaction of jump boundary conditions across interfaces. This technique has recently been modified for increased accuracy in wave propagation problems (McCartin, Meltz, and Bahrmasel, SIAM Nat. Mtg., 1986). This paper describes the application of this method to electromagnetic scattering studies in two dimensional geometries.

In our formulation, we truncate the domain exterior to the scatterer at a finite distance from the scatterer and apply an artificial radiation boundary condition due to Bayliss and Turkel (A. Bayliss and E. Turkel, Comm. Pure Appl. Math 33: 707-725, 1980). The capabilities of this approach will be demonstrated on model problems which will include both perfectly conducting and layered dielectric cylindrical scatterers. The effect on accuracy of the placement of the outer boundary will be discussed and the effects of mesh density and placement will also be explored.

B8-5
1540

A NUMERICAL METHOD FOR TWO-DIMENSIONAL INTEGRATION OF FUNCTIONS WITH HIGHLY OSCILLATORY PHASE

Steven L. Dvorak, Robin S. Lyons
and Ronald J. Pogorzelski
TRW Space and Technology Group
One Space Park
Redondo Beach, CA 90278

Two-dimensional integrals involving functions with highly oscillatory phase are often encountered in physics problems. One of these problems is the calculation of the electric or magnetic fields for a reflector antenna system. The standard computational algorithm for these problems utilizes linear approximations for the phase and amplitude of the rapidly varying integrand (A.C. Ludwig, IEEE Trans. AP-16, Nov. 1968, pp. 767-769).

Another algorithm which effectively handles one-dimensional integrals was recently developed (R.J. Pogorzelski and D.C. Mallery, IEEE Trans. AP-33, June 1985, pp 800-804). This one-dimensional, quadratic phase algorithm approximates the rapidly varying phase by a quadratic polynomial, separates the quadratic phase exponential from the slowly varying part of the integrand, and expands this slowly varying piece in a Chebyshev series. The resulting constituent integrals, which contain Chebyshev polynimials multiplied by quadratic phase exponentials, are computed using recursion.

This quadratic phase algorithm was extended to two dimensions (R.J. Pogorzelski, 1985 North American Radio Science Meeting, Vancouver, B.C.). This extension is complicated to program, can require high precision arithmetic, and requires the one-dimensional quadratic phase algorithm many times. In this paper, a method will be discussed where a two-dimensional recurrence relation is used to evaluate the constituent integrals. This method is straightforward, requires less CPU time, and yields more accurate results then the previous two-dimensional routine. This method also lends itself to error analysis for the constituent integrals.

B8-6 1600 A GENERALIZATION OF THE POLYNOMIAL PHASE ALGORITHM FOR NUMERICAL INTEGRATION

R.J. Pogorzelski and I.K. Strother
TRW Space and Technology Group
One Space Park
Redondo Beach, CA 90278

Recently, the development of a class of numerical integration algorithms was reported. (R.J. Pogorzelski, IEEE Trans. AP-33, 563, 1985) (R.J. Pogorzelski and D.C. Mallery, IEEE Trans. AP-33, 800, 1985) These algorithms are particularly effective in computing integrals having rapidly oscillating integrands such as one might encounter in calculating the far field of a reflector antenna by means of the physical optics approximation. Generalization of this class of algorithms to two dimensional integrals was also recently reported in the context of a method of moments approach to the thin wire using travelling wave basis functions. (R.J. Pogorzelski, Nat. Rad. Sci. Mtg. Digest, June 1986, Pg. 62) In that work and in the entire domain Galerkin approach (L.N. Medgyesi-Mitschang and J.M. Putnam, IEEE Trans. AP-33, 1090, 1980) one encounters integrals which possess not only oscillatory but nearly singular integrands. The present work concerns generalization of the polynomial phase algorithm to accommodate such integrands. This has application in the Galerkin method of moments and in integration of surface currents which possess edge singularities.

The technique employed begins with the computation of a concomitant set of integrals with nonsingular integrands involving Chebyshev polynomials of various degrees. These integrals are then converted to ones with a first order singularity outside the range of integration but possibly very close to one of the limits. This conversion involves asymptotic approximation of a "high order Chebyshev" integral followed by a recursive procedure which generates all of the lower order ones. Subsequently, similar sets of integrals with any desired order singularity can be generated as desired provided, of course, that the singularity lies outside the range. This last requirement may necessitate subdivision of the region of integration and separate treatment of the "singularity region".

B8-7
1620

GALERKIN SOLUTION FOR THE THIN AND THICK CIRCULAR IRIS IN CIRCULAR WAVEGUIDE

Robert W. Scharstein
Department of Electrical and Computer Engineering
Clemson University
Clemson, South Carolina 29634

Arlon T. Adams
Department of Electrical and Computer Engineering
Syracuse University
Syracuse, New York 13210

The integral equation for the transverse electric field in the aperture of a circular iris in a circular waveguide is approximately solved by Galerkin's method. The aperture field is represented by a finite sum of normal TE and TM circular waveguide modes that fit the circular aperture, henceforth denoted as aperture modes. The elements of the aperture admittance matrix are given as infinite summations over the waveguide modes of the inner products between the aperture modes and the waveguide modes. These inner products can be expressed as integrals involving the scalar potential functions from which the TE and TM modal fields are derived. The resultant infinite series involving Bessel functions is approximately summed using a Kummer transform with the asymptotic form of the Bessel functions. The case of a thick circular iris in a circular waveguide is treated by the standard microwave technique of even and odd excitation about the transverse plane of symmetry.

The self convergence of the Galerkin 'solution' is demonstrated via resultant aperture field distributions, scattering parameters, and equivalent circuits for the case of dominant TE_{11} mode incidence. The resultant aperture electric field distribution closely resembles that of the TE_{11} aperture mode alone, except at the edge of the iris where the normal component of the electric field becomes large. This is the manifestation of the edge condition in the finite sum approximation of the Galerkin 'solution'. The agreement between the calculated scattering parameters and experimental data is excellent.

B8-8 1640 DETERMINATION OF THE NATURAL-MODE PARAMETERS OF A DIELECTRIC SLAB FROM MARCHING-ON-IN-TIME RESULTS.

Anton G. Tijhuis
Department of Electrical Engineering
Delft University of Technology
P.O. Box 5031, 2600 GA Delft, The Netherlands

We consider the identification of an inhomogeneous, lossy dielectric slab in vacuo in terms of its natural-mode parameters. To this aim, we try to determine the relevant parameters from the transient reflected and transmitted fields excited by an incident pulse of finite duration with the aid of a Prony-type method. With the marching-on-in-time method outlined in [1], we are able to determine such signals direcly in the time domain up to a specified accuracy. On the other hand, the analysis of [2] has provided us with an accurate procedure to determine the natural frequencies, and with initial instants for the validity of the SEM representation at each space point. Therefore we are in the unique position to test Prony's algorithm for an actual, albeit simple configuration.

The main obstacle to a successful application of Prony's algorithm to a slab signal seems to be the total residual contribution from higher-order poles. Numerical experiments show that this contribution may considerably disturb the reconstruction. This problem cannot be resolved by increasing the sampling rate. This would destroy the accuracy in the reconstruction of the lower-order poles, which are most characteristic for the slab configuration.

A preprocessing procedure will be proposed that adapts the reflected and transmitted fields resulting from a sine-squared incident pulse to the limitations of Prony's algorithm. The procedure consists of successively applying a suitable low-pass frequency filtering, a suitable time-delay filtering, and a suitable resampling to the transient fields computed by the marching-on-in-time method. When this preprocessing procedure is included in the Prony-type computation, the resulting scheme can indeed recover the natural frequencies of a given slab. By repeating the computation several times, even noisy signals can be handled.

Representative numerical results will be presented and discussed.

References

[1] A.G. Tijhuis, IEEE Trans. Antennas Propagat. 29, 1981, pp. 239-245.
[2] A.G. Tijhuis and H. Blok, Wave Motion 6, 1984, pp. 61-78, and Wave Motion 6, 1984, pp. 167-182.

Session C-3 1355-Tues. CR1-9
SPECTRAL ESTIMATION: GENERAL SIGNAL PROCESSING
Chairman: D.J. Thomson, AT&T Bell Labs,
600 Mountain Avenue, Murray Hill, NJ 07974

C3-1
1400 ON THE USE OF MAXIMUM ENTROPY SPECTRUM ESTIMATION IN IONOSPHERIC PROBLEMS: Paul F. Fougere, AFGL/LIS, Hanscom AFB, MA 0111731

The Burg Maximum Entropy Method (MEM) will be presented and briefly described. A series of computer simulations which compare Burg-MEM to periodogram will be reviewed. The simulations show that careful windowing and/or end matching are required for periodograms. Even then, periodograms are much noisier than MEM spectra and if periodograms are stacked and averaged to reduce the spectral variance, time resolution is lost. In contrast, the MEM spectrum is always smooth and requires only a short segment of time series data. Thus MEM is an ideal method for analyzing data sets whose properties change slowly with time in such a way that short segments are approximately stationary (in the weak sense).

MEM will be applied to a number of real ionospheric data sets, including scintillation measured at ground stations on signals launched from satellites, (e.g. MARISAT and HILAT), in-situ ion density and velocity data from the atmospheric explorer (AE) satellite, PIIE rocket campaign data, and neutral air density data measured on a polar orbiting satellite.

We hope to prove convincingly that Burg-MEM is a reliable tool that belongs in every ionospheric experimentalist's tool-kit--and we will even provide a complete Fortran package to assist all those who want to try it.

C3-2
1440

IDENTIFICATION OF TOEPLITZ AND CIRCULANT CORRELATION MATRICES FOR THE SPECTRUM ANALYSIS OF STATIONARY AND PERIODIC TIME SERIES

Louis L. Scharf and Philippe J. Tourtier
Electrical and Computer Engineering
University of Colorado
Boulder, CO 80309

Stationary time series have Toeplitz correlation matrices and periodic time series have circulant correlation matrices. This forms the basis of our claim that the first step when estimating spectra should be to compute maximum likelihood, minimum entropy, or constrained minimum entropy estimates of Toeplitz or circulant matrices. The next step is to pass these matrices to MA, AR, or eigen methods of spectrum modelling.

We review our refinements to the algorithm published by Burg, et. al., for estimating structured correlation matrices and present the results of our numerical experiments.

C3-3
1540

AN EXPERIMENTAL ADAPTIVE SUPER-RESOLUTION RADAR SYSTEM

Simon Haykin, Vytas Kezys, Terry Greenlay and
Ed Vertatschitsch
Communications Research Laboratory
McMaster University
Hamilton, Ontario, Canada L8S 4K1

The subjects of adaptive signal processing and super-resolution spectrum estimation are currently attracting a great deal of attention. In this paper, we describe an experimental radar system intended to provide real data for the experimental evaluation of these techniques in the context of a low-angle tracking radar environment. A distinguishing feature of this environment is the presence of multipath (due to the proximity of the target to a reflecting water surface), which can vary from a highly specular (correlated) to a highly diffuse (uncorrelated) condition. The description includes detailed accounts of the transmitter, the 32-element sampled-aperture receiver, and calibration of the receiver. The experiments are being conducted at a site located on Lake Huron. The apparatus has been designed with the aim of evaluating algorithms for angle-of-arrival estimation and adaptive signal detection in the presence of nonstationary multipath conditions.

The paper also includes a presentation of preliminary results on the modified FBLP and minimum-norm algorithms, obtained with radar data collected from the apparatus.

C3-4
1620

SPECTRAL EXTRAPOLATION WITH POSITIVITY:
Philip Stark, Scripps Institute of Oceanography, LaJolla CA 92093; and David L. Donoho, Dept. of Statistics, Univ. of California, Berkeley, CA 94720

Super-resolution is the (claimed) ability of some nonlinear signal processing algorithms to exceed the fundamental limits of resolution which have been established for linear methods (e.g. the Rayleigh criterion, Backus-Gilbert theory, etc.) For example, some of these methods claim to be able to reconstruct a wide-band signal from noisy band-limited data. Such methods claim to work because they exploit side information about the signal to be recovered (e.g. that the signal is time-limited, or positive, or blocky, or sparse). They are currently of great interest in radio astronomy, absorption and NMR spectroscopy, and in seismic prospecting.

In this talk I will study the resolving power of positivity constraints. I will investigate how positivity can be used in reconstructing wide band signals from narrow-band measurements. Positivity constraints can be very valuable, but only for certain very special classes of positive signals. Computing the resolving power of such constraints requires the solution of certain nonlinear eigenvalue problems whose linear forms remind one of problems familar from the theory of prolate spheroidal functions. I will give results of calculations quantifying the resolving power of positivity constraints. I will also briefly discuss various methods which claim to be super-resolving, such as maximum entropy.

Session E-1 1355-Tues. CR1-42
ELECTROMAGNETIC INTERFERENCE ENVIRONMENT:
MEASUREMENT AND MODELS
Chairman: Prof. Joel Morris, Electrical
Engineering Dept., Howard Univ., 2300 6th St. NW
Washington, DC 20059

E1-1
1400 OUT-OF-BAND RESPONSE OF REFLECTOR ANTENNAS

David A. Hill
Electromagnetic Fields Division
National Bureau of Standards
Boulder, Colorado 80303

The response of antennas to out-of-band frequencies plays an important role in interference and jamming problems. Reflector antennas are of particular interest because they are used so frequently and because they have a strong response to above-band frequencies. The analysis of reflector antennas at above-band frequencies is complicated by the presence of higher-order modes which can propagate in typical waveguide feeds. Frequencies well below the in-band frequency are not important because they are cut off by typical waveguide feeds.

We have analyzed a symmetrical parabolic reflector in the receiving mode using physical optics. Approximate expressions for the fields and the Poynting vector in the focal region can be obtained for either on-axis or off-axis incidence [A.R. Valentino and P.P. Toulios, IEEE Trans., AP-24, 859-865, 1976]. For above-band frequencies, we integrate the Poynting vector over the aperture of the feed horn to obtain the total received power in all the propagating modes. Realistic feed systems respond differently to the different waveguide modes, but the total multimode power provides a useful upper bound to actual received power. The analysis yields an approximate expression for the effective aperture which yields both the receiving pattern and the frequency response.

The theory has been compared with previously published measurements for frequencies from 3 GHz (in-band) to 10 GHz. The pattern agreement is good, but the measured gain falls below the theoretical results. This discrepancy is caused by mismatch loss in the coax-to-waveguide adapter, and this loss tends to increase with frequency. We have analyzed the mismatch loss of the adapter using a variational technique, and it can be included in the theory to improve the agreement with the above-band measurements.

E1-2
1420

POISSON NOISE FIELD MODELS FOR TELECOMMUNICATIONS

David Middleton
127 East 91 Street
New York, NY 10128, USA

Both natural and man-made noise sources, with emitters and emissions randomly distributed in space and time, provide the principal (external) interference against which telecommunication systems must operate. When emissions are independent, or when the location of the (possibly correlated) sources are independent, or both, various forms of poisson space-time processes can be constructed. From these, in turn, it is possible to obtain not only the lower order field moments, e.g., means, variances, and covariances, which are useful in assessing the effects of spatial processing, but even first- and second-order probability densities (pdf's). These latter are critical in the derivation and approximation of optimum and suboptimum algorithms for threshold signal detection and estimation (D. Middleton, IEEE Trans. Electromag. Compat., Vol. EMC-26, No. 1, pp. 19-38, Feb. 1984; D. Middleton, Proc. 6th Int'l. Symp. on EMC, Zürich, Switzerland, pp. 429-435, March 5-9, 1985).

Here we construct a general class of quasi-poisson (q.p.) distributions (e.g., those having at least one set of independent physical parameters, namely, emission times, locations, etc.) (D. Middleton, Proceedings of 20th Conference on Information Sciences and Systems, Princeton Univ., Dept. of E.E., March 1986). From these we obtain the canonical first- and second-order pdf's describing most classes of interference fields, α, (and received noise processes $X = \hat{R}\alpha$, $\hat{R}$ = array operator). The gaussian class is shown to be a limiting case. Specific results illustrate the general model: field moments and first- and second-order pdf's representative of telecommunications interference scenarios arising in multilink transmission and reception are presented and discussed; (based on work supported under contract with ITS/NTIA, Boulder, Colo., U.S. Dept. of Commerce).

E1-3
1440

A MODEL FOR PREDICTING VHF/UHF ELECTROMAGNETIC NOISE FROM POWER LINES

R.G. Olsen, B. Stimson
Electrical and Computer Engineering Department
Washington State University
Pullman, WA 99164-2752

It has been shown that corona discharges on power line conductors can be modeled as electric dipoles driven by impulsive currents. Each dipole induces traveling wave currents in both directions along the conductor. These currents radiate as back to back traveling wave antennas. The response of a receiver to a single discharge can be predicted by calculating the far field of the induced current distribution and using the directional pattern and input impedance of the receiving antenna. Since the corona sources are incoherent at these frequencies (R.G. Olsen, Radio Sci., 18, 399-408, 1983) the received noise power is the sum of the noise powers from each source.

A computer program for an IBM personal computer has been written to implement this model. The output of the program has been calibrated using measured 75 Mhz noise data taken in steady rain conditions. Comparisons will be shown between predictions and measured results in the VHF and UHF ranges.

E1-4
1500

A NEW THEORY OF LEAKAGE FOR BRAIDED COAXIAL CABLE

Charles M. McDowell
Department of Electrical Engineering
University of Missouri-Rolla
Rolla, MO 65401

A new theory that fully accounts for braid periodicity has been developed to explain the leakage mechanisms for braided coaxial cable. The fields and the propagation constant are found for a cable immersed in its own insulating material. The braid is modeled as a multifilar contrawound tape helix, and fields are obtained that satisfy Maxwell's equations and Floquet's theorem. The technique is based on a method developed by Sensiper and applied to analyze a helical delay line (L. Stark, JAP 25, 1155-1162, 1954) and a slow-wave structure for traveling wave tubes (M. Chodorow and E.L. Chu, JAP 26, 33-43, 1955). Perturbation theory is then used to remove the outer dielectric.

The results show than an infinite set of space-harmonic surface waves exists on the braid. The zeroth order wave accounts for all leakage unless a discontinuity occurs in the period of the braid; then space harmonics are converted to radiated modes and leakage may increase by many orders of magnitude. The power contained in the surface harmonics is computed and compared to the power in the zeroth order surface wave.

Another facet of this theory is a more accurate formula for surface transfer impedance Z_T, according to which

$$Z_T = j\,0.2\,\omega\,\frac{\cos\alpha}{\pi F^2 C}\left(\tan^2\alpha - \frac{1}{2}\,\frac{\varepsilon_r - 1}{\varepsilon_r + 1}\right)\sum_{m=1}^{\infty}\frac{\sin^2(m\pi F)}{m^3}\quad(\mu\Omega)$$

where F = fill of braid, C = number of carriers, α = pitch angle, and ε_r = dielectric constant. This formula shows that optimum braid is achieved when

$$\tan\alpha = \sqrt{\frac{1}{2}\left(\frac{\varepsilon_r - 1}{\varepsilon_r + 1}\right)}$$

These formulas will be supported by published measurements (E.F. Vance, IEEE Trans EMC, 17, 71-77, 1975; K.J. Teperek and F.A. Benson, Proc. IEE, 120, 1219-1225, 1973).

E1-5 1540 WIDEBAND HF NOISE AND INTERFERENCE MEASUREMENT SYSTEM

L.G. Abraham, L.S. Dozier, L. Lau, D.C. Rogers,
W.K. Talley, B.G. Thornton, and B.J. Turner

The MITRE Corporation
Burlington Road
Bedford, MA 01730

MITRE is engaged in a comprehensive program to develop and apply wide bandwidth spread-spectrum technology to new HF communication systems. Worldwide characterizations of wide bandwidth interference (signals) and noise (atmospherics) are essential in designing such HF radio systems. These factors are important in sizing the antennas, transmitter power, and receiver sensitivity. More directly, such information is essential in designing interference excision and noise canceling circuits.

It has become practical with VLSI devices to use extensive coding for error correction and to seriously consider the use of wideband (1 MHz) direct sequence (pseudonoise) signals coupled with interference excision techniques. Increasingly powerful digital processing makes it possible to take advantage of short-term (seconds or fractions of seconds) variations in interference and noise and permits more detailed resolution (100 Hz) in the frequency spectrum processed.

In 1986 a wideband HF noise and interference measurement system to record data over instantaneous bandwidths of 1 MHz was completed. This system is able to gather data in the form of four different 100 millisecond long "snapshots" with known time separations between adjacent "snapshots" up to ten seconds. This will permit frequency resolution of at least 100 Hz. The measurement system will be deployed in the field in 1987 to selected spots in the U.S.

This paper will describe that wideband HF noise and interference measurement system. Samples will be presented of the 1 MHz wide bandwidth frequency spectrum that is obtained.

E1-6 1600 TIME DOMAIN ANALYSIS FOR A TRANSMISSION LINE SUBJECTED TO THE ELECTROMAGNETIC PULSE ENVIRONMENT: G. Costache, Univ. of Ottawa, Ontario, Canada K1N 6N5

A time domain analysis for a transmission line subjected to fast transient electromagnetic environment, such as produced by EMP, is presented. The time varying property of the transmission line parameters is taken into account by solving the corresponding field problem in time domain (figure 1).

The analysis has shown that when very fast transients such as EMP, ESD or lightning have to be addressed, a time domain solution can be used to characterize their impact into transmission lines and to obtain the induced voltages and currents for very short time periods.

Based on a time domain solution of the Maxwell's equations a time domain resistance characterizing the losses in transmission lines is taken into account for calculations.

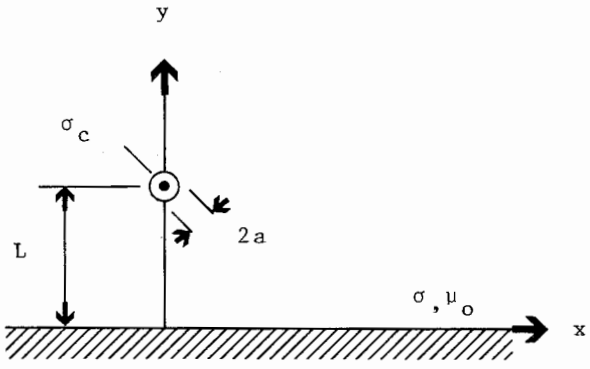

Figure 1. Transmission line above ground

E1-7
1620

SECOND-ORDER NON-GAUSSIAN PROBABILITY DISTRIBUTION OF CLASS B NOISE AND INTERFERENCE FIELDS

David Middleton
127 East 91 Street
New York, NY 10128, USA

First-order probability density functions (pdf's), $w_1(x)$, are usually sufficient to determine optimum threshold algorithms for signal detection and estimation. However, with second-order pdf's $w_2(x_1,x_2)$, it is now possible to obtain estimates of performance improvement, as well as modifications in algorithm structure, which result when sample correlations, in both space and time, are specifically taken into account. Moreover, the "classical" theory of rectification, measurement, and signal detection, which employs zero-memory nonlinear (XMNL) devices can now be implemented explicitly for general nongaussian (e.g., Class A, B, or C) noise (D. Middleton, Proceedings 20th Conference on Information Sciences and Systems, Princeton Univ., Dept. of E.E., March 1986). Noise processes $x(t)$, and noise fields $\alpha(\underset{\sim}{R},t)$, where $x = \hat{R}\alpha$ ($\hat{R}$ = array operator) can be constructed, examined, and employed. It is emphasized that these noise processes (and fields) are not ad hoc, but are physically derived.

Here we are specifically concerned with Class B interference. Class B noise or interference is a nongaussian process characterized by random, overlapping impulsive transients produced in typical receivers by broad-band incoherent sources, EM examples of which are ignition noise, lightning, etc. (D. Middleton, IEEE Trans. on Electromag. Compat., Vol. EMC-26, No. 1, pp. 19-38, Feb. 1984; D. Middleton, ibid., Vol. EMC-19, No. 3, pp. 106-127, Aug. 1977). To obtain explicit results in application, it is necessary to approximate the Class B structure. This is done here by a new model, using a second-order set of gaussian characteristic functions, and associated pdf's, matched to the means, variances, and covariances of the process or field in question. The result is a canonical, manageable four-term sum of gaussian forms. Application to telecommunication noise and interference, as well as other cases (e.g., scattering from random rough surfaces) illustrate the approach; (work supported under Contract N00014-84-C-0417 with Code 1111-SP).

Session F-4 1355-Tues. CR2-26
REMOTE SENSING OF ATMOSPHERIC AND OCEANIC WAVES, SEA ICE AND VEGETATION
Chairman: Calvin Swift, Dept. of Electrical Engineering, Univ. of Massachusetts, Amherst, MA 01003

F4-1
1400 THE LOW FREQUENCY MICROWAVE RADIOMETER FOR THE NAVAL OCEAN REMOTE SENSING SYSTEM: W. Linwood Jones, David E. Ball, and William F. Croswell, Harris Corp., Government Aerospace Systems Division, Melbourne, FL 32902; and Gene A. Poe, Aerojet Electro Systems Company, Azusa, CA 91702

The Naval Ocean Remote Sensing Sytem (NROSS) will be established in FY '91 with the launch of the NROSS-1 Spacecraft. NROSS-1 employs a synergistic complement of four microwave sensors: NASA Scatterometer (NSCAT) operating at 14 GHz to measure ocean surface windspeed and direction; Radar Altimeter (ALT) operating at 13.5 GHz to measure ocean surface height; Special Sensor Microwave Radiometer Imager (SSM/I) operating at 19, 22, 36 and 85 GHz to measure sea ice edge, atmospheric water vapor, cloud mass and precipitation; and Low Frequency Microwave Radiometer (LFMR) operating at 5 and 10 GHz to measure sea surface temperature, ocean surface wind speed and sea ice edge.

The LFMR is a conically scanned, large aperture, precision, 20-channel microwave radiometer to provide accurate brightness temperature images of the ocean surface. The scan geometry matches that of the SSM/I instrument by selecting a nominal earth incidence angle of 53.1° and a swath width of 1400 Km. The LFMR instantaneous field-of-view is 25 Km (along track) by 15 Km (cross track) at 5.4 GHz and 12.5 Km by 7.5 Km at 10.8 GHz. A multi-beam dual polarized feed cluster provides two spot beams at C-band and four beams at X-band; and in conjunction with the 15.8 rpm spin rate and radiometer sampling rate, LFMR achieves Nyquist sampling of the ocean surface in both the along and cross track directions.

This paper presents an overview of the proposed LFMR design with particular emphasis on the radiometric performance, antenna design, and in-orbit scan geometry.

F4-2
1420 THE EFFECTS OF ASYMMETRY AND DOPPLER SHIFT ON GRAVITY WAVE SPECTRA IN THE ATMOSPHERE OBSERVED BY MST RADAR

A. O. Scheffler and C. H. Liu
Department of Electrical and Computer Engineering
University of Illinois at Urbana-Champaign
Urbana, IL 61801-2991

The shapes and levels of observed atmospheric velocity fluctuation spectra can be altered by the presence of vertical and azimuthal asymmetries in the gravity wave spectrum. Such asymmetries can be parameterized in the model spectrum which enables the computation of theoretical radar-observed spectra. The results of these theoretical spectra will be presented and discussed. In addition, asymmetries can be incorporated into the numerical analysis by which the effects of the Doppler shift due to a background wind are evaluated. The results for numerical frequency spectra indicate that the combination of azimuthal asymmetry and Doppler shift can produce significant changes in spectral shape and level in comparison to the non-shifted spectrum.

F4-3
1440

ON THE OBSERVATIONS OF INFRASONIC WAVES AND ACOUSTIC-GRAVITY WAVES AT GROUND LEVEL

XIE Jin-Lai, YANG Xun-Ren, TIAN Shi-Xiu
(Institute of Acoustics, Academia Sinica)
and
LI Qi-Tai
(Meterological Science Institute of Guizhou)

Abstract

The investigation on atmospheric infrasonic waves from various sources is significant in many fundamental aspects concerning atmosphere. In this paper, a systematic description of observations at ground level is given, including the detailed discussions about the equipment system, the multi-element detector array, the data analysis and some typical results.

The infrasonic signals we have detected during the period more than twenty years involve both natural and man-made natures, such as those from typhoon, thunderstorm, hailstorm and other severe weathers and also from the eruption of Volcano St. Helens(1980) referred to the former, and those from atmospheric tests of nuclear bombs and also from the tragic explosion of space shuttle "Challenger"(1986) referred to the latter.

Especially, we have joined the WAGS campaign of October 1985, and lots of data have been recorded at our infrasonic observation stations situated in Yongan, Guiyang and Lasa respectively. The analysis to these data shows there are strong AGWs with periods within 5-42 minutes attached to the variations in solar cycle, and the coupling effects between ionosphere and ground layer is obvious.

The advantages of our observation means lie in the simplicity and economy in equipments, the continuity and reliability in records and the easiness in operation and maintenance. Futhermore, the advantages express also in the intuition of results and in the fact that the analogue data can be reserved on paper or magnetic tapes and thus can be real-time processed.

F4-4
1540

EVOLUTION OF THE DIRECTIONAL WAVE SPECTRUM FROM SHORELINE TO FULLY DEVELOPED

E.J. Walsh*, D.W. Hancock III, D.E. Hines
NASA/GSFC Wallops Flight Facility
Wallops Island, VA 23337
R.N. Swift and J.F. Scott
EG&G Washington Analytical Services Center
Pocomoke City, MD 21851

The Surface Contour Radar (SCR) is a 36-GHz computer-controlled airborne radar which generates a false-color coded elevation map of the sea surface below the aircraft in real-time, and can routinely produce ocean directional wave spectra with post-flight data processing which have much higher angular resolution than pitch-and-roll buoys. A cold air outbreak was occurring on January 20, 1983 when the NASA P-3 aircraft took off from Wallops Flight Facility and flew up the coast to the center of Long Island. The aircraft then turned and proceeded in the downwind direction for 300 km with the SCR measuring the evolution of the directional wave spectrum with fetch.

The surface weather observations were obtained from the National Climatic Data Center, Asheville, NC for sixteen reporting stations from Wallops Flight Facility to Nantucket. The observations indicate a spatially homogeneous offshore wind field in direction during a three day period before the flight. The Long Island shoreline is relatively straight and the contours of constant water depth are approximately parallel to the shoreline. The water depth increases rapidly and is never a factor in influencing the wave field.

When the SCR directional wave spectra are compared to the empirical expressions for wave growth, the JONSWAP growth rates for wave height and period are found to be in best agreement. The expression developed by Donelan et al. in Lake Ontario are furthest off, but they gave the best predictions for the direction of propagation of the waves near shore where the wind was briefly 25^{o} off the normal to the shoreline. Assuming that Donelan et al.'s measurements in Lake Ontario were correct leads to a new expression for the growth of fetch-limited waves which reconciles the disparities.

*Presently on assignment at the NOAA, ERL, Wave Propagation Laboratory, R/E/WP, Boulder, CO 80303

F4-5
1600

OBSERVATION OF SEA ICE USING THE 36-GHZ SURFACE CONTOUR RADAR

Leonard S. Fedor
NOAA/ERL/Wave Propagation Laboratory
Boulder, CO 80303
Edward J. Walsh* and Donald J. Cavalieri
NASA/Goddard Space Flight Center
Greenbelt, MD 20771

In January 1984 a 36-GHz scanning pencil-beam radar was used at 175-m altitude over ice in the Greenland Sea to produce high-spatial-resolution (3 m by 5 m) topographic and backscattered power maps. Incidence angles from nadir to approximately 30° off-nadir were included in the data set. When the radar maps were compared with the ice topography indicated by simultaneous photography and an analysis of the shadows of the ridges cast by the low sun angle (3.5°), it was found that the backscattered power data sharply delineated many of the features observed in the photography. The elevation data were less impressive but still consistent with the general variation of the topography.

For incidence angles more than 5° off-nadir, multiyear floes tended to be uniformly high in backscattered power in contrast to the lower power from the brash ice surrounding them. An observation was made of a composite flow in which two multiyear floes were connected by a band of interstitial first year ice. The multiyear portions produced high backscattered power while the band of first year ice joining them did not. Low backscatter was also produced by the brash ice on one side of the floe and the first year rubble on the other side of it.

*Currently on assignment at the NOAA/Wave Propagation Laboratory

F4-6
1620

RADAR CROSS SECTION MEASUREMENT CHARACTERISTICS OF SIMULATED VEGETATION CANOPY STRUCTURES

C. E. Nance and A. J. Blanchard
Wave Scattering Research Center
Department of Electrical Engineering
University of Texas at Arlington
P.O. Box 19016
Arlington, Texas 76019

Radar return characteristics of vegetation structures has become an important matter to address in order to better understand the remote sensing of the surface of planet earth. The experimental data that could be obtained from living vegetation structures is very difficult and time consuming to aquire due to the uncontrollability of the growth process of the plant matter. Simulation of vegetation structures is very useful due the fact the targets can be configured rather quickly compared to living structures, and can be varied in many different ways to more fully study the effects of the geometric structure on the return characteristics. The symmetry and consistency in structure of plants of a given type lends itself well to simulation of the canopy structure by a collection of identical simulation plants to produce a simulated canopy.

Several theoretical derivations to predict the backscattering cross section of a modeled canopy structure containing discrete scattering elements in a half space have been presented. The radiative transfer theory was applied to a layer of small randomly positioned and oriented ellipsoidal scatterers (L. Tsang, M. C. Kubacsi, and J. A. Kong, Radio Science, 321-329, 1981), and a canopy consisting of randomly oriented circular discs to model a vegetation canopy (M. A. Karam and A. K. Fung, Radio Science, 557-565, 1983) to calculate the backscatter from each modeled vegetation layer. These types of canopy structures could be used for modeling leafy vegetation canopies, but experimental data from live plant structures is difficult to apply for comparison to these models due to the fact that the geometry of the live plants cannot be represented in such models. The use of simulated vegetation canopies with plants comprised of elements with simple geometrical shapes to model branches, leaves, and stalks are simple enough to compare theoretical predictions, but are a good step toward more complex simulation that can be applied when the theoretical derivations can handle more complex geometries.

Previous research has dealt with the measurements of a simulated nodal structured plant canopy (D. F. Zook, Masters Thesis, University of Texas at Arlington) which examined the scattering response when the nodal spacing on a simulated stalk approaches one wavelength. This paper presents a more complex simulation of a vegetation canopy resembling that of soybeans or other leafy ground cover plants. The canopy structure consists of thirty simulated low dielectric plants each having adjustable branch angles. Metal circular disks, attached to the end of each branch, will serve as the leaf structure and the main scattering elements. The branch angle effects of the simulated plants on the scattering characteristics for distributions with small branch angles (0 - 20 degrees) and for uniform branch angle (0 - 90 degrees) will be presented.

F4-7
1640 SHORT-RANGE FM RADAR MEASUREMENTS WITH FINE SPATIAL R4ESOLUTION: R.K. Moore and S.P. Gogineni, Radar Systems and Remote Sensing Lab, Univ. of Kansas Center for Research, Inc

Swept-frequency methods have long been used to accomplish the same kinds of results as short-pulse measurements. Some swept measurements have been based on interpretation of the standing wave patterns caused by reflections using models for the target complex. FM radar, however, uses an approach more like that for short pulses. The received spectrum from a linearly-swept FM radar is essentially the same as a time-domain representation of a pulse return, and most of the same analysis techniques can be used to extract signal information. The PRF of the FM radar acts as a sampling comb in the frequency domain that is equivalent to temporal sampling of a time-domain return.

FM systems have advantages in that high peak powers are not required, and that the spectrum of the transmitted signal may be tailored to compensate for differences in antenna response and medium attenuation. Other processing on the receiving end may be used to compensate for phase distortions in the medium, if the nature of the distortion is known. Coherence cancellation of system and nearby static echoes may be achieved in the receiver.

Examples are given of systems and some of the problems encountered and, in most cases, solved.

Session G-6 1355-Tues. CR1-46
AURORAL AND POLAR CAP IRREGULARITIES
Chairwoman: Sunanda Basu, Emmanuel College,
400 The Fenway, Boston, MA

G6-1 PATTERNS OF POLAR IONOSPHERIC EFFECTS
1400 Herbert C. Carlson, Edward J. Weber and Jurgen Buchau
Air Force Geophysics Laboratory, Hanscom AFB MA 01731

A polar network of radio, radar and optical diagnostics has been applied to the testing, development, and validation of a framework within which major variability of the polar ionosphere can be ordered. Such variability is of direct importance to high latitude communication, tracking, positioning, and imaging by radio or radar techniques over the available portion of the rf spectrum. Deep within the winter polar cap, values of peak electron concentration, total electron content, and bottomside ionization can vary from quiet polar night values to values comparable to midlatitude midday conditions. Furthermore, these dramatic changes can appear to switch on or off in times as short as a few minutes, or more appropriately over distances as short as tens of km. These remarkable enhancements can persist over spatial scales of 10 to 1000 km (or intercept line of sight ray paths from minutes to an hour). Associated amplitude scintillation can switch from negligible to saturated 250 MHz and phase scintillation from negligible to that exceeding auroral and comparable to equatorial spread-F events. Widely diverse observed conditions can be ordered into two basic patterns of behavior, after allowing for identified dependences on interplanetary magnetic field (B_Z and B_Y), universal time, an index of magnetic activity, season and solar cycle. The source, evolution, coupling, and ultimate fate of ionospheric features leading to these polar effects are reviewed in light of the most recent experimental evidence collected to address these specific issues.

G6-2 1420 HF CHANNEL PROBE

R.P. Basler, G.H. Price, C.L. Rino, R.T. Tsunoda, and T.L. Wong
Radio Physics Laboratory
SRI International
Menlo Park, California 94025

An experiment in Greenland has measured the transfer characteristics for HF signals propagating through disturbed regions of the ionosphere. Transmissions over the 1-hop path from Narssarssuaq to Thule have suffered distortions in the range (propagation time) and Doppler domains on the order of hundreds of microseconds and tens of Hertz, respectively. A frequency-modulated continuous wave (FMCW) waveform was used for oblique sounding purposes, and a pseudorandom noise modulation with a 20-kHz bandwidth was used to measure range and Doppler spreads. Spaced receivers were used to measure azimuthal angle of arrival, and independent ionospheric diagnostic data for points along the path were provided by the incoherent-scatter radar and HILAT satellite ground station at Sondre Stromfjord. The results are interpreted in terms of scatter effects produced by high-velocity plasma irregularities encountered along the mean ray paths.

G6-3
1440 HIGH LATITUDE IRREGULARITIES: PLASMA INSTABILITY THEORIES

P.K. Chaturvedi
Plasma Physics Division
Naval Research Laboratory
Washington, DC 20375-5000

The theories on the generation of high latitude irregularities by plasma instability mechanism are discussed. The processes causing the irregularities at short scalesizes (on the order of ion Larmor radius) by kinetic instabilities and at longer scalesizes by fluid instabilities would be included.

G6-4
1540

THE STATE OF THE THEORY OF HIGH LATITUDE IONOSPHERIC PLASMA TURBULENCE

Charles E. Seyler
School of Electrical Engineering
Cornell University
Ithaca, NY 14853

A review is given on the theory of the turbulent plasma dynamics of the high latitude ionosphere. The principal purpose of this review is to draw connections between the existing body of experimental evidence of plasma turbulence in the ionosphere and the predictions of various plasma models which have been proposed to describe the dynamics of the turbulent ionosphere. The description of the macroscopic dynamics of the plasma motion is suggested to be embodied in a low frequency plasma model, which incorporates gradient drift, collisional drift, kinetic Alfven, current convective, and Kelvin Helmoltz processes. Various limiting forms of the model can be analyzed to determine the existence of a similarity range for the spatial power spectra of particular processes. The spatial predictions are testable in those situations where adequate plasma diagnostics exist to determine both electric and density fluctuations as well as potential sources of free energy for instability drive. An attempt is made to correlate the spectral predictions to the existing body of observations.

G6-5 1620 RADAR INTERFEROMETER STUDIES OF HIGH LATITUDE E-REGION IRREGULARITIES

Jason Providakes and Bela G. Fejer
School of Electrical Engineering
Cornell University
Ithaca, NY 14853

This work will review recent experimental results on the study of meter-scale auroral E-region plasma waves. VHF radar observations have shown that in addition to the type 1 (two stream) and type 2 (gradient drift) waves observed in the equatorial region, there are also plasma waves unique to the high latitude E-region. These include resonant echoes with Doppler shifts of about 70 Hz independent of the cross field plasma drift (type 3 waves), and two stream waves with phase velocities sometimes in excess of 900 m/s, associated with very large electron heating events (type 4 waves). High temporal and spatial radar interferometer observations have shown that during active periods strong echoes are often observed from highly localized and very dynamic scattering regions. These localized regions are generally associated with horizontal shears in the cross field plasma flow, and with large scale (> 10 km) irregular structures within the scattering volume. Recently, vertical interferometer measurements have been used to determine the height dependence of the different Doppler spectral components, and the effect of the magnetic aspect angle on the backscattered power and wave spectra. These results will be compared with previous observations and with recent theoretical studies.

G6-6
1640 NUMERICAL MODELING OF HIGH LATITUDE PHASE SCINTILLATION SPECTRA

S. J. Franke and C. H. Liu
Department of Electrical and Computer Engineering
University of Illinois at Urbana-Champaign
Urbana, IL 61801-2991

The theoretical phase scintillation spectrum is computed for irregularity models having scale size dependent anisotropy, and for ionospheric layers that do not satisfy the "thick slab" approximation. These features have been suggested as characteristics of nighttime auroral zone irregularities. The dependence of observed phase spectral indices on propagation geometry will be studied. Applications of the model to interpretation of experimentally measured spectra will be discussed.

Session G/H-1 1355-Tues. CRO-30
ELF/VLF RADIO WAVE PROPAGATION
Chairman: A.C. Fraser-Smith, Space, Telecommunications and Radioscience Lab, Stanford Univ., Stanford, CA 94305

G/H1-1 1400 STRUCTURE OF TM AND TE VLF MODES IN THE DAYTIME EARTH-IONOSPHERE WAVEGUIDE: CALCULATIONS AND MEASUREMENTS

E. C. Field, Jr.
Pacific-Sierra Research Corporation
12340 Santa Monica Boulevard
Los Angeles, California 90025
P. A. Kossey
Air Force Geophysical Laboratory
AFGL/LID
Hanscom Air Force Base, MA 01730

This paper reviews the properties of VLF transverse electric (TE) and transverse magnetic (TM) modes in the earth-ionosphere waveguide and presents measurements of the structure of such modes. Rocket probes launched from Wallops Island, Virginia measured TE and TM fields at all altitudes between the ground and the base of the ionosphere. The fields were radiated from a nearly horizontal airborne transmitting antenna and comprise one or more well-defined TE or TM waveguide modes. Calculated height profiles agree well with the measured ones and correctly reproduce details of profile structure caused by interaction between two or more modes. Additional calculations show the dependence of mode structure on ground conductivity.

G/H1-2
1420

MODELING OF VLF AND LF PROPAGATION USING WAVEGUIDE CONCEPTS

J. A. Ferguson
Ocean and Atmospheric Sciences Division (Code 544)
Naval Ocean Systems Center
San Diego, CA 92152-5000

Propagation in the earth-ionosphere waveguide at very low frequencies (vlf) is sensitive to low levels of electron densities and to the direction of propagation with respect to the geomagnetic field. Signals at vlf propagate to very long ranges introducing the additional complications of varying ground conductivity and ionosphere. The WAVEGUID and MODESRCH computer codes have been developed for application to the earth-ionosphere waveguide at vlf. Use of these computer codes in modeling paths for which experimental data exist will be described.

G/H1-3
1440

EMPIRICAL MODELING OF EASTERLY AND WESTERLY VLF PROPAGATION IN THE EARTH-IONOSPHERE WAVEGUIDE

R. A. Pappert
Ocean and Atmospheric Sciences Division (Code 544)
Naval Ocean Systems Center
San Diego, CA 92152-5000

It has been known for many years that easterly and westerly propagation of VLF in the earth-ionosphere waveguide is non reciprocal with the mean attenuation rate to the west being greater than to the east for ground to ground transmissions. It is also true that nighttime propagation to the west is more difficult to predict than is propagation to the east. For example, a simple exponential $\beta = 0.5$ km^{-1}, $h' = 87$ km (notation of Wait & Spies) profile does an excellent job of predicting nocturnal in-flight measurements over the Hawaii-San Diego path but does not predict nighttime propagation over the Hawaii-Wake path. This is partly due to the fact that propagation to the west is less stable than propagation to the east. In this paper full wave solutions will be used to show that propagation to the west is more sensitive to upper levels of the ionosphere than is propagation to the east. It therefore seems reasonable that propagation to the west senses more variable regions of the ionosphere than does propagation to the east and that this, at least in part, is responsible for the difficulty of predicting westerly propagation. Comparisons between calculations based on empirical electron density profiles and in-flight measurements between Hawaii and San Diego, and Hawaii and Wake will be presented.

G/H1-4
1500

ALFAN: A BALLOON EXPERIMENT TO MEASURE TE & TM NOISE IN THE EARTH-IONOSPHERE WAVEGUIDE

A.C. Fraser-Smith, P. McGill, and R.A. Helliwell
Space, Telecommunications and Radioscience Laboratory
Stanford University
Stanford, CA 94305
J.P. Turtle
Radio Propagation Branch
Rome Air Development Center
Hanscom Air Force Base
Massachusetts, MA 01731

Rome Air Development Center and the STARLAB at Stanford University recently cooperated on an experiment to measure low-frequency TE and TM noise at high altitudes in the Earth-ionosphere waveguide. The experiment, called ALFAN (for Airborne Low Frequency Atmospheric Noise), involved the flight of a specially-designed instrumentation package on a balloon. It took place on August 4, 1986, in New Mexico: the balloon was launched from a location near Roswell, it flew at an altitude of about 18–21 km for roughly five hours, and the flight was terminated near White Sands. The instrumentation package was parachuted to the ground and recovered without damage.

Atmospheric noise was measured throughout the flight using a three-axis loop antenna (two orthogonal vertical loops and one horizontal loop) suspended below the instrumentation package. Each loop had its own receiver circuitry, and the noise was measured in a band of about 1.5 kHz in the range 30 – 60 kHz. The center frequency of the 1.5 kHz band could be changed within its overall range by telemetry from the ground; the outputs from the receiver were digitized during the flight and transmitted to ground, where they were monitored and changes made to the center frequency of the 1.5 kHz measurement band as circumstances warranted.

It was anticipated before the flight that the TE noise levels would be on the order of about 10 dB lower than those of the TM noise. Preliminary analysis of the data suggests that the noise levels were roughly comparable. This result and other features of the noise measurements will be discussed.

G/H1-5
1540 THE SIPLE, ANTARCTICA VLF TRANSMITTER AS A PROBE OF THE EARTH-IONOSPHERE WAVEGUIDE

D.L.Carpenter, T.F.Bell, U.I.Inan, T.Wolf
STAR Laboratory
Stanford University
Stanford,CA 94305
A.J.Smith
British Antarctic Survey (NERC)
Madingley Road
Cambridge CB3 OET, U.K.

Waveguide signals from the Siple, Antarctica VLF transmitter (76S,84W,L=4.3), have been used in studies of (i) burst precipitation into the nighttime D region of the ionosphere,(ii) frequency dependent effects of radiation in the 2 - 10 kHz range from a single horizontal antenna element, and (iii) effects of radiation from crossed horizontal antenna elements. The observation points were at Antarctic stations Halley, Palmer, and South Pole, each about 1500 km from Siple. The burst precipitation experiments revealed fast changes in received signal phase and amplitude (Trimpi effects) associated with whistlers and VLF emissions propagating in the magnetosphere.

The frequency dependent effects included observation in the endfire direction of strong signals at the third harmonic of the half wave antenna resonance frequency. A preliminary explanation of frequency dependent effects in the 2 - 10 kHz range is given in terms of antenna properties and frequency dependent waveguide attenuation.

Recently a crossed element was added to the antenna system at Siple. A series of experiments has been conducted in which the antenna elements were excited so as to simulate radiation from horizontal antenna elements oriented in various directions. Preliminary results from these experiments will be described.

G/H1-6
1600

LIGHTNING-INDUCED ELECTRON PRECIPITATION EVENTS OBSERVED AT L~2.4 AS PHASE AND AMPLITUDE PERTURBATIONS ON SUBIONOSPHERIC VLF SIGNALS

U. S. Inan and D. L. Carpenter
STAR Laboratory, Durand 324
Stanford University, Stanford, CA 94305

Lightning-induced electron precipitation (LEP) events are studied using the Trimpi effect, in which the precipitation induced ionization enhancements in the lower ionosphere (D-region) give rise to rapid perturbations of subionospheric VLF signals. In 1983, the phase and amplitude of signals from the NPM transmitter in Hawaii (23.4 kHz) and the Omega transmitter in Argentina (12.9 kHz) were measured at Palmer, Antarctica ($L \sim 2.4$), together with the magnetospheric whistler background. The long baseline and over-sea great circle paths from these two sources made it possible for the observed perturbations to be interpreted using a single waveguide mode theory. Analytical expressions are used to relate the magnitude of the phase perturbations to differential changes in ionospheric reflection height along a segment of the propagation path. The predicted relationship between relative perturbation sizes on the two different signals is compared with measurements. From this information, the whistler-induced flux levels are inferred to be in the $10^{-4} - 10^{-2}$ erg cm^{-2} s^{-1} range and the precipitation regions are inferred to be roughly 'circular' in shape, rather than elongated along L-shells. Measured amplitude changes tended to be small ($\sim$ 0.5 dB) and negative, as expected from a single mode theory, but the ratios of simultaneous amplitude and phase perturbations were slightly larger than the theory predicts, probably due to to the effects of an additional mode(s). An assessment of the relative detectability of amplitude versus phase perturbations favors phase perturbations by $\sim$ 10 dB, irrespective of the detection scheme used.

G/H1-7
1620

STEERABLE ELF/VLF RADIATION PRODUCED BY AN ARRAY OF IONOSPHERIC DIPOLES GENERATED FROM HF HEATING

D. H. Werner and A. J. Ferraro
Communications and Space Sciences Laboratory
Department of Electrical Engineering
The Pennsylvania State University
University Park, PA 16802

A VLF or ELF dipole source has been created within the lower ionosphere by modulating the atmospheric dynamo currents with a ground based high power HF source from the Arecibo Observatory. The authors and their colleagues have demonstrated that ELF or VLF generated this way and injected into the earth-ionosphere waveguide could be received a few thousand kilometers away. The injection properties due to an array of ionospheric dipoles as a function of array geometry and element currents that will allow steerable ELF/VLF radiation within the earth-ionosphere waveguide are investigated theoretically. The ionospheric array factors for a linear and a planar array of Hertzian dipole sources are developed and their properties examined. The principle of pattern multiplication is then applied to include the effect of the ionospheric array element. This provides a means for predicting the field strengths at a remote receiving site due to a steerable linear or planar array of ionospheric sources generated by high power HF periodic plasma heating.

G/H1-8
1640

DIRECT PROBE MEASUREMENTS RELEVANT TO RADIO WAVE PROPAGATION

L. C. Hale, J. D. Mitchell, C. L. Croskey,
S. P. Blood, and K. J. Goodnow
Communications and Space Sciences Laboratory
Department of Electrical Engineering
The Pennsylvania State University
University Park, PA 16802

In the sensible ionosphere (above about 70 km), parameters affecting radio wave propagation can be measured using radio techniques as well as direct probes, which include RPA's, ion traps, and "Langmuir" and impedance probes. At lower altitudes Gerdien condensers are used for ion conductivity, mobility, and density; but ion conductivity can readily be measured using simple probes, although below about 60 km, this must be done subsonically to reduce error. Simple probes have been used for electron measurements, with some discrepancies. A "last frontier" may be the accurate measurement of free electrons at very low altitudes, even into the stratosphere under disturbed conditions. Electronic conductivity at these altitudes is important to radio propagation, particularly at VLF and ELF.

The design of probe systems for making accurate measurements at low altitudes is considered. Identified problems include:

1. Probe theory including fluid flow, angle of attack, and optimum velocity, the non-linear mobility of electrons, and the effects of negative ions and aerosol particles.
2. Practical considerations such as surface uniformity, the effects of insulating surfaces, outgassing, sensitivity, and time response.
3. Radiation effects, including photo-emission and the effects of energetic particles.
4. The effects of electric fields, including "stray" fields, vehicle potential effects, and environmental fields.
5. The design of "return" and ancillary electrodes, including area and length ratios necessary to minimize error.
6. A fundamental problem that some of these considerations dictate large, and some small, probe radius of curvature.

Strategies for overcoming these problems are discussed and a tentative proposed probe system design is described.

Session H-4 1355-Tues. CR1-40
WAVE, PARTICLE, AND MASS INJECTIONS IN SPACE PLASMAS
Chairman: W.W.L. Taylor, TRW Space and Technology Group, One Space Park, Redondo Beach, CA 90278

H4-1 1400 INSTABILITIES OF ARTIFICIAL FINITE SIZE ELECTRON BEAMS IN THE IONOSPHERE

C. S. Lin
H. K. Wong
Southwest Research Institute
Department of Space Sciences
P.O. Drawer 28510
San Antonio, TX 78284

The linear theory of excitations of electrostatic waves by the interaction of a finite-size electron beam in a cold magnetized plasma is presented. The electron beam is assumed to be cold and to drift along the magnetic field with a beam energy about several keV. Charge and current neutralization are assumed to be maintained. The temporal and spatial growth rates of beam plasma instabilities are computed for frequencies from ion cyclotron frequency to the electron plasma frequency. Initial results indicate that the perpendicular wave length inside the beam is of the order of the beam radius. The spatial damping length outside the electron beam is examined for estimating the heating region and the wave propagation distance. These results are applied to explain measurements from the SEPAC (Space Experiments with Particle Accelerators) and recent Spacelab 2 electron beam experiments.

H4-2
1420

ION RELEASES AT ROCKET ALTITUDES

Craig J. Pollock and Roger L. Arnoldy
Institute for the Study of Earth, Oceans and Space
University of New Hampshire
Durham, New Hampshire 03824

Lawrence J. Cahill and Robert E. Erlandson*
School of Physics and Astronomy
University of Minnesota
Minneapolis, Minnesota 55455

Paul M. Kintner
Department of Electrical Engineering
Cornell University
Ithaca, New York 14853

NASA flight #29.015 was the third in a series of missions designed to study the interaction of injected heavy ion beams with the ambient ionospheric plasma. As in the two previous flights, phenomena associated with ion injections were clearly distinguishable in both the charged particle and plasma wave signatures. In this case, beam-associated waves and particles were observed on the main payload as it moved away from the beam-emitting subpayload up to separation distances of nearly 1 km. The sub-payload featured two Ar+ ion generators with one firing across geomagnetic field lines and the other firing anti-parallel to the field lines, toward the main payload. Each generator was designed to produce a ~200 eV, 100 mA ion beam with an angular spread of ~30 degrees (FWHM). During both perpendicular and parallel firings, strongly ordered and highly reproducible ion populations were observed at the main payload at unexpected energies and pitch angles. Anti-parallel firings produced the expected 200 eV anti-parallel ion component as well as two unexpected components at 90 degrees pitch angle; one near the gun energy and the other at ~15 eV. Cross-field firings also produced two 90 degree populations; one near 100 eV and the other, as in the anti-parallel case, at ~15 eV. The plasma wave data show emissions at several species gyro-harmonics as well as near the local lower hybrid resonance frequency for an Ar+ - 0+ plasma in addition to absorption features at H+ gyro-harmomics.

* Currently at The Applied Physics Laboratory, Johns Hopkins University, Laurel, Maryland.

H4-3
1440

WAVES GENERATED BY AN ARGON ION BEAM

L. J. Cahill, Jr. and R. E. Erlandson
Space Science Center
University of Minnesota
100 Union Street S.E.
Minneapolis, MN 55455

Two argon beams were operated on a spinning subpayload of a sounding rocket at 200 to 400 km altitude. One of the beams was emitted perpendicular to the magnetic field and the other upward, parallel to the field. Waves were observed at the main payload, above the guns, on the same field line at separation distances up to 800 m. During perpendicular beam operations, ion cyclotron harmonics of hydrogen ions were observed near 350 km altitude and harmonics of oxygen ions above that. Line emissions near hydrogen cyclotron harmonics and also near the lower hybrid frequency were observed during parallel beam operations. Near peak altitude at 404 km absorption lines in the auroral hiss band were observed with separations near the hydrogen cyclotron frequency. Ions were also observed at the main payload during gun operation, some with energies and pitch angle appropriate for the beam ions and others at higher and lower energies.

H4-4
1520

INITIAL MOTION AND MOMENTUM COUPLING FOR THE AMPTE COMETS

A. T. Y. Lui
The Johns Hopkins University
Applied Physics Laboratory
Laurel, MD 20707
K. Papadopoulos
SAIC
McLean, VA 22102
J. D. Huba
Naval Research Laboratory
Washington, D. C. 20375-5000

The Active Magnetospheric Particle Tracer Explorers (AMPTE) program has created two artificial comets, one in the solar wind on December 27, 1984 and the other in the magnetosheath on July 18, 1985, with the release of about 2 kg of barium on each occasion. This experiment was conducted with comprehensive in situ plasma diagnosis. One unanticipated feature common in both cases is that the barium cloud did not move initially in the direction of the solar wind flow as a result of momentum coupling between the two plasmas. Instead, the cloud was seen moving perpendicular to both the solar wind flow and the interplanetary magnetic field direction (A. Valenzuela et al., Nature, 320, 700-703, 1986). Based on the in situ magnetic field observations, we deduce that the barium ions within the main portion of the cloud were magnetized. Consequently, the unexpected sideway motion of the cloud can be understood as a $\vec{F} \times \vec{B}$ drift resulting from any momentum coupling force $\vec{F}$ between the barium cloud and the streaming solar wind. Another prominent feature from the AMPTE comet experiments is the occurrence of intense electrostatic waves during the gradual recovery of the compressed interplanetary magnetic field back to the nominal value (D. A. Gurnett et al., Geophys. Res. Lett., 12, 851-854, 1985). We suggest that this wave activity is also a product of momentum coupling between the Ba^+ cloud and the solar wind protons via a cross-field counter-streaming ion instability. The observed wave frequencies and saturation amplitudes are found to be consistent with this interpretation.

H4-5
1540

STRUCTURING OF THE AMPTE MAGNETOTAIL BARIUM RELEASES

J.D. Huba, J.G. Lyon, and P. Bernhardt*
Naval Research Laboratory
Washington, DC 20375-5000
A.B. Hassam**
Science Applications International Corp.
McLean, VA 22102

The AMPTE magnetotail barium releases of March 21, 1985 and May 13, 1985 displayed the expected characteristics of a high kinetic beta (β_k = plasma kinetic energy/magnetic field energy >> 1), radial plasma expansion: (1) the barium plasma forms a relatively dense shell and expands at roughly the magnetosonic speed, (2) diamagnetic currents are set up on the surface of the shell which generate a magnetic cavity, (3) the expansion stops when the initial plasma kinetic energy of the expansion is comparable to the 'swept-up' magnetic field energy, and (4) the magnetic cavity eventually collapses, returning to the pre-release field configuration. These gross features are reasonably well described by ideal MHD theory even though the ion Larmor radius (ρ_i) is comparable to the scale size of the expansion. One aspect of these releases which is not well described by ideal MHD theory is the large scale, field-aligned structuring of the shell; this occurs during the latter half of the expansion phase. We develop a set of one-fluid FLR (finite-Larmor-radius) MHD equations which is applicable to the AMPTE magnetotail barium releases, i.e., $\rho_i \sim R_c$. The gross expansion characteristics are studied using a 2D MHD magnetic-flux-tube-coordinate code. The stability properties of the cloud are studied using standard linear stability theory. Two unstable regimes are found: the usual magnetic interchange mode ($\gamma = \sqrt{g/L_n}$), and a new, faster growing mode ($\gamma = k\sqrt{gL_n}$). Here, γ is the growth rate, g is the deceleration of the cloud, L_n is the scale length of the density at the edge of the cloud, and k is the azimuthal wavenumber. The results are compared to AMPTE data.

* Permanent Address: Los Alamos National Laboratory
Los Alamos, NM 87545
**Permanent Address: University of Maryland
College Park, MD 20742

H4-6
1600

SIMULTANEOUS OBSERVATIONS OF PC 3-4 PULSATIONS IN THE SOLAR WIND AND IN THE EARTH'S MAGNETOSPHERE

M. J. Engebretson
Augsburg College
Minneapolis, MN 55454
L. J. Zanetti and T. A. Potemra
The Johns Hopkins University
Applied Physics Laboratory
H. Lühr
Technische Universität Braunschweig
W. Baumjohann
Max-Planck-Institut für extraterrestrische Physik
M. H. Acuna
NASA/GSFC

The equatorially orbiting AMPTE CCE and IRM satellites have made numerous observations of Pc 3-4 magnetic field pulsations (10-100 s period) simultaneously at locations upstream of the earth's bow shock and inside the magnetosphere. These observations show solar wind/inteprlanetary magnetic field (IMF) control of two categories of dayside magnetospheric pulsations. 1. Harmonically structured, azimuthally polarized pulsations are commonly observed from L = 4 to 9 in association with upstream waves. Varying levels of broadband, compressional wave power are associated with these pulsations. 2. More monochromatic compressional pulsations are clearly evident on occasion, with periods identical to those observed simultaneously in the solar wind. Harmonically structured, azimuthally polarized pulsations also occur in conjunction with these compressional pulsations. In both cases the harmonic pulsations display frequencies characteristic of local resonant conditions. As in earlier studies there is clear control of the occurrence of pulsations both inside and outside the magnetosphere by the cone angle of the IMF, and the amplitude of magnetospheric pulsations increases when the solar wind velocity increases. This data set and other recent observations at cusp latitudes suggest a high latitude entry mechanism for wave energy related to harmonically structured pulsations.

H4-7
1620

SUBSIDIARY DIFFUSE PLASMA RESONANCES IN THE IONOSPHERE: Vladimir A. Osherovich, Cooperative Institute for Research in Environmental Science, Colorado State Univ., Ft. Collins, CO

A recently developed theory of force-free electromagnetic oscillations is employed to interpret the diffuse plasma resonances stimulated by topside ionospheric sounders at the frequencies f_{Dn}. The main prediction of the theory, namely, that the spectrum of frequencies should be proportional to: $n^{1/2}$, $n = 1, 2, 3, \ldots$ has been checked against obserations. It has been found that $f_{Dn} \simeq 0.95 (f_N f_H)^{1/2} n^{1/2}$ is a fair approximation for diffuse ionospheric resonances where f and f are the plasma frequency and electron gyrofrequency, respectively. The author suggested that hybrid frequency $F_n = (f_{Dn}^2 + f_H^2)^{1/2}$ should be found in topside sounder observational data. This second prediction is verified in the paper. The author identifies subsidiary diffuse plasma resonances with hybrid resonances F_n for $n = 1, 2, 3, 4$.

Session J-5 1355-Tues. CR2-6
MILLIMETER AND SUBMILLIMETER TECHNIQUES IN RADIO ASTRONOMY II
Chairman: P.F. Goldsmith, FCRAO, Univ. of Massachusetts, Amherst, MA 01003

J5-1
1400 STATUS OF THE IRAM INTERFEROMETER

J. Delannoy and D. Downes
Institut de Radioastronomie Millimetrique
Voie 10, Domaine Universitaire
38406 St. Martin d' Heres - France

The millimeter Interferometer of the Institut de Radioastronomie Millimetrique (I.R.A.M.) is being constructed on the Plateau de Bure, 100 Km south of Grenoble, France. In its iniial stage, the interferometer will consist of three 15m antennas movable on baselines of 288m EW and 160m NS.

The antennas represent new technology for radio astronomy, in that the panels are carbon fiber, with a Hostaflon film coating, and the reflector support structure has lower and upper struts also made of carbon fiber. The purpose of incorporating carbon fiber in the reflector structure is to obtain high thermal stability.

As of October 1986, all three movable mounts of the telescopes, built by Neyrtec (Alsthom Atlantique, Grenoble) are finished. Of the reflectors, built by Neue Technologie (M.A.N., Munchen), the first one has been mounted on the Plateau, and the initial surface adjustment gave an overall accuracy better than 80 micrometers RMS. The second and third antennas of the interferometer are expected to be finished by Summer 1987.

An additionnal antenna of this series is being completed at La Silla, Chile, under the supervision of I.R.A.M., for the European Southern Observatory (E.S.O.) and the Onsala Space Observatory.

J5-2
1420

IMAGING FOCAL PLANE ARRAY FOR MILLIMETER WAVELENGTH ASTRONOMICAL SPECTROSCOPY

Paul F. Goldsmith
Neal R. Erickson
F. Peter Schloerb
Five College Radio Astronomy Observatory
Department of Physics and Astronomy
University of Massachusetts
Amherst, MA 01003

We have been engaged in the development of a focal plane array receiver for the 14m FCRAO radio telescope. This is a critical area for development of millimeter receiver systems, since the best receivers are approaching being limited by atmospheric emission and imaging is the only way of significantly increasing the data rate. The key frequency range identified is 90-116 GHz which includes the J=1-0 transition of CO (widely used for galactic and extragalactic mapping) as well as tracers of higher-density interstellar material such as CS and HC_3N, and also isotopic variants of carbon monoxide. The Cassegrain focal ratio of 4.15 is not a serious limitation in terms of number of focal plane pixels. Rather, the expense of equiping each pixel with a spectrometer system of broad capability encompassing high resolution ($\Delta f \leq 100$ kHz) for studies of dark clouds to broad coverage ($\Delta V = 1000$ km s^{-1}; $\Delta f = 300$ MHz) limits the number of pixels. An array of 15-16 elements, each with a cooled Schottky barrier diode mixer and FET IF amplifier is the present design concept.

High efficiency cold optics should result in single sideband receiver temperatures ≤ 200 K over the band of interest, with somewhat higher noise at frequencies down to ~ 85 GHz. The focal plane array should result in a greater than order of magnitude reduction in observing time for projects involving extended objects.

Other important aspects of the system include:

1) cooled single sideband filter and image termination;
2) high efficiency scalar feedhorns with high packing density achieved by partial truncation of aperture sections;
3) fixed-tuned mixers for ease of operation;
4) polarization interleaving of beams to minimize area on the sky covered by the array beams.

General aspects of focal plane imaging as well as the logic leading to the present design will be discussed.

J5-3
1440

MILLIMETER/SUBMILLIMETER IMAGING WITH PLANAR FOCAL PLANE ARRAYS

K.S. Yngvesson and J.F. Johansson
Department of Electrical and Computer Engineering
University of Massachusetts
Amherst, MA 01003

Although focal plane arrays are being used in the optical and infrared, efforts at applying similar technology for millimeter and sub-millimeter waves have only started quite recently. Much improved efficiency in the utilization of telescopes, both ground-based and space-based, should result, from the use of multi-beam focal plane array systems.

A planar, integrated circuit type, technology is almost certainly required, for mm/sub-mm focal plane arrays to be affordable. We have made substantial progress with arrays of Tapered Slot Antennas (TSA's), and this talk will review results on these arrays and present a comparison with other planar arrays, as well as arrays of traditional waveguide type feeds. In developing the new technology, one finds it necessary to re-examine a number of issues regarding the design of mm/sub-mm telescope receiver systems. For example, the need to supply LO power to a number of receivers, makes cryogenic operation favored, and especially SIS mixers. The f–# at the position of the array is an important factor to optimize, and in this respect TSA arrays are advantageous since they can be matched to f–#'s as large as 2.0. TSA's have demonstrated Rayleigh resolution in two–dimensional imaging, and imaging telescope systems using such arrays are presently estimated to be able to yield a total aperture efficiency of 50% or higher. We will discuss in detail some recent calculations which show the trade–offs between different factors when attempting to design an imaging mm/sub-mm system with the maximum possible resolution, and compare different focal plane arrays in this context. There are definite upper bounds for the aperture efficiency for any array with a given element spacing, for example, as shown in the Figure below.

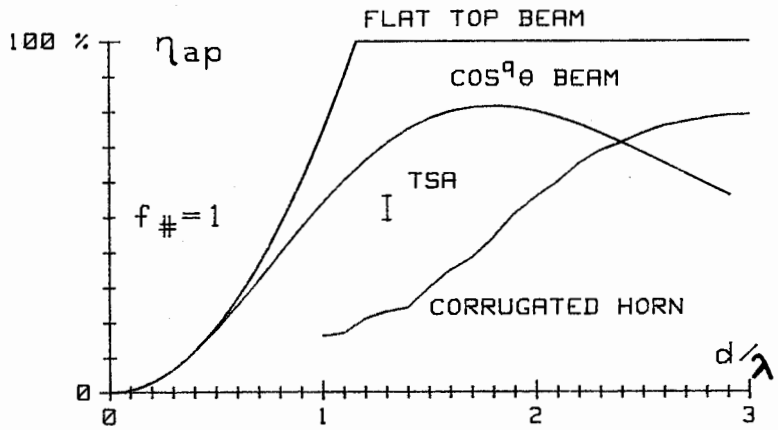

J5-4 1500 CRYOGENIC SUBMILLIMETER HETERODYNE RECEIVERS WITH SOLID STATE LOCAL OSCILLATORS

Neal R. Erickson
Five College Radio Astronomy Observatory
University of Massachusetts
Amherst, MA 01003

Two cryogenic submillimeter receivers are under construction using single mode waveguide mixers and solid state frequency multiplied local oscillators. One receiver is for 490 GHz and is designed for use on an optical telescope. To minimize the complexity of set-up and operation, it uses a miniature self-contained 70 K cryocooler to cool the mixer and IF amplifier, and a solid state local oscillator system. Since the noise of Schottky mixers and FET amplifiers changes relatively little below 70 K there is only a small performance penalty to operating at this temperature. The solid state LO source consists of a 65 mW InP gunn oscillator at 82 GHz followed by a high efficiency tripler and finally a doubler to produce a net output of 0.4 mW at 492 GHz. The mixer uses a rectangular horn tapering to waveguide of 0.5 x 0.15 mm cross section. The mixer diode has Cj = 0.18 fF and Rs = 16 Ω. LO power is injected using a room temperature Martin-Puplett interferometer. All optics are off-axis reflectors. The receiver noise temperature has previously been measured at 20 K to be 1700 K SSB with probably a 20% increase at 70 K.

A second receiver is for 690 GHz, using a similar approach, but with cooling provided by a 20 K refrigerator since this unit is presently for lab tests only. The mixer uses waveguide of 0.09 x 0.30 mm cross section with an integral smooth walled conical horn. The mixer diode has Cj = 2 fF and Rs = 17 Ω. LO will be provided by a two-diode InP oscillator at 86 GHz producing 120 mW output power. This oscillator will drive a balanced doubler using a pair of Schottky varactors with an expected output power of 35 mW. Following this will be a cascaded pair of single diode doublers with a projected output power of 0.3 mW at 692 GHz. While this LO chain is still under construction, the mixer has been tested with a laser LO and gives a noise temperature of 3000 K SSB at 20 K. Required LO power is <0.5 mW and comparable results are expected with the solid-state source.

J5-5
1540

SIS MIXERS FOR RADIOASTRONOMY

M. J. Wengler, D. P. Woody, T. G. Phillips
California Institute of Technology, Pasadena, CA 91125
R. E. Miller
AT&T Bell Laboratories, Murray Hill, NJ 07974

Superconducting tunnel diodes (SISs) are the most sensitive detectors available for broadband near-millimeter heterodyne detection. Quantum heterodyne theory (J. R. Tucker, *IEEE J. of Quantum Electronics*, **QE-15,** 1234–1258, 1979) is extended to include quantization of the electromagnetic field (M. J. Wengler and D. P. Woody, *IEEE J. of Quantum Electronics*, submitted 1986). This theory predicts that good quality NbN SISs will be capable of nearly perfect photodiode response to frequencies as high as 3000 GHz. Computer results from this theory are presented which show the effect of input source impedence on the mixer gain and noise.

We have fabricated lead alloy SISs at the center of bowtie antennas mounted on quartz lenses. A heterodyne receiver based on this quasioptical coupling (M. J. Wengler *et al., Int'l. J. of IR and MM Waves,* **6,** 697–706, 1985) has excellent sensitivity from 115 to 466 GHz. This receiver is the most sensitive heterodyne receiver yet reported for 300 to 466 GHz. Recently, a series array of two SISs cooled to 2 K yielded a receiver temperature T_R = 165 K DSB at 230 GHz, which is nearly as good as the best waveguide results at this frequency.

The beam pattern of a bowtie antenna is not optimum (R. C. Compton *et al., IEEE Trans. Antennas and Propagation,* submitted 1986). Transformed by a small quartz lens and a polyethylene lens, our mixer has a beam describable as the sum of a Gaussian pattern and an extended diffuse pattern. Much of this diffuse pattern is terminated inside the cryostat in which the mixer is mounted. Sensitivity degradation due to beam lost in the cryostat is included in the receiver temperatures we report.

The mixer beam that does see out of the cryostat is not as clean as the nearly Gaussian beams produced by feedhorn-coupled mixers. Our mixer has been tested on one of the 10.4 meter dishes at the Owens Valley Radio Observatory for comparison with the feedhorn-coupled SIS mixers which usually operate there (D. P. Woody *et al., IEEE Trans. on Microwave Theory and Technique,* **MTT-33,** 90–95, 1985). At 115 and 230 GHz, the bowtie beam couples to the telescope with about 3/4 the efficiency of feedhorn coupling. The effect on system sensitivity due to this lower efficiency is to be traded against the advantages of having a single mixer for multi-octave response.

We discuss the design and manufacture of an efficient bowtie mixer. SIS junction area must be $\lesssim .3(\mu m)^2$ to keep capacitance below about 15 fF. Normal state resistance should be below 100 Ω to minimize RC roll-off and the possibility of saturation, but above $\sim$ 30 Ω to avoid mismatch with the 120 Ω bowtie antenna. The design of the mixer optics is discussed. The IF output circuit is designed so the 50 Ω IF amplifier input is transformed to 100 Ω at the junction in the 1 to 2 GHz IF range. Simultaneously, the IF circuit presents a low impedence to the junction from about 3 to 40 GHz. This lowers the root mean square voltage developed across the junction, reducing mixer saturation problems.

J5-6
1600

MEASUREMENT AND CORRECTION OF ANTENNA SURFACE TOLERANCE ERRORS

Charles E. Mayer and John H. Davis
Electrical Engineering Research Lab
The University of Texas at Austin
10100 Burnet Rd
Austin, TX 78758

Surface tolerance losses prove to be the limiting factor of an antenna's high frequency performance. If the antenna surface can be accurately measured, then certain errors may be corrected. Measuring the antenna by an electromagnetic metrology technique allows complete confidence that the measurements correlate strongly to the actual antenna performance. The power of the holographic technique (Mayer, et. al., IEEE Trans. Instrum. Meas., Vol. IM-32, pp. 102-109, 1983) is that the total system phase tolerance, i.e. through secondaries, terciaries, and quasi-optical diplexing and collimating optics is measured. Further, the measured amplitude illumination function can add much insight to evaluating the system.

We at the Millimeter Wave Observatory (MWO) have designed and implemented an error correcting secondary mirror on the 5-m telescope. The antenna aperture efficiency was doubled over the range from 230-300 GHz. The error correcting technique involves modifying the surface of an analytical secondary with a computer controlled milling machine (0.1 mil accuracy) to create a constant phase path length through the entire telescope optics.

5m primary reflector

We have also designed and tested dual shaped reflectors to redistribute the feed energy around the central blockage and to obtain a more desirable taper function.

Use G.O. to go from primary to subreflector
Primary reflector is examined by using a perfect elliptical subreflector and then get aperture phase with holographic techniques
Did at 2 frequencies to test G.O.

Wednesday Morning, 14 Jan., 0830-1200

0830-Weds. Macky Auditorium
PLENARY SESSION

PS-1
0840 PHASE-ONLY ANTENNA SYNTHESIS FOR LINEAR AND PLANAR ARRAYS: John F. DeFord and Om P. Gandhi, Electrical Engineering Dept., Univ. of Utah, Salt Lake City, UT 84112

Minimization of the maximum sidelobe level for a given array geometry by phase-only adjustment of the element excitations is considered. Optimum phases are obtained by using a numerical search procedure to minimize the expression for the pattern sidelobe level with respect to the element phases, and results for both linear and planar arrays of equispaced elements are presented. Data suggests that optimum sidelobe level is a logarithmic function of array size. Optimum patterns kave relatively low efficiencies, with efficiency approaching an asymptotic nonzero limit as the array size is increased. Array efficiencies can be significantly improved by introducing a sidelobe taper, at the expense of raising the peak sidelobes somewhat. An analytic synthesis algorithm is presented for use on very large arrays for which the numerical search technique for the minimization of the sidelobe level is computationally impractical. This method produces patterns with characteristics similar to arrays synthesized using the numerical search method, and it may be used to synthesize either uniform or tapered sidelobes, allowing flexibility in determining the efficiency and peak sidelobe level for a given array.

Numerical search method he used requires large computer times.
His analytical synthesis method treats the whole phase as a random variable Results of this are similar to his numerical results.

PS-2
0900

ACCURATE ANALYSIS OF METAL-STRIP-LOADED IMAGE GUIDE LEAKY WAVE ANTENNAS: M. Guglielmi and A.A. Oliner, Polytechnic Univ., Brooklyn, NY 11201

The disperson behavior of metal-strip-loaded dielectric guide leaky wave antennas is carefully analyzed and completely characterized. Many measurements have been made on this antenna type but until now no satisfactory theory was available from which such antennas could be systematically designed. A new small obstacle equivalent network is developed to accurately describe the multimode metal strip grating at a dielectric interface, a key constituent of these antennas. Finally, it is shown how the dispersion behavior and the antenna performance can be effectively controlled by properly adjusting the structural parameters.

PS-3
0920

CHARACTERISTIC MODES AND DIPOLE REPRESENTATIONS OF SMALL APERTURES: Taoyun Wang (Advisor: Roger F. Harrington), Dept. of Electrical and Computer Engineering, Syracuse Univ., Syracuse, NY 13210

In this paper the characteristic modes of the equivalent magnetic current are related to the dipole representation of a small aperture in an infinitely large conducting screen. The eigenequations for the first three lowest eigencurrents are derived from the low frequency approximation to the integral equation. It is shown that these three characteristic currents are closely related to the three dipoles of Bethe-hole theory. An example of a small circular aperture in an infinite conducting plane is discussed.

PS-5
1015

RECENT SEARCHES FOR MAGNETIC MONOPOLES:
Michael W. Cromar, National Bureau of Standards, Electromagnetic Technology Division, Boulder, CO 80303

Predictions of Grand Unified Theories have stimulated renewed interest in the detection of single magnetic charges. A brief review of the predicted properties of a magnetic monopole will be followed by a description of recent experiments at NBS Boulder and at other laboratories. The next generation of much larger detectors will also be described.

- Dirac in 1931 said there should be one (or more) monopoles.
- Grand Unified Theory: 1970's
  Suggests very large monopole mass 10^6 GeV
  and $10^{-4}c$ velocity
  Will go right thru the earth
  Projects 10^{75} monopoles down to 1 in universe
  One theory predicts 3 per year passing thru a football field

Detector

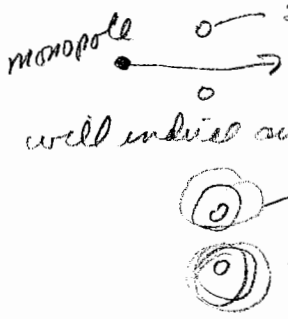

will induce an electric current the remains

Cabrera at Stanford has done this
He saw one event in 150 days Physical Review Ltrs
but not sure it was a monopole May 1982
10 cm² area. This output is thought to be spurious

NBS detector:
3 orthogonal loops 16 cm in diameter
Must traverse 2 loops to qualify
One year (8/84 to 8/85) of operation:
NO candidate events

Other efforts
Fermi Lab - Chicago
IBM - Yorktown Heights
Stony brook
Imperial college

~~PS-6 To be announced~~
~~1100~~

Third generation

Much larger loops with coincidence loops are planned:
Stanford and IBM-BNL
Stanford's has 20cm radius and 5.1m length
On line soon
IBM-BNL proposes an array of detectors

Magnetic monopoles are their own antiparticle so that if two of them get together they would annihilate each other and release a tremendous amount of energy.

Applications are, of course, zero. It's detection would be for basic physics theory sake,

---

Wednesday Afternoon, 14 Jan., 1355-1700

Session A-3 1515-Weds. NW 248
TRANSIENT RESPONSES FROM CW MEASUREMENTS
Chairman: Edmund K. Miller, Nichols Hall,
Univ. of Kansas, Lawrence, KA 66045

A3-1
1520 APPLICATION OF LATTICE FILTERING TECHNIQUES TO CW MEASURED TIME DOMAIN DATA*

S. Giles, H.G. Hudson, S.R. Parker, and R.J. King
Office of Naval Technology/
Lawrence Livermore National Laboratory
P.O. Box 808, L-228
Livermore, CA 94550

Understanding basic phenomenology of EM coupling into configured cavities and onto conductors is important in predicting the vulnerability of electronics systems to EM threats. Often, knowledge of the behavior of these systems is best gained through small scale experiments. Experiments and numerical modeling codes serve to describe the actual response of test systems--in our case, the monopole and cavity-backed spiral antennas exposed to a spherical wave.

The facility used to produce the wave is the EMP Engineering Research omni-directional radiator (EMPEROR). The EMPEROR and accompanying measurement and test systems can be operated in either the pulsed or CW mode. The CW mode is used more often than the pulsed mode primarily because a wider bandwidth is possible, 0.1-18.0 GHz vis-a-vis 0.1-2.5 GHz; and, with the HP8510A system, large improvements in dynamic range and measurement accuracy are possible. However, the data must be transformed to obtain time domain information.

Lattice parameters are generally used in modeling time domain data by building a standard lattice structure (S.M. Kay and S.L. Marble, Proc. IEEE, 69, 1389-1390, 1981). A different lattice structure is needed to model complex data. The theory of the complex data compatible lattice and its application to produce the time domain response of the monopole and cavity-backed spiral antennas are presented in this paper.

* Work performed under the auspices of the U.S. Department of Energy by the Lawrence Livermore National Laboratory under contract number W-7405-ENG-48.

A3-2
1540 THE MEASUREMENT AND CHARACTERIZATION OF A PULSED EDDY CURRENT WAVE IN ALUMINUM AS ALTERED BY A SLOT DEFECT: Dr. Kenneth H. Cavcey, Center for Electronic and Electrical Engineering, Electromagnetic Fields Division, National Bureau of Standards, Boulder, CO 80303

The nondestructive testing of conductors used for shielding purposes dates back as far as the 1950's. By subjecting an aluminum sheet containing a defect on one of its surfaces to an electromagnetic pulsed eddy current source, EM fields are created in and outside of the conductor. As the wave reachers the defect, its time dependent and amplitude characteristics are modified. As a result the detection and interpretation of the wave components are an important way of verifying conductor integrity.

This paper describes a novel way of experimentally measuring the field components of interest. In addition, the problem is modeled mathematically using the method of moments approach. Results are presented for comparison and analysis purposes.

A3-3
1600

TARGET TRANSIENT RESPONSE DETERMINATION FROM FREQUENCY-DOMAIN RCS MEASUREMENTS

L. E. Sweeney, Jr., Lloyd A. Robinson,
Alfred J. Bahr, and William B. Weir
SRI International
333 Ravenswood Ave
Menlo Park, CA 94025

Modern automatic network analyzers (ANAs) when combined with RCS ranges have enabled quick and precise coherent measurement of target scattering as a function of frequency. While frequency domain data has great utility in itself, even greater value can be attained by transforming to the time domain. Such transformations can be performed easily and efficiently via the Fast Fourier Transform (FFT) implemented by software on a separate computer or by firmware incorporated into the ANA itself.

Target transient response measurements made via the frequency domain have the advantage that the target transient response can be determined accurately from a single frequency domain data set for any and all excitation pulses having bandwidths contained within the measurement bandwidth. Derivation of similar data by determining the target impulse response from deconvolution of actual pulse measurements can produce inaccuracies caused by low signal-to-noise ratios where the illuminating pulses lack sufficient spectral content.

This paper will describe the use of frequency-domain measurements in an RCS model range to determine the transient responses of typical targets, and will illustrate how such measurements can be used to characterize targets and understand their scattering mechanisms, particularly in the resonance scattering regime.

A companion paper will discuss how frequency-domain measurements transformed to the time domain can be used to diagnose clutter sources and background scattering within an RCS range itself, and how transforming between the frequency and time domains can be used to excise unwanted range clutter from the data to provide substantially improved RCS data as a function of frequency and azimuth.

A3-4
1620

TIME-DOMAIN DIAGNOSTICS OF RCS RANGES USING FREQUENCY-DOMAIN MEASUREMENTS

Lloyd A. Robinson, L. E. Sweeney, Jr.,
Alfred J. Bahr, and William B. Weir
SRI International
333 Ravenswood Ave.
Menlo Park, CA 94025

Modern automatic network analyzers (ANAs) when combined with RCS ranges have enabled quick and precise coherent measurement of range background as a function of frequency. Extremely valuable information about the sources of range background clutter can be attained by transforming to the time domain. Such transformations can be performed easily and efficiently via the Fast Fourier Transform (FFT) implemented by software on a separate computer or by firmware incorporated into the ANA itself.

This paper will discuss how frequency-domain measurements transformed to the time domain can be used to diagnose clutter sources and background scattering within an RCS range itself, and how transforming between the frequency and time domains can be used to excise unwanted range clutter from the data to provide substantially improved RCS data as a function of frequency and azimuth.

A companion paper will describe the use of frequency-domain measurements in an RCS model range to determine the transient responses of typical targets, and will illustrate how such measurements can be used to characterize targets and understand their scattering mechanisms, particularly in the resonance scattering regime.

A3-5
1640

PULSE-GATED ANTENNA MEASUREMENTS

Doren W. Hess
Scientific-Atlanta, Inc.
P. O. Box 105027
Atlanta, Georgia 30348

Pulse-gated antenna measurements have conventionally been performed out of doors for the purpose of removing the effects of clutter from the measurement. The earlier methods utilized higher power transmitters to make up for the loss in signal caused by the duty factor of the pulse waveform. Since the advent of phase-locked receivers, technology has proceeded without implementation of pulse-gating for antenna measurements.

By special configuration of the instrumentation, it is now possible to construct antenna ranges with the advantage of phase-locked receivers which provide the capability of pulse gating to remove clutter. The configuration promises dynamic ranges of 80 dB or more with rejection of clutter.

Compact range measurements can also be performed in the pulse-gated mode to reduce the chamber related clutter effects. Although operating in a different time regime, the compact range instrumentation is similar to the outdoor range.

In this presentation I review the considerations one makes in designing a system, the current limitations of hardware and the potential benefits of pulse-gated antenna measurements.

Session B-9 1355-Weds. NW 271
GUIDED WAVES
Chairman: K.A. Michalski, Dept. of Electrical Engineering, Univ. of Mississippi, University, MS 38677

B9-1
1400 RADIATIVE AND SURFACE WAVE LOSSES IN MICROSTRIP TRANSMISSION LINES: J. S. Bagby, Department of Electrical Engineering, University of Texas at Arlington, Arlington, Texas 76019, and D. P. Nyquist, Department of Electrical Engineering and Systems Science, Michigan State University, East Lansing, Michigan 48824.

An exact dyadic integral equation is utilized in the analysis of propagation in uniform integrated microstrip transmission lines. The object of the analysis is to predict and quantify the radiative and surface wave losses in such systems.

The axially-transformed surface current $\vec{k}(\vec{\rho};\zeta)$ of a natural mode on an integrated microstrip line satisfies the homogeneous integral equation:

$$\hat{t}\cdot(k_c^2 + \nabla\nabla\cdot) \oint_{\ell} \ddot{g}(\vec{\rho}|\vec{\rho}';\zeta)\cdot\vec{k}(\vec{\rho}';\zeta)\, d\ell' = 0, \quad \vec{\rho} \in \ell$$

where k_c is the wavenumber in the cover region, $\ddot{g}(\vec{\rho}|\vec{\rho}';\zeta)$ is the Hertzian potential Green's dyad of the background structure, ζ is the complex propagation constant of the mode, $\hat{t}$ is a unit tangent to the transmission line, and ℓ is the cross-sectional contour of the line.

The integral representation of the Green's dyad exhibits singularity when the real part of ζ is less than the propagation constant of a surface wave mode in the integrated circuit background structure. It is shown that for the dominant mode of the line the singularity is not implicated, and all losses are due to radiation into the cover medium. For higher order modes, however, the singularity is implicated, requiring inclusion of a residue term representing excitation of surface waves in the film layer. For higher order modes, higher losses are observed due to excitation of surface waves in the film layer.

This equation is solved numerically by the method of moments for narrow and wide microstrip transmission lines. The above-described effects are demonstrated in both cases.

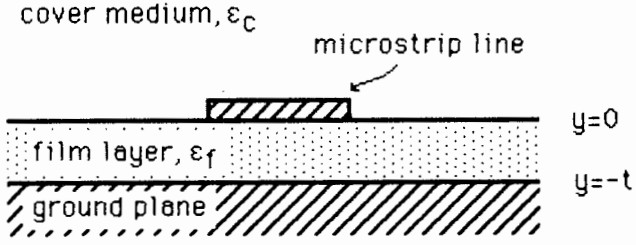

B9-2
1420

EXACT IMAGE THEORY FOR MICROSTRIP GEOMETRY

I.V.Lindell*, E.Alanen, A.T.Hujanen
Dept. E.E., Helsinki Univ. of Technology
Otakaari 5A, Espoo 15, Finland, 02150
*address for the academic year 1986-87:
Dept. EECS, MIT, rm 26-311, Cambridge
MA 02139, USA.

Exact image theory, which was recently introduced for problems involving a plane interface between two homogeneous media (IEEE Trans, Ant. & Prop., vol. AP-32 (1984), pp.126-133, 841-847, 1027-1032), is here extended for problems with the microstrip geometry. The basis field problem for the horizontal current upon a dielectric substrate with ground plane is solved in terms of an image current function, for which an exact expansion in terms of modified Bessel functions is developed. Some asymptotic tests for the image theory are made and the resulting current functions are seen to coincide with those calculated through another, totally different, theory applying Mittag-Leffler expansion (IEE Proc. vol. 133H (1986), pp.297-304). In contrast to the Mittag-Leffler method, there is no need to solve for a large number of poles and their residues in the present method. In practical problems involving the microstrip geometry, the image current functions can be calculated once for all and stored in computer memory for multiple use in field calculations, which allows a rapid means of analysis of microstrip structures.

B9-3
1440

RESONANT FREQUENCY OF RECTANGULAR MICROSTRIP PATCH ON SEVERAL ANISOTROPIC LAYERS

R.M. Nelson, D.A. Rogers, A.G. d'Assuncao
Dept. of Electrical Engineering
North Dakota State University
Fargo, North Dakota 58105

A fullwave analysis for determining the resonant frequency of rectangular microstrip patches using several uniaxial anisotropic layers is presented. The structure considered as shown below consists of two uniaxial anisotropic layers beneath the patch, with one uniaxial anisotropic layer covering the patch.

Two different spectral domain methods were used independently to derive the immittance matrix for the structure considered. The first one uses Hertz vector potentials oriented along the optical axis, which is assumed to be in the y-direction for the three different anisotropic layers (H. Lee, V.K. Tripathi, MTT-30, No. 8, 1188-1193, Aug. 1982). The second method uses a transverse equivalent transmission line (T. Itoh, MTT-28, No. 7, 733-736, July 1980), modified to include anisotropic substrates. Both methods yield the same source immittance matrix. This immittance matrix is then used in conjunction with Galerkin's method to obtain the resonant frequency of the microstrip patch.

Numerical results are presented which show the effect of anisotropy on the resonant frequency for various configurations including patch resonators on both single and double anisotropic layers (with or without an anisotropic overlay) as well as suspended patch resonators with anisotropic media (with or without an anisotropic overlay).

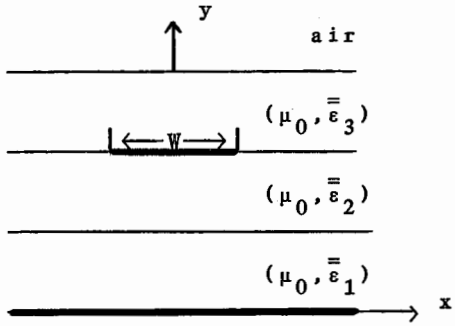

B9-4
1500

SURFACE WAVES AND THEIR DISPERSION RELATIONS IN A DIELECTRIC ROD

A. R. Vaucher, J. V. Subrahmanyam, Gregory Cowart, Mustafa Keskin, and H. Überall
Department of Physics
Catholic University of America
Washington, DC 20064

The conventional formulation of the electromagnetic field solution for a cylindrical dielectric rod is reinterpreted in a novel fashion in order to show the presence of surface waves which propagate over the rod's surface along helical pahts. The eigenfrequencies of the rod are interpreted as the resonance frequencies at which these helical surface waves match phases after each circumnavigation of the rod, effectively forming resonating standing waves around the rod. This interpretation permits us to obtain a continuous interpolation between the resonances, furnishing us with the dispersion curves (phase velocity as a function of frequency) of the surface waves.

The procedure here follows our previous approach in which helical surface waves were studied on the conducting interior walls of cylindrical cavities (J. V. Subrahmanyam et al., IEEE Trans. MTT-29, 1066-1072, 1981). In the dielectic rod, the problem is more complicated due to the mixing of modes.

The merit of the described approach lies in our reinterpretation of the conventional modal solution, which offers little physical insight, in terms of helical surface waves which offer a physical picture of the solution. Based on such a picture, one will be able to modify the solution e.g. by the use of ribs or slots, in a purposeful manner to influence the propagation of the surface waves, and hence the form of the radiated field as desired.

B9-5
1540 ANALYSIS OF A NOVEL O-TYPE MILLIMETER WAVEGUIDE:

J. S. Bagby and C. V. Smith, Department of Electrical Engineering, University of Texas at Arlington, Arlington, Texas 76019.

In the millimeter-wave and sub-millimeter-wave frequency range both metallic closed-pipe waveguides and standard optical fibers exhibit prohibitive losses. In order to overcome this limitation a novel hollow, multi-layered O-type dielectric waveguide is proposed for use at these frequencies.

In contrast to conventional dielectric waveguides, in this proposed waveguide electromagnetic energy is not guided by surface waves; instead, guidance is accomplished in the air-core region by reflection of incident radiation from the inner air/dielectric interface. This results in minimization of energy confined to the lossy dielectric material, and hence lower loss.

The number of layers used, layer thicknesses, and layer composition are chosen to maximize reflection at the inner interface for a large range of incidence angles, in close analogy to the process used in design of dichroic laser cavity mirrors. Fabrication techniques perfected in the construction of optical fibers can be adapted to this configuration.

Numerical results in the form of dispersion curves for the waveguide are presented, demonstrating feasibility with realistic material parameters.

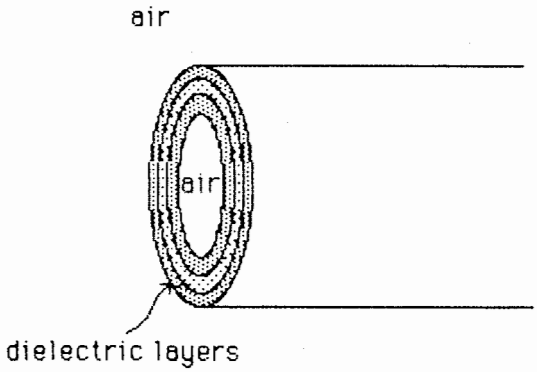

B9-6
1600 THE QUASI-STATIC CHARACTERISTICS OF SLOTTED PARALLEL-PLATE WAVEGUIDES

HESHAM A. AUDA
DEPARTMENT OF ELECTRICAL ENGINEERING
UNIVERSITY OF MISSISSIPPI
UNIVERSITY, MS 38677, USA

The quasi-static characteristics of parallel-plate waveguides with multiple slots in its upper plate (see Figure 1) are investigated. The analysis utilizes the characteristic currents for the slots determined under the quasi-static approximation. The equivalent magnetic currents on the slots and radiation pattern are determined when the array of slots is illuminated by a transverse electromagnetic wave incident in the waveguide or by a transverse electric plane wave incident in the upper half-space. Analytic expressions in the case of a single slot are also given.

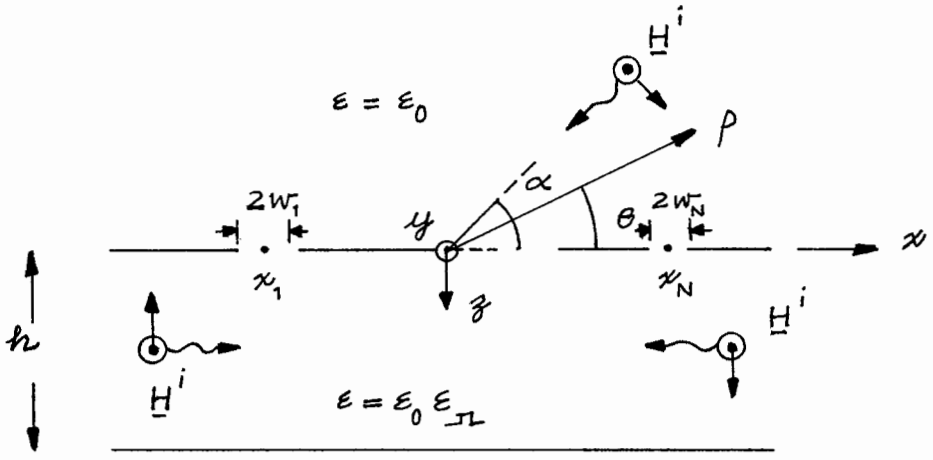

Figure 1. A slotted parallel-plate waveguide.

B9-7 1620 PROPAGATION CHARACTERISTICS OF RECTANGULAR GROOVE GUIDES

Edward K N Yung, K M Luk and K F Tsang

Department of Electronic Engineering
City Polytechnic of Hong Kong
700 Nathan Road, Hong Kong

The open groove guide is a special waveguide for the use at millimeter wavelengths which exhibits low attenuation and wide band characteristics. Using the mode matching technique, a characteristic equation for rectangular groove guides was first developed by Nakahara and Kurauchi (Sumitomo Eectric Tech. Rev., 5, 65-71, 1965). However the characteristic equation is too complicated that it is necessary to ignore all evanescant modes. Nevertheless propagation constants obtained by this first order approximation agree reasonably with experimental results for cases where the step discontinuity of the groove guide is small. Recently a transverse equivalent network for the rectangular groove guide has been derived by Oliner and Lampariello (IEEE Trans. Microwave Theory Tech., 33, 755-763, 1985) and with which a very accurate yet simple dispersion formula for the determination of the propagation constant was developed. The latter approach is semi-empirical because the shunt susceptance of the step discontinuity was determined by comparing its results with guides having a reactive diaphragm experimentally.

In this paper, an innovative technique will be presented for the analysis of the groove guide.

B9-8
1640

CASCADED SYSTEM OF WIRE-GRID POLARIZERS:
Rajendra K. Arora and Devi Chadha, Dept. of Electrical Engineering, Indian Institute of Technology, Delhi, Hauz Khas, New Delhi 110016, India

Wire-grid polarizers, consisting of unidirectionally conducting screens mounted on dielectric substrates, have application as quasi-optical transmission type polarization rotators. In practice, two or more of such polarizers are required to give broadband and wideangle characteristics. A wave matrix method is employed to analyze the transmission and scattering properties of the cascaded system of wire-grid polarizers for the general case of arbitrary polarization and angle of inclination of a plane electromagnetic wave. An optimum design of the system can be obtained with the proper choice of grids and their relative orientations.

Session C-4 1355-Weds. NW 238
SPECTRAL ESTIMATION: MULTI-WINDOW TECHNIQUES
Chairman: A.D. Chave, AT&T Bell Labs,
600 Mountain Avenue, Murray Hill, NJ 07974

C4-1
1400

MULTIVARIATE MULTIPLE-WINDOW SPECTRUM ESTIMATES

David J. Thomson
AT&T Bell Laboratories, Murray Hill, N.J. 07974

We describe the estimation of coherence, cross-spectra, transfer functions, and related multivariate time-series entities using the multiple-window approach. This method of spectrum estimation (Proc.IEEE **70,** pp 1055-96, 1982) differs from conventional approaches in that an orthogonal *set* of data tapers is applied to the data before Fourier transforming. The tapers, or data windows, are discrete prolate spheroidal sequences characterized as being the most nearly bandlimited functions possible among functions defined on a finite time domain and so have very low "leakage". The method is essentially a small-sample inverse method applied to the finite Fourier transform. Major advantages of this approach include: a statistical efficiency typically a factor of 2 to 3 higher than conventional methods with the same degree of bias protection; seperation of the continuous and line parts of the spectrum; estimates of coherence, phase, and similar quantities may be obtained without the usual averaging ambiguities. Sample variances of the frequency-domain entities are estimated by a jackknifing method where each of the different windows is successively dropped from the analysis.

Recent developments in the theory to be discussed include: improved line-extraction methods; maximum-likelihood coefficient weights for multivariate spectral matrix and coherence estimates (the method is closely related to optimum filter theory and the weights are essentially the filters on the prolate basis); narrow band phase-tracking techniques; and combinations with segment averaging methods.

C4-2
1440

MULTITAPER POLARIZATION ANALYSIS OF SEISMIC DATA

F. Vernon
IGPP UCSD
La Jolla, CA 92093
J. Park
Yale University
New Haven, CT 06511

In this paper a technique is presented to estimate the frequency dependent polarization of three component data. This technique is based on the multiple taper spectral analysis methods (D.J. Thomson, Proc.IEEE, 70, No.9, 1055-1096, 1982) which apply a set of orthogonal tapers to the data series. The tapers are constructed such that each taper samples the time series in a statistically independent manner while optimizing resistance to spectral leakage.

The set of K tapers $v_t^{(k)}$ which is used is a subset of discrete prolate spheroidal sequences. These tapers are orthogonal, i.e., $v_t^{(k)} \cdot v_t^{(k')} = \delta_{kk'}$. To construct spectral estimates, one first calculates complex "eigenspectra" $Y_k(f)$ from the time series x_t with N points which are tapered by the respective $v_t^{(k)}$

$$Y_k(f) = \frac{1}{N} \sum_{t=0}^{N-1} v_t^{(k)} x_t e^{i\pi ft}$$

We calculate the "pure state" polarization at frequency f_0 by calculating the first K eigenspectra.

$$Y_0^{(m)}(f_0), Y_1^{(m)}(f_0), \ldots, Y_{K-1}^{m}(f_0)$$

for the three component (m = 1,2,3) wave field. The dominant polarization of motion is given by the linear combination $\hat{z}$ of the three components that contains the greatest fraction of the seismic energy in the frequency neighborhood of f_0. The components of $\hat{z}$ can be complex, allowing for phase lags between components. The phase lags between components represent elliptical partical motion. The vector $\hat{z}$ also defines a specific horizontal azimuth and a vertical angle of incidence.

This technique is applied to three component seismic data recorded on the Anza Seismic Array. Local and regional earthquakes recorded at several different sites are studied in the frequency band from 1 Hz to 30 Hz. Particular emphasis is given towards studying bodywave phases and identifying possible site resonances.

C4-3
1520 HUNTING FOR PALEOCLIMATE PERIODICITIES IN A GEOLOGIC TIME SERIES WITH AN UNCERTAIN TIME SCALE

Jeffrey Park (Dept. of Geology and Geophysics, Yale Univ., P.O. Box 6666, New Haven, CT 06511)
Tim Herbert (Dept. of Geology, Princeton University, Princeton, NJ 08544)

We report results of spectral analysis of $CaCO_3$ weight-% measurements taken at roughly 2 cm intervals from an 8m section of a mid-Cretaceous (Albian) sediment core from Piobbico, Italy. Fourier analysis finds strong evidence for an oscillation correlated with the ~ 100 kyr period oscillations in the eccentricity of the earth's orbit about the sun. The uncertainty in the depth-age relation hampers a more complete assessment. We fit for long-term (time scale > 75 kyr) fluctuations in sedimentation rate by tracking the frequency modulations of the presumed 100 kyr cycle by means of a multiple-taper F-test analysis. Variations in sedimentation rate are determined by fitting a smoothed cubic spline to the set of discrete frequency-modulation estimates, specifying a χ^2 misfit criterion. We infer fluctuations of a factor of two in the sedimentation rate, which occur on a time scale of 400 kyr. When we tune the carbonate series using the inferred age-depth function we obtain greater correlation with the earth's orbital oscillations. The ~ 100 kyr cycle resolves principally into two harmonic components whose frequency ratio corresponds to that of the modern 95.8 and 126 kyr eccentricity oscillations. We also observe a sinusoidal oscillation of lower amplitude with period close to the period of the modern obliquity cycle.

C4-4
1620

DETECTING NONSTATIONARY SIGNALS IN NOISY DATA USING SEVERAL TAPERS

Craig Lindberg,[1] Jeffrey Park,[2] and David J. Thomson[3]

[1]Institute of Geophysics and Planetary Physics,
Scripps Institution of Oceanography,
University of California, San Diego, La Jolla, CA 92093
[2]Department of Geological and Geophysical Sciences,
Yale University, New Haven, CT 06511;
[3]AT&T Bell Laboratories, Murray Hill, NJ 07974

We present a multiple taper method for detecting nonstationary signals in a time series based on a statistical test that measures the confidence one can assign to a signals's existence at any given frequency. We consider the problem of detecting decaying sinusoids immersed in additive white noise. This type of data is common in the analysis of mechanical vibrations and nuclear magnetic resonance experiments. The data are multiplied by K tapers derived by a variational principle, creating K independent time series. A decaying sinusoid model is fit to the K time series in the frequency domain. A statistical test of the fit gives a measure of the chance that a decaying sinusoid is in the data. We compare the method to conventional direct spectral estimates and find it superior. We present a number of examples of the method's use on single and multiple records.

C4-5
1640

REDUCED RANK, RANK-ONE UPDATING OF THE SYMMETRIC EIGENPROBLEM

R.D. DeGroat
R.A. Roberts
University of Colorado
Department of Electrical and Computer Engineering
Boulder, CO 80309

It is often desireable to adaptively update the eigenvalue decomposition (EVD) of a symmetric, nxn matrix when modified by a rank-one matrix, i.e.,

$$\tilde{R} = R + xx^T,$$

where the EVD of $R=UDU^T$ is known, the EVD of $\tilde{R}=\tilde{U}\tilde{D}\tilde{U}^T$ is desired, and xx^T is a rank-one matrix containing new information.

In many signal processing problems, including direction finding, beamforming, and narrow-band spectral estimation, R is used to estimate a "signal space" from which signal information may be extracted. Tufts and Kumarasen showed in (D.W. Tufts and R. Kumaresan, Proc. IEEE, 70, pp. 975-989, 1982) that a low rank approximation to R often gives a better representation of the signal space than the full rank matrix. Combining this idea with the rank-one update method described in (R.D. DeGroat and R.A. Roberts, SPIE Proceedings, 696, 1986), can significantly reduce the computation.

If R is full rank, the rank-one update is $O(n^3)$. But if a rank r approximation, $R^{(r)}$, is used in place of R, the reduced rank, rank-one update is $O(n(r+1)^2)$. The reduction in computation is due to the fact that all but one of the n-r null eigenvalues of $R^{(r)}$ can be deflated out of the update, resulting in a reduced eigenproblem of size r+1.

The reduced rank, rank-one update not only achieves a better representation of the signal, but also a significant reduction in computation.

Session E/B-1 1355-Weds. NW 261
SPECIAL SESSION ON HIGH POWER
ELECTROMAGNETICS I
Chairman: D.V. Giri, Pro-Tech,
125 University Ave., Berkeley, CA 94710
Organizers: C.E. Baum, R.L. Gardner, and D.V. Giri

E/B1-1 1400 AN ANISOTROPIC LENS FOR TRANSITIONING PLANE WAVES BETWEEN MEDIA OF DIFFERENT PERMITTIVITIES

A.P. Stone
University of New Mexico
Department of Mathematics
Albuquerque, NM 87131
C. E. Baum
Air Force Weapons Laboratory
Kirtland AFB
Albuquerque, NM 87117

In this paper we consider a particularly simple geometry in which an anisotropic lens is specified for the transitioning of plane waves between media of different permittivities. In the case of non-normal incidence we can have the situation where a TEM wave propagates with a TM polarization, and the wave can pass through the boundary with no reflection. That is, the angle of incidence is the well known Brewster angle which can be calculated if the properties of the media are known. We show that enforcing the requirements of differential impedance matching and transit-time conservation at boundaries of regions of different permittivities leads to the Brewster angle condition. The case of a plane wave propagating in a region I, normally incident on a boundary between I and a lens region, and on into a region II is investigated. The requirements of impedance continuity and transit-time conservation at all boundaries then lead to the lens design, specified by the shape of the lens region and its permittivity.

E/B1-2
1420

DESIGN PROCEDURES FOR ARRAYS WHICH APPROXIMATE A DISTRIBUTED SOURCE AT THE AIR-EARTH INTERFACE

Y.G. Chen, S. Lloyd and R. Crumley
Maxwell Laboratories, Inc., 8888 Balboa Ave.
San Diego, CA 92123

C.E. Baum
Air Force Weapons Laboratory, Kirtland AFB, NM 87117
and
D.V. Giri
Pro-Tech, 125 University Ave., Berkeley, CA 94710

Abstract

This paper addresses a general electromagnetic problem of simulating a distributed source at an interface of a conducting dielectric by an array of pulsers. One possible application lies in the distributed source at the air-earth interface associated with a nuclear EMP (C.E. Baum, Sensor and Simulation Note 240, January 1978 and Joint Special Issue on the Nuclear EMP, IEEE Trans. on Antennas and Propagation, 26, 35-53, 1978). Other electromagnetic applications may include geological prospecting, detection of buried objects and study of the coupling of the field generated by natural lightning to underground objects. In general, the design procedures of arrays approximating distributed sources considered here are applicable whenever, a need for coupling electromagnetic waves into earth arises. Approximate theoretical considerations, as well as design procedures for the arrays are discussed.

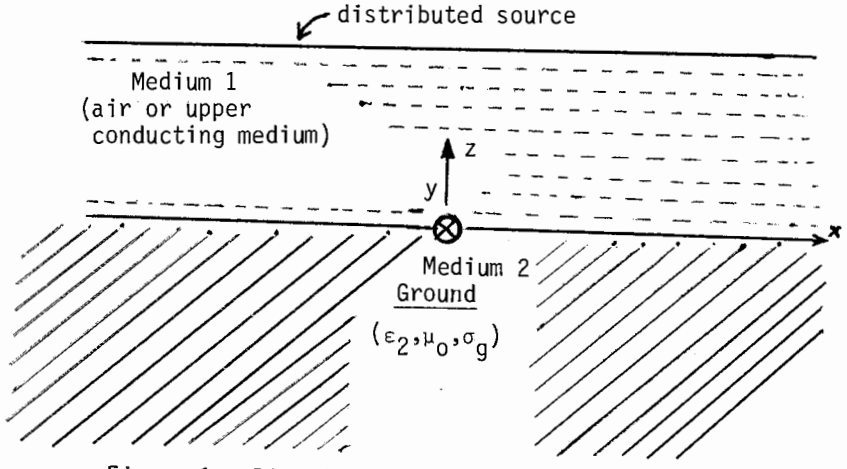

Figure 1. Distributed source near the interface.

E/B1-3
1440

ELECTROMAGNETIC INTERACTION

J. P. Castillo
R & D Associates
P.O. Box 9335
Albuquerque, NM 87119

This paper will address the basic interaction mechanisms and associated modeling for electromagnetic waves impinging on objects of arbitrary shape. Methods which are used to decompose a complex scatterer into simple shapes will be presented. Basic electromagnetic topological approaches will be used in defining the basic interaction problem. This interaction problem will be divided into the following fundamental subproblems:

- Interaction with exterior surfaces
- Interaction with appendages
- Interaction with apertures
- Coupling to interior objects
- Propagation along interior conductors

Limitations of this approach will also be presented. The necessity for complementary experiments will be discussed. Finally, simple examples of how these basic models are applied to abstract objects will be given.

E/B1-4
1500

CALCULATIONAL MODELS FOR LIGHTNING AND EMP INTERACTION WITH LONG LINES *

F.M. Tesche
LuTech, Inc.
P.O. Box 796012
Dallas, TX 75379

The determination of the response of above-ground and below-ground transmission lines to an incident electromagnetic field is necessary in performing an assessment of how communications systems or electrical power systems would behave when exposed to a natural lightning excitation, or to a transient electromagnetic pulse (EMP).

In a recent study of the commercial power transmission and distribution system in the U.S. [1], several computational models for transmission line coupling were discussed. Recently, other models have been developed to permit the analysis of a wider class of electromagnetic coupling problems than those mentioned in [1].

In this paper, a summary of these field to line coupling models is presented. These include models for:

1. Single and multiconductor line over the ground.
2. Single coaxial and shielded multiconductor line over the earth.
3. Single buried cable.
4. Buried coaxial cable.
5. Single transmission line having non-linear and/or time varying parameters.
6. Simple above-ground single conductor transmission line network (no loops).
7. Generalized multiconductor transmission line network.

All of these models involve the use of a TEM transmission line theory which has been suitably modified to account for the effects of the lossy earth. Moreover, these models require only a modest computational capability: all run on the IBM-PC. In this paper, typical computed responses for problems of interest are presented to illustrate the use of these transmission line models.

---

[1] Legro, J.R., et, al., "Study to Assess the Effects of High Altitude Electromagnetic Pulse on Electric Power Systems", ORNL/Sub/4-3374/1/v2, Westinghouse Electric Co. Report, Prepared for Oak Ridge National Laboratory, February, 1986.

* Work Sponsored by the Westinghouse Electric Corporation and Oak Ridge National Laboratory through U.S. Department of Energy Contract DE-AC05-840R21400.

E/B1-5
1520

GROUND BASED C3 SYSTEMS EMP HARDENING

B.K.Singaraju
Air Force Weapons Laboratory
Kirtland Air Force Base
NM 87117-6008

High altitude Electromagnetic Pulse generated by nuclear explosions can cause disruption and damage to electronics components and communications systems and power systems. This disruption and possible damage to associated equipment is in general undesirable and can be a serious problem for critical Department of Defense (DoD) missions. Over the years, DoD and the United States Air Force in particular have been working on hardening critical Command, Control and Communications systems.

Although there are various methods of hardening facilities, United States Air Force has been using shielding and protecting the conductive penetrations as the principal approach for hardening the facilities. Underlying reasons for this approach are: (1) Ease of verification, (2) Ease of modification and (3) Ease of maintenance.

It has been found that it is easier to verify that a facility is meeting its design specifications on a shielded facility rather than other designs. In this procedure, if the specification for the design of the facility are adequate, then it is clear that this verification is adequate to ascertain that the design is implemented properly.

In general, the equipment in these facilities is either modified or replaced on regular basis. This modification and the associated efforts to maintain the survivability originally built into the facility are easier to perform on a facility built using the shielded design rather than by other means.

Maintenance of hardened facilities such that they remain hard is a critical issue. In a facility that is hardened using the integral shielding approach, it is relatively easy to determine when maintenance is necessary and it is even possible to design automated systems that can detect and localize the required maintenance.

In this paper we will discuss the general philosophy used in the design, specifications and verification. We will also discuss the on going programs to automate the hardness maintenance of facilities hardened using the shielding approach.

E/B1-6
1540

NORMS OF TIME-DOMAIN FUNCTIONS AND CONVOLUTION OPERATORS

C. E. Baum
Air Force Weapons Laboratory/NTAAB
Kirtland AFB NM 87117-6008

This paper develops various norms of time-domain functions and convolution operators to obtain bounds for transient system response. Besides the usual p-norm one can define another norm, the residue norm (or r-norm), based on the singularities in the complex-frequency (or Laplace-transform) plane.

E/B1-7 1600 A UNIFIED WAY OF QUANTIFYING EM NOISE ENVIRONMENTS: L. Marin, Kaman Sciences Corp., Dikewood Division, 2800 28th St., Suite 370, Santa Monica, CA 90405

The noise environments that electronic equipment installed in different systems experience can vary drastically depending on the system and the source of the noise environment. The transient stresses induced on wiring by lightning or switching of internal power typically have a complex waveform. This waveform usually has a broadband spectrum covering several decades in the frequency domain.

On the other hand, the test waveforms commonly used in determining the strength (or noise immunity) of equipment are usually a family of simple and relatively narrowband signals. The capability of comparing equipment strength to the stress environment imposed on it is a necessary ingredient in any design validation, surveillance or maintenance program.

The purpose of this paper is to present transient waveform quantities that can be used in:

- quantifying the minimum tolerable strength (or immunity) levels of equipment
- quantifying the maximum allowable stress levels inside a system
- verification that equipment strength is indeed larger than the stress it is subjected to

Quantities used to capture different features of a given waveform f(t) will be discussed. The relationship of these quantities to equipment failure modes will be discussed as well as their application to different system interfaces. Finally, it should be pointed out that the quantities used to characterize the waveform satisfy the properties of a mathematical norm and they are therefore sometimes referred to as waveform norms.

E/B1-8
1620

APPLICATION OF SHIELD TOPOLOGY TO EMP PROTECTION

Edward F. Vance
SRI International
Route 3, Box 268A
Fort Worth, TX 76140

This paper discusses the use of shield topology in interference control, with particular emphasis on high-strength external sources such as lightning and nuclear EMP. Fundamental principles of electromagnetic interference control are identified as spatial separation, orthogonalization, and exclusion by means of a barrier. Space waves and guided waves are introduced to demonstrate the importance of the shield to the proper performance of barrier elements, such as filters and surge arresters, on conductors penetrating the shield. A consistent approach to grounding is deduced from the shielding principles.

Verifiability implies limiting the number of protection features that must be verified. A high-quality closed shield can be made to limit the stresses induced by exterior sources to an arbitrarily low value. Thus, the stress allowed to penetrate the shield can be effectively limited to that guided along input/output, power, and other conductors and that penetrating openings made for ventilation, personnel entry, etc. These stresses must be limited to values that do not cause spurious arcing inside the shield. They must also be limited to values that cannot cause failure of components inside the shield. Since the number of ways that a system can fail when overstressed is virtually unlimited, the latter criteria is tantamount to requiring that the components inside the shield shall not be overstressed by external sources.

A bound on the amount of shielding needed to protect a circuit or system from a known external sources is thus evident. Although the ability to analyze the interaction of broad-spectrum transient with complex structures is limited, it is possible to reduce the transient to a level such that understanding the exact interaction is no longer important. Thus, if the induced transient stresses are much smaller than those that occur during normal operation, it is not necessary to know these smaller stresses. It is shown that protecting system circuits from external sources such as lightning and the EMP is topologically similar to the electromagnetic compatiblity problem of protecting one circuit from the interference produced by another, separately packaged, circuit.

Session H-5 1355-Weds. NW 270
IONOSPHERIC WAVE EXPERIMENTS FROM THE SPACE STATION
Chairman: R. Post, Plasma Fusion Center, MIT, Cambridge, MA 02139

H5-1
1400 **ACTIVE HF WISP (WAVES IN SPACE PLASMAS) EXPERIMENTS FROM THE SPACE STATION**

R. F. Benson
Laboratory for Extraterrestrial Physics, Code 692, Goddard Space Flight Center, Greenbelt, MD 20771

A transition of the WISP instrumentation from the Shuttle/ Spacelab flight called Space Plasma Lab to the Space Station is anticipated. The extended time-line available from WISP operations on the Space Station will allow a large number of experiments to be performed. This paper will discuss some of those in the HF range including experiments investigating Z to ordinary mode wave coupling; wave-mode ducting; transmitter-accelerated particles; stimulated plasma instabilities, nonlinear effects and ion effects on electron resonant phenomena. In addition, coordinated experiments between WISP and particle accelerators and chemical release activity will allow stimulated phenomena in an artifically perturbed ionosphere to be investigated. Coordinated WISP/Space Station operation over low-latitude incoherent scatter facilities will allow repeated simultaneous investigations of naturally-produced equatorial plasma bubble phenomena from both topside and bottomside remote detection facilities. The role of the crew in active participation in the conduct of these experiments and the placement of WISP instrumentation on the main Space Station and polar and co-orbiting platforms will also be discussed.

H5-2
1420

MULTIPLE PULSE RESONANCE ECHO GENERATION IN TOPSIDE IONOSPHERIC SOUNDING

D. E. Kaplan
Lockheed Research Laboratory
Palo Alto, CA 94304

Multiple pulse echoes and allied coherent resonance phenomena, analogous to the spin echo and photon echo in solid state physics, have been observed in laboratory plasmas in the neighborhood of electron cyclotron resonance.[1] The temporal dependence of echo amplitude upon excitation pulse interval provides information relating to momentum and energy relaxation and diffusion of the electron ensemble. A velocity dependent collision frequency mechanism has been demonstrated to dominate laboratory plasma echo formation. The collision frequency regime characteristic of ionospheric plasmas, with naturally occurring density and magnetic field variations, may be expected to support the generation of this type of resonance echo. Evidence available from Alouette ionograms[2] indicates that these echoes occur among the many types of ionospheric plasma responses to pulse stimulation.

Future topsounder satellite platforms provide a unique opportunity to utilize resonance echo observations to obtain data associated with electron collision processes in the ionosphere. Pulse sequences of varying time intervals may be specifically optimized to provide echo data more comprehensive than that available from the Alouette experiments. The collision related process of multiple pulse echo generation is reviewed and topsounder instrumentation parameters and pulse protocols appropriate to resonance echo generation are suggested.

REFERENCES

1. G. F. Herrmann, R. M. Hill and D. E. Kaplan, 'Cyclotron Echoes in Plasmas', Phys. Rev., 156, p. 118, 1967.

2. D. B. Muldrew and E. L. Hagg, 'Stimulation of Ionospheric Resonance Echoes by the Alouette II Satellite', Plasma Waves in Space & in the Laboratory, Vol. 2, Edinburg Univ. Press, 1970, p. 55.

H5-3
1440

USE OF THE SPACE STATION AS ONE SOURCE OF A DP DEVICE*

N. Hershkowitz, D. Diebold, T.Intrator and M.H.Cho
Department of Nuclear Engineering
University of Wisconsin
Madison, WI 53706

Plasma chamber simulations of space phenomena such as double layers (N. Hershkowitz, Space Sci. Rev. 41, 351, 1985), which make use of double plasma (DP)-like devices, have provided increased understanding of space phenomena. Among many good features of such measurements have been; convenience and the possibility of steady state measurements, control of parameters, and relatively low cost. Device size (compared to Alfven wavelength and Debye length λ_D), perturbations by diagnostics and relatively high background neutral density have been some of the major limitations encountered.

This talk will consider five examples of plasma chamber experiments which either have run up against limitations which may be remedied by Space Station measurements or have developed new diagnostic techniques which would be beneficial for space measurements but do not appear to be suited to satellites. In many applications, the Space Station could function as one boundary of a DP device by using electron and ion beams with the background plasma, diagnosed using a satellite, as the other. Applications include experiments to study:

1."Stairstep-like" multiple double layers, non-BGK structures which resemble space double layer data, have been produced in plasma chambers by increasing the normalized chamber length L/λ_D.

2.Plasma wakes. Many laboratory investigations have demonstrated that emissive probes, consisting of small diameter hot wires, operated in "the limit of zero emission", provide a good technique for determining the plasma potential. This diagnostic is ideal for determining plasma wakes but hot wires often must be replaced and are not suited to satellite measurements.

3.Newly discovered ion acoustic and currentless double layers. The structures are difficult to investigate in the laboratory because probe sizes are larger than λ_D and perturbations are significant.

4.Ion acoustic solitons. These structures evolve from arbitrary initial compressive pulses in plasmas. Studies of such phenomena has been limited by device dimensions.

5.Potential dip filling. Recent experiments have demonstrated that filling in of plasma potential dips by charge exchange or Coulomb scattering can alter plasma potential profiles, e.g. near hot cathodes.

*This work was supported by NASA Grant NAGW-275.

H5-4
1500

BASIC RESEARCH EXPERIMENTS THAT CAN BE PERFORMED ON THE SPACE PLATFORM

N. Rynn
Department of Physics
University of California
Irvine, CA 92717

A basic research program, based on the Q-machine, that models plasma phenomena in the magnetosphere, supported by the National Science Foundation has been functioning for some time at U.C. Irvine. A brief explanation of the program will be given, including a description of our laser induced fluorescence (LIF) technique to measure ion velocity distributions in situ in barium plasmas. Some of the experiments will be described, including those involving the electrostatic ion cyclotron (EIC) instability, modeling of ion conics, measurement of three dimensional velocity distributions, and the interaction of lower hybrid waves with the magnetosphere. The region in the vicinity of the space platform could be an exciting laboratory and raises the possibility of translating some of these experiments to the space environment. In particular, the possibility of launching large amplitude EIC, or ion Bernstein waves, or an EIC instability along a magnetic held line in space and then probing the effects over large distances, either via a diagnostic package on a satellite, or via ground-based transmitters will be discussed. Some of the effects to be looked for would be particle trapping, non-linear effects in general, ion heating, and stochasticity and enhanced diffusion. It may be possible to build what is effectively a long Q-machine, without vacuum chamber walls, in space.

This work supported by the National Science Foundation Grant Nos. ATM-8411189 and PHY-8606081.

Commission H - Waves in Plasmas
Chairman: K. J. Harker
Session: Ionospheric Wave Experiments from the Space Station (R. S. Post)

H5-5
1520

THERMAL PLASMA PERTURBATIONS IN THE VICINITY OF LARGE COMPLEX SPACE STRUCTURES AS OBSERVED IN THE VICINITY OF THE SPACE SHUTTLE

J. M. Grebowsky
Laboratory for Atmospheres/614
NASA/Goddard Space Flight Center
Greenbelt, MD 20771

Large space structures produce significant perturbations of the ambient thermal plasma medium. These effects may compromise the reliability of measurements in their vicinity of ambient plasma properties and ambient wave phenomena. On the other hand they can provide useful scientific platforms for the study of plasma phenomena that cannot be duplicated in the laboratory. Not only the size of the structures is significant, but under conditions requiring artificial atmospheres and water releases, or precise attitude control through frequent thruster firings, or the use of gas releasing experiments the structure will be encompassed by a complex contaminant gas cloud that will extend and perturb the ambient plasma environment far from the source regions. Such effects were measured directly by the thermal ion spectrometer measurements made as part of the Plasma Diagnostic Package (PDP) experiment flown on two Shuttle missions: OSS-1 and Spacelab 2. Plasma contaminating effects on these missions were most readily apparent in the presence of water ions throughout the missions. These ions were particularly evident in the deep wake of the Shuttle and in many instances comprised the dominant ion species current collected by the spectrometer. Other contaminant ions notably the moleculars NO^+ and O_2^+ were also present which could not be clearly distinguished from similar ambient ion species that are present up to F-Region altitudes. Thruster firings, water dumps and the interaction of neutral gases and ions with the Shuttle surfaces also are associated with changes in the immediate plasma environment. Thruster firings produce short burstlike concentration enhancements of several molecular ion species. Water releases on the other hand provide a very effective chemical sink for ambient O^+ ions. Measurements made during PDP free flight indicate that the interactions of the Shuttle with the plasma produce not only a prominent wake effect which is detected far downstream, but also has an influence several hundred meters upstream where water ions were detected. The Shuttle geometry as well as the necessarily complex bayload bay configurations introduced further complexity in the nearby plasma environment e.g., attitude dependent ion scattering and/or production effects were observed in the vicinity of the open bay.

H5-6
1600 A VIEW TOWARD SPACE PLASMA PHYSICS INVESTIGATIONS FROM THE SPACE STATION: N.H. Stone, Space Science Lab, NASA Marshall Space Flight Center, Huntsville, AL 35812

A brief review of scaling concepts and the investigation of space plasma phenomena (particularly the plasma dynamics of orbiting spacecraft) in ground-based laboratories will be given, followed by several example comparisons between the results of ground-based investigations and measurements obtained in space. The advantages of extending the simulation techniques used in ground-based laboratories to an orbiting ionospheric laboratory will be assessed. The investigation of space plasma processes from the Space Shuttle Orbiter will be discussed, including a brief review of initial investigations conducted on the STS-3 and Spacelab-2 missions and their preliminary results, and investigations planned for future space shuttle missions. Finally, the question as to why the Space Station should be used will be addressed in light of the capabilities of ground-based laboratories and the Space Shuttle Orbiter, followed by some general requirements such experiments would place on the Space Station.

H5-7
1620

AMBIENT PLASMA INTERACTION WITH EXTENDED MAGNETIC FIELD STRUCTURES FROM THE SPACE STATION AND IMPLICATIONS FOR RADIO NOISE GENERATION

B.G. Lane, R.S. Post, J.D. Sullivan
Plasma Fusion Center, MIT
Cambridge, MA 02139

The possibility of flying magnets on the Space Station opens up new possibilities for research on plasma interactions. For example, the ASTROMAG magnet would create an extended magnetic field whose strength drops to the ambient level of 0.2 G over a scale length of approximately 10 m. The combined cusp field from the magnet and the earth field produce a complex extended configuration with ring nulls which separate open from closed field lines. This configuration will move through the ambient 1×10^5 cm^{-3} plasma at a velocity of approximately 7×10^5 cm/sec. The ambient plasma crosses the field structure in a time short compared to an ion Larmor period, but long compared to an electron Larmor period. Thus electrons behave as a magnetized fluid while ions move ballistically through the ambient field and reflect from the stronger magnetic field of the cusp. Since the ambient plasma Debye length is short compared to the field scale length, an electrostatic shock structure forms to achieve quasi-neutrality. Fluctuations at the lower hybrid frequency as well as instabilities driven by the ion two stream instability may be expected. We will compare the estimated plasma currents and resulting collisionless shocks with situations where experimental data exists. The associated fluctuation levels and detection schemes will be discussed.

The proposed addition of an rf plasma source creates the possibility of introducing an auxiliary plasma in the wake whose turbulent wavelength spectrum extends from approximately 10 m to the Debye length of 1 cm. Measurements beyond the wake make it possible to measure the nonlinear mixing of the convective modes.

Earlier information and detailed measurements of these phenomena could be performed in laboratory based experiments with a significant impact on the understanding of the space station plasma interactions.

H5-8
1640 A ROTATING MAGNETOSPHERE SIMULATION EXPERIMENT: S.M. Kaye and F.W. Perkins, Princeton Univ., Plasma Physics Lab, Princeton, NJ 08544

Rotating magnetospheres are found in astrophysical objects ranging from the earth to Jupiter to pulsars and accretion discs. Experimental study of these objects is quite limited, apart from the terrestial magnetosphere. This work outlines a rotating magnetosphere simulation experiment to be carried out in the vicinity of the space station. The idea is to create, either by mechanical or equivalent electrical means, a highly conducting sphere of 1m radius with a rotating dipolar magnetic field frozen into its surface. In general, the dipole will not be aligned. The sphere contains a source BaI atoms which are ionized by r.f. cyclotron resonance heating at a radius of 2-3m. Barium is chosen as a working gas because the 455 nm resonance of BaII line will permit flow visualization under solar illumination. For reasonable plasma densities, a balance between outward centrifugal forces and inward magnetic confinement forces should occur in the region 5-10m radius, beyond which the centrifugally-driven flow becomes super Alfvenic. The space environment will this permit, for the first time, experimental study of magnetic angular momentum transfer from a central object to surrounding plasma flow.

H5-9
1700 Coulomb Lattice of Dust Particles in Plasmas.

I. IKEZI, GA Technologies Inc., P. O. Box 85608, San Diego, CA 92138--Dust particles in a plasma accommodate many electron charges. The Coulomb energy of the dust particles, q^2/b, can become much greater than the kinetic energy in the ionosphere. (q = the charge on a particle, b = the average distance between particles.) As a result, a Coulomb lattice of dust particles may be formed. The dust changes the electron-to-ion density ratio. It also introduces potential ripples in the plasma. Thus the feature of the wave propagation in the dusty plasma is significantly modified.

Session J-6 1355-Weds. NW 268
SIGNAL PROCESSING IN RADIO ASTRONOMY
Chairman: J.R. Fisher, NRAO, Greenbank, WV

J6-1
1400

FAST PULSAR SEARCH MACHINE

D. C. Backer, D. R. Werthimer, T. R. Clifton
University of California
Berkeley, CA 94720

S. R. Kulkarni
California Institute of Technology
Pasadena, CA 91125

We are using a fast, digital processor to search for highly dispersed signals from new pulsars with rotation periods as fast as 2000 Hz. A survey of the sky has been initiated at the NRAO 300-ft telescope. In each beam area 192 possible dispersions and as many as 131,072 possible periods are explored for the signature of a pulsar signal. Most of the computation required in this search is executed in real-time with the pipeline of CPU's in our processor.

The initial task in a pulsar search is a two-dimensional Fourier tranform of samples in the radio frequency-time plane. We execute one dimension of the transform by sampling the autocorrelation products of the video signal. We employ the Berkeley Radio Astronomy Laboratory, 80-MHz, 3-level correlator. Data from 64 autocorrelator channels is processed by a pair of Intel 80286 CPUs, and stored in one of two 4 MB buffers. The alternate buffer, which contains data from the previous observation, is read into one of two Mercury 3216 array processors. The AP's do the time to fluctuation frequency transform, and reduce the data to power spectrum peaks above a 4-sigma threshhold. Thresholded data is stored in a third buffer. A fourth buffer containing the previous results is simultaneously analyzed for the signature of a pulsar: a dispersed signal with many harmonics.

Final reduction of data is conducted offline. The most promising candidates are reobserved either by the original search technique, or by folding the data from the correlator at the candidate period and dispersion.

J6-2
1420

PULSAR DISPERSION REMOVAL: A SIGNAL PROCESSING PROBLEM

Daniel R. Stinebring, Physics Department
Princeton University, Princeton NJ 08544
Timothy H. Hankins
Department of Electrical Engineering
Thayer School, Dartmouth College
Hanover, NH 03755

Recent advances in the timing of millisecond pulsars have opened up new areas of investigation, including high precision studies of the interstellar medium and a search for long-wavelength gravitational radiation. Dispersion caused by propagation in the ionized interstellar medium must be removed from the signal before detection in order to achieve the maximum possible time resolution. We will discuss dispersion removal as applied to pulsar timing, concentrating on the signal processing aspects and emphasizing cost and processing speed constraints.

Radio pulses from the millisecond pulsar PSR 1937+21, the most stable known clock over intervals longer than a few months, sweep downward in frequency at the rate of α = 1MHz / 214 μs at 1400 MHz. To remove dispersion, the incoming signal must be convolved with a quadratic phase function $h(t) = \exp(-i\pi\alpha n^2/N)$, where n is the lag number and N is the number of lags in the filter. N = 214 for processing across a 1 MHz bandwidth, and N scales as $(\Delta\nu)^2$ as the bandwidth $\Delta\nu$ is increased. We want to perform this convolution, or its equivalent in the frequency domain, over a total bandwidth of 40 MHz. We will be able to use a 32 x 1.25 MHz filter bank that provides baseband outputs for each of the filter channels. The large data rate requires a real-time or nearly real-time solution, since a daily observation lasts approximately two hours. Square-law detection and synchronous averaging at the pulsar period of 1558 μs can be done once dispersion has been removed from the signal.

We have successfully performed pre-detection dispersion removal on this pulsar over a 1.6 MHz bandwidth using a Reticon 5601A de-chirping chip. This time-domain chip has fixed lag coefficients, requiring a different sampling rate and bandwidth for each observing frequency and pulsar. If the sweep rate becomes too rapid, as it does for frequencies and pulsars of interest, the required sampling rate increases above the chip limit of 2.0 MHz. This limitation leads us to look for other solutions to this problem. We will present our Reticon results and discuss other approaches to this problem. We encourage suggestions from the audience.

J6-3
1440

PULSE DETECTION IN THE SETI MCSA

I.R. Linscott, J. Duluk, J. Burr, and
A.M. Peterson, Radio Science Laboratory
Stanford University, Stanford, CA 94305,
A. Szentgyorgyi, Columbia University, and
P. Backus, SETI Institute

A special computer architecture for signal detection and pattern recognition is being developed at Stanford University for the SETI Multi-Channel Spectrum Analyzer (MCSA). The architecture features two custom VLSI chips that are the hearts of two signal processors, one for numeric and the other for symbolic computation. These processors are programmable and connected on a parallel interconnection network. The MCSA is designed to detect patterns of weak, narrow band signals among a large number of noisy narrowband channels. The MCSA can, in addition, be configured to detect weak, broadband, dispersed pulses, and is suitable for the study of pulsars. An implementation of matched filter signal processing in the MCSA will be presented appropriate for sensitive pulsar pulse recognition.

J6-4
1500

TWO MEGACHANNEL HIGH RESOLUTION DIGITAL SPECTRUM ANALYZER FOR SETI APPLICATIONS

M. Garyantes, M. Grimm,
E. Satorius, and H. Wilck
Jet Propulsion Laboratory
4800 Oak Grove Drive
Pasadena, California 91109

With the recent advent of fast fixed and floating point arithmetic chip sets, the development of wideband high resolution digital spectrum analysis hardware is now possible. In this paper, we present a flexible FFT architecture for providing two megachannels of spectral data at a maximum throughput rate of 40 MHz. This system is currently under development at JPL for use in various applications of the Deep Space Network including the Search for Extraterrestrial Intelligence (SETI) program.

J6-5
1520

AN FFT SPECTROMETER WITH PULSAR DEDISPERSION CAPABILITIES

Richard J. Lacasse and J. Richard Fisher
National Radio Astronomy Observatory
Green Bank, WV 24944

NRAO is constructing a signal processor which incorporates some novel approaches to both pulsar radiometry and spectroscopy. Using a pipelined FFT, the processor operates on individual output points of each transform to calculate, in real time, functions that have traditionally been done with analog electronics or after data have been averaged in a computer. The signal processor consists of two parallel pipelines, only one of which is described below.

The heart of the spectrometer is a pipelined 10-stage FFT engine that can process real data at up to 80Ms/s, producing 1024 point complex, 40 MHz spectra every 25 μsec. Ahead of the FFT engine are 8 IF-to-video converters and 6-bit analog-to-digital converters. A high speed memory acquires, sorts, and orders the data from the converters for 1, 2, 4, or 8 input processing. User selectable windows are applied to the data before transformation. Modules following the FFT pipeline include a self- or cross-power calculator, a stokes parameter calculator, a faraday rotation corrector, and an accumulator/dedisperser. Dedispersion is accomplished by a high speed, complex memory addressing scheme which can accommodate the anticipated ranges of observation bandwidths and dispersion measures. In addition, spectra can be accumulated independently in as many as 8 recurring time periods of programmable width and spacing.

J6-6
1600

SIGNAL PROCESSING IN THE MARK IIIA VLBI CORRELATOR SYSTEM

A. R. Whitney
MIT Haystack Observatory
Westford, MA 01886

The Mark IIIA correlator system is currently operating at the U.S. Naval Observatory in Washington, D.C. in support of VLBI geodetic measurements being made by NASA, NGS, NRL, and USNO. A similar system, to be used for astronomy measurements as well, is being installed at Haystack Observatory. This correlator system, developed at Haystack Observatory, is a second-generation version of the original Mark III correlator, and adds significant new capabilities.

Data processed by the Mark IIIA correlator system is taken using the Mark III or Mark IIIA data acquisition system, which results in data rates up to 224 Megabits/seconds/station. Data from up to 5 stations (10 baselines) may be simultaneously processed.

The Mark IIIA is a highly-parallel, baseline-based system which uses signal-processing algorithms that follow generally along the lines of traditional VLBI correlators. Sample-by-sample fringe-rotation and cross-correlation is performed over a specified number of lags for each of a number of several-second integration periods over the duration of an observation. Fourier transforms are then performed to create cross-spectral and delay functions for each integration period, which are then combined to make estimates of various observables (correlation amplitude, phase, group delay, phase-delay rate, etc.) Special algorithms are used for bandwidth-synthesis measurements which span RF bandwidths of several hundred Megahertz.

The Mark IIIA correlator module incorporates an internal microprocessor to maintain a high-precision *a priori* model for several seconds, even under conditions of very high delay rates or acceleration. This allows processing of data collected from artificial earth-satellites, and from earth-orbitting antennae receiving signals from natural sources; these capabilities were critical in supporting the first space-based VBLI astronomy observations between ground-based antennae and an earth-orbitting satellite.

J6-7
1620

GOLDSTONE SOLAR SYSTEM RADAR PERFORMANCE ANALYSIS

E.H. Satorius, S.S. Brokl, R.F. Jurgens,
C. R. Franck, and R.M. Taylor
Jet Propulsion Laboratory
4800 Oak Grove Drive
Pasadena, California 91109

The Goldstone Solar System Radar (GSSR) has been developed to operate in both CW and PN ranging modes. In this paper, we present the results of a computer-aided performance analysis of the GSSR operating in the PN mode. The intent of this analysis is to quantify the effects of digital quantization errors on the performance of the GSSR in terms of system sensitivity. The results of our analysis not only quantify system performance, but also provide useful quidelines for choosing various GSSR parameters to enhance system performance.

J6-8
1640

CORRELATOR ARCHITECTURE FOR THE AUSTRALIA TELESCOPE

W. E. Wilson,
CSIRO Division of Radiophysics, Epping, NSW, Australia, and
M. S. Ewing,
Caltech Owens Valley Radio Observatory, Pasadena, CA

The Australia Telescope (AT) is a versatile array of 6 new 22 m antennas at Culgoora NSW in a 6 km east-west "compact array." Another 22 m antenna at Siding Spring NSW and other existing Australian antennas will be added to form the AT "long baseline array." Wavelength coverage extends from decimeters to millimeters (327 MHz—116 GHz). Completion of the compact array is expected in 1988.

The AT will have separate correlators for the compact and long-baseline arrays; they are based on a novel custom integrated circuit, the XCELL. Designed by CSIRO Division of Radiophysics and Austek Microsystems Ltd, an Australian firm, the chip incorporates an 8×8 array of multiplier-accumulators, operating at a 16 MHz clock rate. Either 1- or 2-bit samples may be correlated.

XCELL is suitable for correlation of very high speed data streams which are blocked into N-sample parallel words before correlation. The AT correlator "module" consists of a 4×4 array of XCELLs which effectively produce a 32×32 multiplier-accumulator array. With a word length N=32 samples, a data stream of 512 Msample/sec can be correlated. Intermediate "reconfigurations" of the array permit efficient use of the XCELLs for higher resolution and lower sample rates, down to 16 or 8 Msamples/sec (1-bit or 2-bit sampling, respectively). This resolution versatility is readily achieved through data switching. Recirculation may be added for even higher resolution.

J6-9
1700

THE HAT CREEK HYBRID SPECTROMETER

J. Carlstrom, D. Thornton, J. Hudson, L. Urry
Radio Astronomy Laboratory
University of California Berkeley, CA 94720

A hybrid spectrometer designed for millimeter-wave interferometry has been developed for use at the Hat Creek Observatory. Details of the spectrometer may be found in W. L. Urry, D. D. Thornton, J. A. Hudson, PASP, 97, 745-751, 1985. Here we give a brief overview of the spectrometer and then concentrate on recent developments pertaining to the use of the spectrometer. A strong emphasis will be placed on online passband calibration.

The spectrometer is ideally suited for multi-line astronomical observations. For each correlated IF pair, there are 512 complex channels. Quadrature phase shifting of the first LOs allow the sidebands to be separated resulting in 256 complex channels per sideband. These channels may cover a total bandwidth per sideband of 1.25 MHz (4.88 KHz per channel) to 320 MHz (1.25 MHz per channel). The spectrometer uses up to four single sideband mixers with separate LOs for each IF. The bandwidth of the sampled IF at these LOs may be set from 1.25 to 80 MHz. The spectrometer may also be used for single dish observing (autocorrelating each IF) with the same bandwidths as above but with a factor of two higher spectral resolution.

To accurately calibrate the passband of data taken with an interferometer it has been customary to observe a strong continuum source with the same spectrometer configuration that was used to take the data. The continuum source must be observed long enough to achieve high signal to noise spectra. This is often a prohibitively long time, especially when narrow bandwidths are used. We have developed a quick way to determine the passband by splitting the IFs one at a time and feeding them into the spectrometer. The complex gain corrections are then applied to the data online. One still needs to observe an astronomical continuum source to determine the receiver phase response and the difference between the upper and lower sideband amplitude gains. However, these are both slowly varying functions of the IF frequency and may be determined by fitting a low order polynomial to relatively quickly obtained noisy broadband spectra of a continuum source.

Thursday Morning, 15 Jan., 0835-1200

Session A-4 0855-Thurs. NW 248
MICROWAVE MEASUREMENTS AND STANDARDS
Chairman: Harry M. Cronson, The Mitre Corp., MS R 35 O, Burlington Road, Bedford, MA 01730

A4-1 0900 MMIC WAFER PROBING TO 26GHz: Aditya K. Gupta, Rockwell International, Microelectronics Research & Development Center, 2427 W. Hillcrest Drive, Newbury Park, CA 91320

With the development of Monolithic Microwave Integrated Circuit (MMIC) technology, a strong need has evolved for accurate, on-wafer RF probing of microwave devices and circuits. In response to this need, Cascade Microtech Inc. has recently introduced an RF probe station for measurements up to 26 GHz (E.W. Strid, Microwave Journal, 71-82, Aug. 1986). This system utilizes tapered 50 ohm coplanar transmission lines. The manufacturer provides coplanar impedance standards to eliminate systematic measurement errors (due to the probes, cables, etc.) by using standard techniques of automatic network analysis. This measurement scheme works well with coplanar circuits, but if the MMIC transmission medium is microstrip, a coplanar-to-microstrip transition at each RF port of the chip is required. The implications of these transitions on measurement accuracy is the subject of this paper.

A4-3
0940 MILLIMETER WAVE REFLECTED POWER FROM MOVING STRIP ILLUMINATED SEMICONDUCTOR PANEL

M. H. RAHNAVARD, A. HABIBZADEH

Electrical Engineering Department
Shiraz University, Shiraz, Iran

One of the needs in air trafic is to know the environmental situation under any weather condition. Visble and IR radar will fail in adverse weather because of high attenuation (B. J. Levin. "Millimeter Wave Image Conversion, "PH. D. Dissertation, the Moore School of Elect. Engg. University of Pennsylvania, Philadelphia 1967.)but there are several windows in millimeter wave region with low attenuation in bad weather condition (Weibel, G. H. and Dressel, H. O., "Propagation Studies in Millimeter Wave Link Systems", Proc. IEEE, Vol. 55, April 1967, pp. 497-513). One of the method to convert millmeter wave to visible light is by using illuminated semiconductor panel (J. Bordogna, et. al. "Millimeter Wave Image Conversion", Task, D-2, The Moore School of Elect. Eng. University of Pennsylvania, Philadelphia.). Semiconductor panels are used as image convertors in both transmission and reflection mode of operation (H. Jacobs, et. al., "Interformetric Effect with Semiconductor in Millimeter Wave Region," J. Opt. Soc., V. 57, No. 8, Aug. 1967). In both cases the response of illuminated panel is important. Excess carrier in semiconductor panel under stationary illumination is obtained by Levin et. al. (B. J. Levin, "Spot Illumination of Semiconductor Panel, "IEEE Letters Vol. 56, pp. 1230-1231, July 1968, R. Mavaddat and B. J. Levin "Surface Illumination of Semiconductor Panel," J. of Applied Physics vol. 40 pp. 5324-5332 (1967)). Using the above result reflection coefficient and attenuation coefficient for this case is also studied (R. Mavaddat, "Millimeter Wave Attenuation Through Illuminated Semiconductor Panel," IEEE Trans. on Microwave Theory and Techniques, Vol. MTT-18, No. 7, July 1970 pp. 360-364, R. Mavaddat, "Millimeter Wave Power Transmission and Reflection in Semiconductor Image-Convertion Systems". IEEE Transaction on Microwave Theory and Technique pp. 555-558, July 1971.). Practically, the response of semiconductor panel to moving illumination is required. In reference (M. RAHNAVARD, et. al. "Moving Spot Illumination of Semiconductor Panelys", Journal of Applied Physics Vol. 46, No. 3, pp.1229-1234 March 1975.) excess carrier in moving spot illuminated semiconductor panels is studied and profiles of excess carrier for moving strip illuminated semiconductor panel vs. different parameters is obtained. In this paper using the excess carrier results, reflected millmeter wave from strip illuminated semiconductor panel vs. scanning velocity, position, thickness of the strip and time is studied and the resultant curves are plotted.

A4-4 1000 LOSS CALCULATION IN SYMMETRICALLY SPHERICAL WITH CIRCULAR APERTURE UNSTABLE OPTICAL RESONATORS USING DIFFERENT TECHNIQUES

M. H. RAHNAVARD, H. ZARE-MOODI
Electrical Engineering Department
Shiraz University, Shiraz, Iran
Telephone Number: Iran, Shiraz 34064-2712

Unstable Optical resonator is used in medium and high power laser. In stable resonator when Fresnel number is greater than 0.5 all of the energy is not absorbed by 1st mode but energy is absorbed in higher order modes. For absorbing maximum energy from the material we should operate in higher modes with higher power loss capability. In unstable resonator with proper gain it is possible to have mode with lowest power loss and this mode will absorbe most of the energy from the laser material and it is possible to have optical resontor with smaller length. For this reason power loss calculation is important in unstable optical resonators.

Session B-10 0835-Thurs. NW 271
BACKSCATTERING ENHANCEMENT
Chairman: I.M. Besieris, Dept. of Electrical Engineering, Virginia Polytechnic Institute, Blacksburg, VA 24061

B10-1 0840 BACKSCATTERING ENHANCEMENT: EXPERIMENT AND THEORY

Akira Ishimaru and Yasuo Kuga
Department of Electrical Engineering
University of Washington
Seattle, Washington 98195

In 1984, Kuga and Ishimaru published a paper describing experimental evidence for the backscattering enhancement from a dense distribution of discrete scatterers. Tsang and Ishimaru then explained this effect theoretically by demonstrating that two wave paths which transverse through the same particles in opposite directions can constructively interfere and produce the backscattering enhancement and that the angular width is of the order of (wavelength)/(mean free path). In recent years, this enhancement has been recognized as evidence of weak Anderson localization effects, and similar experiments have been conducted by others. The backscattering enhancement from rough surfaces appears to be caused by similar mechanisms. However, the backscattering enhancement from turbulence appears to be based on different mechanisms with different angular widths.

B10-2
0900

MEASUREMENTS OF ENHANCED OPTICAL BACKSCATTERING FROM ROUGH SURFACES

J. C. Dainty, M.-J. Kim, E. R. Mendez and K. A. O'Donnell
Blackett Laboratory, Imperial College, London SW7 2BZ, United Kingdom

Significant enhanced backscattering by randomly rough surfaces has recently been observed (E. R. Mendez and K. A. O'Donnell, submitted to Phys. Rev. Lett.) at $\lambda = 0.63$ μm.

The surfaces are fabricated by exposing photoresist to suitable laser speckle patterns, processing the resist and overcoating with aluminium (or gold). The probability density of surface height approximates a Gaussian of standard deviation σ_z; in our experiments, $\sigma_z \approx 1$-2 μm. The autocorrelation of surface height is also Gaussian of correlation length ℓ in the range 1-20 μm.

For surfaces with a large correlation length ℓ and low rms slope, e.g., $\ell \approx 20$ μm, $\sigma_z \approx 1$ μm, the scattered intensity v angle of observation agrees well with the Beckmann prediction for small or moderate angles of incidence. However, if $\ell/\sigma_z \approx 1$ (e.g. $\ell \approx \sigma_z \approx 1.5$ μm), the scattered intensity shows significant enhanced backscatter with an interesting polarization structure.

A simple geometrical/physical optics multiple scattering model can explain the phenomenon qualitatively but, to our knowledge, there is no quantitative theory that predicts this effect. In this paper, measurements for several surfaces will be presented.

B10-3
0920

BACKSCATTER ENHANCEMENT: GENERIC MODEL AND ESSENTIALS

David A. de Wolf
Department of Electrical Engineering
Virginia Polytechnic Institute and
State University
Blacksburg, VA 24061

Backscatter enhancement is the term used to describe the phenomenon that scattered EM energy appears to be stronger in a narrow cone around the backwards direction than in other directions. The enhancement can be up to a factor 2 for 180 degree backscatter. The phenomenon has been studied intensively in the USSR, and to lesser extent in the USA.

Simple and general models for the phenomenon for large-scalesize continuously random and for discrete random media will be given. For the continuous case, a fairly worked out result can be expressed in terms of radiative transfer theory, based on previously published work. In the case of discrete (particulate) media, an argument for enhancement can be given by regarding the average scattered intensity in terms of the iterated integral-equation series for the electric field. This model is rather general, but it already incorporates several features typifying much more specific and limited models.

We will discuss some of the existing work on backscatter enhancement, and attempt to make a comparison with what is presented here.

B10-4
0940

BACKSCATTERING ENHANCEMENT FOR RANDOM DISCRETE SCATTERERS OF MODERATE SIZE

Leung Tsang and Akira Ishimaru
Department of Electrical Engineering
University of Washington
Seattle, Washington 98195

Backscattering enhancement for random discrete scatterers was previously studied by calculating the contributions of cyclical scattering terms in multiple scattering processes. The method was applied to the case of small particles, where it was shown that the cyclical scattering processes exhibit a peak in the backscattering direction with angular width 2K"/K' with K' and K" being the real and imaginary parts of the effective propagation constant. In this paper, the method is extended to the case of scatterers comparable to or larger than a wavelength. The problem of a plane wave normally incident on a half space of dielectric spheres is considered. The problem is of particular interest because besides the peak due to cyclical scattering, there can also be a peak due to single scattering in the Mie phase function. Numerical results are illustrated as a function of particle size and concentration. The relative importance of the two peaks will be discussed.

B10-5 PANEL DISCUSSION: Walter A. Flood,
1000 Moderator

Session C-5 0835-Thurs. NW 238
ROBUST SPECTRAL ESTIMATION
Chairman: J. Park, Yale Univ., P.O. Box 6666, New Haven, CT 06511

C5-1
0840 ROBUST ESTIMATION OF POWER SPECTRA, COHERENCES, AND TRANSFER FUNCTIONS: Alan D. Chave and David J. Thomson, AT&T Bell Labs, Murray Hill, NJ 07974

Reliable calculation of power spectra for single data sequences or of transfer functions and coherences between multiple time series is of central importance in many fields of science and engineering. Problems arise in conventional time series analysis with many types of data because the methods are essentially copies of classical statistical procedures parameterized by frequency. Because these techniques are based on the least squares or Gaussian maximum likelihood approach to statistical inference, their advantages include simplicity and the optimality properties established by the Gauss-Markov theorem. In practice, this type of model is rarely an accurate description due to the presence of a small fraction of unusual data or "outliers" that do not share the statistical characteristics of the bulk of the sample. Outliers can destroy conventional spectral estimates, often in a manner that is difficult to detect.

Over the past two decades, the field of robust statistics has been developed to handle outlier contamination and yield reliable estimates under non-ideal circumstances. We have adapted the principles of robust statistics, and especially M-estimation theory, to univariate and multivariate spectral analysis using section-averaging techniques (Chave, Thomson, and Ander, J Geophys. Res., in press). This results in robust spectral estimates, and operates in an automatic, data-adaptive, high-efficiency fashion. Because robust methods involve nonlinear operations and implicitly identify abnormal data, we emphasize the importance of monitoring the statistical behavior of the output using diagnostics like quantile-quantile plotting. We also find that nonparametric techniques like the jackknife yield more reliable confidence limits and inference tests than the conventional, distribution-based types.

We have developed a new type of robust spectral estimator based on the multiple prolate window method of Thompson (Proc IEEE, 70, 1055-1096, 1982). Individual multiple window estimates with large time-bandwidth products for spectra, coherences, or transfer functions are first obtained for individual blocks that are subsets of longer time series. These quantities have sufficient degrees of freedom to be individually stastically meaningful, and are combined using an M-estimator to yield a robust result. A major

C5-2
0920

TOPICS IN SPECTRUM ESTIMATION

R. D. Martin, D. B. Percival and A. T. Walden
Department of Statistics, GN-22
University of Washington
Seattle, WA 98195 USA

Long-Memory Processes. Various methods have been proposed for estimating "long-memory" spectrum which are characterized by linearity near zero frequency, on a log-log scale. We compare the sampling properties of several methods, including the following: (1) the periodogram estimator studied by Mohr (1981); (2) the extension of Mohr's scheme to include multiple window estimation techniques due to Thomson; and (3) the maximum entropy method as recently investigated by Fougere.

Bias-Robust Spectrum Estimation. Averaging of the periodogram over time, at each discrete Fourier transform frequency, is a very commonly used method in spectrum estimation. However, this method is very non-robust, just as is the sample mean for estimating location. We propose a bias-robust estimate of the spectrum by replacing the sample mean with an exceedingly simple kind of M-estimate of scale for exponential random variables. Here, a bias-robust estimate is one which minimizes the maximum asymptotic bias over epsilon-contaminated families of nearly exponential distributions.

Robust Filtering and Spectrum Estimators for Unequally Spaced Data. We describe algorithms for extending robust-filtering based spectrum estimation (Thomson, 1977; Kleiner, Martin and Thomson, 1979) to the case of unequally-spaced data. The method is improved by extending robust smoothing based spectrum estimation (Martin and Thomson, 1982) to the case of unequally spaced data, and using a robust smoother in place of a robust filter. Applications are described.

C5-3
1040 IMPLEMENTATION CONSIDERATIONS FOR TIME AND FREQUENCY DOMAIN PARTIALLY ADAPTIVE ARRAY PROCESSING

Barry Van Veen
Richard Roberts
Department of Electrical and Computer Engineering
University of Colorado
Boulder, CO 80309

The computational complexity of fully adaptive arrays employing thousands of sensors is often prohibitive and thus, one is led to processors which only use a fraction of the total adaptive degrees of freedom available. Time (B. Van Veen, Ph.D. Thesis, Univ. of Col., 1986) and frequency domain (N.L. Owsley, Array Signal Processing, chap. 3, Prentice Hall, 1985) implementations of partially adaptive processors based on the generalized sidelobe canceller (L.W. Griffiths and C.W. Jim, IEEE Trans. Antennas Propagat., 30, 27-34, 1982) have been proposed. The present work reviews time and frequency domain partially adaptive implementations and compares them on the basis of performance and complexity.

A fixed number of adaptive degrees of freedom are assigned to each spectral bin in a frequency domain implementation. Time domain implementations make more effective use of their adaptive degrees of freedom by distributing them throughout the the spectrum of interest and are more robust to a variety of channel errors. Frequency domain implementations require more computational resources but the computations are performed in parallel.

C5-4
1120 DEVELOPMENT AND APPLICATION OF A MULTIVARIATE ERRORS-IN-VARIABLES MODEL FOR THE ANALYSIS OF GEOMAGNETIC ARRAY DATA

G. D. EGBERT and J. R. BOOKER (both at Geophysics Prog. AK-50, Univ. of Wash., Seattle, WA 98195)

In regional geomagnetic array studies, where array dimensions are smaller than typical source scales, it is usually assumed that the time varying external source fields can be approximated by plane waves of infinite horizontal extent. If this assumption holds exactly and measurements are made without error, it is easy to show that all field components can be related by linear transfer functions to the two horizontal components of the magnetic fields at any chosen reference station. Such interstation and intercomponent transfer functions have typically been estimated, one at a time, from the Fourier transformed time series using least squares methods. To do this, it is assumed that the reference fields are measured without error, and that the discrepancy between predictions and observations due to the failure of model assumptions can be treated as incoherent noise in the predicted field component.

We have developed a more physically realistic statistical model for the estimation of this plane wave response which allows for (potentially correlated) noise in all measured field components. We find that much of the "noise" is highly coherent across the array and can be ascribed to violations of the uniform source field assumption. The covariance structure for the noise can be parameterized, based on simple physical models, in a way which allows for the separation of coherent source "noise" from the desired signal. In statistical terms, the model is a (complex) multivariate errors-in-variables model with a generalized, but identifiable, error covariance. We will emphasize in particular the statistical methods we have developed for parameterization and estimation of the error covariance structure. We will also discuss some simple ways to "robustisize" the standard errors-in-variables estimates which are particularly relevant to geomagnetic arrays.

C5-5
1120

SMOOTH EM RESPONSE FUNCTIONS FROM NOISY DATA

J.C. Larsen
Pacific Marine Environmental Lab, NOAA
Seattle, WA 98115

Least squares methods are typically used to determine band average estimates of magnetotelluric response functions yielding estimates that are often not smooth functions of frequency due to noisy data. MT response functions should, however, be smooth function of frequency since the electromagnetic data can usually be treated as independent of the wavenumber of the source. Therefore a weighted least squares method has been developed to determine response functions and variances that will be smooth functions of frequency with the effects of noisy data removed.

To carry out the objective of obtaining smooth response functions that can also be approximated, as far as possible, by a response functions based on a one dimensional earth, the response is represented by a response based on a best fitting D+ Parker one dimension model earth (a stack of thin conducting sheets) times a smooth distortion factor given by a finite sum of simple frequency dependent functions. The response is then interatively estimated whereby a one dimensional model is computed at the end of each iteration and a new distortion factor for the next iteration is then computed by least squares from the electromagnetic data.

Since least square methods are sensitive to outliers, a time and a frequency weighting series are generated that are based, respectively, on the time and frequency residuals. The present iterative method then incorporates these weights and provides an unbiased method for removing the effects of outliers. The weighted residuals are plotted to determine whether a gaussian distribution is satisfied.

Session E/B-2 0835-Thurs. NW 261
SPECIAL SESSION ON HIGH POWER
ELECTROMAGNETICS II
Chairman: R.L. Gardner, Mission Research Corp.
1720 Randolph Road, SE, Albuquerque, NM 87801

E/B2-1
0840 LIGHTNING RESPONSE OF AIRCRAFT: K.S.H. Lee and F.C. Yang, Dikewood Division of Kaman Sciences Corp., 2800 28th Street, Suite 370, Santa Monica, CA 90405

The 1984 and 1985 F-106B lightning test data have been processed and analyzed. Representative internal and external response data are presented, in both the time and frequency domains. Peak values, other norm quantities and spectral envelopes are tabulated and graphed. These norm quantities and spectral envelopes can be used for the lightning specification development. The interaction of natural lightning with aircraft is also discussed with the aid of the test data. A mathematical model is then suggested for calculating aircraft external responses to direct-strike lightning.

+

E/B2-2 0900

PULSE DATA PREPROCESSING TECHNIQUES TO RECOVER SEM PARAMETERS

C. D. Taylor*, S. Giles**, and E. Harper***
* Stocker Visiting Professor
Ohio University
Athens, OH 45701-2979
** Lawrence Livermore National Laboratory
Livermore, CA 94550
*** Air Force Weapons Laboratory
Kirtland AFB, NM 87117

Generally, the response of a system to a high power electromagnetic transient can be expressed in terms of a singularity expansion. This technique is called the singularity expansion method (SEM). Knowning the SEM parameters it is possible to characterize the system response and to search for conditions required to maximize a particular attribute of the response signal. Thus it is the goal of this study to present techniques whereby the SEM parameters can be extracted from measured data, and in particular, data with a low signal-to-noise ratio. Both linear and nonlinear filter techniques are considered.

A nonlinear digital filter technique that uses a serial correlation test is shown to provide a preprocessing technique which allows the classic Prony method to be applied to the data. The technique also estimates the noise level and detects the presence of nonstationary noise. Results are presented for typical noisy data, as well as for analytical data with added White-Gaussian noise.

E/B2-3 MOTION OF ION CLOUDS IN AIR
0920

C. E. Baum
Air Force Weapons Laboratory/NTAAB
Kirtland AFB NM 87117-6008

After the initial processes in a natural lightning event there can exist clouds of positive and/or negative ions in air. This paper considers some of the processes involved in the subsequent motion of such ion clouds in spherical and cylindrical geometries. In the case of spherical geometry such a cloud can stay around for a long time. Such clouds of ions can also be moved by other electric fields in the environs.

E/B2-4 0940 CORONA EFFECTS ON POWER SYSTEMS DUE TO LIGHTNING AND EMP INDUCED SURGES: J.P. Blanchard, LuTech, Inc., 3742 Mt. Diablo Blvd. Lafayette, CA 94549

Corona discharge effects on power systems have been studied for many years, particularly because of the power loss and radio frequency interference noted due to these discharges. More recently, changes in the shape of lightning induced transient surges on power lines due to corona influences have been studied. These studies have led to related investigations of the effect of corona on currents induced in power lines by transient electromagnetic pulses (EMP).

This paper will review the concept of corona as related to transmission lines. Following a brief discussion of the nature of corona formation and its impact on transmission lines in their normal operating state, the bulk of this paper will be devoted to the effects of corona arising from lightning and EMP induced transient current surges. Comparisons between analytical predictions and experimental results will be discussed.

E/B2-5 1000 PROGRESS IN THE DERIVATION OF ELECTRICAL CHARACTERISTICS OF LIGHTNING FROM ITS OPTICAL OUTPUT*

R. L. Gardner, A. H. Paxton, and L. Baker
Mission Research Corporation, 1720 Randolph Road, S.E., Albuquerque, New Mexico 87106

W. Rison
New Mexico Institute of Mining & Technology
Socorro, New Mexico 87801

C. E. Baum
Air Force Weapons Laboratory/NTAAB
Kirtland Air Force Base
New Mexico 87117

In order to develop techniques for remote sensing of lightning currents and other internal electrical parameters a detailed model of the energy balance of a lightning discharge has been constructed. We present here a detailed one-dimensional hydrodynamic model of a slice of unit length of a lightning channel.

The energy is input to the channel by joule heating. A known current is impressed on a channel whose resistance is calculated from a conductivity profile which is a function of the local gas temperature. Energy is distributed across the cross section of channel as if it were a set of parallel resistors. The current is assumed to vary slowly enough that the diffusion time is negligible.

Energy losses are more varied. The hot gas loses energy immediately through radiation. In this model radiation losses and redistribution of energy throughout the gas are calculated using multi-group diffusion. Eight frequency bands are chosen and for each a diffusion calculation is performed. The bands are chosen in such a way that the opacity varies by no more than a factor of two over a single band. Hydrodynamic expansions, including pseudo-viscous pressure for shocks is included to complete the energy balance. A complex equation of state for an idealized air molecule is used in the calculations.

This model is intended for use in remote sensing of lightning currents. For that purpose, the model must be experimentally verified. The model is compared to available experimental data from the KIVA Laboratory on S. Baldy Peak.

---

*This work was performed under Air Force Contract F29601-85-C-0009.

E/B2-6
1020

AN EXPERIMENTAL TEST OF THE "TRANSMISSION-LINE MODEL" OF ELECTROMAGNETIC RADIATION FROM TRIGGERED LIGHTNING RETURN STROKES

J. C. Willett
Naval Research Laboratory
Washington, D. C. 20375;
V. P. Idone
State University of New York
Albany, NY 12222;
C. Leteinturier
CNET MER/GER
22301 Lannion
France;
A. Eybert-Berard and L. Barrett
CEA 38041 Grenoble
France;
E. P. Krider
Institute of Atmospheric Physics
University of Arizona
Tucson, AZ 85721.

The "transmission-line model" of return-stroke radiation, first proposed by Uman and McLain (J. Geophys. Res., 75, 5143-5147, 1970), and invoked frequently thereafter to infer peak currents from remote fields or to estimate propagation velocities from measured fields and currents, has never received a thorough experimental test. During the summer of 1985, we were able to measure peak currents (with a coaxial shunt), two-dimensional average propagation speeds (with a high-speed streak camera), and electric field waveforms (at 5.2 km range) for a number of subsequent return strokes in rocket-triggered lightning flashes at the Kennedy Space Center, Florida. Because of the temporal ambiguity on the streak-camera films, it has been possible to identify only the velocity of one individual stroke for which current and field data are available. Two other multi-stroke flashes, however, each yielded a tight cluster of velocity measurements and a group of peak field/current ratios, though not necessarily for the same strokes. A further six flashes provided more current and field measurements for which no velocity information was obtained. It will be shown that these data indicate reasonable agreement between the propagation speeds measured with the streak camera and those inferred from the transmission-line model.

E/B2-7 1100 PANEL: WHERE WE ARE AND WHERE WE ARE GOING IN HIGH POWER ELECTROMAGNETICS

Session G-7 0835-Thurs. NW 270
HF IONOSPHERIC PROPAGATION
Chairman: C.M. Rush, NTIA/ITS, Boulder, CO 80303

G7-1
0840 CALCULATED AND OBSERVED WINTERTIME NMAX(F2) VALUES AT THULE

D.N. Anderson, J. Buchau, E.J. Weber and H.C. Carlson, Jr.
Air Force Geophysics Laboratory
Hanscom AFB MA 01731

Extensive observations of the diurnal variation in polar cap ionospheric densities at Thule, Greenland have been made during winter months from solar cycle maximum to solar minimum periods. Experimental evidence strongly suggests that the daytime plasma densities in the ionospheric F-region originate equatorward of the dayside cusp region and are produced primarily by solar ultraviolet radiation rather than by precipitating low energy electrons. To study the process in more detail, the time-dependent ion continuity equation is solved numerically including the effects of production by solar radiation and precipitating particles, loss through charge exchange with N_2 and O_2 and transport by ambipolar diffusion, neutral wind and high latitude E x B convection drift velocity. Calculated electron density values as a function of local time at Thule are compared with recent observations during a period of declining sunspot activity. The relative contributions from solar production and precipitating particle production are discussed for various E x B plasma convection patterns.

G7-2
0900

METHODS FOR IMPROVING ACCURACY OF RADARS TRACKING OBJECTS AT IONOSPHERIC HEIGHTS

D. B. Odom, The Raytheon Company
Wayland, MA 01778
J. A. Klobuchar, Ionospheric Physics Division
Air Force Geophysics Laboratory
Hanscom AFB, MA 01773

The problem of accurately determining the contribution which the ionosphere provides to the time of arrival of a signal scattered from an object being tracked by the new generation of long range high precision radars is addressed in this talk. For older radars, the estimate of the ionospheric contribution is often either not made, or is obtained from a simple set of correction tables. A few of the older radars utilize indirect observations, such as Total Electron Content (TEC) measurements and overhead soundings. These latter measurements do not provide a sample in the region of space from which the ionospheric contributions actually come.

The new radar, which requires a special high precision measurement of the ionospheric contribution, is a long range phased array radar used by the United States for early warning and space track missions. The procedure used by this type of radar is referred to as "self sounding". The radar makes two measurements (called pulse pairs) of the total time delay from the radar to the target and back. Each measurement is at a different frequency; the difference in time delays is used to obtain the total ionospheric contribution. Since this contribution is applicable for only this region of space, and for a limited period of time, a procedure is described which allows this measurement to be applied to other surveillance sectors. A series of 62 measurements, each made up of thousands of radar observations, will be reviewed. The precision which was achieved in the measurement of the ionospheric range contribution during these observations is described in detail. A comparison of these results with a series of standard TEC measurements taken at the same time is provided.

G7-3 0920 PRECISION TARGETING EXPERIMENT: Eli Tichovolsky, Rome Air Development Center, Electromagnetic Sciences Directorate, Hanscom AFB, MA 01731

A Precision Targeting Experiment (PTE) was performed in 1984 during which 15 hours of OTH-B FM/CW radar range-Doppler data were collected by SRI international from a target aircraft (Air Force Geophysics Laboratory's Airborne Instrumentation Observatory) of precisely known location and speed. Exhaustive ionospheric diagnostics were collected via three vertical sounders at the path mid and end points, a wide-sweep backscatter sounder at the radar, a radar-to-target oblique sounder, and a tilt-measuring sounder array operated by the University of Lowell Center for Atmospheric Research at mid-path. This database will be used to analyze HF radar propagation modes and their impact upon accurate radar range to ground range conversion. The objective of this experiment was to detect and identify deficiencies in the wide-sweep backscatter inversion process--an element critical to range conversion.

G7-4
0940

A NEW WIDEBAND HF TEST FACILITY

M.N. Richard, E. A. Palo, and B.D. Perry
The MITRE Corporation
Burlington Road, MS E025
Bedford, MA 01730

The MITRE Corporation has maintained and periodically operated a wideband HF experimental test facility for the past 5 years. With this facility we have been able to demonstrate the feasibility of the concept of wideband (megahertz-bandwidth) HF communications using pseudo-noise (PN) spread spectrum signaling techniques and have established a useful data base covering wideband HF skywave propagation, channel equalization techniques (including pre-transmit equalization), reciprocity of the wideband HF skywave channel, and PN spread spectrum signal processing techniques as applied to the wideband HF channel.

We are currently undertaking a major redesign of the test facility, creating a flexible test bed for performing communications experiments. A transportable transmit terminal provides a programmed and remotely controlled selection of transmission parameters. The fixed receive site includes several antennas, an analog wideband HF receiver, and an alternative, nearly-all digital HF receiver. There are two types of real-time narrowband interference mitigation processors; a 128-tap, adaptive (FIR) filter and a 16,384-point DFT processor. The PN Matched Filter (for the despreading of the PN signal) is capable of processing gains in excess of 10,000 (40 dB). The data waveform (DPSK) demodulator is supported by several flexible channel distortion compensation subsystems. All of these signal processing subsystems are selected, linked, and controlled in real time by a powerful microprocessor control system.

When the upgrade is completed later this year, we will have the capability to perform extended duration experiments requiring minimal operator control. The facility will allow for real-time control of the transmission parameters and data collection test points. Test configurations will include multiple PN spread spectrum modes (for data communication) and linear frequency modulation probe modes (for channel characterization). We are planning a series of experiments aimed at assessing real world HF communications performance with megahertz-bandwidth spread spectrum waveforms over selected paths with lengths ranging from 1000 km to 3000 km.

In this paper we shall review previous wideband HF results; describe the test facility, its capabilities and motivation; summarize experimental results to date; and preview the experiments to follow.

G7-5
1000

HF MUF MODEL UNCERTAINTY ASSESSMENT

T.N. Roy and D.B. Sailors
Ocean and Atmospheric Sciences Division
Naval Ocean Systems Center
San Diego, CA 92152-5000

To assess the accuracy of MUF model prediction, a statistical analysis of observed oblique sounder median maximum observed frequencies (MOF) and predicted maximum usable frequencies (MUF) was conducted. A data base consisting of 13,054 hours of oblique sounder MOFs measured on 70 paths were compared against the predicted MUF values from MINIMUF-3.5, MINIMUF 85 and an unrelated MUF model, the HF Broadcast WARC Model (HFBC 84). The data was screened into subsets to determine the effect of particular paths, path length and orientation, season, month, latitude, sunspot number, diurnal trends, geographic region and sounder type. The accuracy of all three models was very close, with the MINIMUF-3.5 model having the lowest rms error of 4.44 MHz. MINIMUF 85 was next with an rms error of 4.58 MHz and HFBC 84 was last with an error of 4.67 MHz. Correlation was good for all three models. Coefficients were .824, .819 and .827 for MINIMUF-3.5, MINIMUF 85 and HFBC 84, respectively.

The primary difference between MINIMUF-3.5 and MINIMUF 85 appeared when detailed analysis of the accuracies was conducted. When the variation in error was noted as a function of season, sunspot number, or range, for instance, there was less variation in the accuracy of MINIMUF 85. In some cases, MINIMUF-3.5 would exhibit high error, and in other cases it would exhibit low error.

When the accuracy of the models was investigated as a function of mid-path local time a large diurnal error was found in all three models. In the case of the MINIMUF models, linear regression showed that the bias could be removed and the rms error be reduced. It also showed that the error is common to both MINIMUF models. Further investigation for path lengths less 4000 km, also showed that linear regression could reduce the rms error and remove the bias. This implies that the error in the models could be attributed to the f_oF2 portion of the model. A method for improving this portion of the model is suggested.

G7-6
1040

GENERATION OF INTENSE HF FIELD IN THE IONOSPHERE: S. Ganguly, Center for Remote Sensing, McLean, VA 22102

A scheme to produce intense HF electric fields in the ionosphere and the potential applications that could result is discussed When two strong UHF beams with a frequency difference equal to the plasma frequency of the ionosphere, propagates through a common volume in the plasma, the beat frequency could generate intense electric field fluctuations in the HF range.

Generation of the electric field fluctuations at the beat frequency will depend on the nonlinear processes in the ionospheric plasma. For parametric and similar processes, arising through the ponderomotive forces, the efficiency of conversion is given by Manley- Rowe relation, e.g. $\eta = f_{HF}/f_{UHF}$.

For a 10 MHz HF field generated by beating two radars at frequencies near 430 MHz, the efficiency is 2×10^{-2}. With the Arecibo radar radiating 5×10^{12} watts of ERP, about one watt m^{-2} of power density might be deposited in the ionosphere. In order to produce equivalent power densities using conventional ground-based HF facilities, it would require an ERP of the order of 10^{11} watts. This is at least three orders of magnitude larger than what can be attained by any existing ground-based facility. The wealth of physical processes and the practical applications that could result from such a facility are numerous. Applications will range from problems relating to cosmos, fusion research, particle acceleration, radar, and communications.

G7-7
1100

LUF MODEL UNCERTAINTY ASSESSMENT

D.B. Sailors and W.K. Moision
Ocean and Atmospheric Sciences Division
Naval Ocean Systems Center
San Diego, CA 92152-5000

A statistical analysis of observed oblique sounder lowest observed frequency (LOF) and predicted lowest usable frequency (LUF) was used to assess the accuracy of the PROPHET algorithm QLOF version 2.0. A LOF data base of 1814 LOFs from 29 paths was established for the assessment. The data was screened into subsets to determine the effect of particular paths, universal and local time, sounder type, path length and orientation, season, month, sunspot number, and mid-path latitude. Version 2.0 had a bias of 0.55 MHz low, an rms error of 1.95 MHz, and a correlation coefficient with the observed data of 0.89. The rms error increases with increasing range. A higher residual was noted for the months of July through October. An increase in residual at mid-latitude was noted. Reasons for these errors are given. A modification to the absorption index term which determines the latitudinal and seasonal variation is suggested.

G7-8
1120

A PROCEDURE WHICH ALLOWS AN UPDATE OF ABSORPTION CALCULATIONS UTILIZING IONOSPHERIC SOUNDINGS

D.B. Odom and N.P. Viens
Raytheon Company
Wayland, Massachusetts 01778

Most predictions of signal strength of energy propagated through the ionosphere utilize simple median parameter models to estimate the value of the nondeviative absorption component which is expected for a selected high frequency communication or radar system configuration. These median models (see, for example, K. Davis, Ionospheric Radio Propagation, 1965) typically rely upon semi-empirical fits to experimental data bases in which variations in time of day, location, season, geomagnetic activity, etc. are modeled.

The problems associated with utilizing this type median absorption estimation technique are two fold: First, the absorption data corresponding to the generic environmental conditions of interest (location, time of day, etc.) must be available and second, the RMS fitting techniques provide only typical values for the expected absorption along with estimates of the deviation which is observed about these typical values. In an attempt to overcome the limitations inherent in these simple absorption modeling procedures a raytracing procedure through a realistic three-dimensional model of the ionosphere that can be readily derived from vertical and ground backscatter soundings has been developed. This propagation modeling procedure provides an updated estimate of both the deviative and non-deviative absorption components for propagation geometries over which ionospheric soundings are available. The modeling procedure utilizes a standard (ARDC, 1960) collisional frequency profile and provides updates of the ionospheric layer parameters using the observed sounder data. A comparison with vertical incidence data collected over a full sunspot cycle has been made and will be described during the talk. The results of this comparison are very promising. The importance of including the deviative absorption term will also be discussed as well as the results which this modeling procedure provides in both Northern and mid latitudes.

G7-9
1140 INCOHERENT SCATTER OBSERVATIONS OF D-REGION MODIFICATIONS: S. Ganguly, Center for Remote Sensing, McLean, VA 22102

Under the action of a strong HF signal, D-region electron temperature is increased and the electron density is modified. For the first time, these changes have been measured using the incoherent scatter technique. Increases in Te by a factor of about 2 have been observed. We shall present the details of this technique for interpretation of D-region results.

Session G/H-2 0835-Thurs. NW 268
IONOSPHERIC MODIFICATION
Chairman: Lewis M. Duncan, Los Alamos National Lab, Mail Stop D-466, Los Alamos, NBM 87545

G/H2-1
0840

THE SATURATION OF PARAMETRIC INSTABILITIES IN IONOSPHERIC MODIFICATION AT ARECIBO

J.A. Fejer
Department of Electrical Engineering and Computer Sciences
University of California San Diego, C-014
La Jolla, CA 92093

Observations with the 430 MHz radar at Arecibo have yielded considerable information on three mechanisms for the saturation of parametric instabilities excited in ionospheric modification experiments.

Observations of backscatter by Langmuir waves below threshold confirm the results of fluctuation theory. Observation in which the strength of the modifying HF wave exceeded the threshold of the parametric decay instabilities by factors of only 2-3, are reasonably well explained by the theory of saturation involving repeated parametric decay, resulting in a cascade of Langmuir waves. This represents the first saturation mechanism.

Observations (W.T. Birkmayer, T. Hagfors, and W. Kofman, Phys. Rev. Lett. , 57, 1008, 1986) with a much stronger HF wave show that the backscatter comes from Langmuir waves trapped inside cavitons (localized density depletions), from only slightly below the reflection height of the HF wave. The formation of cavitons represents the second saturation mechanism.

A third saturation mechanism, the acceleration of electrons by the parametrically excited Langmuir waves, has been suggested during the early stages of ionospheric modification experiments by several authors. Observations at night, in the absence of photoelectrons, of the temporal development after HF switch-on of incoherent backscatter by Langmuir waves, enhanced by the presence of accelerated electrons, does not seem to confirm the importance of such a saturation mechanism. Similar observations in daytime show a considerable enhancement in the fluxes of photoelectrons. The time development of this enhancement, following the switching on of the HF transmitter, closely follows the time development of the well known overshoot in the enhanced plasma line.

G/H2-2
0900 OBSERVATIONS OF HF-INDUCED LARGE-SCALE IONOSPHERIC CAVITIES: Lewis M. Duncan, Los Alamos National Lab; James P. Sheerin, KMS Fusion; and Richard A. Behnke, National Science Foundation

High-power electromagnetic radiation incident on a plasma, acting through the nonlinear ponderomotive force or collisional thermal forces, can generate self-consistent density profile modifications resulting in spatial localization of the pump field. These localized plasma density cavities, when supported by trapped electromagnetic radiation or associated electrostatic plasma waves, may be considered as large-scale cavitons. Cavity formation, evolution and collapse have been observed during recent HF ionospheric modification experiments at the Arecibo Observatory.

Cavities are seen to develop on three distinct spatial and temporal scales. Ponderomotively-driven cavitons form on millisecond time scales near the ionospheric resonance height. Radar observations of the early-time enhanced plasma waves are used to infer the basic characteristics of these rapid, small-scale structures. Thermal self-focusing of the incident HF radiation leads to kilometer-scale field-aligned density striations studied by radar scanning techniques. These irregularities, forming in seconds and decaying in tens of minutes also are believed responsible for the reported preconditioning phenomenon. Typical density variations associated with these effects are on the order of a few percent. Our most recent Arecibo experimental results have detected a new process leading to severe profile steepening and several kilometer density cavities with depletions exceeding 75%. The resultant cavities are supported by thermal forces and trap the incident electromagnetic radiation and associated parametrically-excited electrostatic turbulence. These thermal cavities develop in a manner identical to computer simulations of ponderomotively-driven cavitons in laboboratory wave-plasma interactions. In addition, multiple cavities move along the profile density gradient and are observed to propagate through each other, a characteristic unique to wave solitons. Other soliton-like behavior phenomena are observed, including cavity nucleation, fission and collapse.

G/H2-3 0920

CONVECTION OF THE 630.0 NM AIRGLOW EMISSIONS IN AN ARTIFICIALLY HEATED IONOSPHERE

P. A. Bernhardt and L. M. Duncan
Los Alamos National Laboratory
Los Alamos, NM 87545

C. A. Tepley
Arecibo Observatory
Arecibo, PR 00613

Images from a low-light-level CCD camera show the 630.0 nm airglow clouds resulting from ionospheric heating by the HF facility near Arecibo, Puerto Rico. The enhanced airglow is a result of electron excitation of metastable oxygen. Observations from directly beneath heated ionosphere show elliptical airglow clouds which outline the radiation pattern of the heater. The clouds are initially formed at the zenith and convect to the east. This motion is due to transport of the modified plasma regions by ambient electric fields. Large cavities in the F-region are produced by parametric instabilities and by thermal expansion. As these cavities drift eastward, the intense HF beam is refracted in the same direction. The airglow clouds follow the movement of the parametric interaction regions. When cavities can no longer trap the HF radio waves the high power beam returns to the zenith and the airglow cloud disappears in the east and reforms directly overhead. This process yields pulsation of the zenith airglow intensity. Occasionally, the airglow clouds contain field aligned structure which may be indications of irregularities produced by the high power HF.

G/H2-4
0940

PLASMA LINE PREDICTIONS FOR A 138.8 MHz RADAR

D.B. Muldrew, Communications Research Centre
Department of Communications
P.O. Box 11490, Stn H, Ottawa, Ontario K2H 8S2

An experimental study of the plasma line, PL, using a 138.8-MHz radar has been proposed by F.T. Djuth for the January 1977 ionospheric heating campaign at Arecibo. Calculations of expected PL characteristics have been made for this radar frequency using the magnetic field-aligned duct model (D.B. Muldrew, J. Geophys. Res., 84, 2705-2714, 1979). Some of the assumed parameters for daytime conditions are: HF frequency of 5.1 MHz, field-aligned electron density scale height of 50 km, ion temperature of 800 K, electron temperature of 2000 K, field intensity E^2 at the first Airy-function maximum of 0.5 - 1.0 $(V/m)^2$, photoelectron damping rate of 1790/s, and a vertical-looking radar. Based on previous 430-MHz radar observations, it is assumed that the Langmuir waves resulting from parametric decay of the HF wave must grow convectively by a factor of e^{10} in intensity above the photoelectron enhanced level to be observed by the radar. This growth factor was assumed even though a somewhat larger factor might be required for the 138.8-MHz radar.

The calculated decay line frequency displacements from 138.8 ± 5.1 MHz vary between 1.05 and 1.14 kHz for the upshifted PL, UPL, and 1.20 and 1.36 kHz for the downshifted PL, DPL. The calculated asymmetry for fields with E^2 = 1.0 $(V/m)^2$ at the first Airy maximum is about 0.09 kHz; for E^2 = 0.6 $(V/m)^2$ it is about 0.2 kHz. In a given duct the calculated DPL grows to the assumed observable level for significantly smaller fields than those required for the UPL; hence, DPL can be observed at times when UPL are not. A few DPL have been observed with the 430-MHz radar when UPL are absent (L.M. Duncan, M.S. Thesis, Rice Univ., Fig. 4.5, 1976) but this should be more common for 138.8 MHz observations. The calculated height of observation of the UPL for E^2=1.0 $(V/m)^2$ is 35-60 m above the DPL height. For E^2 = 0.6 $(V/m)^2$ the UPL is about 80 m or more above the DPL height. A height measurement is likely the best way to verify if the PL mechanism requires field-aligned ducting of Langmuir waves since the theory predicts that for the 430-MHz radar the UPL height is below the DPL height. Calculated PL rise times for E^2 = 1.0 $(V/m)^2$ are between 1.3 and 1.7 ms; for E^2 = 0.5-0.7 $(V/m)^2$ they vary from 2.5-6 ms. Although the required density deviation $\Delta N/N$ in the duct is about one half or less for 138.8-MHz observations than it is for 430-MHz observations, the duct diameter must be about 3 times as great. Hence, it is difficult to say whether the required ducts will be more easily created by the HF wave for the 138.8-MHz observations or for the 430-MHz observations.

G/H2-5
1000

NEW INTERPRETATION OF PLASMA-LINE OVERSHOOT PHENOMENON

S.P. Kuo
Polytechnic University
Farmingdale, New York 11735
M.C. Lee
Massachusetts Institute of Technology
Cambridge, Massachusetts 02139
F.T. Djuth
The Aerospace Corporation
El Segundo, California 90245

One of the most reproducible HF-enhanced plasma line phenomena in the F region over Arecibo is the so-called main plasma line overshoot (R.L. Showen and D.M. Kim, J. Geophhys. Res., 83, 623, 1978). Based upon the experimental observation of Coster et. al. (J. Geophys. Res., 90, 2807, 1985), it seems unlikely that anomolous absorption by HF-induced short-scale (1-10m) irregualarities can account for the overshoot observed at Arecibo. In addition, recent efforts to carefully measure the differential absorption of the ionospherically reflected HF wave at Arecibo, have yielded an upper bound on the anomolous absorption of $\sim$10% in power at an HF frequency of 5.1 MHz, (J.A. Fejer, F.T. Djuth and M.P. Sulzer, private communication, 1985). Given the fact that strong plasma line overshoot was present during the absorption measurements, this data supports the point that anomolous absorption does not play a key role in the overshoot effect.

It is known that the resonance broadening effect (T.H. Dupree, Phys. Fluids, 9, 773, 1966) can lead to the saturation of the parametric instability and further to the mode suppression. This is because the anomolous damping introduced by the resonance broadening effect of the instability is proportional to the total spectral intensity of excited waves, and the growth rate of individual spectral line is a function of the angle θ between the propagation direction of the spectral line and the geomagnetic field, and of the wavenumber k of the line. As the total energy of the instability increases, it enhances the anomolous damping (uniformly) to every plasma line. Consequently, the spectral line having small growth rate (which depends on θ and k) will be suppressed when the anomolous damping exceeds the linear growth rate of this line. A model based on this process has been developed to describe the plasma-line overshoot phenomenon. This model will be discussed and the results compared with the experimental data will be presented.

G/H2-6
1040

IONOSPHERIC MODIFICATION AT ARECIBO - 5 MHz VERSUS 3 MHz HEATING

F. T. Djuth [1], B. Thidé [2], H. M. Ierkic [3], M. P. Sulzer[3], J. A. Fejer [4]

[1] Space Sciences Laboratory, The Aerospace Corporation, El Segundo, CA 90245
[2] Uppsala Ionospheric Observatory, S-755 90, Uppsala, Sweden
[3] Arecibo Observatory, P. O. Box 995, Arecibo, Puerto Rico 00612
[4] Department of Electrical Engineering and Computer Sciences, University of California San Diego, La Jolla, CA 92093

Recent results at Arecibo indicate that the nature and extent of the F region modifications by high-power, high-frequency radio waves near 3 MHz are substantially different from those observed at 5 MHz. While HF-enhanced plasma lines (HFPLs) are maintained during continuous wave (CW) heating at frequencies near 5 MHz, HFPLs are never sustained at 3 MHz. However, HF-enhanced ion lines may be excited at either frequency during CW operations. At 3 MHz, HFPLs are detected only during an "overshoot" period lasting on average several hundred milliseconds. Typically, 4-8 seconds of HF off time is required to produce detectable HFPLs during the 3 MHz overshoot. In addition, considerably more absorption of the pump wave due to HF-induced instabilities is evident at 3 MHz than at 5 MHz. At both frequencies, strong stimulated electromagnetic emissions are observed to emanate from the modified ionospheric volume, but the character of the emissions tends to be different at the two frequencies. Finally, large HF-induced enhancements in electron temperature are observed at 3 MHz that, up to this point, have not been reproduced at 5 MHz. As part of this presentation, several plasma processes that may play increased roles at low HF frequencies will be described and examined within the context of the current observations.

G/H2-7
1100

LONG TERM EVOLUTION OF THERMAL DENSITY CAVITIES PRODUCED BY HF HEATING*

J. D. Hansen, G. J. Morales, Merit Shoucri, and J. E. Maggs
Physics Department
University of California at Los Angeles
Los Angeles, CA 90024

The results of a previous theoretical study (M. Shoucri, G. J. Morales, and J. E. Maggs, J. Geophys. Res., 89, 2907, 1984) indicated that macroscopic density cavities (few km in width) could be generated at the reflection height of a HF wave due to localized ohmic heating of the ionosphere arising from the Airy-swelling of the wave's electric field. Density depletions on the order of a few percent were predicted to be produced within 60 seconds of heater turn-on. Detailed experimental observations (J. P. Sheerin, D. R. Nicholson, G. L. Payne, and L. M. Duncan, APS Bull., 30, 1467, 1985) have been made in Arecibo of rather large density cavities ($\delta n/n_o > 20\%$) produced under long term heating conditions (i.e., larger than 60 seconds). The present analytical and numerical study examines the evolution of such density cavities beyond the initial formation stage. In particular, we investigate the role of cross field drift and self-consistent displacement of the reflection layer. The possibility of developing rippling of the reflection surface and consequences of the resulting shorter density scale length are examined.

* Work supported by ONR

G/H2-8
1120

RECENT IONOSPHERIC MODIFICATION EXPERIMENTS USING ENERGETIC ELECTRON BEAMS ON SPACECRAFT

B.E. Gilchrist, P.M. Banks, A.C. Fraser-Smith
STAR Laboratory, Stanford University
Stanford, CA 94305-4055

Energetic electron beam generators on spacecraft provide opportunities for conducting a variety of new ionospheric modification experiments, including, in particular, the creation of plasma density structures such as plasma sheets and filaments. The properties of these structures necessarily depend on certain beam and spacecraft parameters, including beam energy, current, pulsing rate, and spacecraft altitude and velocity, but the form of the dependence has not yet been well established (Banks, P.M. and B.E. Gilchrist, GRL, 12, no.4, 175-178, 1985).

During 1985, the Fast Pulsed Electron Generator (FPEG), a low power (100W) electron gun, on Spacelab-2 and the CHARGE-2 rocket was utilized to provide information on the detection and form of any structures produced by electron beams. Because of FPEG's low beam power and the high (orbital) velocity associated with Spacelab-2 it was calculated that low undisturbed nighttime background electron density levels (near 10^{+3} cc^{-3}) in the 160-200 km altitude range would be needed to detect any electron beam ionization enhancement. For the most part this did not appear to have been achieved. The Charge-2 rocket had a much slower horizontal velocity which allowed the predicted ionization enhancement density to be some forty times higher than Spacelab-2. Because of anomalous gun operation during the rocket flight, actual beam current was down by a factor of ten early in the flight, increasing to a level down by a factor of two late in the flight.

A description of results from both of these missions will be presented with emphasis given to 50MHz radar data obtained from the Charge-2 rocket flight, which showed possible indications of electron beam effects. Suggestions for future experiments will also be outlined.

G/H2-9
1140

RECENT RESULTS ON HIGH POWER IONOSPHERIC HEATING EXPERIMENTS USING THE HIPAS FACILITY*

P. Y. Cheung, P. J. Barrett, A. Y. Wong, and K. L. Lam
University of California, Los Angeles
Department of Physics
Los Angeles, CA 90024

Recent results of ionospheric heating and profile modification experiments using the UCLA HIPAS facility near Fairbanks, Alaska will be presented. The HIPAS transmitters has a total power output of 800 KW and can be operated in either CW or pulsed mode. On site diagnostics include two digital ionosondes, a computer controlled multi-channel phase array detection system, and computer controlled HF receiving systems. Experiments are performed under various ionospheric conditions, including during the occurrences of aurora. Artifically created spread-F, i.e., the spreading of return echoes of both O (ordinary) and X (extraordinary) waves, are observed quite frequently during the heating experiments. Evidence of heater induced Z-mode will also be presented. A preview of future experimental program will also be presented.

*Work supported by ONR grant N00014-78-C-0754 and the UCLA Physics Department.

INDEX

TUESDAY, 13 JANUARY
(Paper presentations will be held in the Engineering Center)

0835-1200

B-7	Scattering	CR2-28
C-2	Mobile Satellite Systems	CR1-9
H-3	Wave, Particle, and Mass Injections in Space Plasmas I	CR1-40

0855-1200

A-2	Antenna and EM Field Measurements	CR1-42
F-3	Theoretical Studies of Propagation in Non-Ionized Media	CR2-26
G-5	What is There Left to Study About the Ionosphere and Why?	CR0-30
J-4	Millimeter and Submillimeter Techniques in Radio Astronomy I	CR2-6

1200-1300
Radio Science Editors Luncheon — Aspen Room, UMC

1355-1700

B-8	Numerical Techniques	CR2-28
E-1	Electromagnetic Interference Environment: Measurement and Models	CR1-42
F-4	Remote Sensing of Atmospheric and Oceanic Waves, Sea Ice and Vegetation	CR2-26
G-6	Auroral and Polar Cap Irregularities	CR1-46
G/H-1	ELF/VLF Radio Wave Propagation	CR0-30
H-4	Wave, Particle, and Mass Injections in Space Plasmas II	CR1-40
J-5	Millimeter and Submillimeter Techniques in Radio Astronomy II	CR2-6

1700-1800

Commission B Business Meeting	CR2-28
Commission C Business Meeting	CR1-9
Commission E Business Meeting	CR1-42
Commission H Business Meeting	CR1-40

WEDNESDAY, 14 JANUARY
(Afternoon paper presentations will be held in the Events/Conference Center)

0830-1200
Plenary Session — Macky Auditorium

1130-1300
USNC/URSI Executive Committee — Aspen Room, UMC

1355-1700

B-9	Guided Waves	NW 271
C-4	Spectral Estimation: Multi-Window Techniques	NW 238
E/B-1	Special Session on High Power Electromagnetics I	NW 261
H-5	Ionospheric Wave Experiments From the Space Station	NW 270
J-6	Signal Processing in Radio Astronomy	NW 268

1515-1700

A-3	Transient Responses From CW Measurements	NW 248

THURSDAY, 15 JANUARY
(Paper presentations will be held in the Events/Conference Center)

0835-1200

B-10	Backscattering Enhancement	NW 271
C-5	Robust Spectral Estimation	NW 238
E/B-2	Special Session on High Power Electromagnetics II	NW 261
G-7	HF Ionospheric Propagation	NW 270
G/H-2	Ionospheric Modification	NW 268

0855-1200

A-4	Microwave Measurements and Standards	NW 248